VIBRATIONAL SPECTROSCOPIC STUDIES OF MATRIX ISOLATED MOLECULES

by

Richard Evans

A thesis submitted for the degree of Doctor of Philosophy in the University of Oxford

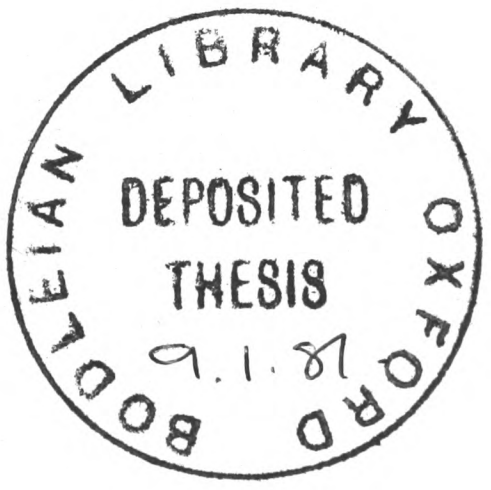

Jesus College, Oxford

1980

TITLE: Vibrational Spectroscopic Studies of Matrix Isolated Molecules

AUTHOR: R Evans, Jesus College, Oxford

DEGREE: D Phil

DATE: Trinity Term 1980

ABSTRACT: The Raman spectrum of polycrystalline or matrix-isolated S_2N_2 shows three bands attributable to its Raman active fundamentals, including two in close proximity; the possibility of Fermi resonance is discounted. The infrared spectrum of polycrystalline S_2N_2 shows five bands, including three attributable to the infrared active fundamentals, while the others are associated with some intermediate species in the polymerisation of S_2N_2.

The vibrational spectra of matrix-isolated S_4N_4 are consistent with previous observations in the solid state and in solution, also with the established cage structure of the molecule.

The stretching force constants of S_2N_2 and S_4N_4, lower than those predicted on the basis of observations on acyclic S-N molecules, are correlated with the strain in the molecules and their associated thermodynamic instability. The interaction force constants indicate delocalised π -bonding, apparently more extensive in S_2N_2. Substantial cross-ring S-S bonding is evident in S_4N_4; S-S interactions in S_2N_2 are apparently non-bonded and repulsive in nature.

The infrared spectrum of matrix-isolated $CrOCl_3$ contains bands attributable to the fundamentals of this molecule, along with several indicating the presence of CrO_2Cl_2 and possibly other related molecules. The Raman spectrum shows just three strong bands, all below 250 cm^{-1}, assumed to arise from the deformation fundamentals of $CrOCl_3$; the form of the spectrum is attributed to absorption or fluorescence. The force constants derived for $CrOCl_3$ correspond closely to their counterparts in $VOCl_3$ and CrO_2Cl_2, suggesting similar force fields in the three molecules.

The infrared spectrum of the volatile products of the reaction between PCl_3 and NaN_3 indicates the presence of several molecules, possibly including Cl_2PN_3 and oligomers of $Cl_2 P \equiv N$, although no definite conclusions are drawn. Spectroscopic evidence also suggests that the reaction between $(CH_3)_2PCl$ and NaN_3 yields $(CH_3)_2PN_3$ as a major product, although observations such as the effect of ultra-violet photolysis remain unexplained.

ACKNOWLEDGEMENTS

It is impossible to begin without expressing most heartfelt gratitude to my supervisor, Dr A J Downs, for his extremely helpful advice, constant encouragement and unfailing good humour throughout the course of this work.

I should also like to thank the following:-

Dr G P Gaskill for a most useful introduction to the wonders of Raman spectroscopy and matrix isolation;

Mr M Hawkins for assistance with, and useful discussions relating to, computing matters;

The other 'inmates' of T.13 and S.8 who all helped to provide the best possible atmosphere in which to work;

Mrs L Robertson for provision of an efficient typing service;

and Dr R V Paterson for his services as a proof reader.

CONTENTS

Chapter 1

INTRODUCTION

The first study of reactive chemical species by the method of trapping in a rigid matrix at low temperatures was the work of Lewis and Lipkin on large organic radicals;[1] this followed earlier reports of luminescence following irradiation or electron bombardment of solids at low temperatures.[2,3] The term 'matrix isolation' was introduced, however, by Pimentel and his associates in 1954,[4] and it was from this point that the technique as we know it really developed. The species studied are typically those which under normal conditions have only a short lifetime, undergoing either unimolecular or bimolecular reactions to yield longer-lived products.

There are, in fact, two alternative approaches to the study of such species. The first of these involves generation of the species in the gaseous or liquid state followed by rapid spectroscopic observation, as in flash photolysis,[5] pulse radiolysis[6] and related techniques. The second method is to trap the species in a large excess of inert material at low temperatures (typically 4-40K), in order to prolong its lifetime and allow the use of conventional methods of spectroscopic characterisation. This effective isolation of the species concerned limits the chances of bimolecular reactions, while the low temperatures employed limit the thermal energy available and hence the chances of unimolecular decay.

A variety of spectroscopic methods has been used to study matrix-isolated molecules: these include the methods of infra-red,[7-9] Raman,[10] optical,[11] esr,[12] and Mössbauer[13] spectroscopy. The methods of vibrational spectroscopy have found the widest application, making up for their relative insensitivity by the extent and chemical significance of the information which they yield. As well as qualitative information about the number and nature of the species present, infrared and Raman methods usually give some indication of molecular

symmetry and allow some sort of definition of the molecular force field, which may be correlated with the nature of the bonding in the molecule.

If matrix isolation is to be a useful tool in the characterisation of novel molecular species it is important that the spectroscopic properties observed are not significantly perturbed by the matrix environment. Such perturbations have been identified by characterisation of stable molecules in the matrix-isolated state and comparison with gas-phase measurements. Certain spectral changes induced by a matrix environment, such as slight differences in frequencies and absorption coefficients, are analogous to those which occur upon dissolution of molecules in a liquid solvent. In addition, however, there are effects peculiar to matrices, such as the possibility of observing a multiplet where only a single spectroscopic feature is expected, commonly attributable to variations in the matrix environment experienced by the guest molecules.

An important effect of the matrix environment is the quenching of rotational motion for all but the smallest molecules. This, together with the elimination of vibrational 'hot bands', leads to considerable simplification and sharpening of observed spectral features. The consequences of such sharp bands include enhanced sensitivity, the possibility of meaningful determination of vibrational frequencies to $\pm$ 0.1 cm^{-1}, and greater ease of resolution of nearly degenerate features, often allowing clear observation of the effects of isotopic substitution. These characteristics compare favourably with the diffuseness of the bands in the vibrational spectra of high-temperature vapours.

Where comparisons are possible, the vibrational frequencies of a matrix-isolated molecule are found to correspond quite closely to those of the same molecule in the gas phase. The frequency perturbation induced by the matrix environment are of the same order of magnitude as anharmonicity corrections, and relationships such as the isotopic sum and product rules may be usefully applied to matrix-isolated species. Hence matrix isolation may be useful in the vibrational analysis of stable molecules, particularly because of the improved definition of the

molecular force field allowed by observations on isotopically distinct species. This has proved to be the case in a variety of examples, such as the molecules $H_3B_3N_3H_3$,[14] CH_3OH,[15] and ClF_3.[16] Similarly matrix isolation has been employed in attempts to explain the behaviour of molecules such as xenon hexafluoride; in this case the apparent dependence of the infrared spectrum on the thermal history of the sample has been attributed to the existence of three electronic isomers.[17]

Chemical reactions may also be monitored using the methods of vibrational spectroscopy. Spectroscopic evidence about chemical changes has been obtained, for example, following the photolysis of matrix-isolated metal carbonyls, either alone (eg $Ni(CO)_4$[18]) or in conjunction with other reagents (eg $M(CO)_6$ with N_2, M = Cr, Mo or W[19]). Sample-warning experiments may be informative when diffusion results in polymerisation or other reactions, leading either to known or to new products. Examples are provided by the dimerisation of such species as CH_3[20] and CCl_2[21] and the behaviour on diffusion of group IV B oxide species, resulting in spectroscopic characterisation of the molecules $(MO)_n$ (M = Si, Ge, Sn or Pb; n = 2, 3 or 4).[22-25]

This thesis is concerned with the study of a variety of species in low-temperature matrices. These include both unstable molecules, such as the products of high-temperature and photochemical reactions, and others which are actually relatively stable under normal conditions. In all cases a combination of Raman and infrared techniques has been employed either simply to characterise the species or to determine its vibrational and structural properties and, ultimately, the nature of the molecular force field.

Chapter 2

VIBRATIONAL SPECTROSCOPY[26-31]

2.1 Introduction

The interaction of light with a molecule causes a distortion of its electron cloud, leading to the possibility of elastic (Rayleigh) scattering of the incident photons. When there is a change in electrical polarisability of a molecule in the course of a vibrational transition, there is also the possibility of inelastic (Raman) scattering. If ν_0 is the frequency of the incident light, then the frequency ν' of the scattered light is given by the equation:

$$\nu' = \nu_0 \pm \nu \qquad (2.1)$$

where ν is the frequency of the vibrational transition. Thus the Raman effect is a scattering phenomenon, normally induced by monochromatic light subject to the condition $\nu_0 \gg \nu$.

By contrast, infrared spectroscopy normally relates to an absorption phenomenon in which energy is transferred to the vibrational motion of the molecule by interaction of the electric vector of the incident radiation with the molecular dipole moment. It is because the mechanisms of the two processes are different that vibrational transitions allowed in infrared absorption may be forbidden in Raman scattering, and vice versa. In various respects the two methods are complementary.

2.2 Normal Modes and Normal Coordinates

A molecule consisting of N atoms requires 3N coordinates to define completely the positions of the nuclei in space. Three of these coordinates relate to translational motion, three to rotational motion (or two in the special case of a linear molecule), and the remaining 3N-6 (or 3N-5) to vibrational motion. This vibrational motion is generally complex but may be regarded as a superposition of a number of so-called 'normal modes', in each of which the atoms execute simple harmonic motion about their equilibrium positions with

the same frequency and phase.

The classical equation of motion for the i^{th} mass has the form

$$\frac{d}{dt}\left(\frac{\partial T}{\partial \dot{x}_i}\right) + \left(\frac{\partial V}{\partial x_i}\right) = 0 \qquad (2.2)$$

where T is the kinetic energy and V the potential energy, and x_i is a displacement coordinate. The total kinetic energy of the system is given by

$$2T = \sum_{i=1}^{3N} m_i \dot{x}_i^2 \qquad (2.3)$$

and the potential energy by

$$2V = \sum_{i=1}^{3N-1} \sum_{i+1}^{3N} k_{ij}(x_i - x_j)^2 \qquad (2.4)$$

assuming simple harmonic motion. These expressions may be simplified, firstly by using mass-weighted displacement coordinates, defined, for example, by the relation

$$q_i = m_i^{\frac{1}{2}} x_i \qquad (2.5)$$

and secondly by constructing linear combinations of these, the normal coordinates Q_i defined as follows:

$$Q_a = l_{1a}q_1 + l_{2a}q_2 + l_{3a}q_3 \ldots + l_{3Na}q_{3N}$$
$$Q_b = l_{1b}q_1 + l_{2b}q_2 + l_{3b}q_3 \ldots + l_{3Nb}q_{3N} \qquad (2.6)$$

where the coefficients of the q_i's are normalised such that $\sum_{1}^{3N} l_{ia}^2 = 1$. The expressions for the kinetic and potential energies reduce to:

$$2T = \sum_i \dot{Q}_i^2 \quad \text{and} \quad 2V = \sum_i \lambda_i Q_i^2 \qquad (2.7)$$

where λ_i is a constant characteristic of the i^{th} mode. The equation of motion may be expressed in terms of the normal coordinates, thus:

$$\frac{d}{dt}\left(\frac{\partial T}{\partial \dot{Q}_i}\right) + \frac{\partial V}{\partial Q_i} = 0 \qquad (2.8)$$

whence it follows that

$$\sum_i \ddot{Q}_i - \sum_i \lambda_i Q_i = 0 \qquad (2.9)$$

For the i^{th} coordinate the equation $\ddot{Q}_i - \lambda_i Q_i = 0$ has a solution of the type

$$Q_i = A_i \cos (\lambda_i^{\frac{1}{2}} t + \varepsilon) \qquad (2.10)$$

where A_i is the amplitude of vibration and ε is a phase angle; also, if ν_i is the frequency of the vibration in cm^{-1}, then $\lambda_i = 4\pi^2 c^2 \nu_i^2$. The solution implies that nuclei vibrating in the i^{th} mode represented by Q_i do so with a common frequency ν_i.

2.3 Normal Coordinate Analysis

It can be shown[26] that the quadratic expression for the kinetic energy may be written in matrix form as:

$$2T = \dot{\underset{\sim}{X}}^{+} \underset{\sim}{M} \dot{\underset{\sim}{X}} \qquad (2.11)$$

where $\dot{\underset{\sim}{X}}$ is a column matrix of the derivatives with respect to time of the Cartesian displacements, $\dot{\underset{\sim}{X}}^{+}$ is its transpose, and $\underset{\sim}{M}$ is a diagonal matrix of the nuclear masses, each appearing three times. This refers to the total kinetic energy; in the treatment of the purely vibrational problem for a non-linear molecule it is convenient to introduce a set of 3N-6 internal coordinates by a transform matrix $\underset{\sim}{B}$:

$$\underset{\sim}{D} = \underset{\sim}{B}\underset{\sim}{X} \qquad (2.12)$$

where $\underset{\sim}{D}$ is a (3N-6) column matrix with elements D_i and $\underset{\sim}{X}$ is a 3N column matrix with elements x_i . If the matrix $\underset{\sim}{A}$ is defined as the inverse of $\underset{\sim}{B}$, so that $\underset{\sim}{X} = \underset{\sim}{A}\,\underset{\sim}{D}$, then the vibrational kinetic energy may be expressed in terms of the internal coordinates as follows:

$$2T = \dot{\underset{\sim}{D}}^{+} \dot{\underset{\sim}{A}}^{+} \underset{\sim}{M}\, \underset{\sim}{A}\, \dot{\underset{\sim}{D}} \qquad (2.13)$$

In deriving this expression it is assumed that there is no interaction between the internal vibrations and other forms of molecular motion, particularly rotation; this is normally a good approximation.[26]

The potential energy may also be expressed as a function of the internal coordinates. When the molecule is in its equilibrium configuration, the potential energy is at a minimum, leading to the vanishing of all terms of the form $(\partial V/\partial D_i)_0$ evaluated at $D_i = 0$; if this position is taken as the arbitrary zero from which the potential energy is measured, then the required expression is as follows:

$$V = \tfrac{1}{2}\sum_i \left(\frac{\partial^2 V}{\partial D_i^2}\right)_0 D_i^2 + \sum_i \sum_j \left(\frac{\partial^2 V}{\partial D_i \partial D_j}\right)_0 D_i D_j \qquad (2.14)$$

The force constants are defined as $F_{ii} = \left(\frac{\partial^2 V}{\partial D_i^2}\right)_0$ and $F_{ij} = \left(\frac{\partial^2 V}{\partial D_i \partial D_j}\right)_0$, so that the expression for the potential energy may be rewritten as

$$2V = \sum F_{ii} D_i^2 + 2\sum F_{ij} D_i D_j \qquad (2.15)$$

This may be expressed in matrix form as follows:

$$2V = \underset{\sim}{D}^{+} \underset{\sim}{F}\, \underset{\sim}{D} \qquad (2.16)$$

where $\underset{\sim}{F}$ is a square matrix whose elements are the force constants F_{ij}.

2.4 The Wilson G Matrix

The vibrational kinetic energy T may be expressed in terms of the internal coordinates by the use of the matrix $\underset{\sim}{G}$, defined as[27]

$$\underset{\sim}{G} = \underset{\sim}{B}\, \underset{\sim}{M}^{-1} \underset{\sim}{B}^{+} \qquad (2.17)$$

Here $\underset{\sim}{B}$ is the transform matrix of equation (2.12) and $\underset{\sim}{M}^{-1}$ is the inverse of the diagonal matrix $\underset{\sim}{M}$ of equation (2.11). If $\underset{\sim}{A}$ again denotes the inverse of $\underset{\sim}{B}$ it can be shown that the inverse of $\underset{\sim}{G}$ may be expressed in the following way:

$$\underset{\sim}{G}^{-1} = \underset{\sim}{A}^{+} \underset{\sim}{M}\, \underset{\sim}{A} \qquad (2.18)$$

Thus, comparison with the equation derived in the previous section leads to the following relation for the vibrational kinetic energy:

$$2T = \dot{\underset{\sim}{D}}^{+} \underset{\sim}{G}^{-1} \dot{\underset{\sim}{D}} \qquad (2.19)$$

Introduction of this, together with the corresponding expression for the potential energy, into the equation of motion results in a series of equations of the form

$$\sum_i \sum_j (F_{ij} - \lambda_i G_{ij}^{-1}) D_i = 0 \qquad (2.20)$$

These equations may be expressed in the form of a square matrix of order 3N-6, and the solutions λ_i, which lead directly to the vibrational frequencies, may be obtained by solving the corresponding secular equation. Written in the form of a determinant

$$| \underset{\sim}{F} - \lambda \underset{\sim}{G}^{-1} | = 0 \qquad (2.21)$$

this generates a polynomial in λ of order 3N-6. The left-hand side of equation (2.21) may be either pre-multiplied or post-multiplied by $|\underset{\sim}{G}|$ to obtain the alternative forms

$$| \underset{\sim}{GF} - \lambda \underset{\sim}{E} | = 0 \quad \text{and} \quad | \underset{\sim}{FG} - \lambda \underset{\sim}{E} | = 0 \qquad (2.22)$$

where $\underset{\sim}{E}$ represents a unit matrix of the appropriate order.

2.5 Molecular Symmetry and the Factorisation of the Secular Equation

The internal coordinates generally form a number of distinct sets (eg stretching of a particular type of bond), within each of which the members may be interchanged by a symmetry operation of the molecular point group. Although the internal coordinates form the basis of a representation of the molecule,[28] this representation is generally reducible; by reference to the appropriate character table, however, it is possible to generate internal symmetry coordinates S_i which take the form of a series of linear combinations of the original internal coordinates, and which form the basis of a fully reduced representation. If this transformation is expressed in matrix form as $\underset{\sim}{S} = \underset{\sim}{U}\,\underset{\sim}{D}$, then symmetrised $\underset{\sim}{F}$ and $\underset{\sim}{G}$ matrices $\underset{\sim}{F}_s$ and $\underset{\sim}{G}_s$ may be generated as follows:

$$\underset{\sim}{G}_s = \underset{\sim}{U}\,\underset{\sim}{G}\,\underset{\sim}{U}^+ \quad \text{and} \quad \underset{\sim}{F}_s = \underset{\sim}{U}\,\underset{\sim}{F}\,\underset{\sim}{U}^+ \qquad (2.23)$$

$$\text{so that} \quad 2T = \dot{\underset{\sim}{S}}^+ \underset{\sim}{G}_s^{-1} \dot{\underset{\sim}{S}} \quad \text{and} \quad 2V = \underset{\sim}{S}^+ \underset{\sim}{F}_s \underset{\sim}{S} \qquad (2.24)$$

The effect of the transformation is to reduce the $\underset{\sim}{F}$ and $\underset{\sim}{G}$ matrices to a number of independent blocks, or, in other words, to factorise the secular equation; this leads to considerable simplification of the vibrational problem.

2.6 Solution of the Secular Equation

In order to solve the secular equation (2.21) or (2.22), it is necessary to construct the symmetrised $\underset{\sim}{F}$ and $\underset{\sim}{G}$ matrices. The elements of the $\underset{\sim}{G}$ matrix are expressed in terms not only of the atomic masses but also of the bond lengths and bond angles of the molecule (derived from experimental data or otherwise estimated by comparison with the dimensions of related molecules. The relation between the components of the $\underset{\sim}{F}$ matrix and the force constants of the molecule demands some knowledge of the molecular force field. In practice, the problem is usually one of calculating the components of the $\underset{\sim}{F}$ matrix and hence the force constants from observed vibrational frequencies. The number of unknown quantities exceeds the number of measured frequencies for any given molecule containing more than two atoms, and although the amount of information available may be increased, for example, by isotopic labelling, it is commonly necessary to make certain assumptions about the force field, for example, that certain force constants are transferable from one molecule to another, or that certain force constants are zero. The case where all interaction force constants are zero corresponds to a simple valence force field, characterised by a diagonal $\underset{\sim}{F}$ matrix. Alternative approaches include the Urey-Bradley approximation, a force field which makes use of repulsive force constants between non-bonded atoms as well as the usual stretching and bending force constants.[32]

2.7 Isotopic Substitution

Isotopic labelling of a molecule increases the amount of experimental information available, since it gives rise to new vibrational frequencies because of the change of mass, but leaves the force field unaffected to a good approximation. However, the increase in the number of independent observed parameters is not as great as might be expected at first sight, because the frequencies of one isotopic version of a molecule are related to those of another by the so-called product rule.[26,33] This rule follows from the fact that the product $\pi\lambda$ of all the roots of an equation of the

form $|\underset{\sim}{D} - \lambda\underset{\sim}{E}| = 0$ is equal to the determinant $|D|$. If there is no change in symmetry on isotopic substitution, then the $\underset{\sim}{F}$ matrix remains unchanged, and it follows that for any symmetry block

$$\frac{\pi\lambda}{\pi\lambda'} = \frac{\pi(\nu^2)}{\pi(\nu'^2)} = \frac{|G|}{|G'|} \qquad (2.25)$$

where the primes denote the frequencies and $\underset{\sim}{G}$ matrix appropriate to the second isotopic version of the molecule In practice, the anharmonicity of real vibrations causes deviations from this rule, but these are appreciable (> ca 2%) only when the anharmonicity correction is relatively large. This in turn occurs only for very light nuclei with their relatively large vibrational amplitudes. An example is provided by the totally symmetric (A_1) vibrations of the phosphine molecule, for which the observed frequencies (2327 and 992 cm^{-1} for PH_3,[34] 1694 and 730 cm^{-1} for PD_3[35]) show a slight deviation from the product rule. The rule is generally useful as a means of confirming a particular assignment. Its application requires a knowledge of the molecular geometry, moreover, and if sufficient isotopic information is available, the rule may be exploited to define the limits of a particular interbond angle[36].

2.8 Selection Rules for Infrared Absorption

According to classical theory, a molecule is capable of emitting or absorbing electromagnetic radiation by virtue of periodic changes in its electric dipole moment μ. This dipole moment is a vector quantity which may be expressed in terms of the vibrational normal coordinates Q as follows:

$$\underset{\sim}{\mu} = \underset{\sim}{\mu}_0 + \sum_k \left(\frac{\partial \underset{\sim}{\mu}}{\partial Q_k}\right)_0 Q_k + \text{higher terms}, \qquad (2.26)$$

the zero subscripts signifying the values appropriate to the equilibrium configuration of the molecule ($Q_k=0$). Provided that the amplitudes of the vibrations are small, then the higher (anharmonic) terms of equation (2.26) may be ignored. Then the condition that the molecular dipole moment

oscillates with the frequency ν_k (corresponding to the normal coordinate Q_k) is that

$$(\frac{\partial \mu_i}{\partial Q_k}) \neq 0 \qquad (2.27)$$

for at least one of the Cartesian components i = x, y or z.

Using the language of quantum mechanics, this may be expressed in terms of the transition moment, which determines the intensity of absorption. For a transition between two states characterised by the wavefunctions $\psi(n)$ and $\psi(m)$ the transition moment μ_{nm} is defined as follows:

$$\underset{\sim}{\mu}_{nm} = \int \psi(n) \underset{\sim}{\mu} \psi(m)^* \, d\tau \qquad (2.28)$$

in which $d\tau$ is a volume element in configurational space and the integral is to be extended over the whole of this space. Substitution of the Taylor expansion value of the dipole moment given by equation (2.26) leads to the expression

$$\underset{\sim}{\mu}_{nm} = \underset{\sim}{\mu}_0 \int \psi(n)\psi(m)^* \, d\tau + \sum_k [(\frac{\partial \underset{\sim}{\mu}}{\partial Q_k})_0 \int \psi(n) Q_k \psi(m)^* \, d\tau] \qquad (2.29)$$

The mutual orthogonality of the wavefunctions means that the first term vanishes unless n = m, a condition clearly corresponding to no transition; the condition for the second term to be non-vanishing leads to a selection rule analogous to that obtained <u>via</u> the classical treatment.

Thus a vibrational transition is forbidden in infrared absorption unless at least one of the three components of the transition moment, $\int \psi(n) \mu_i \psi(m)^* d\tau$, i = x, y or z, does not vanish; whether this happens depends on the symmetry properties of the wavefunctions of the initial and final states on the one hand and those of the dipole moment μ on the other. For a vibration to be active in infrared absorption, the product $\psi(n) \mu_i \psi(m)$ must belong to a representation containing the totally symmetric species for at least one of the components μ_i of the dipole moment (i = x, y or z) ; for a fundamental transition this condition is met only if the wavefunction

or normal coordinate of the vibrational mode belongs to a representation containing the same symmetry species as at least one of these components.

2.9 Selection Rules for Raman Scattering

The first generally accepted theory concerning the origin of Raman scattering was developed by Placzek[37]; recent accounts have normally favoured the bond polarisability approach first introduced by Wolkenstein[38] and subsequently developed by Long[39]. The Placzek theory requires firstly that the molecules are in a non-degenerate electronic ground state, and secondly that the frequency of the exciting radiation is far removed from any absorption of the molecules. The intensity I of Raman scattering at a displacement $\Delta\nu$ from the exciting frequency ν_o is given by

$$I = \frac{KM(\nu_o - \Delta\nu)^4}{\Delta\nu[1 - \exp(-h\Delta\nu/kT)]} [\underset{\sim}{P}_{nm}]^2 \qquad (2.30)$$

where K is a constant, M is the molar concentration of the scattering species, and the denominator includes a Boltzmann factor allowing for the initial molecular populations of the two vibrational levels designated by the labels m and n to which the transition moment $\underset{\sim}{P}_{nm}$ relates. $\underset{\sim}{P}_{nm}$ in turn determines the possibility of a transition between these two vibrational levels, being related by the expression

$$\underset{\sim}{P}_{nm} = \int \psi(n) \underset{\sim}{P} \psi(m)^* \, d\tau \qquad (2.31)$$

to the induced dipole moment $\underset{\sim}{P}$ generated by interaction of the molecular electron cloud with the electric field associated with the exciting radiation. For field strengths of the magnitude ordinarily used, the induced dipole moment is itself determined by the product of the field $\underset{\sim}{E}$ and the molecular polarisability α:

$$\underset{\sim}{P} = \alpha \underset{\sim}{E} \qquad (2.32)$$

The molecular polarisability has the properties of a symmetric tensor, characterised by six distinct components α_{xx}, α_{yy}, α_{zz}, α_{xy}, α_{yz} and α_{zx}.

Like the dipole moment, the polarisability is in general a function of all the normal vibrational coordinates, and may be expanded as a Taylor series with respect to these coordinates, neglecting terms higher than the first. Thus

$$\alpha = \alpha_0 + \sum_k \left[\left(\frac{\partial \alpha}{\partial Q_k} \right)_0 Q_k \right] \qquad (2.33)$$

In this equation, which is analogous to equation (2.26), α_0 is the polarisability tensor in the equilibrium configuration of the molecule and $(\partial \alpha / \partial Q_k)_0$ is the so-called derived polarisability (also at the equilibrium configuration) for the k th normal mode. Like α itself, $(\partial \alpha / \partial Q_k)_0$ is a symmetric tensor, each of its components being the value, at the equilibrium configuration, of the derivative $\partial \alpha_{ij} / \partial Q_k$ of the corresponding component of α (i or j = x, y or z). Then the induced dipole moment of a vibrating molecule may be expressed as

$$\underset{\sim}{P} = \alpha_0 \underset{\sim}{E} + \sum_k \left[\left(\frac{\partial \alpha}{\partial Q_k} \right)_0 Q_k \right] \underset{\sim}{E} \qquad (2.34)$$

The first term $\alpha_0 E$ gives rise to a component of $\underset{\sim}{P}$ which oscillates with the frequency ν_0 characteristic of $\underset{\sim}{E}$, corresponding to the phenomenon of Rayleigh scattering. On the other hand, the second term contains the product of <u>two</u> time-dependent factors, namely Q_K, which oscillates with the normal frequency ν_k, and $\underset{\sim}{E}$, which oscillates with the incident frequency ν_0; the corresponding contribution to the induced dipole moment is characterised by the two new frequencies $\nu_0 + \nu_k$ and $\nu_0 - \nu_k$. It is this contribution which corresponds to Raman scattering. For a particular vibrational mode with the normal coordinate Q_K to be active in Raman scattering it follows that

$$\left(\frac{\partial \alpha_{ij}}{\partial Q_k} \right) \neq 0 \qquad (2.35)$$

for at least one of the components (i or j = x, y or z) of the polarisability tensor. Expressed in quantum-mechanical terms, this selection rule amounts to the requirement that

$$\int \psi(n) \alpha_{ij} \psi(m)^{*} \, d\tau \neq 0 \qquad (2.36)$$

for a transition between the vibrational states represented by $\psi(m)$ and $\psi(n)$. By anology with the case of infrared absorption, therefore, a fundamental transition is inactive in Raman scattering unless its vibrational representation contains the same symmetry species as at least one of the components of the polarisability tensor (or one combination of these components).

Like the corresponding conditions for infrared absorption, these selection rules are "restricted" in the sense that their derivation is based on certain assumptions, in particular, that the vibrations of a molecule are simple-harmonic. Relaxation of the simplifying assumptions means a change in the nature of the potential energy and hence also in the wave equation and its solutions. For example, the eigenfunctions associated with anharmonic rather than harmonic vibrations no longer possess the special properties of the Hermite polynomials which form the basis of the restriction of transitions to $\Delta v = \pm 1$ in infrared absorption or in the Raman effect. It is a consequence of anharmonicity that overtones and combination tones of vibrational fundamentals may become active in infrared absorption or Raman scattering although, generally speaking, the 'restricted' selection rules give a fairly good account of the observed spectra.

2.10 Polarisation of Scattered Light

The radiation scattered by a molecule has components in planes parallel and perpendicular to the direction defined by the incident electric vector (see Figure 2.1); in general, the intensities of these two components $I_{\parallel}$ and $I_{\perp}$ are unequal, the ratio $I_{\parallel}/I_{\perp}$ being termed the depolarisation ratio or degree of depolarisation. According to the Placzek theory[37], the depolarisation ratio of Rayleigh scattering emitted in a direction at 90°

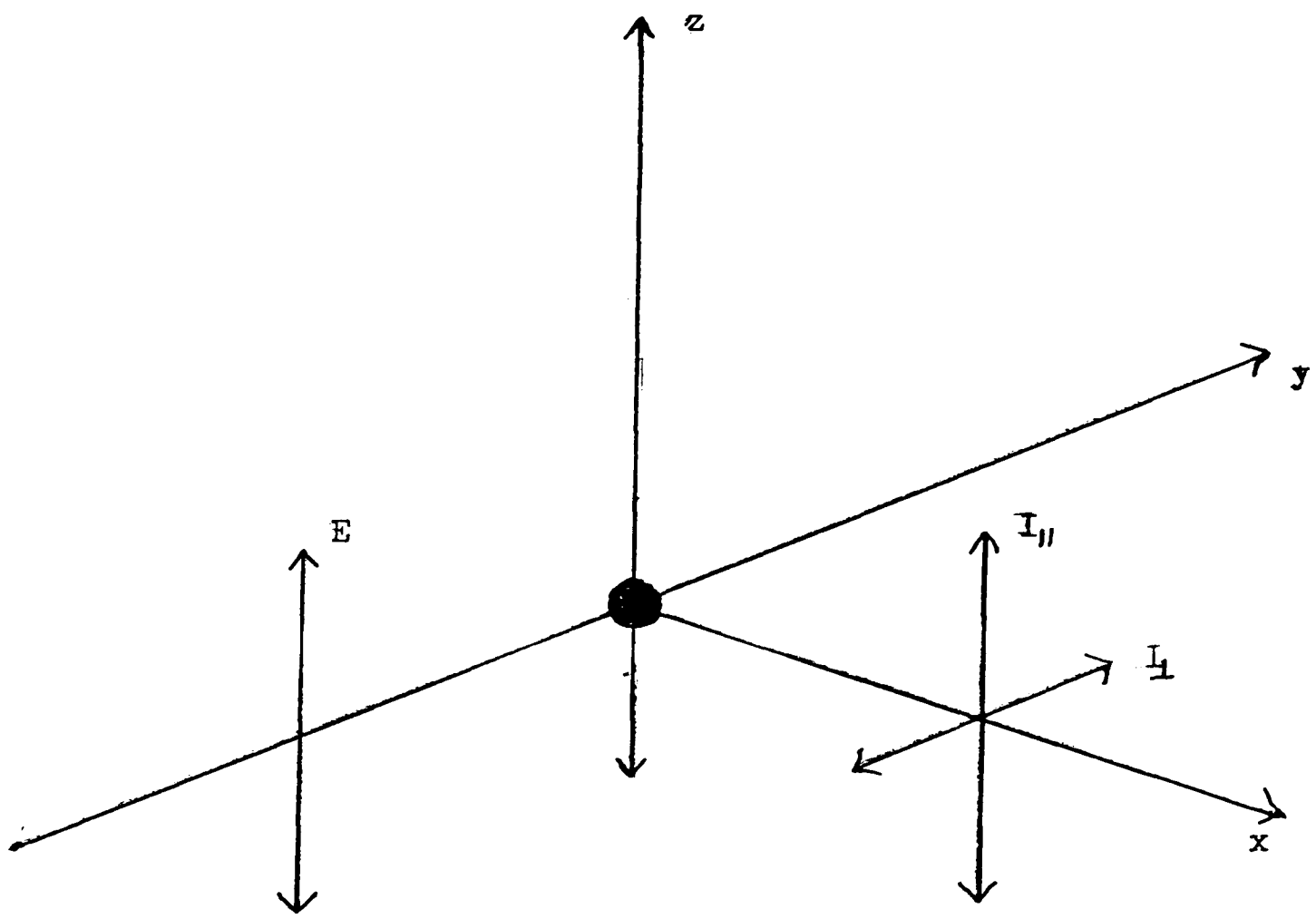

Fig. 2.1. Polarisation of scattered light.

to that of the incident light by a large number of molecules in random orientations is given by

$$\rho_P = \frac{I_{\parallel}}{I_{\perp}} = \frac{3\gamma^2}{45\bar{\alpha}^2 + 4\gamma^2} \qquad (2.37)$$

Here $\bar{\alpha}$ and γ are the mean value and anisotropy invariants respectively of the polarisability tensor, their definitions being as follows:

$$\bar{\alpha} = \tfrac{1}{3}(\alpha_{xx} + \alpha_{yy} + \alpha_{zz}) \qquad (2.38)$$

and

$$\gamma^2 = \tfrac{1}{2}\left[(\alpha_{xx}-\alpha_{yy})^2 + (\alpha_{yy}-\alpha_{zz})^2 + (\alpha_{zz}-\alpha_{xx})^2 + 6(\alpha_{xy}^2 + \alpha_{yz}^2 + \alpha_{zx}^2)\right] \qquad (2.39)$$

A similar expression applies to the depolarisation ratio of Raman scattering emitted under analogous conditions, except that the mean value and anisotropy invariants employed relate not to the polarisability but to the derived polarisability tensor $(\partial\alpha/\partial Q_k)_0$ with components conveniently denoted by α_{ij}'. If $\bar{\alpha}' = 0$, $\rho_P = \frac{3}{4}$ and the scattered radiation is said to be 'depolarised'; if $\bar{\alpha}' \neq 0$, $\rho_P < \frac{3}{4}$ and the radiation is said to be 'polarised'. Group theoretical methods show that the condition $\bar{\alpha}' \neq 0$ for which $\rho_P < \frac{3}{4}$ arises only for vibrational modes belonging to the totally symmetric representation of the molecular point group, so that the degree of depolarisation can be used as a test of molecular symmetry or as evidence for a particular vibrational assignment. At a more quantitative level, polarisation measurements may provide an insight into details of the molecular force field, providing information, for example, about the extent of coupling between totally symmetric normal modes.[40]

2.11 Fluorescence and Resonance Effects

The Placzek treatment shows that, if the frequency of the exciting radiation

ν_0 is far removed from any absorption region of the molecule, the intensity of the Raman scattering is roughly proportional to ν_0^4 [see equation (2.30)]; deviations from this fourth power dependence are an indication that the pre-conditions of the Placzek treatment have lapsed. Thus, when the frequency of the exciting radiation coincides with an absorption band of the molecule under investigation, absorption and re-emission of radiation with a different frequency commonly leads to the phenomenon of fluorescence, in the presence of which the relatively weak Raman scattering may be difficult to detect. As little as 1 ppm of a fluorescent material can seriously affect the observed spectrum. Fluorescence bands are, however, easy to detect, being generally broad and intense and extremely sensitive to variations in the frequency of the exciting radiation.[41]

As the exciting frequency approaches the origin of an electronic transition of the molecule, the Raman lines due to one or more fundamentals show a pronounced enhancement in intensity, a change often accompanied by the development of progressions of overtone or combination bands.[42-44] This so-called resonance Raman effect is also marked by deviations from the dependence of the scattered intensity on the fourth power of the existing frequency. In fact, the following expression has been derived to accommodate the scattered intensity in circumstances such as these:[45]

$$I \propto (\nu_0 - \nu)^4 \frac{(\nu_{eg}^2 + \nu_0^2)^2}{(\nu_{eg}^2 - \nu_0^2)^4} \qquad (2.37)$$

Hence, it appears that, as the frequency difference ν_{eg} between two electronic states approaches ν_0, the intensity of the scattered radiation departs from its approximate dependence on ν_0^4. It is generally observed, however, that the increase in intensity varies from one Raman line to another. With a knowledge of the symmetry properties of the electronic transition, characterised by the frequency ν_{eg}, certain predictions can be made

concerning the changes in intensity,[46] and it has been shown that the lines subject to intensity enhancement as $\nu_0 \rightarrow \nu_{e_g}$ arise from vibrational modes which contribute, via vibronic mixing, to the 'forbidden' intensity of the electronic transition.

One feature which distinguishes resonance Raman from fluorescence effects is the time-scale of the two processes. Fluorescence is an absorption and re-emission phenomenon in which the lifetime of the excited state is about 10^{-7} s; Raman scattering, on the other hand, occurs on a time-scale of about 10^{-15} s. This difference has been used to record the resonance Raman spectra of fluorescent species.[47] One problem which is common to both resonance Raman and fluorescence phenomena is that of sample heating; the heat produced may be enough to destroy a thermally sensitive sample, or to volatilise a matrix if the matrix isolation technique is being employed. This problem may be overcome in some cases by surface scanning of the laser beam over the sample.[48]

Since resonance Raman spectra may be observed at very low concentrations ($\sim 10^{-3}$M), the phenomenon may find increasing use in conjunction with the matrix isolation technique, where the usual problem is one of low Raman intensities. Resonance Raman spectra of matrix-isolated Cl_2^-,[49] O_3^- [50] and NO_2[51] have been reported, for example, and valuable information about anharmonicities of vibrations has been obtained from the overtone progressions in certain of the fundamentals.

Chapter 3

MATRIX ISOLATION: EXPERIMENTAL TECHNIQUES

3.1 Introduction

The principles of matrix isolation have already been outlined in Chapter 1. The use of the technique was originally limited by ready access to suitable cryogenic facilities, but with the commercial development of miniature refrigerators, it has now become a widely exploited method. The extent of current interest in matrix isolation may be judged by the number of books and reviews which have been devoted to the subject.[36, 52-57]

The matrix-isolation technique has been applied in conjunction with a wide variety of spectroscopic techniques, the deposition surface being modified to suit the technique. Thus, alkali halide windows have found widespread use for studies of infrared and electronic spectra; a polished copper or aluminium block has commonly been the deposition surface for Raman, a sapphire rod for esr, and a beryllium disc for Mössbauer studies. The projects to be described in this thesis have been confined to studies of the infrared and Raman spectra of the species concerned.

The essence of the technique is that the species under study is trapped in a large excess of an inert, rigid matrix at low temperatures. The conditions employed lead to considerable simplification and sharpening of the spectral features associated with the trapped molecules. There are three main reasons for these significant improvements: (i) vibrational 'hot' bands are eliminated because of the all but negligible probability of a vibrational transition originating from any but the lowest vibrational level; (ii) rotation of all but the smallest molecules is inhibited by the matrix, leading to sharply defined vibrational bands; and (iii) resonance fluorescence effects, which often mask the Raman spectra of gaseous molecules,[58] appear often to be quenched when the molecules are trapped

in a matrix. The sharpness of the vibrational bands allows the effects of isotopic substitution to be assessed, to striking advantage.

3.2 Generation of Species

The generation and reactions of matrix-isolated species are summarised in Figure 3.1. The methods employed for bringing molecules into a matrix environment generally fall into the following classes:

(a) Trapping from the vapour phase. For stable molecules having a vapour pressure greater than ca 10^{-4} mm Hg at or below room temperature, vapour-phase mixing with the matrix gas, followed by deposition, is a straightforward procedure. In some cases the use of elevated temperatures is necessary, the species being generated by evaporation from an oven or Knudsen cell and the effusing molecular beam caused to co-condense with an excess of matrix gas. High temperature species such as S_2 [59] and Al_2O [60] have been studied in this manner.

(b) Production in a discharge in the vapour phase. An example of this method is provided by the production of xenon dichloride when a mixture of xenon and chlorine gases is passed through a microwave discharge prior to deposition on a surface cooled to 20K.[61] The dangers of this method, however, are illustrated by the fact that the species obtained by similar treatment of a mixture of krypton and chlorine, originally thought to be Cl_3,[62] is now believed to be Cl_3^-.[63]

(c) Co-condensation. This technique, developed by Andrews and Pimentel,[64] entails the co-deposition of a beam of metal atoms with a potential reagent, such as a molecular halide. Hence, for example, radicals such as CH_3 [65] and CCl_3 [66] have been generated by halide-abstraction.

(d) Photolysis. The most fruitful method of producing free radicals and other species of interest has been photolysis in situ using ultra-violet or vacuum-ultraviolet radiation, as in the production of radicals of the type NX (X = H, F, Cl, Br or CN) and OX (X = H, F or Cl)

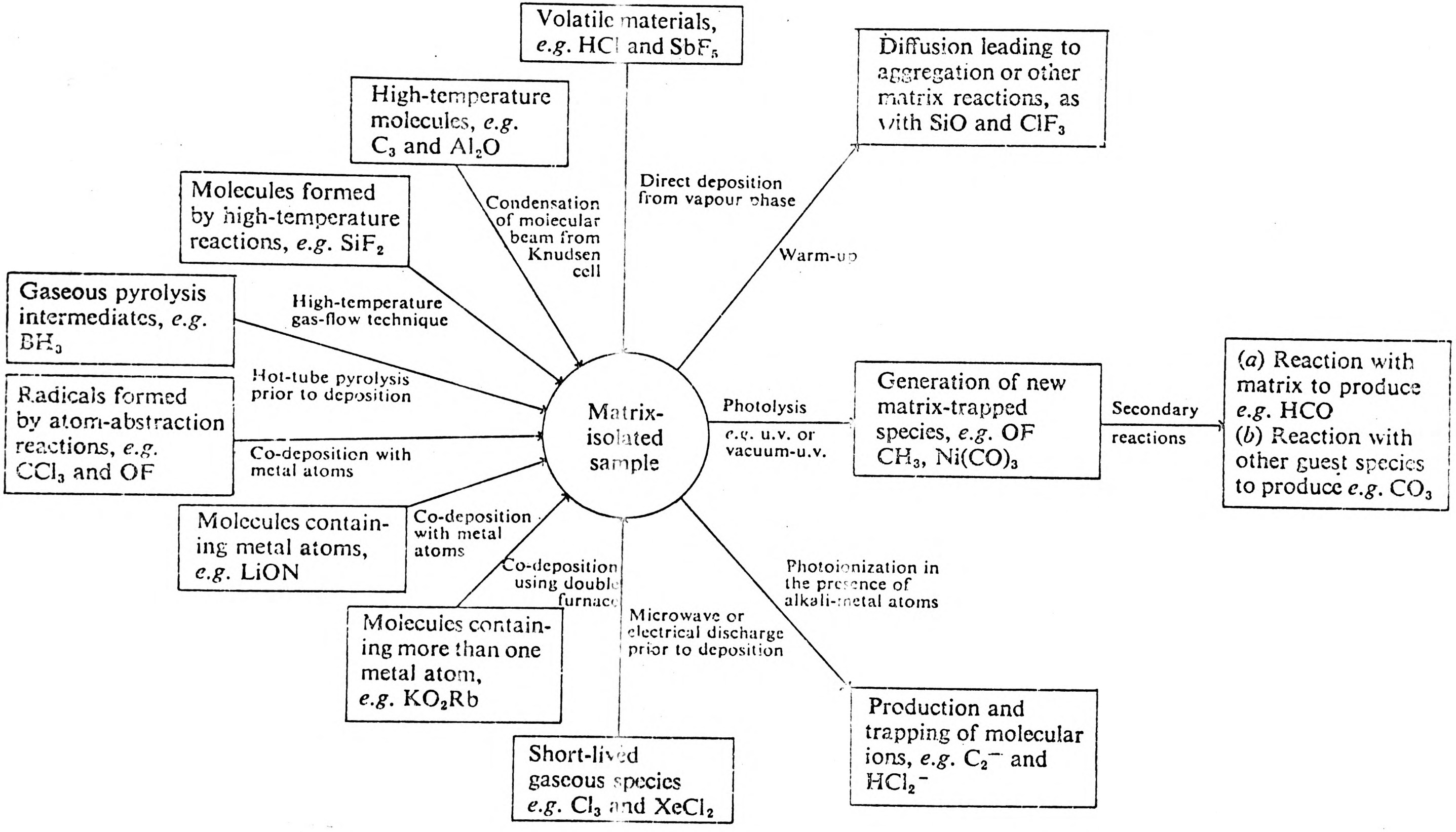

Fig. 3.1. A schematic summary of the types of system studied by matrix isolation.

from the parent molecules XN_3 and OX_2 respectively. The success of this method depends on the coincidence of the frequency of the photolysing radiation with an absorption band of the parent molecule, on the condition $h\nu \geqslant D(X-Y)$ if the fission of a bond X-Y is to occur, and on the ability to counteract the 'cage effect' of the host lattice. Possible expedients for coping with the last of these problems include (i) the production of an unreactive fragment which remains trapped in an adjacent matrix site; (ii) production of a fragment small enough to diffuse away from the photolysis site; (iii) stimulation of diffusion by warming the matrix;[67] and (iv) photolysis during deposition of the matrix to take advantage of the greater mobility implied by the act of quenching.

3.3. Conditions of Deposition

The matrix normally obtained by rapid quenching from the gas phase appears to consist of a collection of randomly oriented microcrystallites characterised by weak host-host and guest-host interactions. The actual choice of matrix material is governed by such factors as volatility, inertness, rigidity etc[67, 68] and also by its spectroscopic properties and the nature of the species to be isolated.

The aim of most matrix-isolation experiments is to produce a sample with optimum isolation of the species concerned within the host lattice, which is itself transparent to the radiation used for spectroscopic measurements. For Raman measurements, the latter requirement may be formulated, in part, in terms of the ratio of the intensities of the inelastic (Raman) and elastic (Rayleigh and Tyndall) scattered radiation. In addition, the matrix material should itself be relatively free from Raman scattering, although such scattering from materials such as nitrogen and methane can prove useful for the purpose of alignment of the sample with respect to the incident radiation and spectrometer optics. The scattering of radiation

is less of a problem with infrared studies, since the particle size of the microcrystallites is then small compared with the wavelength of the radiation used.

In practice, the requirements of isolation and transparency tend to be mutually incompatible, and a balance has to be sought between the experimental factors which may be varied in order to achieve the best compromise. These factors are as follows:

(a) The deposition rate. This affects both the degree of isolation and the transparency of the matrix. Deposition rates are typically in the order of 1-5 mmol of matrix gas per hour, with deposition times of several hours; an alternative to this "slow spray-on" (SSO) method is the "pulsed matrix isolation" (PMI) technique, in which the sample is deposited in a matter of minutes in a series of pulses each involving a volume of perhaps 10-20 cm^3 of gas at a pressure in the order of 10-20 cm Hg.[69,70] This leads to a better degree of isolation than slow spray-on [71] and to more transparent matrices, probably because of local seeding and crystallising effects, but is applicable only in those cases where the species to be isolated is sufficiently volatile to allow pre-mixing with the matrix gas.

(b) The deposition temperature. The sample must normally be condensed rapidly enough to restrict diffusion of molecules during condensation and held at a temperature low enough to inhibit subsequent diffusion of the trapped species. A general, empirical rule is that the deposition temperature should be appreciably less than half the melting point (Tm/K) of the matrix material.[68] It is often found that deposition at a temperature slightly higher than the lowest attainable improves the transparency of the matrix, possibly through improved annealing with the elimination of imperfections arising from phase changes within the solid matrix (eg the α-β phase change of

methane at 20.2K[72]).

(c) The matrix ratio. True isolation is likely to be achieved only at high ratios of matrix to solute molecules (M/S), usually greater than 1000:1, but dependent also on the relative sizes of the matrix and solute molecules. At lower M/S ratios, molecular aggregates are likely to be trapped, a condition usually identifiable by the dependence of the measured spectrum on the matrix ratio and by the results of controlled warm-up experiments in which the aggregation of monomeric molecules initiated by diffusion is monitored spectroscopically.

3.4 Matrix Effects

The vibrational properties of a molecule are invariably perturbed by its interaction with a matrix environment, just as solvation modifies the vibrational properties of a molecule with the transition from the vapour to the solution phase. The following effects may interfere with the characterisation of molecular species but at the same time may also bear information about intermolecular forces within the matrix:

(a) Frequency shifts. Vibrational frequencies are subject to matrix shifts which are usually less than 1-2% of the frequency associated with the gaseous molecule, though shifts of up to 10% have been reported for highly polar molecules.[53]

There have been several attempts to give a quantitative account of these matrix-induced perturbations of the vibrational energy levels of a trapped molecule;[68, 73] these have mostly been based on the correlation between the polarisability of the matrix material and the frequency of a particular vibrational mode of the isolated molecule. The intermolecular potential energy, and hence the matrix shifts, may be expressed as the sum of dispersive, inductive, electrostatic and repulsive contributions, and expressions for the various

terms have been derived on a semi-empirical basis; the results of this sort of treatment lend themselves to presentation in the form of so-called 'Buckingham plots',[74] whence the vibrational frequency of the gaseous molecule may be estimated by extrapolation.

In many cases, the measured frequencies of isotopically distinct species have been used to analyse the force field of a matrix-isolated molecule. The matrix shifts are normally comparable in magnitude with anharmonicity corrections, so that the errors introduced by the use of frequencies uncorrected for such shifts are likely to be no greater than those incurred by assuming the force field to be harmonic. In fact, the ratio of the frequencies exhibited by two isotopic versions of a molecule for a particular vibrational mode is usually indistinguishable for the gaseous and matrix-isolated species, so that the methods of normal coordinate analysis, including the isotopic sum and product rules, may be legitimately applied to matrix-isolated molecules. With the aid of the frequencies for two or more isotopically distinct molecules, such methods often allow the possibility of determining certain of the molecular parameters which contribute to the Wilson G matrix, and bond angles, for instance, have thus been deduced for a variety of simple molecules. Where it has been possible to make comparisons between the molecular parameters calculated for gaseous and matrix-isolated molecules, satisfactory agreement emerges, as in the case of SO_2, for which the bond angle of 119° 37' calculated for the matrix-isolated species agrees closely with the value of 119° 19' obtained from the microwave spectrum of the gaseous molecule.[75]

(b) Molecular distortion. Both positive and negative matrix shifts are observed, and there is substantial evidence to suggest that the shift tends to be more positive for low-frequency bending modes than for

the higher frequency stretching modes of a particular molecule. This observation has been rationalised[76] in terms of the incompatibility of the guest molecule with the matrix cage, those internal coordinates associated with low force constants being most likely to be found in a 'tight cage' as the molecule seeks out the most economical way of accommodating itself in the space available. The principal effects of such distortions are frequency shifts and variations in the relative intensities of the vibrational bands, but it is conceivable that the symmetry of the trapped molecule may also be lowered, leading to changes in the selection rules and in the degeneracy of particular modes.

(c) Matrix splitting. It is often found that a multiplet is observed where only a single band is expected; this may arise from different orientations of the guest species within a particular matrix cage, or from the population of more than one type of cage from the range of opportunities offered by substitutional, interstitial and dislocation sites within the matrix. Changes in either of these circumstances result in slight differences in the intermolecular forces between the guest species and its environment which may manifest themselves in discernible perturbations of the vibrational energy levels of the guest species. In addition, the degeneracy of certain vibrational modes may be lifted by the symmetry of the matrix site; again, perturbations by the proximity of another guest molecule may be sufficient to produce observable differences in the vibrational frequencies of the trapped molecule. In practice, the various mechanisms of matrix splitting may be distinguished by studying the effects of diffusion and of systematic variations of the matrix material and matrix ratio.

(d) Molecular orientation. The possibility of matrix splitting arising from different orientations of the guest molecule within the matrix

cage has already been referred to; in some cases, for example that of NF_2,[77] esr studies have provided evidence that the guest molecules actually adopt preferred orientations relative to the trapping surface, particularly in less rigid matrix supports such as neon. This effect is particularly significant in relation to the interpretation of polarisation measurements involving the Raman scattering due to matrix-isolated molecules for which a random orientation has usually been assumed, though not proved. A possible method of testing whether the isolated molecules are randomly oriented is to measure the depolarisation ratio as a function of the angle of incidence of the laser beam with respect to the deposition surface.[19]

3.5 Application of Raman Spectrometry to Matrix Isolation

Studies of the Raman spectra of matrix-isolated species were rather slow to develop in comparison with those involving the more sensitive technique of infrared spectroscopy, but preliminary experiments reported in 1971[78-80] established the feasibility of such studies, showing, for example, that as little as 1 ppm of carbon disulphide could be detected in a carbon dioxide matrix. Raman spectroscopy possesses a number of advantages over other methods of investigating matrix-isolated species: for example, almost the entire energy range of vibrational transitions can be covered in a single scan without the need to change the optics of the spectrometer, and, in contrast with infrared studies, there is no problem of interference from atmospheric carbon dioxide or water vapour. In addition, there is the opportunity of observing totally symmetric modes, which are commonly seen as the strongest bands in the Raman spectrum while being weak or even inactive in infrared absorption. This often leads to a fuller knowledge of the vibrational properties of a matrix-isolated molecule and to a better definition of the molecular force field. Other advantages of the technique include the possibilities of testing the uniformity of a matrix by focussing the incident laser beam on different regions of the deposit,

and of carrying out polarisation measurements (q.v.).

Apart from the difficulties associated with the inherent weakness of the Raman effect, the main problems posed by the application of the technique to matrix-isolated species arise from the photolytic and thermal effects of the laser radiation, from the limited resolution attainable with the relatively large spectral slit widths normally required to achieve an acceptable signal-to-noise ratio, from the optical properties of the matrix, and from fluorescence originating either in impurities or in the matrix-isolated species itself. The optical properties of the matrix are particularly important if spectra of good quality are to be secured, the level of background scattering varying markedly with the nature of the matrix according to whether it is a transparent glass, an opaque film or a microcrystalline solid.

3.6 The Apparatus

The main components of the apparatus used for the present programme of research were common to all the experimental systems studied using the matrix isolation technique.

(a) Cryogenic equipment. All the experiments to be described were carried out using an Air Products CS-202 'Displex' closed cycle refrigerator, which enabled matrices to be deposited and maintained at temperatures as low as 10K. The principle of operation of this unit involves a modified Stirling cycle,[81] in which helium is compressed to ca 330 psi, fed to the expander (Fig 3.2), where it undergoes cooling as a result of the work which it is allowed to do, and then returned to the compressor. The heat of compression is removed by heat exchange with either air or cold water.[82] The temperature of the deposition surface was monitored in practice either by means of a hydrogen vapour pressure bulb, which could be used to measure temperatures in the range 12-25K, or using a

Fig. 3.2. **The Air Products CSA-202 Displex closed cycle refrigeration system. The expander.**

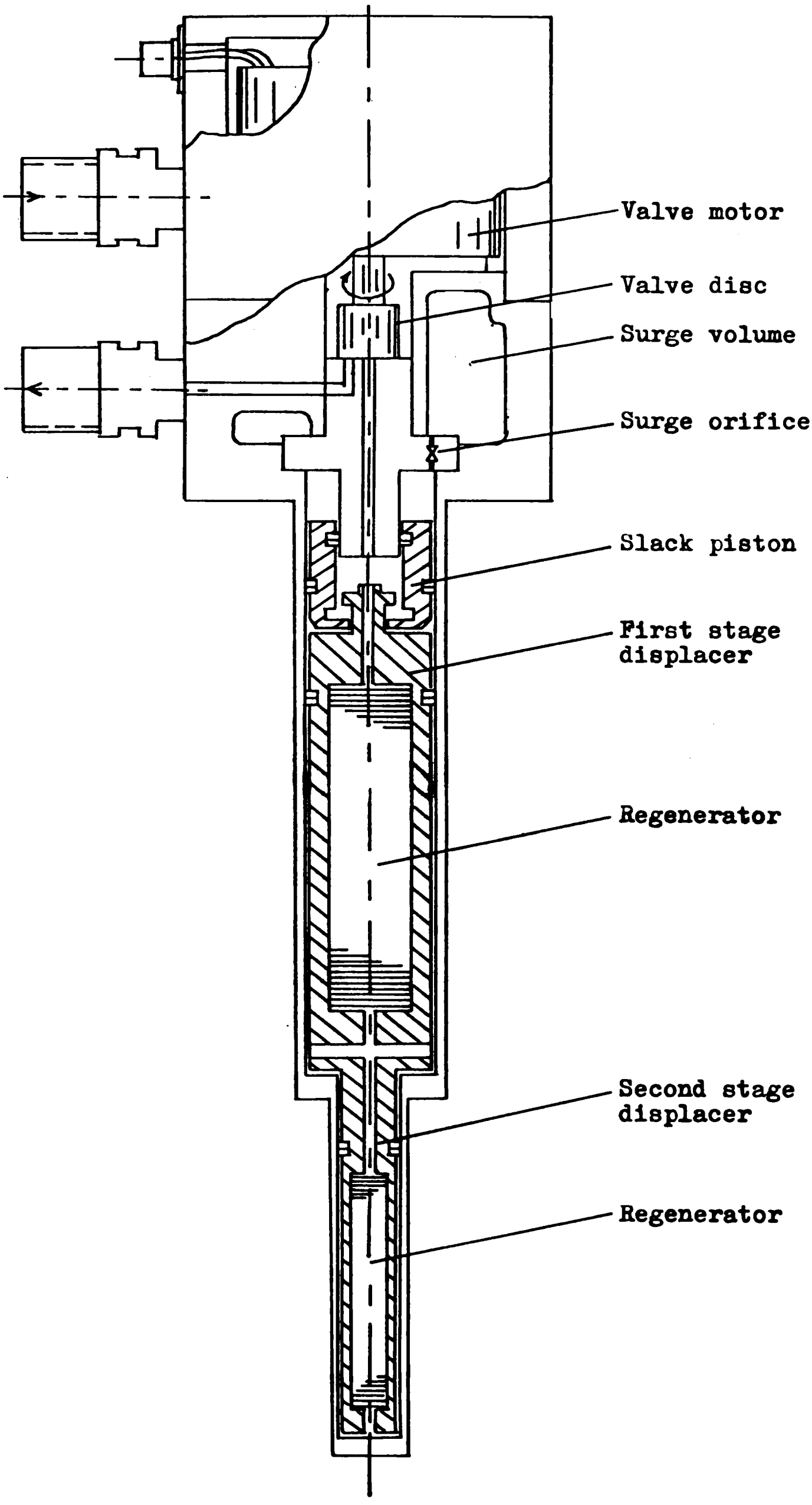

thermocouple of chromel and gold doped with 0.07 atom per cent iron, the output of which was delivered to an Air Products APD-T3 'direct temperature readout'. By balancing the power of a small electrical heater wrapped around the cold end of the refrigerator against that of the refrigeration system, it was possible to provide for variations of temperature and temperature control in the range 10-150K.

The Displex expander was contained in a demountable vacuum shroud (Fig 3.3) in which it could be rotated without loss of vacuum or interruption of the gas flow. For infrared experiments, caesium iodide windows secured to opposite faces of the shroud were used to give spectroscopic access to the central caesium iodide window, whereas in Raman studies the incident radiation and scattered radiation were transmitted through Pyrex windows secured to adjacent faces, the sample being deposited on a polished rectangular block of high purity copper. The shroud was evaculated by an NGN OPA-25 oil diffusion pump ($1\frac{1}{2}$" internal diameter) backed by a PSR-2 rotary pump, the pump unit being connected to the shroud by means of copper tubing and flexible couplings of 1" internal diameter.

(b) The Handling of Matrix Gases. Matrix gases and substances with appreciable vapour pressures at room temperature were handled using a conventional high-vacuum line (Fig 3.4) evacuated by a rotary pump in conjunction with a mercury diffusion pump. Continuous deposition was carried out via a needle valve coupled with an Edwards CG3 Bourdon gauge to control and monitor the flow of gas; in the case of pulsed matrix isolation, the delivery of gas was controlled by two taps separated by a reservoir with a capacity of 20 cm^3. The matrix gases, supplied by the British Oxygen Company, were of 'Grade X' quality, for which a purity of 99.95% or better was claimed; they were used without any attempt at further purification.

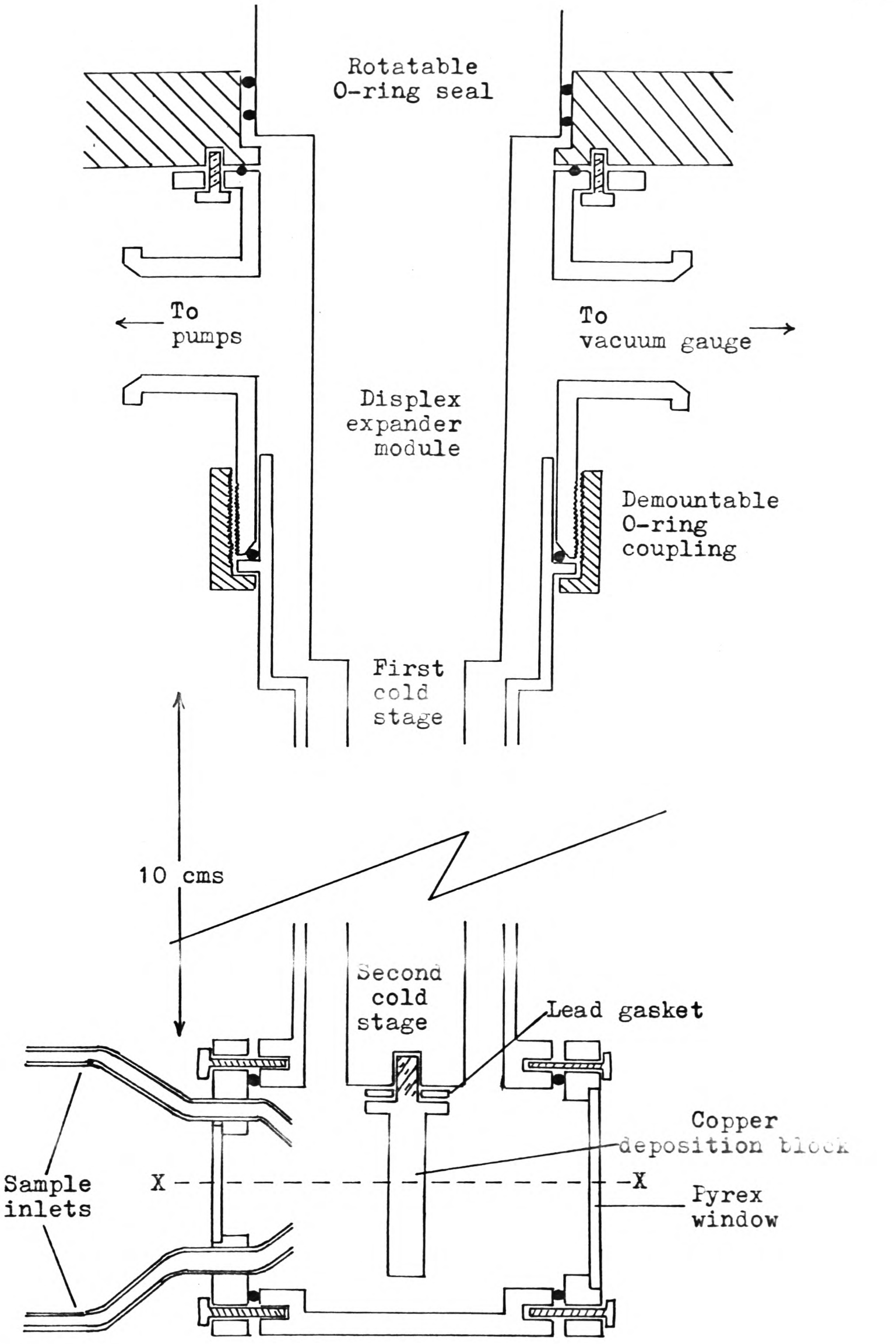

Fig. 3.3. Horizontal section of the vacuum shroud

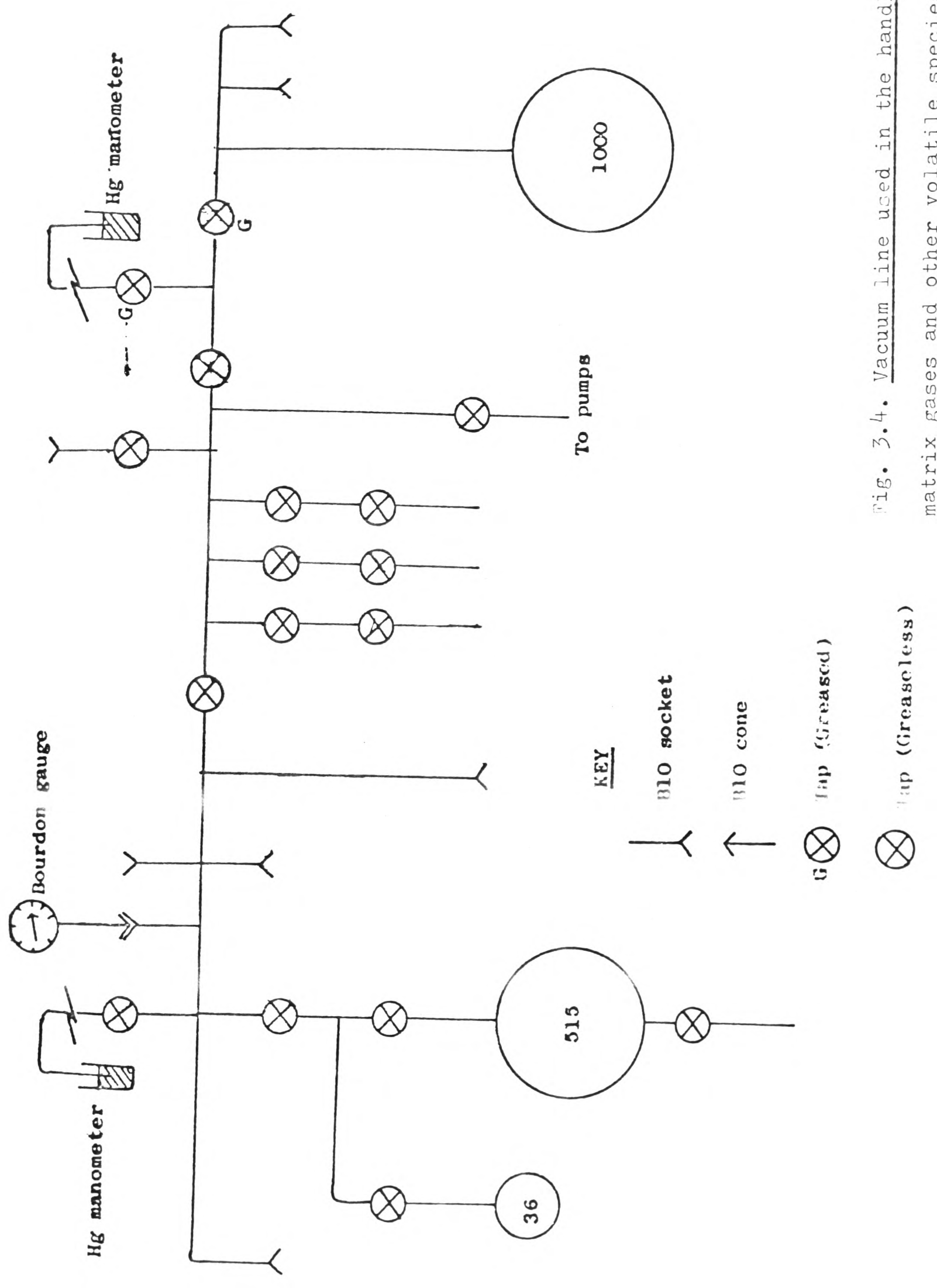

Fig. 3.4. Vacuum line used in the handling of matrix gases and other volatile species.

(c) Furnace Techniques. For the deposition of materials with low vapour pressures at normal temperatures, and for pyrolysis studies, it was necessary to maintain the sample at a temperature somewhat above room temperature and to co-condense the vapour with a large excess of matrix gas introduced from the vacuum line through the needle valve. The sample was contained in a length of Pyrex tubing having an internal diameter of 6 mm connected to the shroud *via* a constriction and heated by a small furnace wound with Nichrome wire. The temperature of the sample was controlled by adjustment of the heating current using a Zenith 'Variac' potentiometer and monitored by means of a copper/constantan thermocouple, the output of which was delivered to an Advance Instruments DMM2 digital multimeter.

(d) Photolytic Techniques. The source of radiation for photolysis experiments was a Hanovia Uvitron 100 high-pressure mercury arc. The thermal effects of the radiation were minimised by the use of a water filter with a path length of 4 cm. Matrices were irradiated *via* a quartz window mounted in one face of the vacuum shroud adjacent to the deposition surface.

(e) Infrared Spectrometers. For infrared studies of matrix-isolated species, the 'Displex' expander unit was supported vertically in the sample chamber of a Perkin-Elmer Model 225 infrared spectrophotometer. This is a double-beam, optical null instrument which covers the range 5000-200 cm^{-1} in four steps, and is capable of a resolution better than 0.5 cm^{-1}. Radiation from a 'Globar' (silicon carbide) source is predispersed by a potassium bromide prism (in the range 5000-450 cm^{-1}) or by scatter plates (below 450 cm^{-1}) before reaching the principal monochromator and is finally detected by a thermocouple. The frequency of the radiation scanned determines which grating of the monochromator is used, as well as the spectral order in which it functions. A dry-air purging system was used to improve the quality of the spectra in regions of atmospheric

absorption, particularly at frequencies below 500 cm^{-1}. Spectra were calibrated by superposition of sharp lines in the vibration-rotation spectra of water vapour, carbon dioxide and ammonia.[83]

Preliminary studies of solids held at 77K using the apparatus described in Section 3.6(g) were carried out with the aid of a Perkin-Elmer Model 457 spectrophotometer. This is again a double-beam, optical null instrument; it covers the range 4000-250 cm^{-1} in three steps, and is capable of a resolution of about 2 cm^{-1} throughout the range. Calibration of the spectra thus obtained was achieved by reference to sharp bands in the infrared spectrum of a polystyrene film.[84]

(f) Raman Spectrometer. Raman studies were carried out using a Spex Ramalog 5 spectrophotometer. In order to investigate the effects of varying the angle of incidence of the exciting laser beam with respect to the matrix deposit, it was appropriate to mount the 'Displex' expander and vacuum shroud horizontally. In addition, the entire system was supported on a movable trolley to allow maximum flexibility in the precise position of the matrix sample.

The optical arrangement of the spectrometer is shown schematically in Figure 3.5. The laser light passes firstly through a beam expander and then through a so-called Claassen filter assembly,[85] a prism monochromator with a narrow bandpass which allows discrimination against unwanted plasma lines. The light is then focussed on the sample by a microscope objective; the collection optics collimate the light scattered by the sample in a direction at 90° to that of the incident radiation and focus it on the entrance slit of the monochromator. The principal monochromator has two holographic gratings each with 1800 lines mm^{-1} set in a Czerny-Turner optical arrangement; the gratings are blazed for highest efficiency near 500 nm and used in their first order. In addition, there is the option of a third

Fig.3.5.. SCHEMATIC DIAGRAM OF THE RAMAN SPECTROMETER

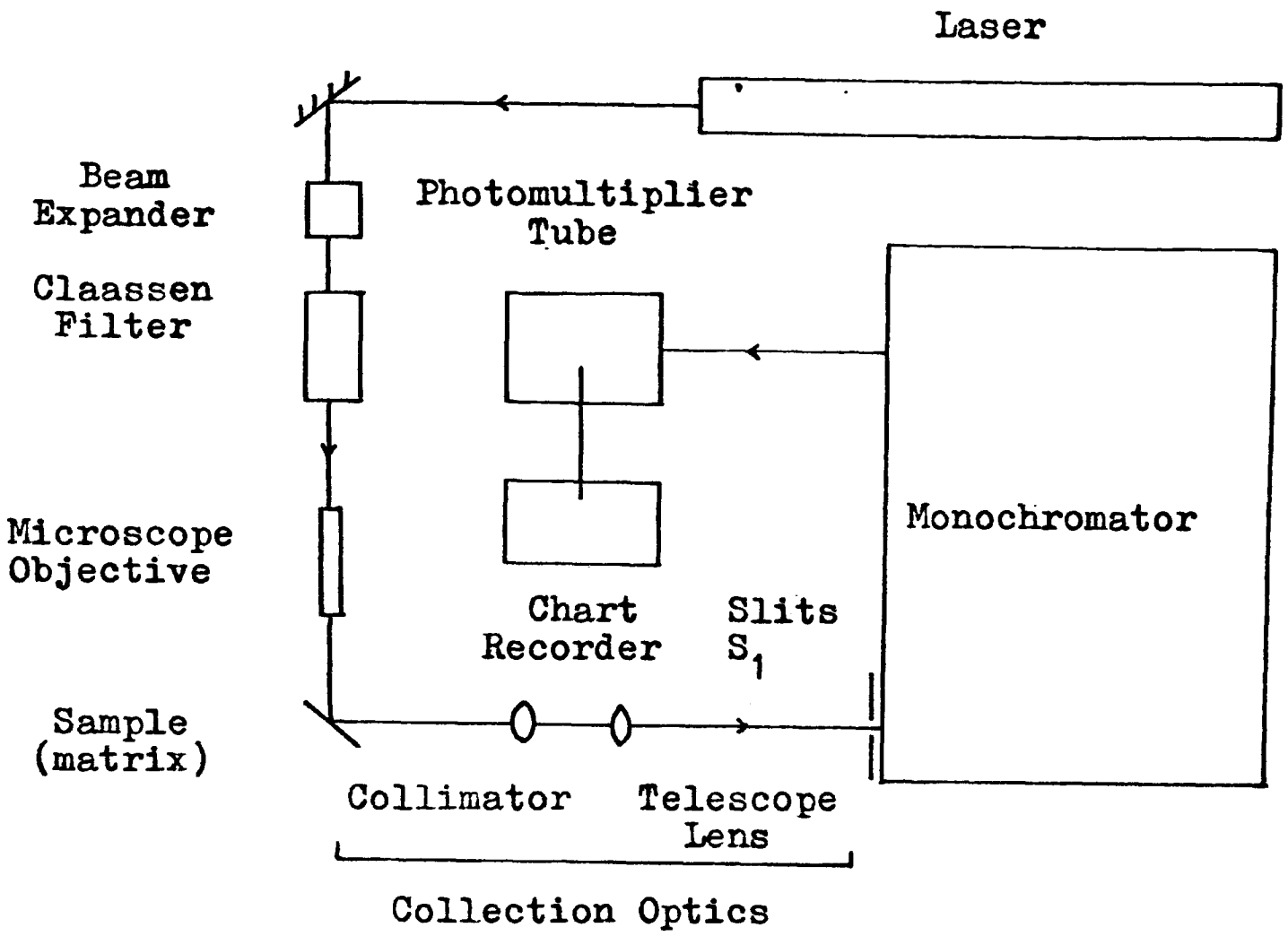

THE DOUBLE MONOCHROMATOR: OPTICAL ARRANGEMENT

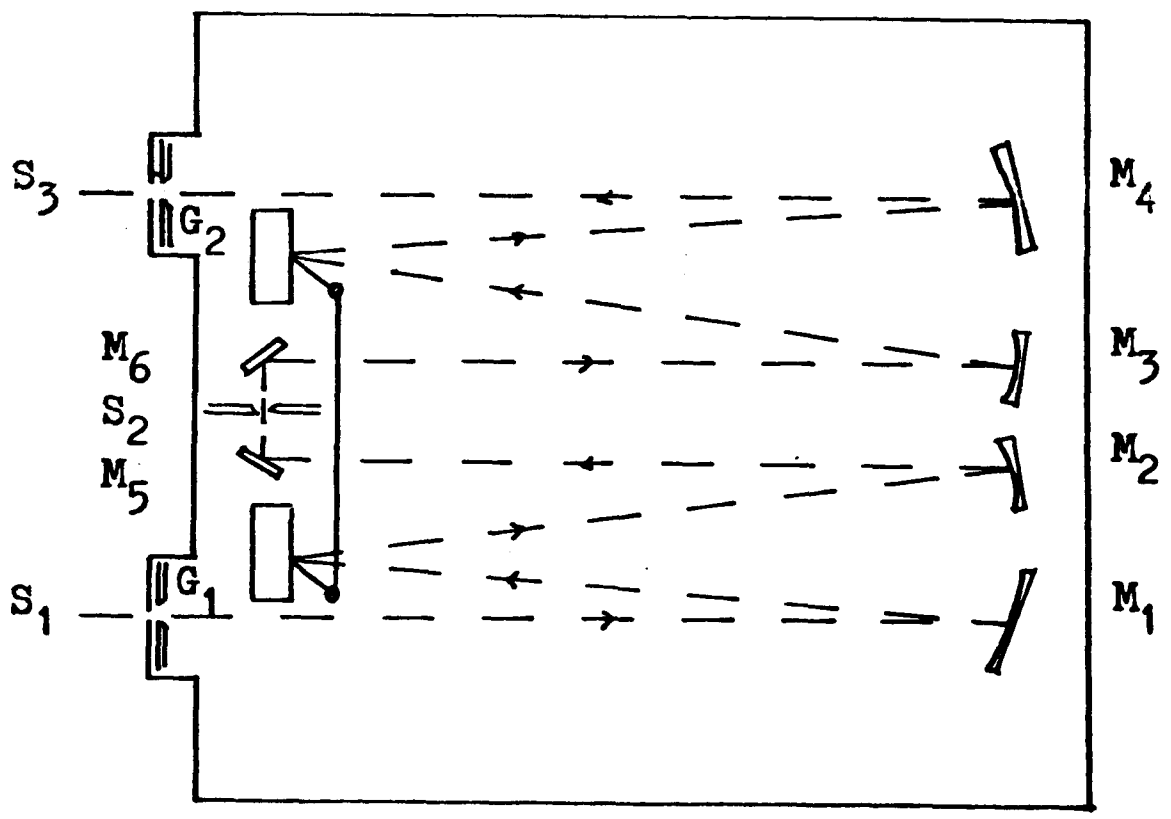

M_n Mirrors
S_n Slits
G_n Gratings

monochromator directly preceding the detection system; this improves spectral quality by reducing the amount of stray scattered light, particularly at frequencies close to that of the exciting line. The scattered light is detected by an RCA C31034 photomultiplier, which is contained in a chamber cooled to -30°C to reduce the 'dark noise' count and so improve the signal to noise ratio. This photomultiplier shows approximately 9% variation in quantum efficiency throughout the visible region of the spectrum. After amplification, the signal from the detector is relayed to a 'photon counting' system, the output being monitored by a chart recorder. Raman spectra were calibrated by superposition of the atomic emission lines of a low-pressure neon discharge lamp.[86]

One of two lasers was used to excite the Raman spectra measured in the course of the present study. The first, a Spectra-Physics Model 165 argon-ion laser, has two principal emissions, at 514.5 and 488.0 nm, each with a maximum power output of about 1.5W; in practice, the emission at 514.5 nm was generally preferred because of its comparative freedom from secondary emission lines. The second was a Spectra-Physics Model 125 helium-neon laser having its principal emission at 632.8 nm. This proved generally to be of limited use in matrix-isolation studies because of its modest power output (in the order of 50 mW) combined with the reduction in intensity of Raman scattering and the reduced sensitivity of the photomultiplier at longer wavelengths. Nevertheless, its use was sometimes enforced by the photosensitivity or absorption exhibited by certain samples with respect to the radiation produced by the argon-ion laser.

(g) Preliminary Solid-Phase Studies. In some cases, preliminary studies of the infrared spectra of solid species held at low temperatures were carried out prior to any matrix-isolation experiments. The apparatus used for these studies, which is shown in Figure 3.6, consisted

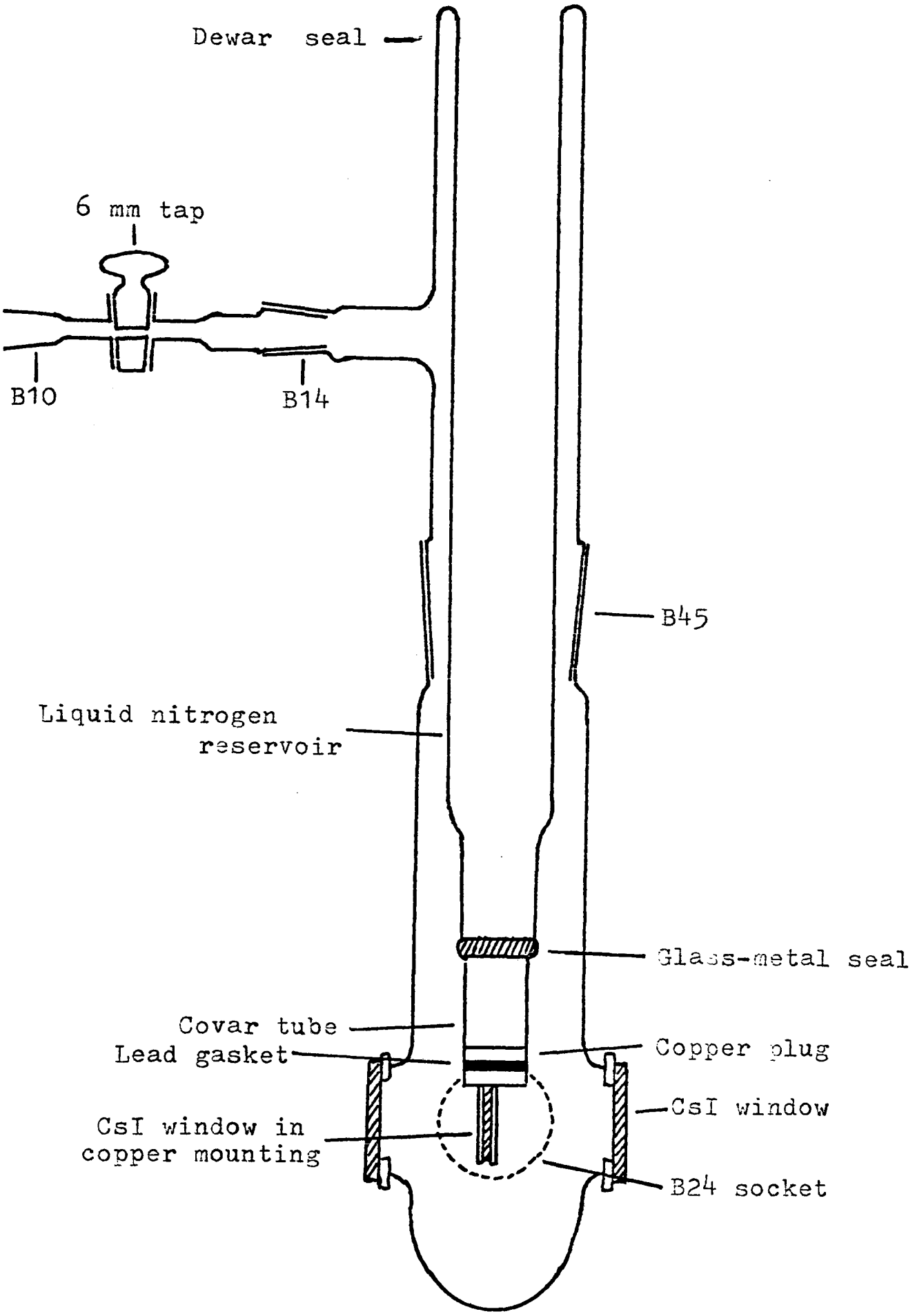

Fig. 3.6. Low temperature infrared cell.

essentially of an evacuable cell having a path length of 10 cm fitted with caesium iodide windows. In the centre of the cell, secured between two copper mounting plates, was a central caesium iodide window on which the solid sample could be condensed. After deposition, this window could be rotated in order to introduce the sample into the beam of the infrared spectrometer. The window could be cooled *via* a copper block mounted at the base of a reservoir capable of holding liquid nitrogen; good thermal contact between the window and the reservoir was ensured by the inclusion of two lead gaskets between the copper block and the mounting plates.

3.7 Experimental Procedure

A matrix-isolation experiment was initiated by cooling of the 'Displex' unit, requiring a pressure inside the vacuum shroud not exceeding *ca* 10^{-4} torr. Within about 45 minutes, the temperature of the cold station of the 'Displex' normally fell to a level where cryopumping caused the pressure inside the shroud to fall to *ca* 10^{-7} torr, before the minimum operating temperature was reached. The temperature of the deposition surface could then be adjusted by balancing the power of the electrical heater against that of the refrigerator itself. The matrix was then formed by either continuous or pulsed deposition, the deposition times for the two processes being in the order of 2–3 hours and 10–15 minutes respectively. Where continuous deposition was employed, the deposition surface was generally 'primed' by condensation of a thin layer of matrix gas prior to deposition of the sample itself. The build-up of the matrix was monitored spectroscopically from time to time by rotating the 'Displex' expander so as to align the deposition surface for spectroscopic measurements and recording the infrared or Raman spectrum of the deposit. When the bands associated with the isolated species had developed sufficient intensity, deposition was halted, and the spectrum was examined in detail; this normally occurred after deposition of a total of 4–6 mmol of material.

It was desirable, though not always possible, to have some knowledge of the matrix ratio used in a particular experiment. Matrix ratios for pre-mixed samples were simply equated with the composition of the gaseous mixture, although this set no more than an upper limit to the ratio since the sticking probability of the matrix gas is invariably lower than that of the less volatile guest species, and may be as low as 15 per cent.[87] Determination of the matrix ratio in a co-condensation experiment proved difficult. Moskovits and Ozin[88] have used a quartz microbalance to estimate the rate of deposition of metal atoms effusing from a furnace. In the present study, however, it was sometimes possible, for substances with a low vapour pressure at room temperature, to estimate the matrix ratio simply by weighing the central deposition block or window before and after deposition for a fixed time in the absence of any matrix gas; the block or window was allowed to warm up to room temperature in an atmosphere of dry nitrogen prior to the second weighing. The amount of matrix gas deposited during the course of an experiment was then estimated by measurement of the pressure differential produced in a known volume of the vacuum line.[8]

Chapter 4

STUDIES OF SULPHUR-NITROGEN SYSTEMS. PART I: DISULPHUR DINITRIDE, S_2N_2

4.1 Introduction

Sulphur and nitrogen form a variety of compounds, whether binary in nature or incorporating one or more other elements as substituents of a sulphur-nitrogen framework. The simplest of these compounds is the diatomic thiazyl radical, SN, which has been detected, for example, by its electronic emission spectrum in a mixture of nitrogen and sulphur vapour when subjected to the action of an electric discharge,[90] and by its photoelectron spectrum.[91] On the other hand, most sulphur-nitrogen compounds favour structures having a cyclic -S-N framework which may be rationalised by the assumption that delocalised π - type interactions play a major part in the bonding.[92] Each sulphur atom is assumed to donate two electrons to the π - system, as in the case of the $S_4N_3^+$ ion (a planar seven-membered ring incorporating an S-S bond linked by a sequence of alternating sulphur and nitrogen atoms[93]), which emerges as a 10π system on the basis of a semi-empirical self-consistent field treatment of the molecular orbitals.[94] Interest in this and other aspects of sulphur-nitrogen compounds may be gauged by a number of general reviews which have been published.[95-99]

The simplest ring system of the type $(SN)_n$ is disulphur dinitride, S_2N_2, formed by passing the vapour of tetrasulphur tetranitride over silver wool at elevated temperatures.[100-104] Crystal-structure determinations involving the dinitride itself[105] and the adduct $S_2N_2\ (SbCl_5)_2$[106] show that the four-membered ring of alternating sulphur and nitrogen atoms is characterised by trans-ring sulphur-sulphur distances of 2.33 and 2.37Å respectively, short enough to imply a bonding sulphur-sulphur interaction in terms of overlapping van der Waals radii (the van der Waals radius for the sulphur atom being 1.85Å[107]). The relative stability of the nearly square-planar S_2N_2 molecule may be related to the fact that the ring has six π- electrons in accordance with the Hückel $4n + 2$ rule;[105] simple Hückel molecular-orbital theory suggests

that the molecule has one pair of electrons occupying a π - type bonding orbital. There have, in fact, been several theoretical studies of this and other sulphur-nitrogen compounds, mainly at the CNDO[109] or Xα[110] level; more recently, an ab initio molecular-orbital study of S_2N_2[111] has led to a minimum energy for a square-planar structure in good agreement with the geometry established experimentally for the crystalline solid. This treatment employed a basis set including 3d orbitals on sulphur; the presence of these was found to be necessary to give a good account of the geometry of the molecule, although their importance has been a matter of some controversy in accounts of sulphur-nitrogen compounds.

The thermal instability exhibited by disulphur dinitride arises partly from dimerisation to tetrasulphur tetranitride, S_4N_4, but more importantly from the formation of the polymeric species $(SN)_x$ - so called 'polythiazyl' - which has recently aroused much interest because of the pronounced metallic character implied by properties such as its electrical conductivity.[112-116] The polymerisation is normally induced simply by allowing the dinitride to warm up to room temperature, but it has been shown that it may also be induced photolytically at temperatures as low as -65°C.[117] A theoretical study of the polymerisation[118] has proposed two symmetry-equivalent reaction modes involving 'one-point cleavage' of the S_2N_2 ring and producing chains related by a centre of symmetry (Fig. 4.1). In the light of such observations, it appeared that a study of the effects of controlled warming on the vibrational spectrum of disulphur dinitride would repay investigation.

The main aim of the present study, however, was to obtain further information concerning the structure of the isolated S_2N_2 molecule and its vibrational properties and to shed further light on the bonding by carrying out a normal coordinate analysis on the basis of the measured vibrational frequencies. Certain other molecules of the type X_2Y_2 are thought to exist in the form of planar rings, notably the alkali halide dimers M_2X_2,[119] the lithium oxide

dimer Li_2O_2,[120] and molecules of the type M'_2O_2 (where M' = Si, Ge, Sn or Pb)[22-25] referred to in Chapter 1. Frequencies of the infrared-active fundamentals of such molecules have been measured; hence partial normal coordinate calculations have been carried out for the alkali halide and lithium oxide dimers assuming a central force field, and for the Group IV oxide dimers assuming a general valence force field.

The infrared spectrum of disulphur dinitride has been reported[121, 122] and interpreted on the basis of a planar rhombic structure with D_{2h} symmetry. There remains some doubt about these assignments, however, with the reporting of no less than five bands widely separated in frequency in the spectrum of the solid compound, as opposed to the three infrared-active fundamentals expected for the isolated S_2N_2 molecule with its assumed D_{2h} symmetry. Previous matrix-isolation studies in this Laboratory[123] have confirmed the assignment of the three infrared-active fundamentals but further investigation was necessary to determine the origin of the other two bands exhibited by solid disulphur dinitride.

Since Raman-active fundamentals have not been observed for any other cyclic molecules of the type X_2Y_2, it was of particular interest to measure the Raman spectrum of disulphur dinitride in order to complete the assignment of frequencies to all six vibrational fundamentals of the molecule, thereby allowing a complete normal coordinate analysis to be undertaken. Earlier attempts to measure the Raman spectrum of disulphur dinitride were frustrated by the thermal instability of the compound.[121] Preliminary studies of the Raman scattering due to the solid and the matrix-isolated molecule carried out previously in this Laboratory[123] met with more success but left open to doubt the assignment of the features observed. One of the main purposes of the present study was to carry out a more thorough and systematic examination, seeking to establish the polarisation properties of the Raman lines and to determine the effects of isotopic substitution at nitrogen in order to

establish conclusively the origin and assignment of the observed scattering.

4.2 Experimental

Tetrasulphur tetranitride was prepared by the formation first of thiotrithiazyl chloride, S_4N_3Cl, from disulphur dichloride and ammonium chloride,[124] followed by treatment of this intermediate with ammonia.[125] The dinitride was then prepared *in situ* by pyrolysis of the vapour of tetrasulphur tetranitride which was passed over heated silver wool. The apparatus for effecting this pyrolysis, illustrated in Figure 4.2, consisted of a simple two stage furnace incorporating a Pyrex glass ampoule approximately 15 cm long and having an internal diameter of 6 mm, connected directly to the vacuum shroud of the matrix isolation assembly *via* a constriction. The ampoule, containing at one end a sample of tetrasulphur tetranitride, was packed with a column 10 cm long of very fine silver wire as supplied by Johnson Matthey Metals Ltd. Pyrolysis temperatures as high as 300°C[100] and as low as 130°C[103] have been reported elsewhere; in the present study the best results were obtained when the silver wool was maintained at a temperature of 180–200°C during deposition. A convenient deposition rate was achieved by vaporising the tetrasulphur tetranitride at 70–75°C (no definite details about the vapour pressure of tetrasulphur tetranitride are available, but qualitative observations have been taken to suggest a vapour pressure of about 1 mm Hg at 130°C[90]). In some experiments, particularly those concerned with the study of 15N-labelled species, it was found more convenient to generate the tetrasulphur tetranitride *in situ* by controlled pyrolysis of thiotrithiazyl chloride, S_4N_3Cl, at 95–100°C.[123]

In order to study the volatile products of pyrolysis, the material effusing from the heated column of silver wool was co-condensed with a stream of matrix gas on a cold caesium iodide window or copper block. The matrix gas – argon, krypton, nitrogen or methane – was deposited typically at a rate of 2 mmol/hr, total deposition times generally being about 2–3 hours. These deposition conditions led to matrix ratios, S_2N_2: matrix gas, in the order

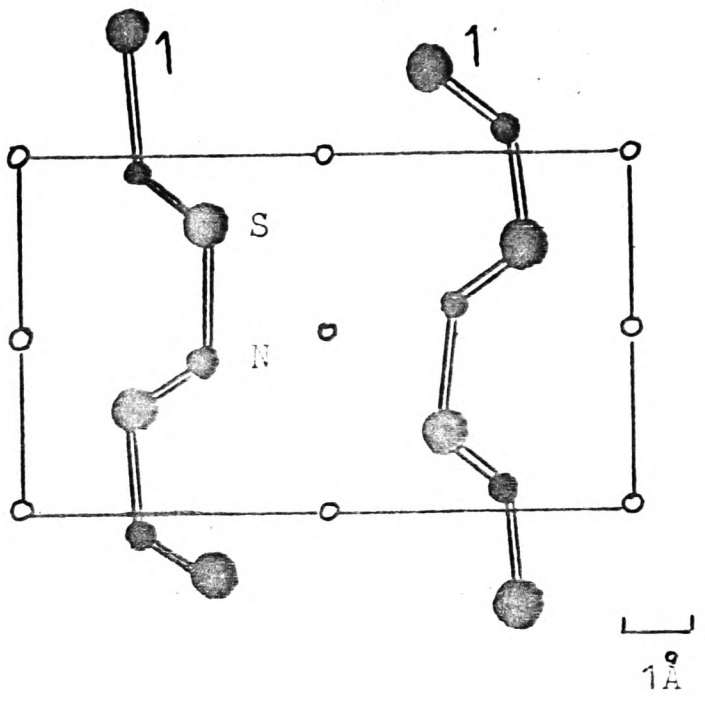

Fig. 4.1. Projection of prevalent chains in $(SN)_x$ showing 2_1 axes (1) and centres of symmetry (•) (ref. 118).

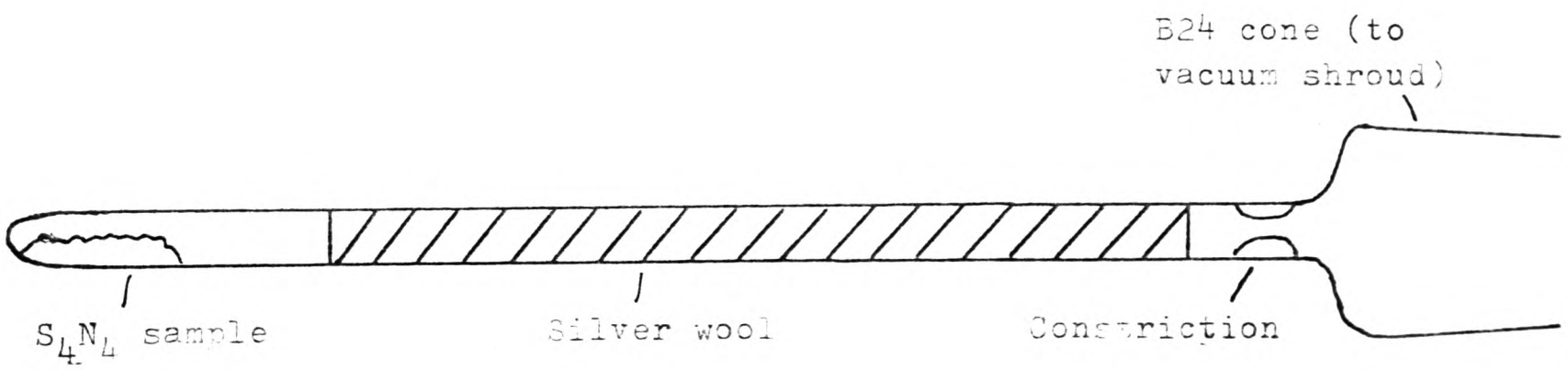

Fig. 4.2. Apparatus for the pyrolysis of tetrasulphur tetranitride.

of 1:800. Preliminary infrared studies of films of solid disulphur dinitride held at 77K were carried out using the apparatus described in Section 3.6(g); deposition times were then in the order of 30-45 min.

4.3 Infrared Spectra

Figure 4.3 illustrates a spectrum typical of those obtained during preliminary studies involving a film of solid disulphur dinitride held at 77K. The frequencies of the absorptions thus observed are listed in Table 4.1, together with those previously reported in the literature.[121, 122] The Table also includes the frequencies of the infrared bands attributed to the S_2N_2 molecule isolated in an argon matrix at 20K; these are derived from the earlier studies carried out by Peake.[123] Selected regions of the infrared spectrum of the matrix-isolated molecule are illustrated, for reference, in Figures 4.4 and 4.5.

The infrared spectrum of polycrystalline disulphur dinitride shows a total of five bands.[121, 122] Of these the two at 660 and 230 cm^{-1} have been shown[123] to be absent from the spectra not only of the matrix-isolated species, but also of the solid condensed from the vapour phase at 20K. In addition, the band at 660 cm^{-1} appears to be absent from the spectrum of the dinitride in the vapour phase and in solution.[121] Of the bands observed in the present study, those occurring at approximately 940, 710, 550 and 340 cm^{-1} originate in traces of tetrasulphur tetranitride,[121, 122, 126] and weak bands near 1000 cm^{-1} exhibited by some samples may be attributable to the polymer $(SN)_x$.[127] The presence of both of these impurities arises presumably either from improperly adjusted conditions of pyrolysis or from thermal annealing of the condensate occasioned, for example, by poor thermal contact between the deposition surface and the refrigerant.

On the evidence of this and previous studies, it appears therefore that the infrared spectrum of the S_2N_2 molecule contains only three absorptions attributable to vibrational fundamentals. It appears too that the solid

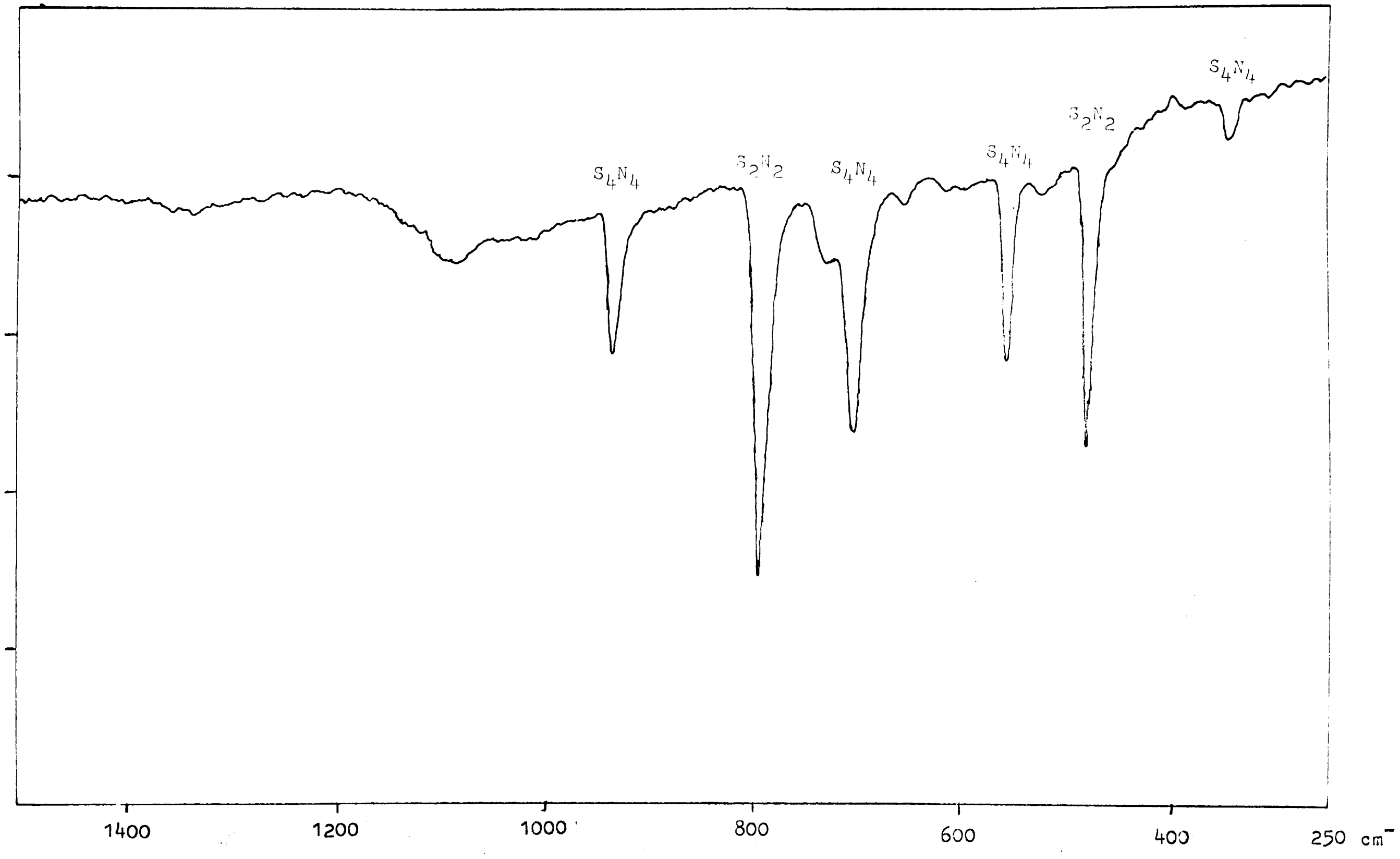

Fig. 4.3. Infrared spectrum observed during preliminary studies of solid S_2N_2 at 77K.

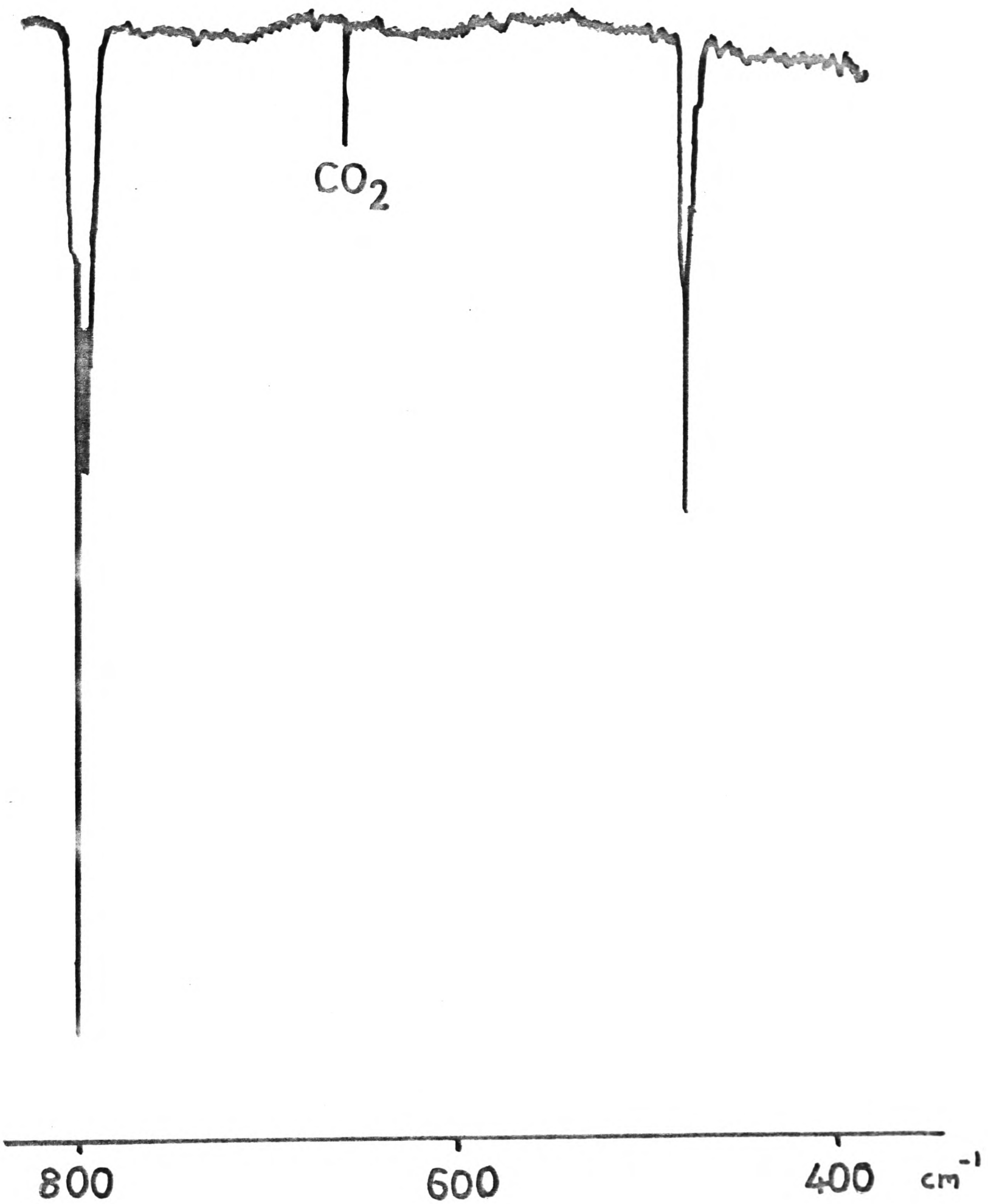

Fig. 4.4. Infrared spectrum of S_2N_2 isolated in an argon matrix (ref. 123)

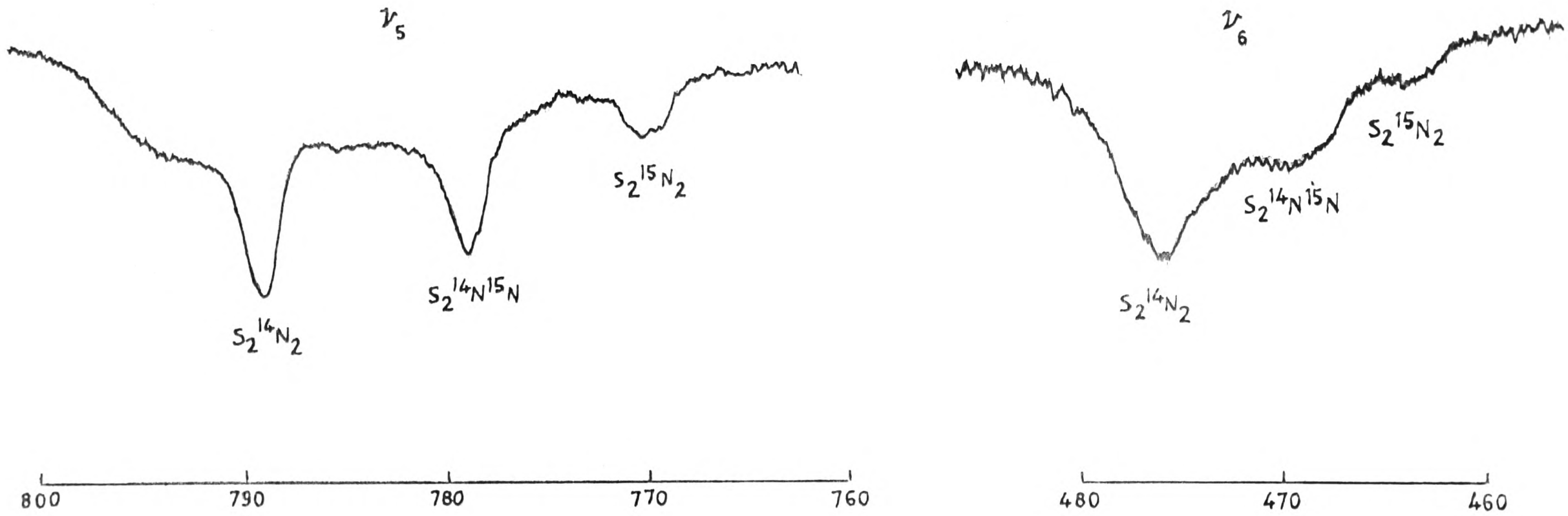

Fig. 4.5. Infrared spectrum of ^{15}N-enriched S_2N_2 isolated in an argon matrix (ref. 123).

Table 4.1. Frequencies and Assignments of the Infrared Bands Observed in Studies of Disulphur Dinitride

Frequency/cm^{-1} [a]				Assignment
Solid,77K (here)	Solid,80K (ref. 118)	Solid,193K (ref. 119)	Ar matrix,20K (ref. 120)	
936				S_4N_4
793	795	785	789.2	$\nu_6(b_{3u})S_2N_2$
705				S_4N_4
	663	665		S_2N_2? [b]
558				S_4N_4
480	474	476	473.7	$\nu_5(b_{2u})S_2N_2$
346				S_4N_4
		221		S_2N_2? [b]
		91	86.0	$\nu_4(b_{1u})S_2N_2$

Footnotes

(a) Frequencies measured to ± 2 cm^{-1} in the present study.

(b) See text.

quenched at 20K has a random arrangement of S_2N_2 units, which are effectively 'self-isolated'. The three bands located at 789, 473 and 90 cm^{-1} in the infrared spectrum of matrix-isolated S_2N_2 have already been assigned by Peake,[123] in accordance with the details given in Table 4.1, to the three infrared-active fundamentals ($b_{1u} + b_{2u} + b_{3u}$) expected for a planar S_2N_2 molecule having D_{2h} symmetry. Such an interpretation is also consistent with the assignment of these bands favoured by Bragin and Evans,[122] and nothing brought to light by the present study has given cause to alter the consensus of opinion.

Further experiments were carried out in which a film of solid disulphur dinitride was deposited on a caesium iodide window at 20K and then allowed to warm up in a controlled manner, in order to investigate the effects of annealing on the infrared spectrum of the solid. Illustrations of the results of these experiments are given in Figures 4.6 and 4.7, which demonstrate the appearance on warming, apparently independently of each other (at approximately 100K and 150K respectively) of the additional bands at 660 and 230 cm^{-1} normally associated with polycrystalline disulphur dinitride. Consideration has been given to a variety of possibilities in seeking to account for these extra bands: (i) that they arise through the reduction in effective symmetry impressed on the S_2N_2 molecule by the site which it occupies in the crystal lattice; (ii) that they result from correlation between the molecules which make up the unit cell of crystalline disulphur dinitride; (iii) that they correspond to translational or librational motions of the S_2N_2 molecules within the unit cell; (iv) that they originate in defects of the crystal lattice; or (v) that they are due to a different phase either of disulphur dinitride itself or of some other compound, eg $(SN)_x$.

The possibility that the extra bands arise through the reduction in effective symmetry imposed on the S_2N_2 molecule by the crystal site has

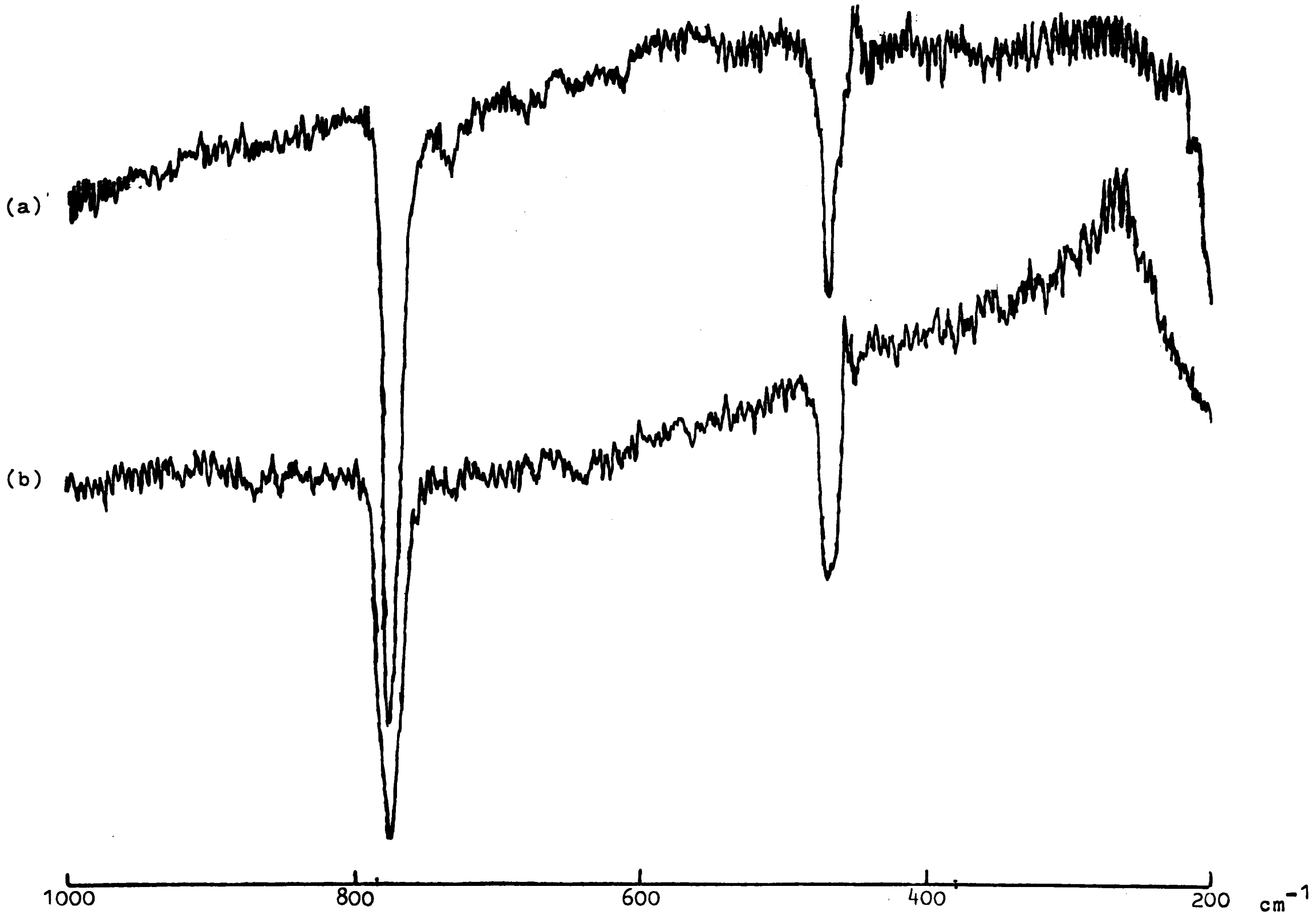

Fig. 4.6. Infrared spectrum of solid S_2N_2 at (a) 30K (b) 70K.

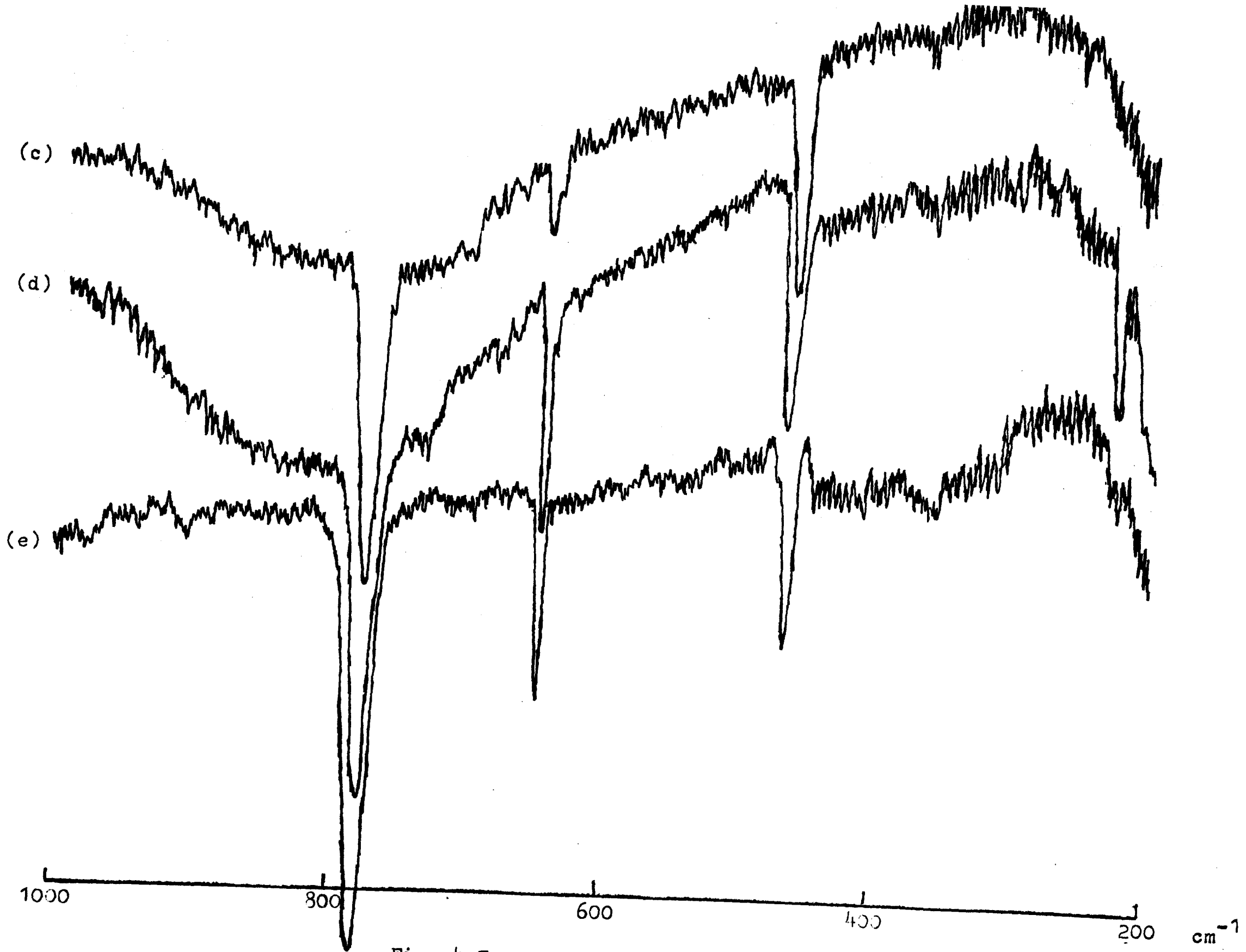

Fig. 4.7. Infrared spectrum of solid S_2N_2 at (c) 120K (d) 160K (e) 200K.

been investigated by the method of factor group analysis.[128, 129] The effective symmetry group in the crystal is C_{2h} (Figure 4.8) and the correlation chart shown in Table 4.2 may be constructed for the internal vibrations of the two S_2N_2 molecules which make up the unit cell. There is clearly no correlation of infrared-active and Raman-active modes, and on this basis there is no reason for expecting extra bands to appear because of the reduction in effective symmetry. In fact, there should be six infrared-active modes for crystalline disulphur dinitride, but unless there is strong correlation between the molecules (ie strong intermolar forces), these will appear as three absorptions each consisting of two virtually coincident components. The fact that the frequencies of the internal vibrations of the S_2N_2 molecule suffer little change with the transition from the solid to the matrix-isolated condition provides a strong argument against the presence of "strong intermolecular forces" in crystalline disulphur dinitride.

On the basis of the foregoing arguments, then, explanations (i) and (ii) seem unlikely. In addition, explanation (iii) is made relatively implausible by the fact that the frequencies of the extra bands are substantially higher than those normally associated with the "lattice modes" of molecular solids.[130] Hence the most likely explanations of those listed appear to be (iv) and (v). Defects simply involving packing of S_2N_2 molecules are unlikely to cause the appearance of the extra bands, but the defects could arise from a change of form of some molecules, possibly as a prelude to polymerisation (Figure 4.9); in this sense there is really no distinction between (iv) and (v).

As noted previously, there are two symmetry-equivalent reaction pathways open to the polymerisation of disulphur dinitride involving 'one point cleavage' of the S_2N_2 ring,[118] and the exact course of the polymerisation may depend on the conditions of thermal annealing. The existence of these

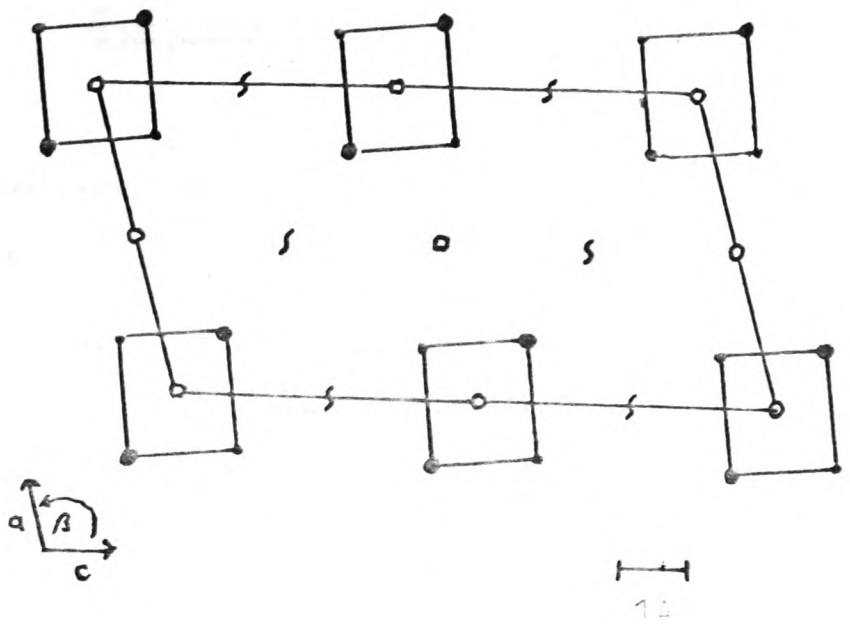

Fig. 4.8. The b-axis projection of the crystal structure of S_2N_2 showing symmetry elements - centres of symmetry (•) and 2_1 axes (§) (ref. 118).

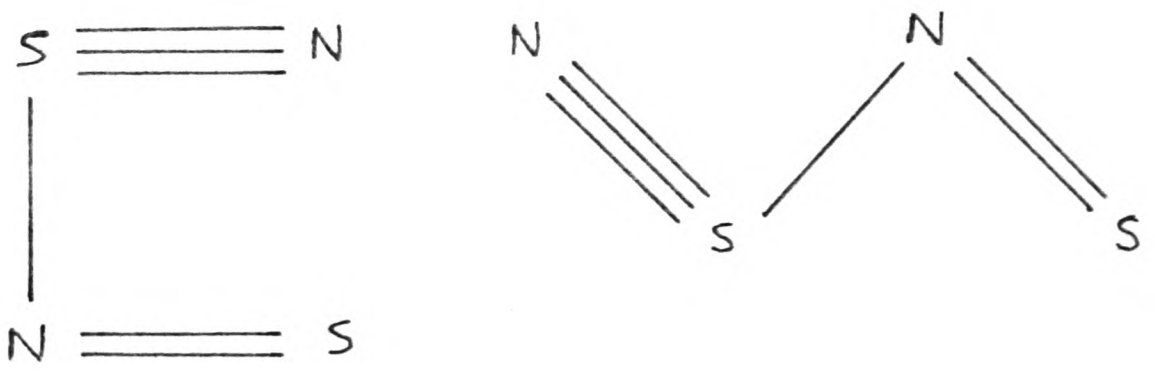

Fig. 4.9. Possible intermediates in the polymerisation of S_2N_2.

Table 4.2. Correlation Chart for the Internal Vibrations of the S_2N_2 Molecules in Crystalline Disulphur Dinitride

Isolated molecule, D_{2h}	C_i, site	C_{2h}, factor group
$2A_g$	$3A_g$	$3A_g$
B_{1g}		$3B_g$
B_{1u}	$3A_u$	$3A_u$
B_{2u}		$3B_u$
B_{3u}		

two distinct modes could well have a bearing on the apparently independent appearance of these two extra absorptions. The band at 660 cm^{-1} possibly reflects the stretching vibration of an open-chain S_2N_2 moiety. The origin of the band at 230 cm^{-1} is rather less obvious, although it would rise from a deformation mode of a unit of the type shown in Figure 4.9.

4.4 Raman Spectra

The Raman spectrum attributed to disulphur dinitride, whether in the form of the solid condensed from the gas phase at 20K, of the annealed solid, or of a matrix-isolated sample, consistently showed just three bands comparable in intensity at approximately 615, 890 and 930 cm^{-1}. Examples of the spectra recorded for the solid at 20K and for S_2N_2 molecules isolated in a solid nitrogen, argon, krypton or methane matrix are shown in Figures 4.10 to 4.14, and the measured frequencies are listed in Table 4.3. In some experiments, the scattering included other bands, either in addition to, or actually in place of, those associated with disulphur dinitride (Figure 4.15). The frequencies of these bands are also included in Table 4.3. Two such bands, at 560 and 720 cm^{-1}, evidently arose from the presence of tetrasulphur tetranitride,[126] while the broad feature at 470 cm^{-1}, often very intense, and a weaker, broad feature at about 670 cm^{-1} are probably due to polythiazyl, $(SN)_x$, the Raman spectrum of which has been reported.[131]

The simplicity of the vibrational spectrum associated with disulphur dinitride both in the solid state and in the matrix-isolated condition, combined with the apparent operation of the mutual exclusion rule governing the activity of vibrations in infrared absorption and Raman scattering, is consistent with a centrosymmetric structure of D_{2h} symmetry for the S_2N_2 molecule. This view is supported by measurement of the depolarisation ratios of the Raman lines due to matrix-isolated disulphur dinitride; the results of such measurements involving a nitrogen matrix are shown in Figure 4.16. Two of the three Raman-active fundamentals associated with an S_2N_2 molecule having D_{2h} symmetry are

Fig. 4.10. Raman spectrum of solid S_2N_2 at 20K.

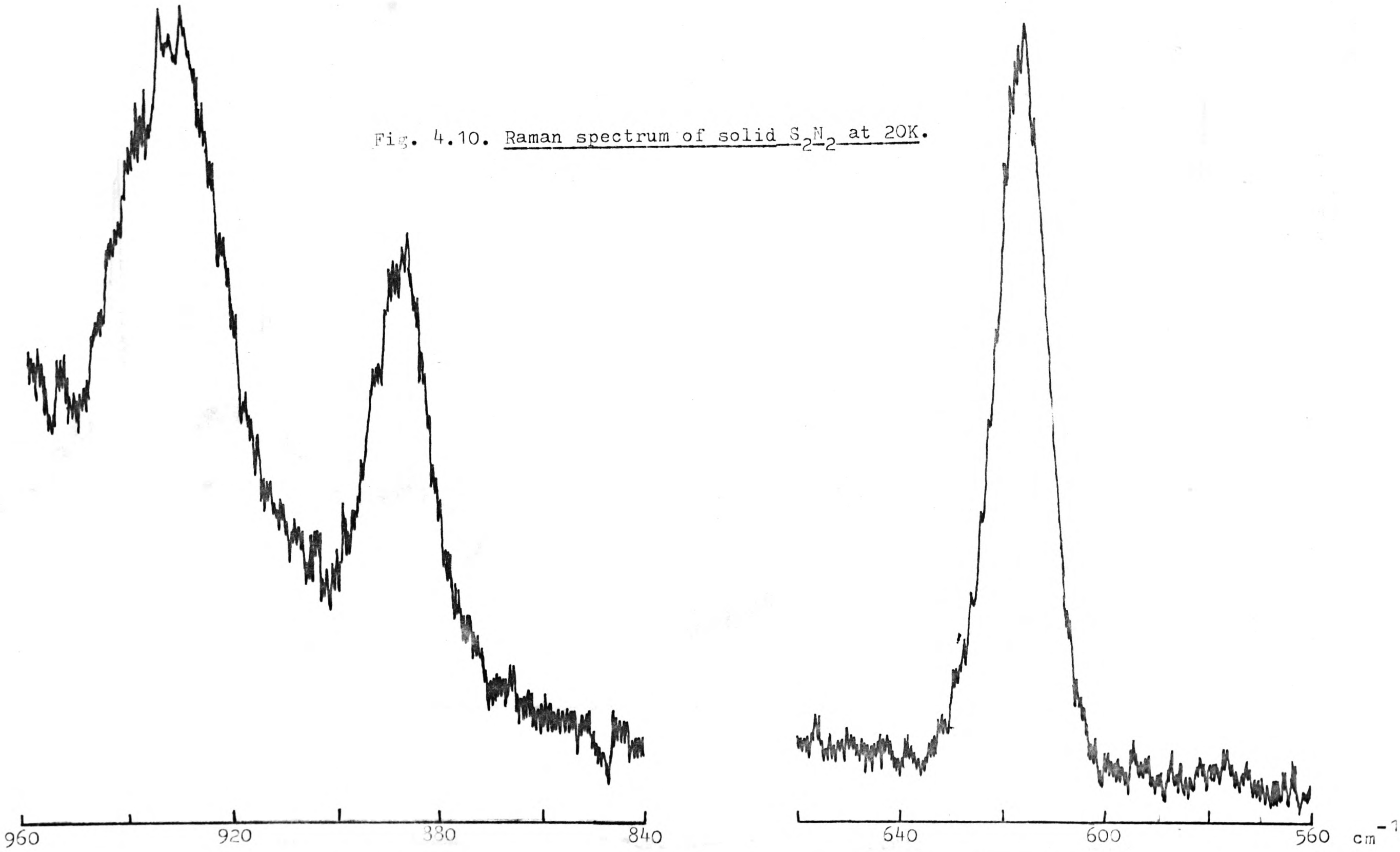

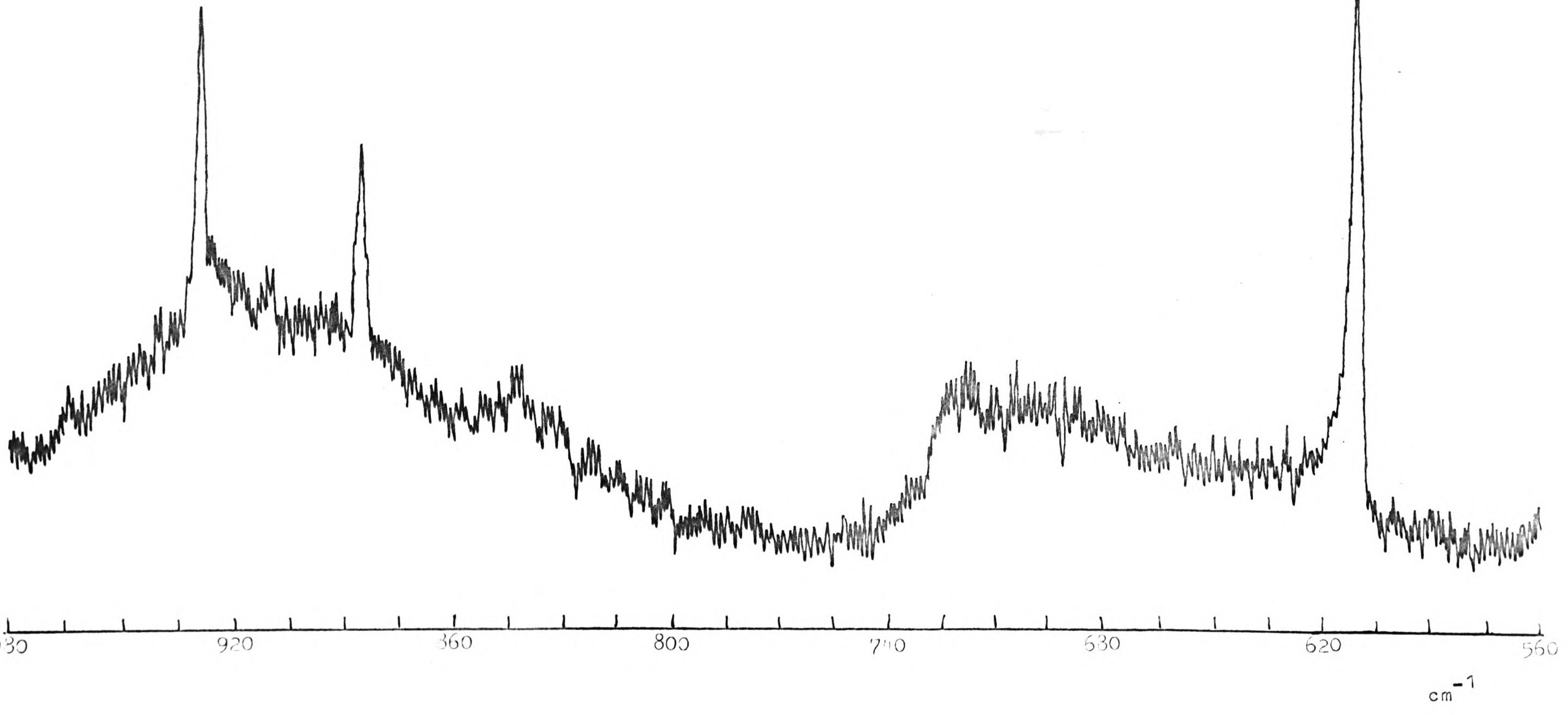

Fig. 4.11. Raman spectrum of S_2N_2 isolated in a nitrogen matrix at 20K.

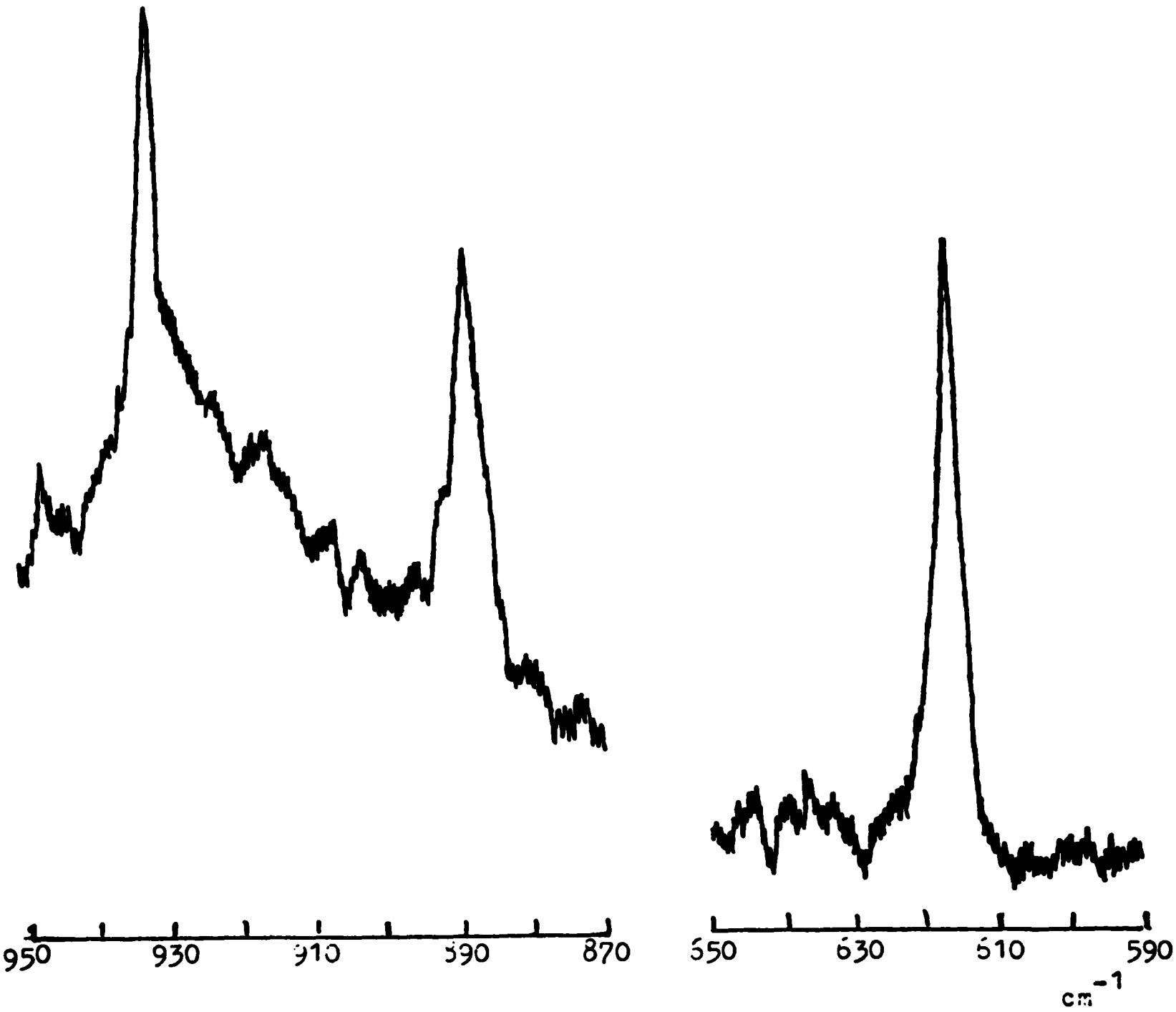

Fig. 4.12. Bands in the Raman spectrum of S_2N_2 isolated in an argon matrix at 20K.

Fig. 4.13. Raman spectrum of S_2N_2 isolated in a krypton matrix at 20K.

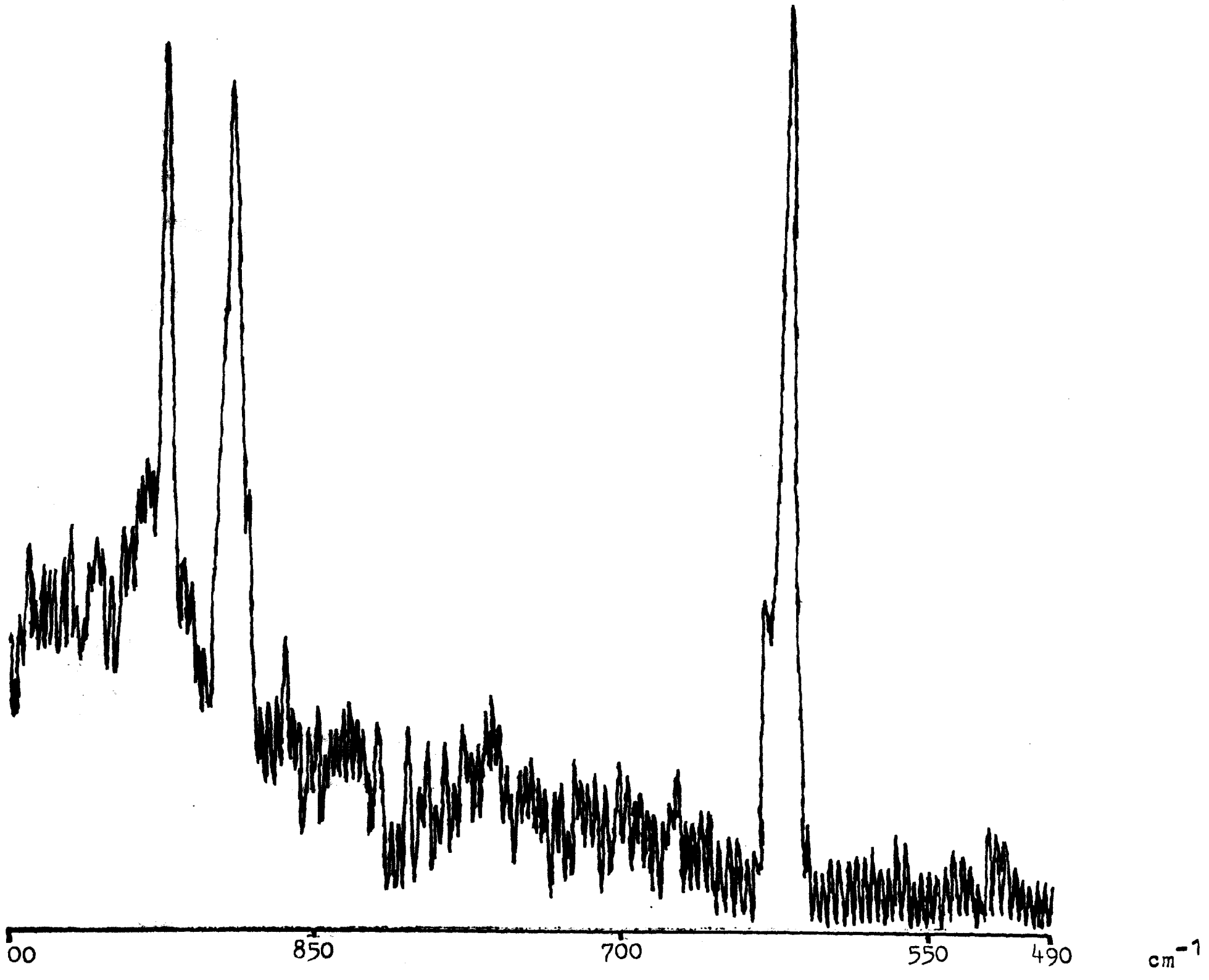

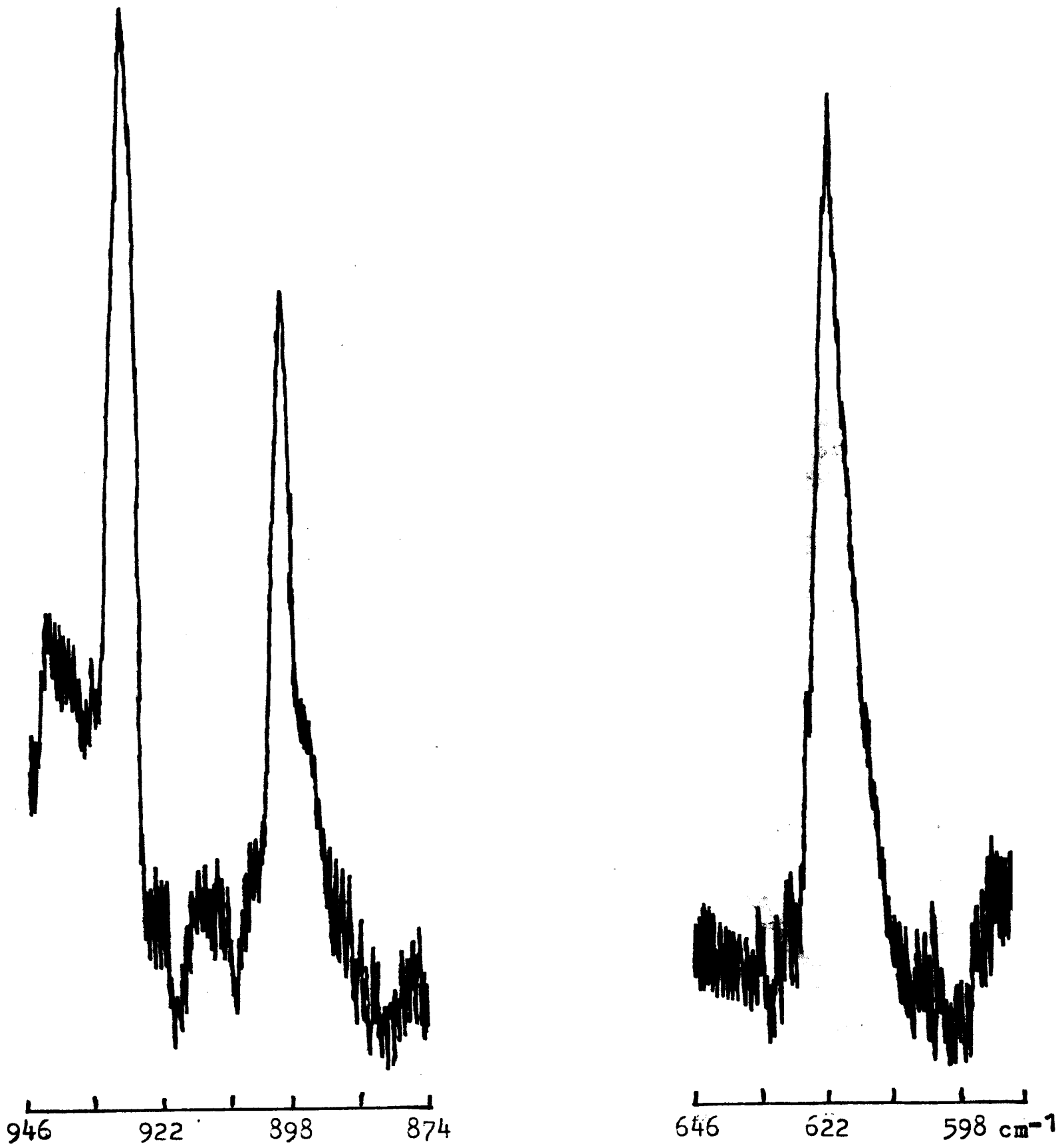

Fig. 4.14. Bands in the Raman spectrum of S_2N_2 isolated in a methane matrix at 20K.

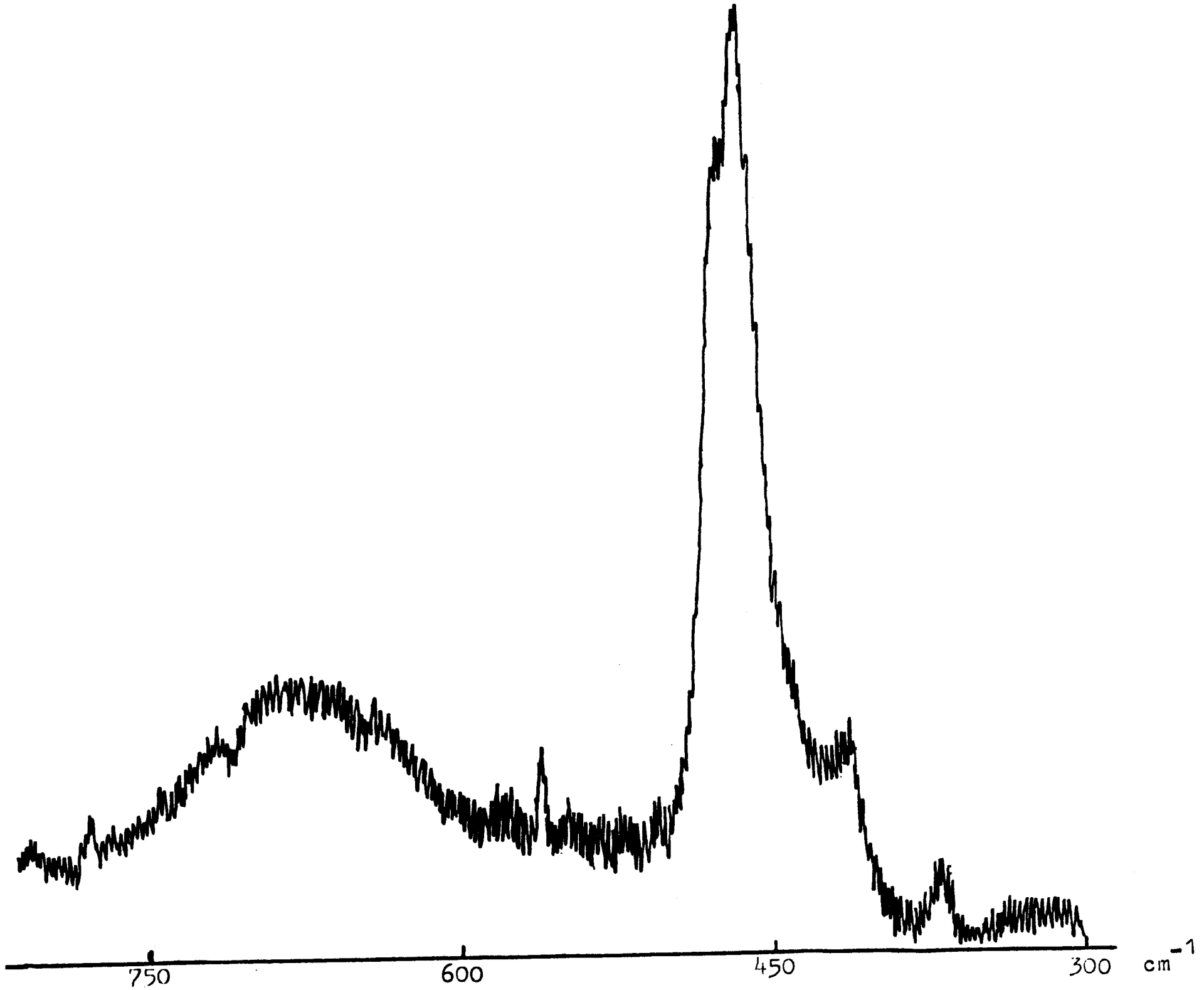

Fig. 4.15. Additional bands (other than those attributable to the presence of S_4N_4) observed during Raman studies of matrix-isolated S_2N_2.

Table 4.3. Frequencies and Assignments of Raman Bands Observed in Studies of Solid and Matrix Isolated Disulphur Dinitride

Frequency/cm^{-1} [a]					Assignment
Solid	N_2 matrix	Ar matrix	Kr matrix	CH_4 matrix	
30K	20K	20K	20K	20K	
	470[b]	470[b]	470[b]	470[b]	$(SN)_x$?
	560[c]	561[c]		560[c]	S_4N_4
615	613	617	617	621	$\nu_2(a_g)S_2N_2$
	670[b]	670[b]	670[b]	670[b]	$(SN)_x$?
	725[c]	724[c]		723[c]	S_4N_4
890	836	839	892	899	$\nu_3(b_{1g})S_2N_2$
928	929	934	926	928	$\nu_1(a_g)S_2N_2$

Footnotes

(a) Frequencies of S_2N_2 bands measured to ± 1 cm^{-1}.

(b) Usually observed in absence of S_2N_2 bands.

(c) Occasionally observed in conjunction with S_2N_2 bands.

Table 4.4. Frequencies and Assignments of Raman Bands Associated with the $S_2{}^{15}N_2$ Molecule in an Argon Matrix at 20K

Frequency/cm^{-1} [a]	Assignment
617	$\nu_2(S_2{}^{15}N_2)$
868	$\nu_3(S_2{}^{15}N_2)$
902	$\nu_1(S_2{}^{15}N_2)$

Footnote

(a) Frequencies measured to ± 1 cm^{-1}.

totally symmetric (A_g) and indeed two of the three Raman lines believed to originate in matrix-isolated S_2N_2 molecules were found to be polarised, a feature clearly in evidence in Figure 4.16. Although the results of polarisation measurements on the Raman spectra of matrix-isolated molecules should be interpreted with caution,[19] the observed Raman lines have therefore been assigned in accordance with the scheme detailed in Table 4.3. The assignment of the scattering at 615 cm^{-1} to the symmetrical in-plane deformation rather than the corresponding S-N stretching mode, despite its being the most intense of the three Raman lines, was found to be necessary in order to solve the secular determinant defining the A_g fundamentals of the S_2N_2 molecule (see section 4.5).

The appearance in the Raman spectrum of two bands in close proximity (near 890 and 930 cm^{-1}) and of almost equal intensity led initially to consideratio of the possibility of Fermi resonance. Such an interaction might involve, on the one hand, an overtone of an unobserved fundamental having a frequency of about 450 cm^{-1} and, on the other hand, a genuine fundamental belonging to the same symmetry class (A_g) also with a frequency close to 900 cm^{-1}. Thus, two alternative sets of frequencies were initially considered for the Raman-active fundamentals, namely 930, 890 and 615 cm^{-1} (in the absence of Fermi resonance) and ca 900, 615 and ca 450 cm^{-1} (if Fermi resonance is assumed to occur).

The eventual assignment of all three lines in the observed Raman spectrum to vibrational fundamentals of the S_2N_2 molecule was based on two pieces of evidence. In the first place, the measured depolarisation ratios already referred to were totally in keeping with such an assignment; in the event of Fermi resonance, all three lines should be polarised. In addition, the Raman spectrum of the molecule $S_2{}^{15}N_2$ isolated in an argon matrix was measured, with the results illustrated in Figure 4.17 and the frequencies listed in Table 4.4. The measured frequency shifts of the three bands

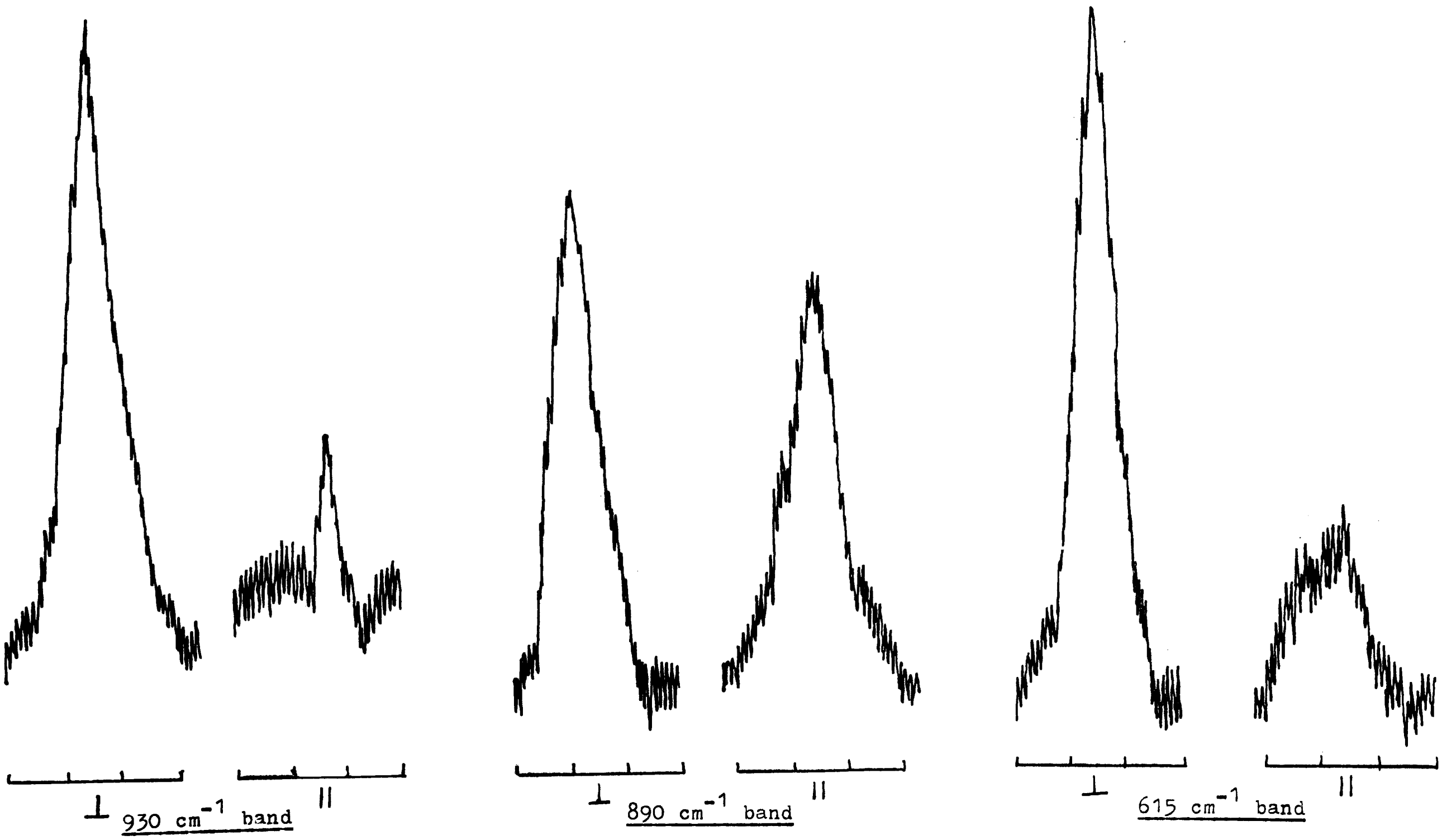

Fig. 4.16. Polarisation measurements on the Raman spectrum of S_2N_2 isolated in a nitrogen matrix.

Fig. 4.17. Raman spectrum associated with the molecule $S_2{}^{15}N_2$ isolated in an argon matrix at 20K.

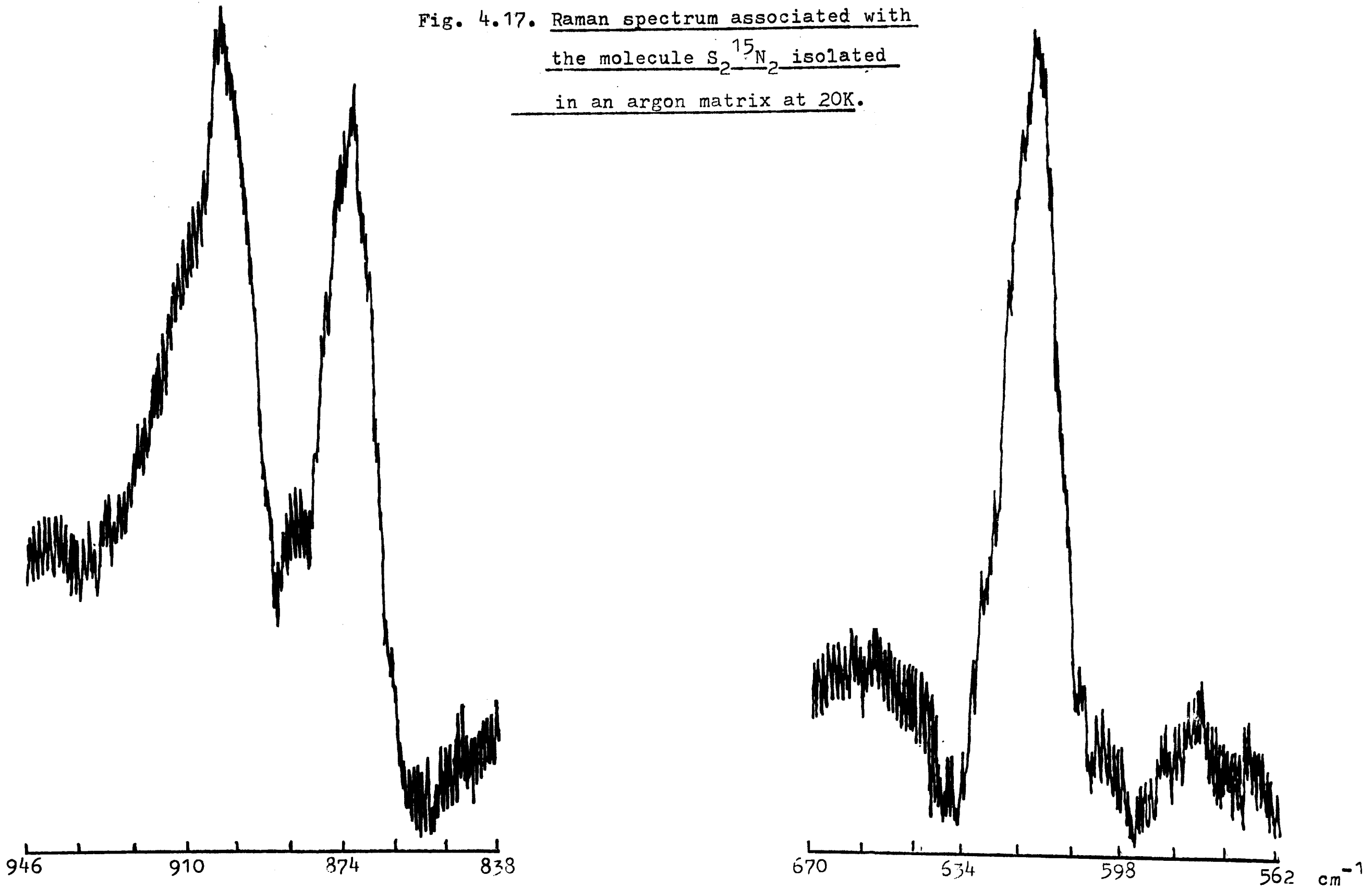

relative to those for $S_2{}^{14}N_2$ corresponded closely to the results of calculations based on the assumption that the bands originate in the three Raman-active fundamentals of the S_2N_2 molecule.

After deposition at 20K of a sample of polycrystalline disulphur dinitride free from impurities, as judged by its Raman spectrum, attention was focussed on the effects of controlled warming on the Raman spectrum of the deposit. No additional bands were observed to develop under these conditions, in marked contrast to the response of the infrared spectrum; the bands due to disulphur dinitride merely decreased in intensity at temperatures above 150K. A very poorly scattering yellow-black deposit was eventually obtained at room temperature, and shown by its infrared spectrum to contain tetrasulphur tetranitride. Again this contrasts with the conclusions drawn from the infrared studies, which gave no evidence for the formation of tetrasulphur tetranitride on annealing. It is possible that annealing follows a different course in the Raman studies either because of irradiation of the deposit by the laser or because of the replacement of caesium iodide as the deposition surface by a copper block.

4.5 Normal Coordinate Analysis

Reference has already been made to the influence of delocalised π-type bonding on the structure of the S_2N_2 molecule (see Section 4.1). The fact that the highest frequency ascribed to a vibrational fundamental of S_2N_2 does not exceed 940 cm^{-1} is in keeping both with this delocalisation and with the cyclic structure of the molecule; by contrast, acyclic S-N species are generally characterised by much higher S-N stretching frequencies (eg 1324 and 1372 cm^{-1} for the gaseous molecules NSCl[132] and NSF[133] respectively). In view of the knowledge already gained about the structure of S_2N_2, calculation of the force constants on the basis of the measured vibrational frequencies may be expected to lead to various interaction terms reflecting the influence of π-type and transannular S-S interactions.

In the first instance, however, the possibility of obtaining an estimate of the bond angle of the matrix-isolated S_2N_2 molecule warrants investigation since it is not obvious that the isolated molecule should have the same geometry as the S_2N_2 molecule in crystalline disulphur dinitride. In the case of the unique b_{1g} mode ν_3, the corresponding blocks of the symmetrised $\underset{\sim}{F}$ and $\underset{\sim}{G}$ matrices each consist of a single element, given in the case of the $\underset{\sim}{G}$ matrix by the expression

$$G_{11} = 2(\mu_N \sin^2 \theta + \mu_S \cos^2 \theta) \qquad (4.1)$$

Here μ_N and μ_S are the reciprocals of the appropriate atomic masses and $2\theta = \angle$ S-N-S. The secular equation therefore becomes

$$2F_{11}(\mu_N \sin^2 \theta + \mu_S \cos^2 \theta) = 4\pi^2 c^2 \nu_3^2 \qquad (4.2)$$

in which F_{11} is the corresponding F matrix element. Hence, if values of ν_3 are known for two different values of μ_N, ie if the frequencies are available for two different isotopic versions of the molecule in which its D_{2h} symmetry is preserved, it is possible to obtain a value for the bond angle at nitrogen. For the S_2N_2 molecule isolated in an argon matrix, the Raman line assigned to the b_{1g} fundamental was found to occur at 889 and 868 cm^{-1} for $S_2{}^{14}N_2$ and $S_2{}^{15}N_2$ respectively. These frequencies lead to a value for $\angle$ S-N-S of $90.9 \pm 1.5^\circ$, which is in remarkably close agreement with the value of 90.42° obtained by X-ray diffraction for the S_2N_2 molecule in crystalline disulphur dinitride.[105] The error limit quoted refers to the continued assumption of simple harmonic motion and not to any allowance for anharmonicity, which is considered unlikely to be important for this particular vibration. Hence it appears that the geometry of the S_2N_2 molecule in the matrix-isolated condition is essentially the same as that in the crystalline solid, lending further support to the view that the molecular units of the crystal are subject to comparatively weak intermolecular forces.

In order to determine a set of force constants for the molecule, it was

necessary to calculate all the elements of the Wilson $\underset{\sim}{G}$ matrix. This calculation requires a knowledge of the bond lengths and bond angles of the molecule, and the values assumed correspond to those determined by X-ray diffraction for single crystals of disulphur dinitride (all S-N bond lengths equal at 1.65A and $\angle$S-N-S = 90.42°).[105] The $\underset{\sim}{G}$ matrix has been obtained in the first place by manual calculation, the method adopted being to choose a set of six internal coordinates (Figure 4.18), express these in terms of Cartesian displacement coordinates by means of the transform màtrix $\underset{\sim}{B}$, and determine the product $\underset{\sim}{B}\,\underset{\sim}{M}^{-1}\,\underset{\sim}{B}^{+}$ (see Chapter 2). The calculation has been repeated using a computer programe GMAT, which is based on the Wilson vector method and again requires for its input the molecular dimensions and a suitable set of internal coordinates; there is extremely close agreement between the results obtained by the two methods. The algebraic expressions linking the internal symmetry coordinates employed to the internal coordinates are listed in Table 4.5. The expressions for the $\underset{\sim}{G}$ matrix elements derived by the first method are listed in Table 4.6 and the numerical values of the elements obtained by the second method appear in Table 4.7.

Once the $\underset{\sim}{G}$ matrix has been evaluated, the next step is to obtain expressions for the elements of the corresponding $\underset{\sim}{F}$ matrix in terms of the molecular force constants. A general valence force field has been chosen initially, and details of the corresponding unsymmetrised and symmetrised $\underset{\sim}{F}$ matrices are given in Tables 4.8 and 4.9 respectively. In fact, the calculations have shown that considerable simplification of the force field is possible since all the observed frequencies are satisfactorily accommodated by a symmetrised $\underset{\sim}{F}$ matrix in which the off-diagonal elements are set equal to zero. On this evidence, the stretch-bend interaction involving the coordinates of the A_g block appears to be negligible.

The calculation of $\underset{\sim}{F}$ matrix elements complying with the observed frequencies has been carried out using a second computer program FGSOL.[134, 135] This

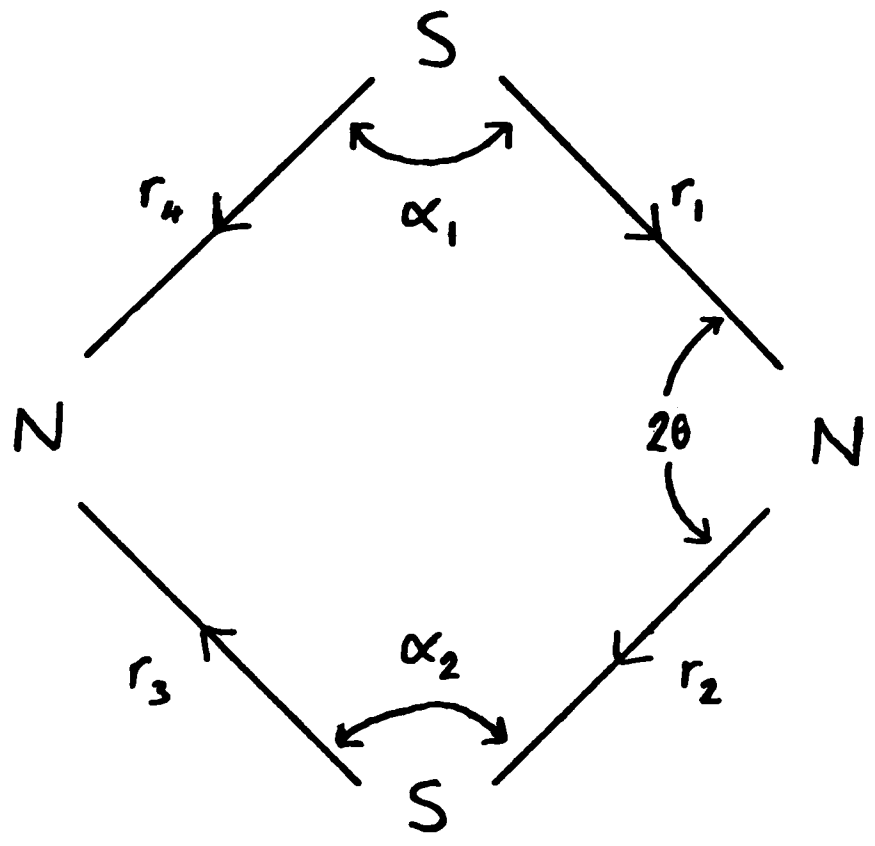

8. <u>Internal coordinates of the S_2N_2 molecule</u>.

Table 4.5a. Internal Symmetry Coordinates Used in the Normal Coordinate Analysis of the S_2N_2 Molecule

(See Figure 4.18 for an explanation of the symbols)

Symmetry block	Coordinate
A_g	$S_1 = \frac{1}{2}(r_1+r_2+r_3+r_4)$ $S_2 = \frac{1}{\sqrt{2}}(\alpha_1+\alpha_2)$
B_{1g}	$S_3 = \frac{1}{2}(r_1-r_2+r_3-r_4)$
B_{2u}	$S_4 = \frac{1}{2}(r_1+r_2-r_3-r_4)$
B_{3u}	$S_5 = \frac{1}{2}(r_1-r_2-r_3+r_4)$ $S_6 = \frac{1}{\sqrt{2}}(\alpha_1-\alpha_2)$

Footnotes

1. The b_{1u} fundamental (the out-of-plane deformation) has been ignored.
2. The redundancy affecting the b_{3u} coordinates is later eliminated as a zero root in the solution of the relevant secular equation.

Table 4.6. Elements of the Symmetrised G Matrix for the S_2N_2 Molecule

Symmetry block	Element
A_g	$G_{11} = 2(\mu_N \cos^2\theta + \mu_S \sin^2\theta)$ $G_{12} = \frac{2\sqrt{2}}{r}(\mu_S - \mu_N) \sin\theta \cos\theta$ $G_{22} = \frac{4}{r^2}(\mu_N \sin^2\theta + \mu_S \cos^2\theta)$
B_{1g}	$G_{33} = 2(\mu_N \sin^2\theta + \mu_S \cos^2\theta)$
B_{2u}	$G_{44} = 2(\mu_N + \mu_S) \sin^2\theta)$
B_{3u}	$G_{55} = 2(\mu_N + \mu_S) \cos^2\theta$ $G_{56} = \frac{2\sqrt{2}}{r}(\mu_N + \mu_S) \sin\theta \cos\theta$ $G_{66} = \frac{4}{r^2}(\mu_N + \mu_S) \sin^2\theta$

Table 4.7. Numerical Values of the Symmetrised G Matrix Elements for the S_2N_2 Molecule[a]

Symmetry block	Element	Value[a]
A_g	G_{11}	1.02366
	G_{12}	-0.34365
	G_{22}	0.75541
B_{1g}	G_{33}	1.02954
B_{2u}	G_{44}	1.03413
B_{3u}	G_{55}	1.01908
	G_{56}	0.87934
	G_{66}	0.75377

Footnote

(a) Actual values multiplied by 10, as calculated using the computer program GMAT.

Table 4.8. Unsymmetrised F Matrix for the S_2N_2 Molecule based on the Assumption of a General Valence Force Field

	Internal Coordinate					
	r_1	r_2	r_3	r_4	α_1	α_2
r_1	f_r	$f_{r_1r_2}$	$f_{r_1r_3}$	$f_{r_1r_4}$	$f_{r_1\alpha_1}$	$f_{r_1\alpha_2}$
r_2	$f_{r_1r_2}$	f_r	$f_{r_1r_4}$	$f_{r_1r_3}$	$f_{r_1\alpha_2}$	$f_{r_1\alpha_1}$
r_3	$f_{r_1r_3}$	$f_{r_1r_4}$	f_r	$f_{r_1r_2}$	$f_{r_1\alpha_2}$	$f_{r_1\alpha_1}$
r_4	$f_{r_1r_4}$	$f_{r_1r_3}$	$f_{r_1r_2}$	f_r	$f_{r_1\alpha_1}$	$f_{r_1\alpha_2}$
α_1	$f_{r_1\alpha_1}$	$f_{r_1\alpha_2}$	$f_{r_1\alpha_2}$	$f_{r_1\alpha_1}$	f_α	$f_{\alpha\alpha}$
α_2	$f_{r_1\alpha_2}$	$f_{r_1\alpha_1}$	$f_{r_1\alpha_1}$	$f_{r_1\alpha_2}$	$f_{\alpha\alpha}$	f_α

Table 4.9. Elements of the Symmetrised F Matrix for the S_2N_2 Molecule Expressed in terms of Valence Force Constants

Symmetry block	Elements
A_g	$F_{11} = f_r + f_{r_1r_2} + f_{r_1r_3} + f_{r_1r_4}$ $\quad F_{12} = \sqrt{2}r(f_{r_1\alpha_1} + f_{r_1\alpha_2})$ $F_{21} = \sqrt{2}r(f_{r_1\alpha_1} + f_{r_1\alpha_2})$ $\quad F_{22} = r^2(f_\alpha + f_{\alpha\alpha})$
B_{1g}	$F_{33} = f_r - f_{r_1r_2} + f_{r_1r_3} - f_{r_1r_4}$
B_{2u}	$F_{44} = f_r + f_{r_1r_2} - f_{r_1r_3} - f_{r_1r_4}$
B_{3u}	$F_{55} = f_r - f_{r_1r_2} - f_{r_1r_3} + f_{r_1r_4}$ $\quad F_{56} = \sqrt{2}r(f_{r_1\alpha_2} - f_{r_1\alpha_1})$ $F_{65} = \sqrt{2}r(f_{r_1\alpha_2} - f_{r_1\alpha_1})$ $\quad F_{66} = r^2(f_\alpha - f_{\alpha\alpha})$

employs the so-called method of stepwise coupling, in which all off-diagonal elements in the $\underset{\sim}{F}$ and $\underset{\sim}{G}$ matrices are initially ignored but then introduced in several stages, corresponding to successive coupling of individual vibrational modes. As the symmetry blocks of the $\underset{\sim}{F}$ and $\underset{\sim}{G}$ matrices for the S_2N_2 molecule are small, however, it is a relatively simple task to perform this calculation manually.

The numerical values determined for the elements of the symmetrised $\underset{\sim}{F}$ matrix are listed in Table 4.10, together with the calculated isotopic shifts associated with the switch from $S_2{}^{14}N_2$ to $S_2{}^{15}N_2$; these shifts are seen to match the observed values (also listed in Table 4.10) within experimental error. Table 4.11 lists the magnitudes of the actual stretching and bending force constants. Reference has already been made in Section 4.4 to the need to assign the Raman lines near 930 and 615 cm^{-1} to the S-N stretching and in-plane deformation modes respectively in order to secure a satisfactory solution of the secular equation. In fact, replacement of ^{14}N by ^{15}N produces an isotopic shift of 32 cm^{-1} for the scattering at higher frequency and practically zero for that at lower frequency, leaving little room for doubt that the former corresponds to a vibration in which motion of the nitrogen atoms predominates, whereas the latter corresponds to a vibration in which motion of the sulphur atoms predominates.

The value of 328.5 N m^{-1} obtained for the principal stretching force constant of S_2N_2 is appreciably lower than the value of about 430 N m^{-1} predicted on the basis of the relationship between bond length and force constant derived by Glemser _et al._[136] for sulphur-nitrogen bonds. However, this relationship was based on the properties of acyclic molecules and its predictions may well be invalid when applied to cyclic systems, particularly in view of the much lower stability of S_2N_2 as compared with its acyclic counterparts and the considerable strain imposed by its almost square-planar geometry.

Table 4.10. Calculated F Matrix Elements and Isotopic Shifts for the Matrix Isolated S_2N_2 Molecule

Symmetry block	$\underset{\sim}{F}$ matrix element	Numerical value[a]	Isotopic shift/cm^{-1} ($S_2{}^{14}N_2$-$S_2{}^{15}N_2$)	
			calc	obs
A_g	F_{11}	374.4	31.	32.0
	F_{22}	469.4	0.1	0.0
	F_{12}	0.0		
B_{1g}	F_{33}	452.0	20.3	21.0
B_{2u}	F_{44}	127.3	11.0	12.1
B_{3u}	F_{55}	359.3	18.4	13.3
	F_{66}	0.0		

Footnote

(a) Units are as follows: F_{11}, F_{33}, F_{44} and F_{55}, N m^{-1}; F_{22}, N m rad^{-2}.

Table 4.11. Calculated Valence Force Constants for the S_2N_2 Molecule

Force constant	Numerical value[a]
f_r	328.5
$f_{r_1r_2}$	-77.4
$f_{r_1r_3}$	34.7
$f_{r_1r_4}$	38.6
$f_\alpha + f_{\alpha\alpha}$	172.3

Footnote

(a) Units are as follows: f_r, $f_{r_1r_2}$, $f_{r_1r_3}$, $f_{r_1r_4}$, f_α and $f_{\alpha\alpha}$, N m^{-1}.

The molecule is characterised by substantial stretch-stretch interaction force constants which are associated presumably with the delocalised bonding implied by the results of molecular-orbital studies.[109-111] The seemingly large value of 172.3 N m^{-1} deduced for the sum of the principal bending and bend-bend interaction force constants is suggestive, as is the short S-S distance, of substantial cross-ring interactions between the sulphur atoms. However, the results of the most recent ab initio molecular-orbital study[137] indicate that while adjacent atoms are bonded (positive overlap), cross-ring bonding is absent, presumably as a result of repulsive interactions between lone-pair electrons. The unusual negative value of fr_1r_2 (Table 4.11) might also be indicative of such interactions. Hence any interactions between the sulphur atoms in the S_2N_2 molecule appear to be of a non-bonded nature; this contrasts with the S_4N_4 molecule for which there is evidence of considerable cross-ring bonding involving the sulphur atoms (Chapter 5).

Chapter 5

STUDIES OF SULPHUR-NITROGEN SYSTEMS. PART II: TETRASULPHUR TETRANITRIDE, S_4N_4

5.1 Introduction

After a detailed investigation of the vibrational spectra of disulphur dinitride and their relationship to its molecular structure, the next step was to tackle its precursor, tetrasulphur tetranitride, in a similar vein in order that the two compounds might be compared. Tetrasulphur tetranitride, the most familiar sulphur-nitrogen compound, was first prepared as long ago as 1835,[138] but little was known about its structure until comparatively recently. It is formed as either the main product or a by-product in a variety of reactions; standard methods of preparation include the interaction of a sulphur chloride with ammonia in an inert solvent such as carbon tetrachloride.[139] The chemistry of tetrasulphur tetranitride has been the subject of two fairly detailed reviews published comparatively recently.[98, 140]

The S_4N_4 molecule is now known, as a result of electron diffraction[141] and X-ray diffraction[142] studies, to consist of a buckled eight-membered ring of D_{2d} symmetry, in which the nitrogen atoms form a square and the sulphur atoms lie at the corners of a slightly distorted tetrahedron (Figure 5.1). The following features of this structure are particularly noteworthy.

(i) The eight S-N bond lengths are identical at 1.616 ± 0.01Å,[142] a distance significantly shorter than that normally associated with an S-N single bond (ca 1.74Å[140]). It has been suggested in one quarter[143] that the bond length corresponds to a bond order of about 1.65.

(ii) The S----S distances along the edges of the tetrahedron (2 x 2.58Å and 4 x 2.69Å) are appreciably shorter than the sum of the van der Waals radii (3.69Å in orthorhombic sulphur[144]) and actually at the upper limit of the range normally associated with S-S single bonds (ca 2.00-2.60Å depending on the relative contributions made by the valence s- and p- orbitals of the sulphur atoms[145]).

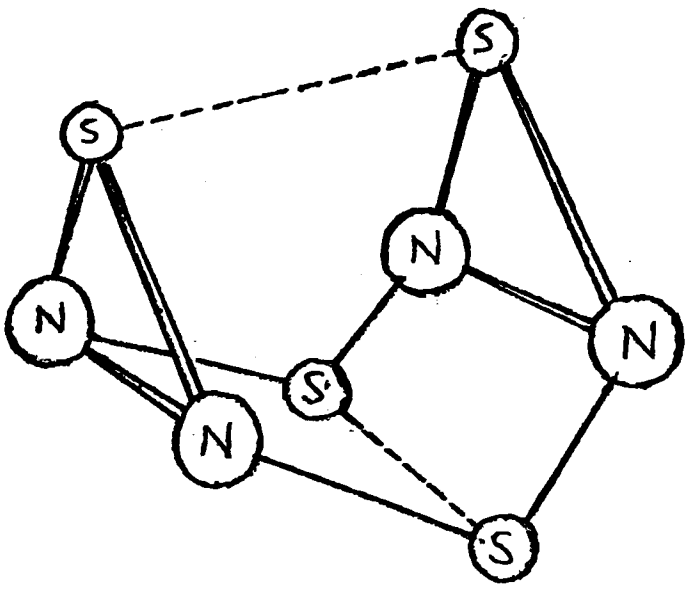

Fig. 5.1. The S_4N_4 molecule.

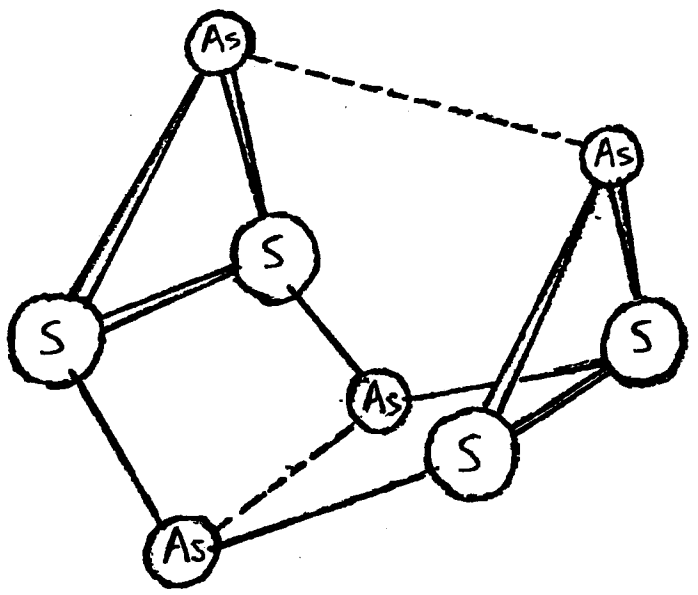

Fig. 5.2. The As_4S_4 molecule.

(iii) The N-N distances along the sides of the square are again much shorter than the sum of the relevant van der Waals radii (3.1Å)[146], but there is no conclusive evidence for significant N-N bonding.[147, 148]

Several attempts have been made to explain the observed geometry of the S_4N_4 molecule. One such interpretation,[149] based on symmetry arguments concerned with the effects of various distortions of a planar structure of D_{4h} symmetry, leads to the conclusion that the configuration of lowest energy should consist of eight single S-N bonds and two transannular S-S bonds. Two relatively strong S-S interactions are also implied by CNDO/2 calculations,[150] but these also indicate an S-N bond order of 1.5 arising from highly delocalised 'islands' of electron density superimposed on the σ-framework emulating the features attributed to the cyclophosphazenes.[151] The second interpretation, unlike the first, assumes a contribution from the 3d-orbitals of the sulphur atoms.

It has been suggested by Banister[152] that the sulphur atoms each provide two electrons for the σ-bonds and that one of the two 'lone pairs' on each atom acquires a contribution from certain of the 3d-orbitals to give two further bonding electrons of higher energy. If one non-bonding pair of electrons is allocated to each atom, fourteen pairs of bonding electrons remain; eight of these are allocated to the S-N σ-framework, leaving six pairs of higher energy to bind together the sulphur atoms making up the near-tetrahedral S_4 unit. The structure of S_4N_4 may also be contrasted with that of As_4S_4 (Figure 5.2),[153] in which the electronegativity values of the constituent atoms (As, 2.2; S, 2.6; N, 3.0[154]) are such that the 3d-orbitals of the sulphur are no longer contracted by an excess positive charge, and which is thought to be fairly well represented by a model involving ten localised single bonds.[152]

More recently, however, a self-consistent field/CNDO treatment of S_4N_4[155] discounts the possibility of significant d-orbital participation. The S-N

and S-S bonds are considered to be relatively localised, slightly bent single bonds (cf P_4 [156]) implicating almost pure p-orbitals, with the lone pairs occupying almost pure 3s-orbitals in the case of sulphur, and orbitals having both 2s- and 2p-character in the case of nitrogen. The bent form of the bonds explains the classical 'strain' in the S_4N_4 molecule and its thermal instability,[157] while the electron delocalisation suggested by diamagnetic ring currents[148] is thought to arise from interaction between the lone pair electrons on each nitrogen atom and the p-orbitals on the adjacent sulphur atoms. The question of the electronic structure of tetrasulphur tetranitride still appears to be unresolved, therefore, although it seems to be generally agreed that there are appreciable S-S but negligible N-N interactions.

There has also been some uncertainty about the interpretation of the vibrational spectra of the S_4N_4 molecule. Infrared and Raman spectra attributed to tetrasulphur tetranitride were reported as long ago as 1953,[157] but the assignment of the observed features attempted then was based on an incorrect molecular structure. Further confusion was added by Griffith and Rutt[158] in their studies of the Raman spectrum of tetrasulphur tetranitride in solution, leading to the assignment of Raman lines at 474 and 156 cm^{-1} to fundamentals of the S_4N_4 molecule; in fact, these lines almost certainly arose from the presence of sulphur in the sample of tetrasulphur tetranitride.[159] Bragin and Evans[122] carried out a complete normal coordinate analysis of the S_4N_4 molecule but this still left considerable room for doubt about the vibrational assignments on which it was based.

In this Laboratory, Cunningham[126] carried out further investigations on the vibrational spectra of tetrasulphur tetranitride and performed a partial normal coordinate analysis of the molecule, but here again the absence of a complete and reliable vibrational assignment limited the scope and significance of the calculations. More recently, Sawodny and his co-workers have reported

a complete assignment of the fundamental vibrations of the S_4N_4 molecule;[160] in this they have sought, for example, to distinguish between the b_2 and e modes, which are active in both infrared absorption and Raman scattering, by the splitting of the e modes in the spectra of solid tetrasulphur tetranitride. Again force constant calculations were carried out but were incomplete, only the principal S-N and S-S stretching force constants being quoted in the published account; the major difficulty, as with all previous studies of this nature, was simply the lack of sufficient information (relating, for example, to the effects of isotopic substitution) to provide a proper definition of the molecular force field.

The aim of the present study was, therefore, to obtain the information required for a complete normal coordinate analysis by measuring for the first time the infrared and Raman spectra of the matrix-isolated S_4N_4 molecule. As well as yielding accurate values of the vibrational frequencies and, in principle, such aids to assignment as the polarisation properties of the Raman scattering, such a study would also lend itself particularly well to the vibrational characterisation of a different isotopic version of the molecule, namely $S_4{}^{15}N_4$. The additional information made available in this way might reasonably be expected to enable the performance of a complete normal coordinate analysis of the S_4N_4 molecule. With this achieved, the force constants would naturally invite comparisons with those of related molecules (particularly disulphur dinitride) for the light which they might shed on the electronic structures of the molecules.

5.2 Experimental

Orange crystals of tetrasulphur tetranitride were prepared by the method referred to in Chapter 4, Section 4.2. The vaporisation of the tetrasulphur tetranitride was achieved in apparatus similar in design to that used for the preparation of disulphur dinitride, but with the pyrolysis stage now omitted; accordingly the assembly took the form of a simple Pyrex-glass

ampoule approximately 6-7 cm long and having an internal diameter of 6 mm, again giving direct access to the vacuum shroud *via* a constriction. Convenient rates of deposition were achieved by vaporising the tetrasulphur tetranitride at 55-60°C prior to infrared studies and at 70-75°C prior to Raman studies. Experiments involving ^{15}N-enriched tetrasulphur tetranitride were most conveniently performed by generating it *in situ* by controlled pyrolysis of ^{15}N-enriched thiotrithiazyl chloride, S_4N_3Cl.[123] The conditions of deposition were otherwise similar to those employed in the studies of disulphur dinitride.

5.3 Infrared Spectra

The infrared spectra exhibited by matrices containing tetrasulphur tetranitride isolated in solid nitrogen, argon or krypton are illustrated in Figures 5.3 to 5.5, and expanded versions of portions of these spectra are reproduced in Figure 5.6. Figure 5.7 depicts the spectrum of an argon matrix incorporating the products of controlled pyrolysis of ^{15}N-enriched thiotrithiazyl chloride; here the bands are predominantly attributable to the infrared-active fundamentals of the molecule $S_4{}^{15}N_4$. The measured frequencies of the absorptions occurring in all these spectra are listed in Table 5.1.

The S_4N_4 molecule belongs to the D_{2d} point group and therefore possesses fourteen distinct vibrational fundamentals which are accommodated by the representation $3a_1 + 2a_2 + 2b_1 + 3b_2 + 4e$. According to the selection rules, the two a_2 fundamentals respond neither to infrared absorption nor to Raman scattering. All twelve of the remaining fundamentals are expected to be Raman-active ($3a_1 + 2b_1 + 3b_2 + 4e$), but only the b_2 and e modes to be infrared-active. In principle, therefore, seven vibrational fundamentals should be observable in the infrared spectrum, although previous measurements[122, 126, 160] suggest that at least one of these occurs at a frequency less than 250 cm^{-1}, the effective limit of detection of the apparatus used in the present study.

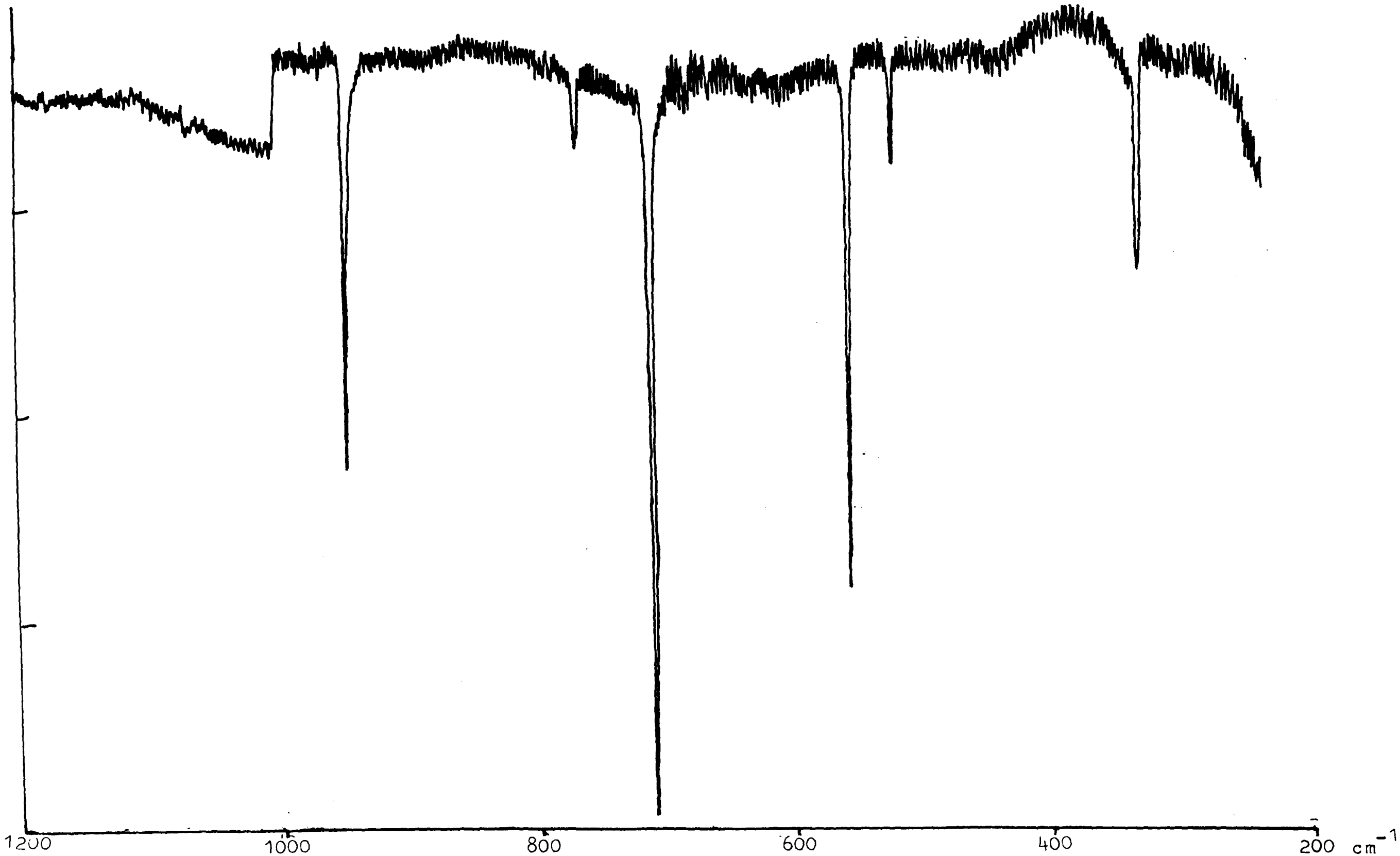

Fig. 5.3. Infrared spectrum of S_4N_4 isolated in a nitrogen matrix.

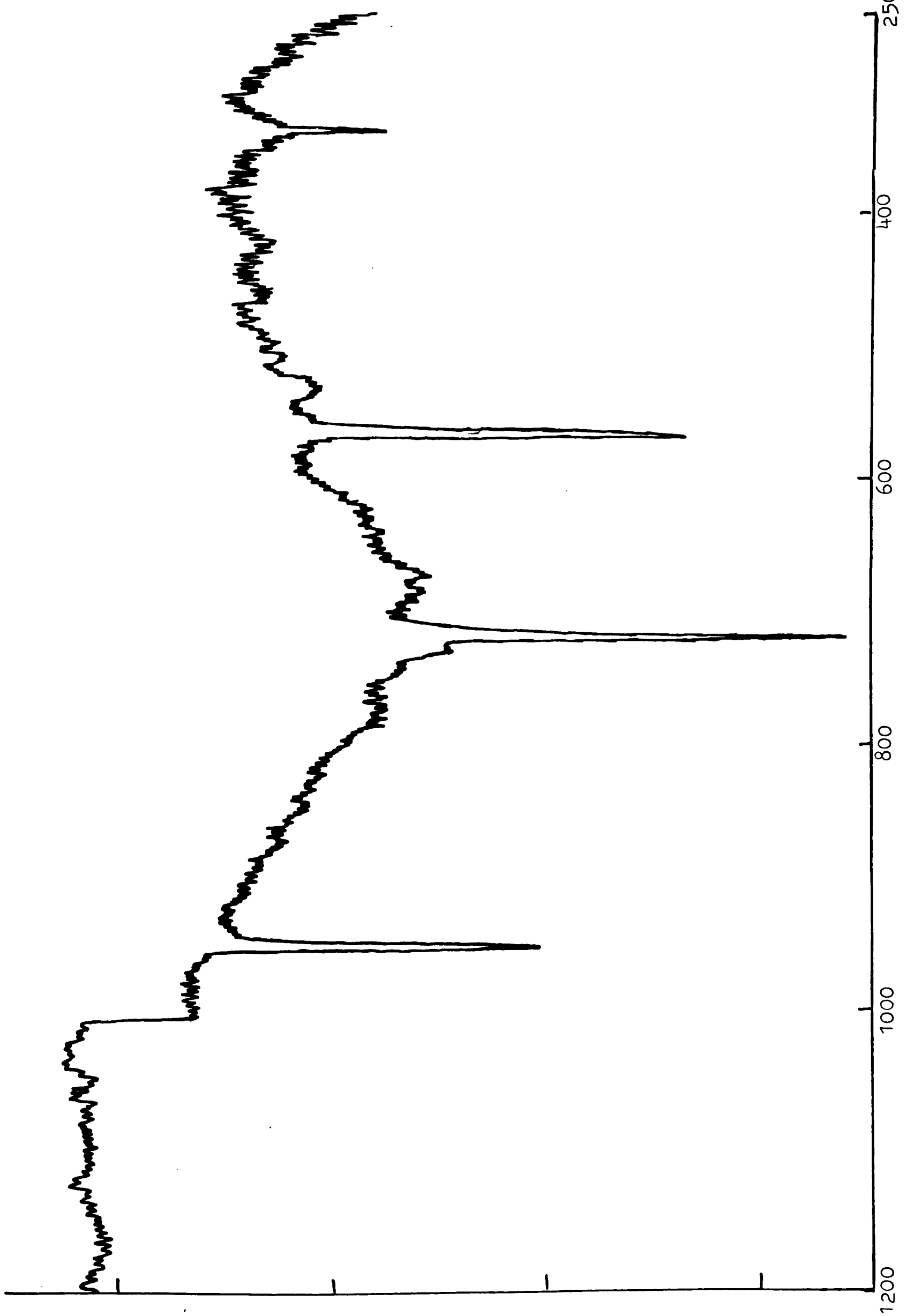

Fig. 5.4. Infrared spectrum of S_4N_4 isolated in an argon matrix.

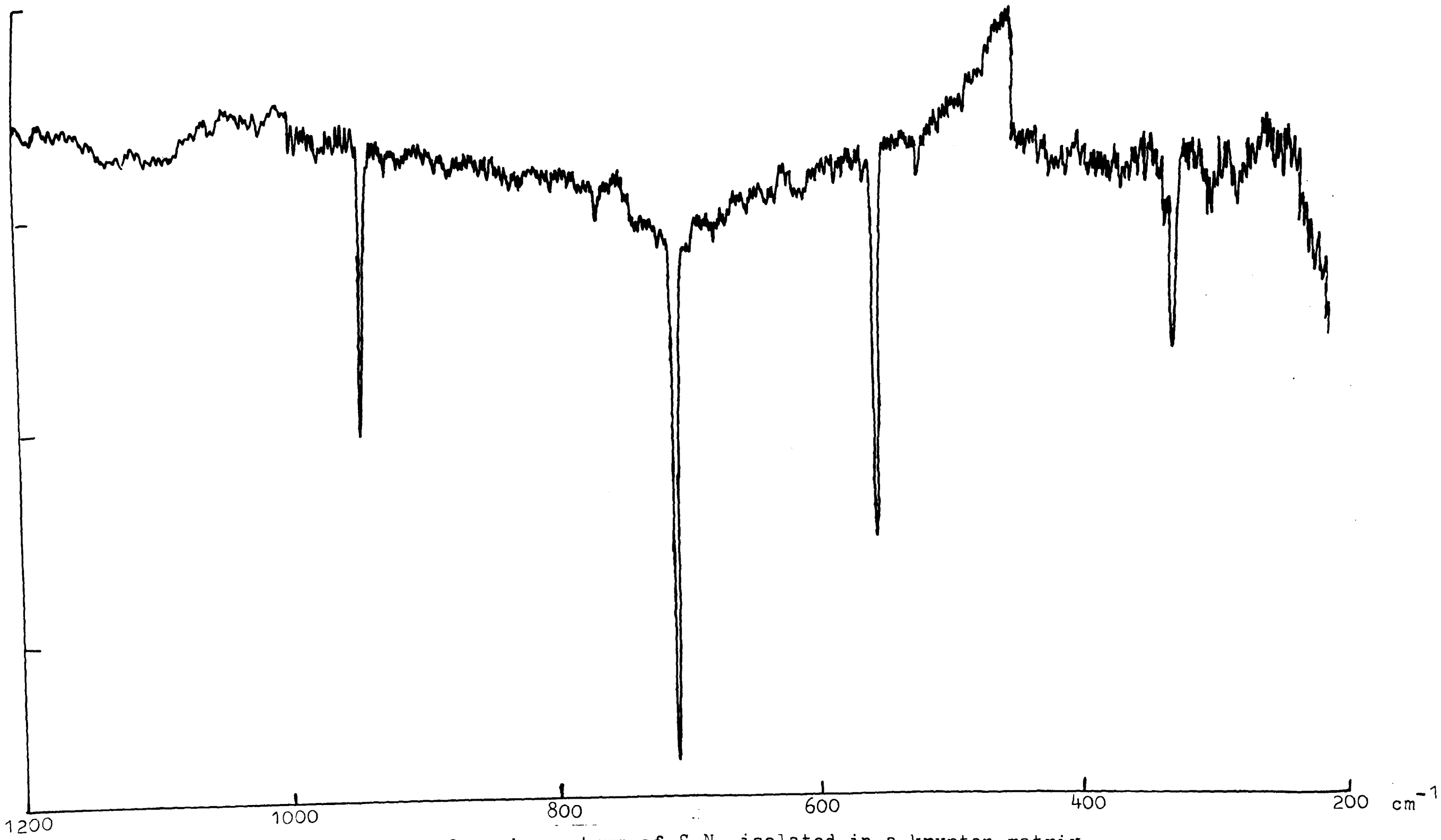

Fig. 5.5. Infrared spectrum of S_4N_4 isolated in a krypton matrix.

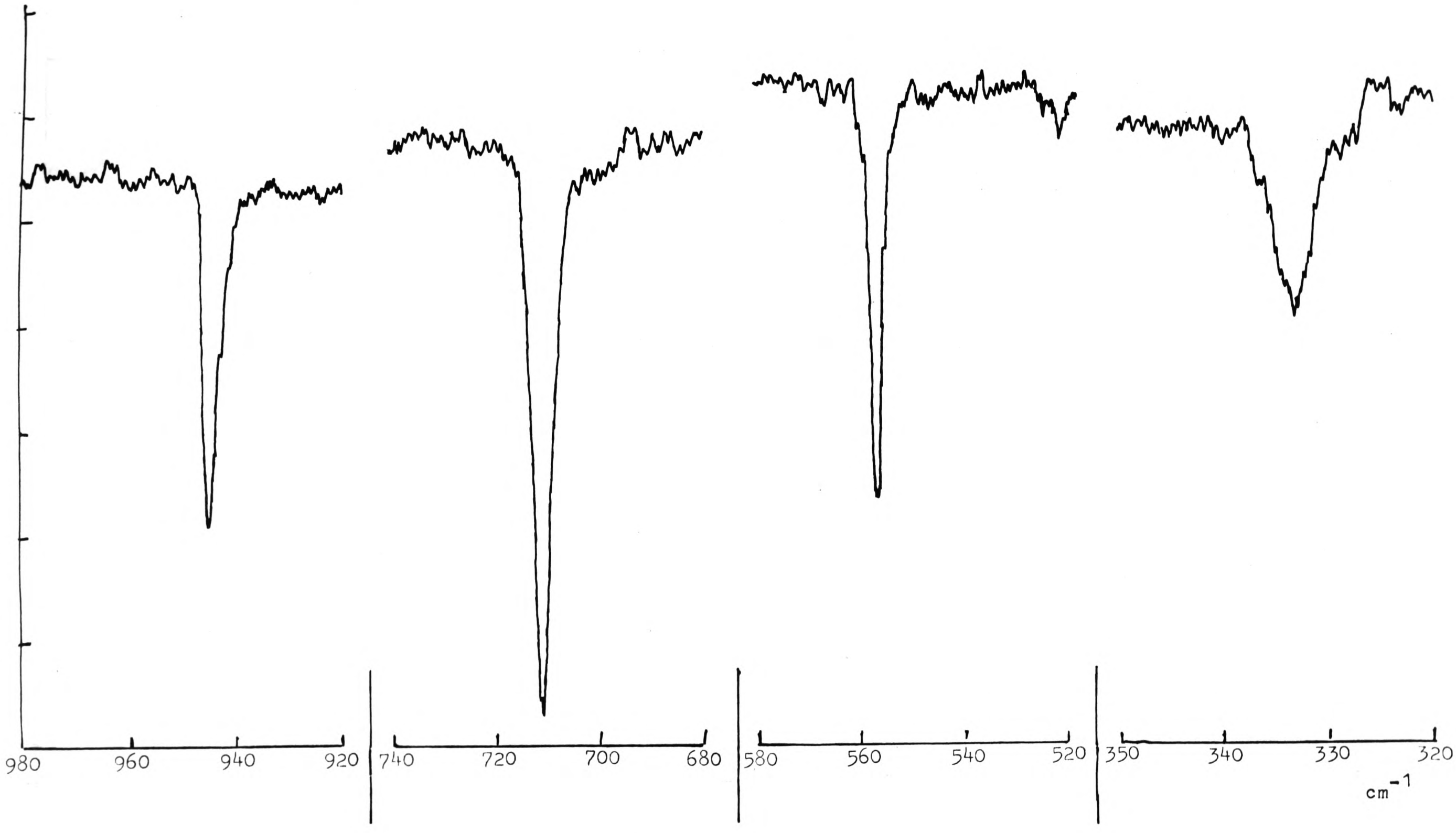

Fig. 5.6. Bands in the infrared spectrum of S_4N_4 isolated in an argon matrix.

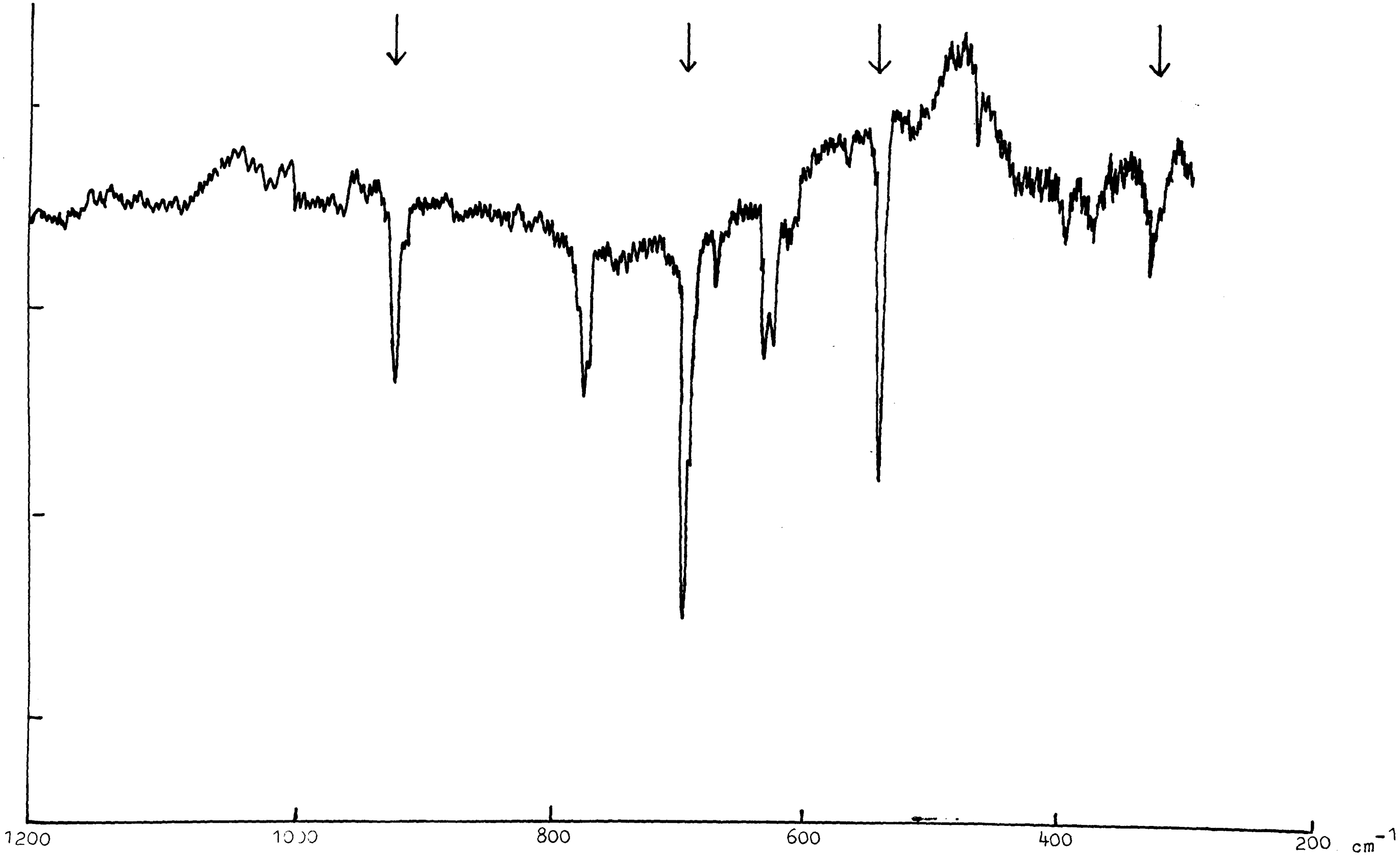

Fig. 5.7. Infrared spectrum of an argon matrix containing the products of pyrolysis of ^{15}N-enriched S_4N_3Cl showing bands attributed to $S_4{}^{15}N_4$.

Table 5.1. Frequencies of Infrared Bands Observed in Studies of Matrix Isolated Tetrasulphur Tetranitride

	$S_4{}^{14}N_4$		$S_4{}^{15}N_4$
N_2 matrix	Ar matrix	Kr matrix	Ar matrix
944.8	945.7	944.2	919.8
768.0		768.0	
710.7	707.6	710.5	693.0
556.5	554.2	557.4	540.5
519.3	519.0	519.0	519?
342.0	337.3	337.0	331.0

The infrared spectrum exhibited by tetrasulphur tetranitride invariably contained four strong absorptions: with the molecules isolated in an argon matrix, these were located at 945.7, 707.6, 554.2 and 337.3 cm^{-1}. In addition, two weaker features were often, but not always, observed at 768 and 519 cm^{-1}, the intensities appearing to vary in sympathy with those of the stronger bands. All six bands may be assigned to infrared-active fundamentals of the S_4N_4 molecule, in agreement with the assignments made in previous investigations.[122, 160] The frequencies of the four strong absorptions are also in close agreement, it may be noted, with those attributed to the presence of tetrasulphur tetranitride in the studies of disulphur dinitride described in Chapter 4.

On the basis of the infrared spectrum of the molecule $S_4{}^{14}N_4$ alone, it is not possible to distinguish between the b_2 and e fundamentals. Such a distinction has been claimed, however, by Sawodny et al.[160] on the basis of the splitting developed by the absorptions due to the degenerate vibrations and attributable to the lowering to C_s of the site symmetry of the S_4N_4 molecules in solid tetrasulphur tetranitride. Additional evidence has been afforded in the present study by measurements of the vibrational spectra of $S_4{}^{15}N_4$ tetrasulphur tetranitride, allowing the distinction between the b_2 and e modes to be made within the context of the normal coordinate analysis of the S_4N_4 molecule. In fact, this evidence supports the assignments proposed by Sawodny et al;[160] on this basis, the infrared absorptions located at 707.6 and 554.2 cm^{-1} (for the $S_4{}^{14}N_4$ molecule isolated in an argon matrix) are assigned to the b_2 fundamentals ν_8 and ν_9, while those at 945.7, 768, 519 and 337.3 cm^{-1} are assigned to the e fundamentals ν_{11}, ν_{12}, ν_{13} and ν_{14} respectively.

5.4 Raman Spectra

The Raman spectrum of matrix-isolated tetrasulphur tetranitride exhibited two very strong bands at approximately 200 and 220 cm^{-1} and two somewhat lower in intensity at approximately 560 and 720 cm^{-1}, along with several

other weaker features. Examples of the Raman scattering from $S_4{}^{14}N_4$ isolated in a nitrogen, argon or methane matrix are shown in Figures 5.8 to 5.10. Figure 5.11 shows the Raman spectrum of an argon matrix containing the products of controlled pyrolysis of ^{15}N-enriched thiotrithiazyl chloride; again this consisted predominantly of bands attributable to the $S_4{}^{15}N_4$ molecule. The measured frequencies of the Raman lines occurring in all these spectra are listed in Table 5.2.

The selection rules imply that, in principle, all but the a_2 fundamentals of the S_4N_4 molecule should be active in Raman scattering. Although it appears that some of the Raman lines are so weak as to escape detection, the main concern is to locate those fundamentals which are inactive in infrared absorption, namely the a_1 and b_1 modes. In fact, the Raman lines occurring near 220, 560 and 720 cm^{-1} have previously been assigned to the three a_1 fundamentals on the evidence of the depolarisation ratios which they display when tetrasulphur tetranitride is in solution.[122, 126] The results of polarisation measurements involving S_4N_4 molecules isolated in a nitrogen matrix, as carried out in the present investigation, are illustrated in Figure 5.12, and afford added evidence in favour of the assignment of these three lines to the a_1 fundamentals.

The two b_1 fundamentals are easily identifiable in principle as the only ones which do not respond to infrared absorption and give rise to depolarised Raman lines. The lower in frequency of the two intense bands in the region of 200 cm^{-1} has previously been assigned to the third b_2 fundamental,[160] but the frequency measured in the present investigation (205.5 cm^{-1} for the molecule isolated in an argon matrix) does not coincide with that of the infrared absorption previously assigned to this fundamental (ca 180 cm^{-1}).[122, 126, 160] The results of the present study suggest that a weaker feature, occurring at 185 cm^{-1} for an argon matrix and apparently unresolved in previous measurements, should be assigned to ν_{10}, the third b_2 fundamental, leaving the strong band at 205.5 cm^{-1} to be ascribed to one of the two b_1

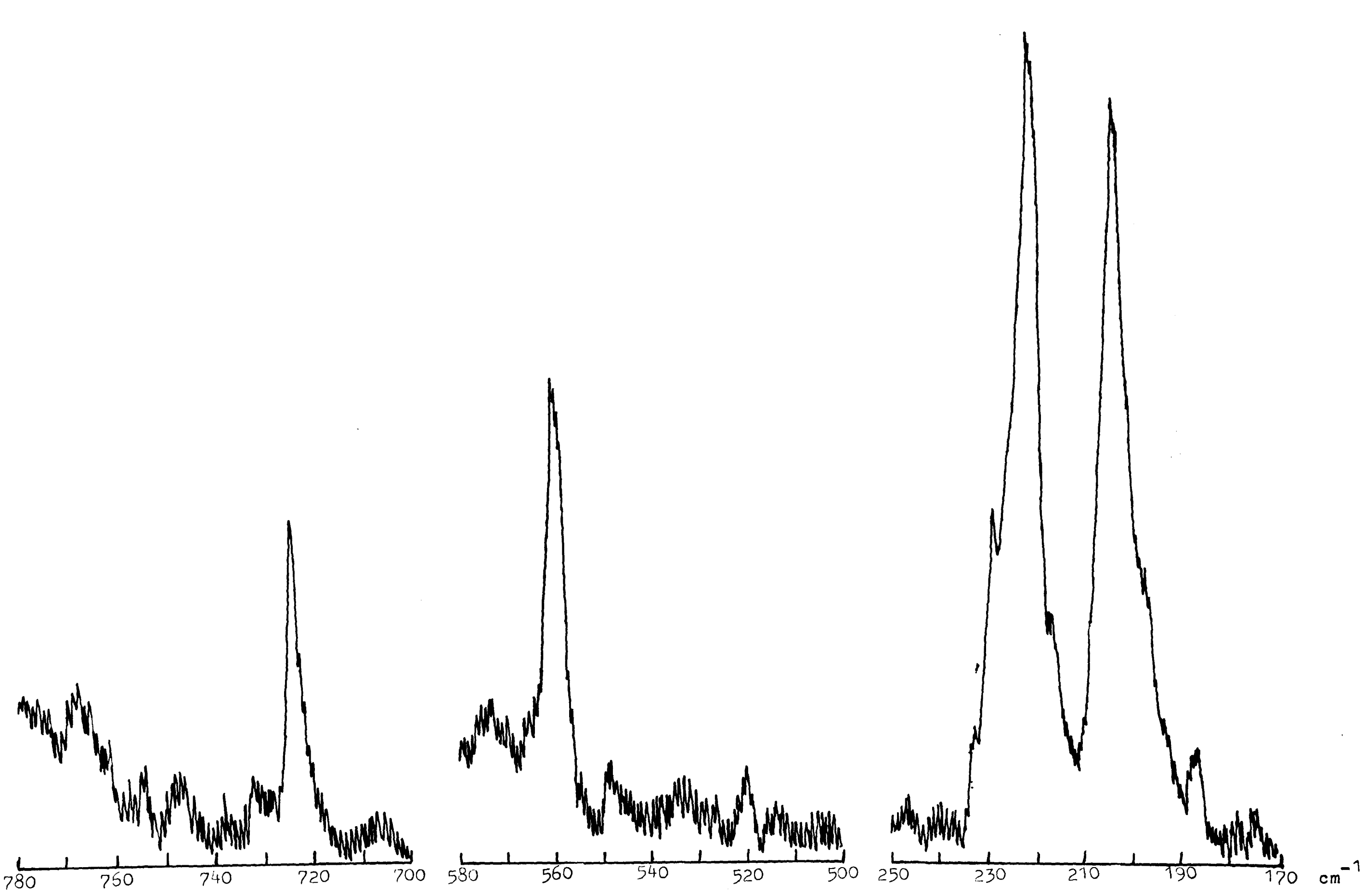

Fig. 5.8. Raman spectrum of S_4N_4 isolated in a nitrogen matrix.

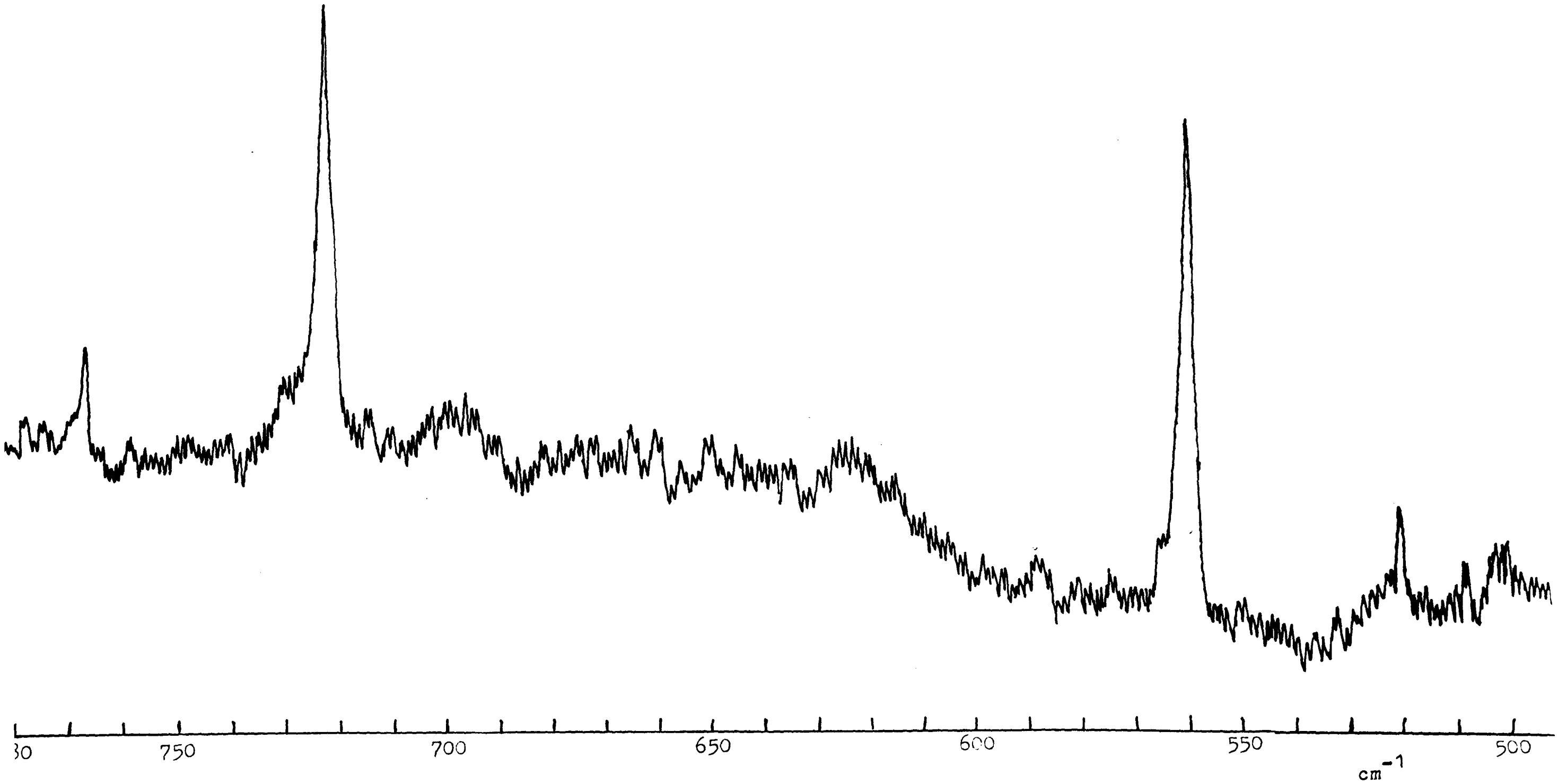

Fig. 5.9. Raman spectrum of S_4N_4 isolated in an argon matrix.

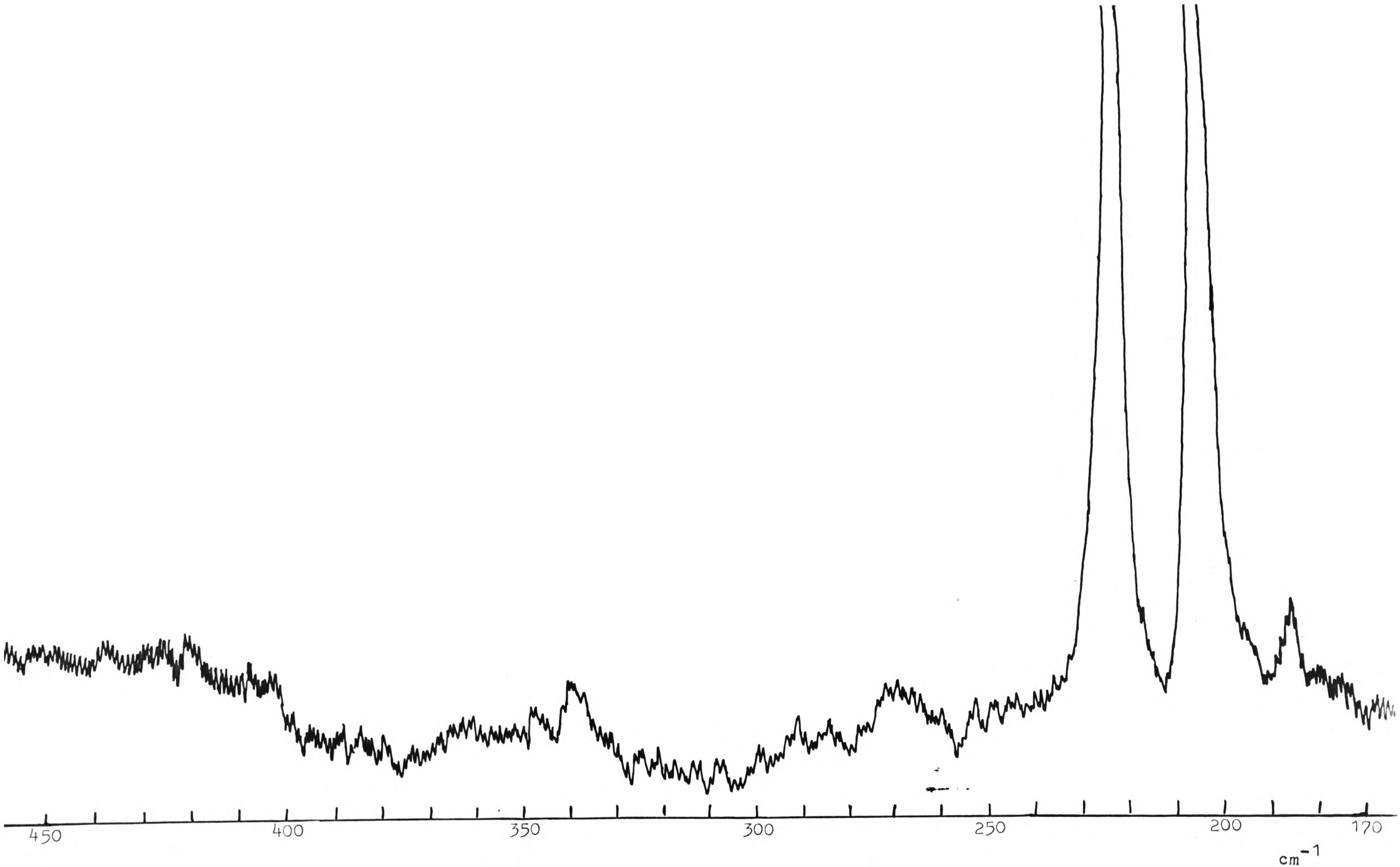
450
400
350
300
250
200
170
cm⁻¹

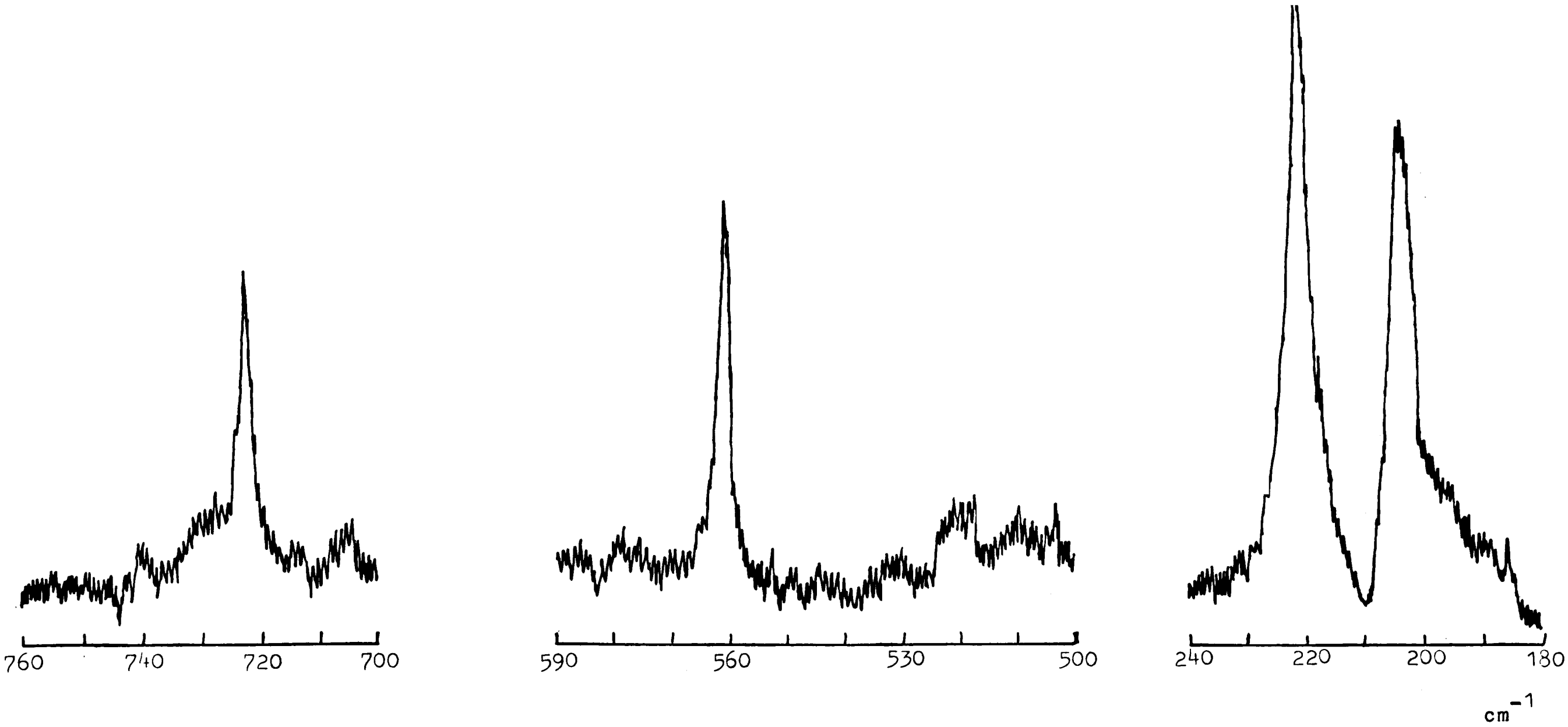

Fig. 5.10. Raman spectrum of S_4N_4 isolated in a methane matrix.

Fig. 5.11. Raman spectrum attributed to the molecule $S_4{}^{15}N_4$ isolated in an argon matrix.

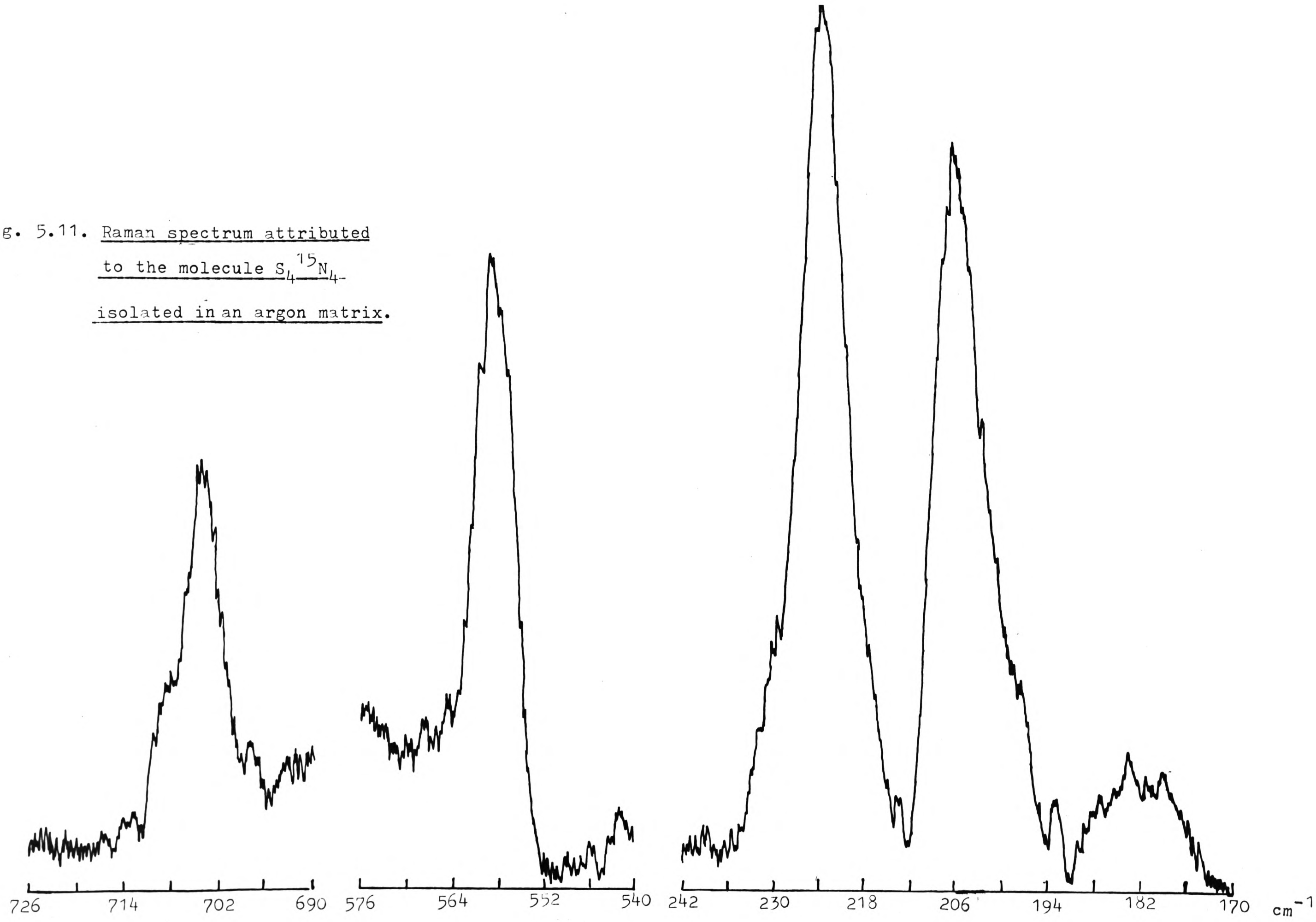

Table 5.2. Frequencies of Raman Bands Observed in Studies of Matrix Isolated Tetrasulphur Tetranitride

$S_4{}^{14}N_4$			$S_4{}^{15}N_4$
N_2 matrix	Ar matrix	CH_4 matrix	Ar matrix
186.0	185.0	188.0	183.0
206.0	205.5	202.0	204.0
223.5	223.0	221.0	221.0
	343	336	
	521		
561.0	560.5	560.0	559.5
725.0	723.0	723.5	704.0

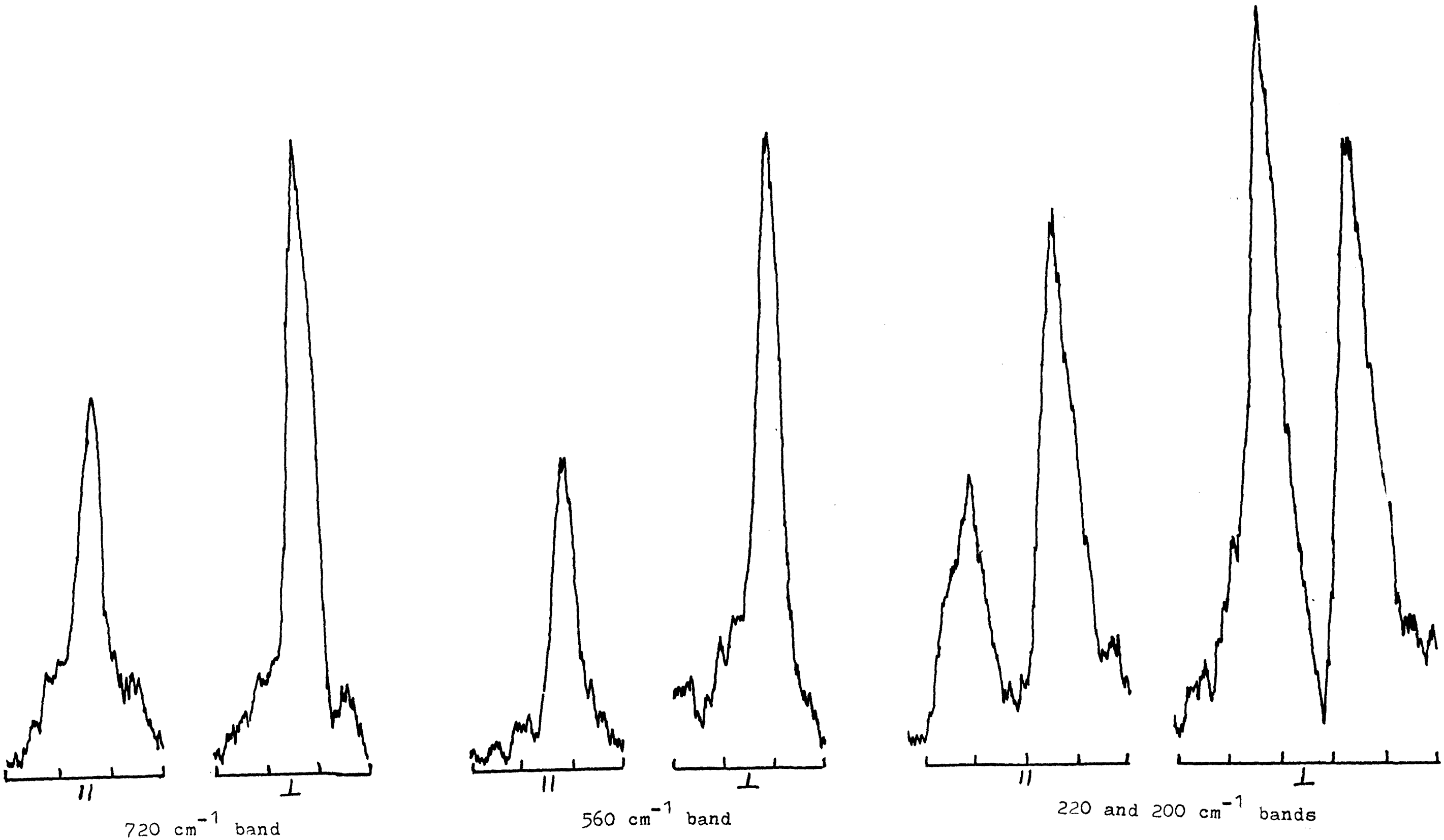

Fig. 5.12. Polarisation measurements on the Raman spectrum of S_4N_4 isolated in a nitrogen matrix.

fundamentals (ν_7).

The assignment of the other b_1 mode (ν_6) is even less clear-cut, with no evidence, for example, to support the existence either of the bands at 888 and 615 cm^{-1} assigned to the b_1 fundamentals by Bragin and Evans,[122] or of that at 528 cm^{-1} suggested as an alternative candidate by Sawodny et al.[160] There is, however, weak scattering at 731 cm^{-1} in the Raman spectrum of solid tetrasulphur tetranitride which has been provisionally assigned to $\nu_6(b_1)$ by Cunningham,[126] and although there was no clear sign of such a band in the spectra of matrix-isolated tetrasulphur tetranitride recorded in the present investigation, this assignment has been adopted on the strength of its apparent consistency with the ensuing normal coordinate analysis.

Table 5.3 summarises the conclusions reached on the basis of the measurements described here or elsewhere by providing a complete list of the assignments favoured for those vibrational fundamentals of the S_4N_4 molecule which are amenable to detection in either infrared absorption or Raman scattering.

5.5 Normal Coordinate Analysis

As in the case of the S_2N_2 molecule, calculation of a set of force constants consistent with the measured vibrational frequencies may be expected to bring to light interaction terms reflecting the influence of electron delocalisation, and comparison with the force constants already deduced for S_2N_2 may highlight important similarities or differences between the two molecules.

For the S_4N_4 molecule, as for the S_2N_2 molecule, the first step in the determination of a set of force constants was to calculate the elements of the Wilson $\underset{\sim}{G}$ matrix. The values of the interbond angles and bond lengths assumed for this purpose were those determined by X-ray diffraction using single crystals of tetrasulphur tetranitride, namely an N-S-N angle of 104°,

Table 5.3. Assignments of the Vibrational Fundamentals of the S_4N_4 Molecule

Symmetry species	Fundamental	Frequency
A_1	ν_1	723.0[a]
	ν_2	560.5[a]
	ν_3	223.0[a]
B_1	ν_6	731[c]
	ν_7	205.5[a]
B_2	ν_8	707.6[b]
	ν_9	554.2[b]
	ν_{10}	185.0
E	ν_{11}	945.7[b]
	ν_{12}	768.0[b]
	ν_{13}	519.0[b]
	ν_{14}	337.3[b]

Footnotes

(a) Raman spectrum, Ar matrix.

(b) Infrared spectrum, Ar matrix.

(c) Raman spectrum, solid (ref. 126).

an S-S-N angle of 90°, and all the S-N bond lengths set equal at 1.62Å. The set of internal coordinates chosen was similar to that employed by Bragin and Evans,[122] comprising eight S-N stretching, two S-S stretching and eight S-S-N bending coordinates (Figure 5.13). These result in a complete set of internal symmetry coordinates, the algebraic expressions for which are given in Table 5.4, with no redundancies. The numerical values of the $\underset{\sim}{G}$ matrix elements derived from these coordinates using the computer program GMAT are listed in Table 5.5.

Having calculated the elements of the $\underset{\sim}{G}$ matrix, it was then possible to check some of the vibrational assignments for the S_4N_4 molecule using the product rule,[26, 33] which relates the frequencies of different isotopic versions of the same molecule as described in Chapter 2. In the case of the S_4N_4 molecule the rule was applied to those symmetry classes for which all the frequencies of the molecule $S_4{}^{15}N_4$ had been measured, namely the a_1 and b_2 classes. The calculations were carried out using the rule as expressed in equation (2.25), which involves the determinants of the appropriate blocks in the $\underset{\sim}{G}$ matrix. The results are listed in Table 5.6 and appear to afford additional evidence in favour of the proposed assignments.

With reference to the $\underset{\sim}{F}$ matrix, a general valence force field was chosen, and Tables 5.7 and 5.8 record the details of the corresponding unsymmetrised and symmetrised $\underset{\sim}{F}$ matrices respectively. In this case, it was found necessary to retain most of the off-diagonal elements in order to accommodate all the observed frequencies. The method of calculating the off-diagonal elements was essentially one of trial and error until the values inserted, together with those computed for the diagonal elements, yielded an $\underset{\sim}{F}$ matrix which would satisfactorily accommodate all the observed frequencies for both isotopic versions of the molecule. The numerical values determined for the elements of the symmetrised $\underset{\sim}{F}$ matrix are catalogued

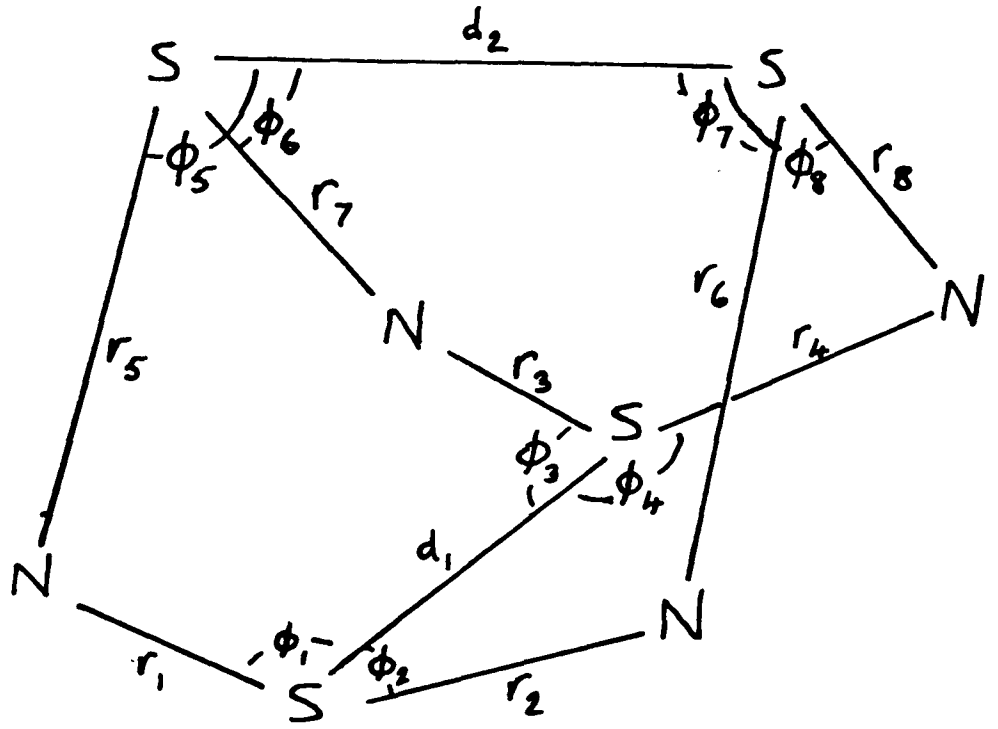

Fig. 5.13. Internal coordinates of S_4N_4.

Table 5.4. Internal Symmetry Coordinates Used in the Normal Coordinate Analysis of the S_4N_4 Molecule

(See Figure 5.13 for an explanation of the symbols)

Symmetry block	Coordinate
A_1	$S_1 = \frac{1}{\sqrt{8}}(r_1 + r_2 + r_3 + r_4 + r_5 + r_6 + r_7 + r_8)$ $S_2 = \frac{1}{\sqrt{8}}(\Phi_1 + \Phi_2 + \Phi_3 + \Phi_4 + \Phi_5 + \Phi_6 + \Phi_7 + \Phi_8)$ $S_3 = \frac{1}{\sqrt{2}}(d_1 + d_2)$
B_1	$S_4 = \frac{1}{\sqrt{8}}(r_1 - r_2 - r_3 + r_4 + r_5 - r_6 - r_7 + r_8)$ $S_5 = \frac{1}{\sqrt{8}}(\Phi_1 - \Phi_2 - \Phi_3 + \Phi_4 + \Phi_5 - \Phi_6 - \Phi_7 + \Phi_8)$
B_2	$S_6 = \frac{1}{\sqrt{8}}(r_1 + r_2 + r_3 + r_4 - r_5 - r_6 - r_7 - r_8)$ $S_7 = \frac{1}{\sqrt{8}}(\Phi_1 + \Phi_2 + \Phi_3 + \Phi_4 - \Phi_5 - \Phi_6 - \Phi_7 - \Phi_8)$ $S_8 = \frac{1}{\sqrt{2}}(d_1 - d_2)$
E	$S_9 = \frac{1}{2}(r_1 + r_2 - r_3 - r_4)$ $S_{10} = \frac{1}{2}(r_5 + r_6 - r_7 - r_8)$ $S_{11} = \frac{1}{2}(\Phi_1 + \Phi_2 - \Phi_3 - \Phi_4)$ $S_{12} = \frac{1}{2}(\Phi_5 - \Phi_6 + \Phi_7 - \Phi_8)$

Footnote

The a_2 fundamentals, inactive in both infrared absorption and Raman scattering, have been ignored.

Table 5.5. Numerical Values of the Symmetrised G Matrix Elements for the S_4N_4 Molecule[a]

Symmetry block	Element	Value[a]
A_1	G_{11}	0.67990
	G_{12}	0.34738
	G_{13}	0.00000
	G_{22}	0.50975
	G_{23}	-0.38502
	G_{33}	0.62373
B_1	G_{11}	0.83079
	G_{12}	0.04374
	G_{22}	0.51010
B_2	G_{11}	1.22114
	G_{12}	-0.34736
	G_{13}	0.00000
	G_{22}	0.50978
	G_{23}	-0.38502
	G_{33}	0.62373
E	G_{11}	0.95052
	G_{12}	-0.27062
	G_{13}	-0.13533
	G_{14}	0.34737
	G_{22}	1.10141
	G_{23}	0.34736
	G_{24}	0.00000
	G_{33}	0.65505
	G_{34}	0.00000
	G_{44}	0.27210

Footnote

Actual values multiplied by 10, as calculated using the computer program GMAT.

Table 5.6. Product Rule Calculations for the S_4N_4 Molecule

A_1 block

	$S_4{}^{14}N_4$	$S_4{}^{15}N_4$	Ratio
|G|	0.040116	0.037449	0.933
Frequencies	723.0 560.5 223.0	704.0 559.5 221.0	
$\pi(\nu^2)$	8.167×10^{15}	7.578×10^{15}	0.928

B_2 block

	$S_4{}^{14}N_4$	$S_4{}^{15}N_4$	Ratio
|G|	0.013199	0.011752	0.890
Frequencies	707.6 554.2 135.0	693.0 540.5 133.0	
$\pi(\nu^2)$	5.264×10^{15}	$.[illegible] \times 10^{15}$	0.893

Table 5.7. Unsymmetrised F Matrix for the S_4N_4 Molecule Based on the Assumption of a General Valence Force Field

	Internal Coordinate																	
	r_1	r_2	r_3	r_4	r_5	r_6	r_7	r_8	ϕ_1	ϕ_2	ϕ_3	ϕ_4	ϕ_5	ϕ_6	ϕ_7	ϕ_8	d_1	d_2
r_1	f_r	f_{r,r_2}	f_{r,r_3}	f_{r,r_4}	f_{r,r_5}	f_{r,r_6}	f_{r,r_6}	f_{r,r_8}	f_{r,ϕ_1}	f_{r,ϕ_2}	f_{r,ϕ_3}	f_{r,ϕ_4}	f_{r,ϕ_5}	f_{r,ϕ_6}	f_{r,ϕ_7}	f_{r,ϕ_8}	f_{r,d_1}	f_{r,d_2}
r_2	f_{r,r_2}	f_r	f_{r,r_4}	f_{r,r_3}	f_{r,r_6}	f_{r,r_5}	f_{r,r_8}	f_{r,r_6}	f_{r,ϕ_2}	f_{r,ϕ_1}	f_{r,ϕ_4}	f_{r,ϕ_3}	f_{r,ϕ_7}	f_{r,ϕ_8}	f_{r,ϕ_5}	f_{r,ϕ_6}	f_{r,d_1}	f_{r,d_2}
r_3	f_{r,r_3}	f_{r,r_4}	f_r	f_{r,r_2}	f_{r,r_6}	f_{r,r_8}	f_{r,r_5}	f_{r,r_6}	f_{r,ϕ_3}	f_{r,ϕ_4}	f_{r,ϕ_1}	f_{r,ϕ_2}	f_{r,ϕ_6}	f_{r,ϕ_5}	f_{r,ϕ_8}	f_{r,ϕ_7}	f_{r,d_1}	f_{r,d_2}
r_4	f_{r,r_4}	f_{r,r_3}	f_{r,r_2}	f_r	f_{r,r_8}	f_{r,r_6}	f_{r,r_6}	f_{r,r_5}	f_{r,ϕ_4}	f_{r,ϕ_3}	f_{r,ϕ_2}	f_{r,ϕ_1}	f_{r,ϕ_8}	f_{r,ϕ_7}	f_{r,ϕ_6}	f_{r,ϕ_5}	f_{r,d_1}	f_{r,d_2}
r_5	f_{r,r_5}	f_{r,r_6}	f_{r,r_6}	f_{r,r_8}	f_r	f_{r,r_3}	f_{r,r_2}	f_{r,r_4}	f_{r,ϕ_5}	f_{r,ϕ_6}	f_{r,ϕ_7}	f_{r,ϕ_8}	f_{r,ϕ_1}	f_{r,ϕ_2}	f_{r,ϕ_3}	f_{r,ϕ_4}	f_{r,d_2}	f_{r,d_1}
r_6	f_{r,r_6}	f_{r,r_5}	f_{r,r_8}	f_{r,r_6}	f_{r,r_3}	f_r	f_{r,r_4}	f_{r,r_2}	f_{r,ϕ_6}	f_{r,ϕ_5}	f_{r,ϕ_8}	f_{r,ϕ_7}	f_{r,ϕ_3}	f_{r,ϕ_4}	f_{r,ϕ_1}	f_{r,ϕ_2}	f_{r,d_2}	f_{r,d_1}
r_7	f_{r,r_6}	f_{r,r_8}	f_{r,r_5}	f_{r,r_6}	f_{r,r_2}	f_{r,r_4}	f_r	f_{r,r_3}	f_{r,ϕ_7}	f_{r,ϕ_8}	f_{r,ϕ_5}	f_{r,ϕ_6}	f_{r,ϕ_2}	f_{r,ϕ_1}	f_{r,ϕ_4}	f_{r,ϕ_3}	f_{r,d_2}	f_{r,d_1}
r_8	f_{r,r_8}	f_{r,r_6}	f_{r,r_6}	f_{r,r_5}	f_{r,r_4}	f_{r,r_2}	f_{r,r_3}	f_r	f_{r,ϕ_8}	f_{r,ϕ_7}	f_{r,ϕ_6}	f_{r,ϕ_5}	f_{r,ϕ_4}	f_{r,ϕ_3}	f_{r,ϕ_2}	f_{r,ϕ_1}	f_{r,d_2}	f_{r,d_1}
ϕ_1	f_{r,ϕ_1}	f_{r,ϕ_2}	f_{r,ϕ_3}	f_{r,ϕ_4}	f_{r,ϕ_5}	f_{r,ϕ_6}	f_{r,ϕ_7}	f_{r,ϕ_8}	f_ϕ	f_{ϕ,ϕ_2}	f_{ϕ,ϕ_3}	f_{ϕ,ϕ_4}	f_{ϕ,ϕ_5}	f_{ϕ,ϕ_6}	f_{ϕ,ϕ_7}	f_{ϕ,ϕ_8}	f_{d,ϕ_1}	f_{d_2,ϕ_1}
ϕ_2	f_{r,ϕ_2}	f_{r,ϕ_1}	f_{r,ϕ_4}	f_{r,ϕ_3}	f_{r,ϕ_6}	f_{r,ϕ_5}	f_{r,ϕ_8}	f_{r,ϕ_7}	f_{ϕ,ϕ_2}	f_ϕ	f_{ϕ,ϕ_4}	f_{ϕ,ϕ_3}	f_{ϕ,ϕ_7}	f_{ϕ,ϕ_8}	f_{ϕ,ϕ_5}	f_{ϕ,ϕ_6}	f_{d,ϕ_1}	f_{d_2,ϕ_1}
ϕ_3	f_{r,ϕ_3}	f_{r,ϕ_4}	f_{r,ϕ_1}	f_{r,ϕ_2}	f_{r,ϕ_7}	f_{r,ϕ_8}	f_{r,ϕ_5}	f_{r,ϕ_6}	f_{ϕ,ϕ_3}	f_{ϕ,ϕ_4}	f_ϕ	f_{ϕ,ϕ_2}	f_{ϕ,ϕ_6}	f_{ϕ,ϕ_5}	f_{ϕ,ϕ_8}	f_{ϕ,ϕ_7}	f_{d,ϕ_1}	f_{d_2,ϕ_1}
ϕ_4	f_{r,ϕ_4}	f_{r,ϕ_3}	f_{r,ϕ_2}	f_{r,ϕ_1}	f_{r,ϕ_8}	f_{r,ϕ_7}	f_{r,ϕ_6}	f_{r,ϕ_5}	f_{ϕ,ϕ_4}	f_{ϕ,ϕ_3}	f_{ϕ,ϕ_2}	f_ϕ	f_{ϕ,ϕ_8}	f_{ϕ,ϕ_7}	f_{ϕ,ϕ_6}	f_{ϕ,ϕ_5}	f_{d,ϕ_1}	f_{d_2,ϕ_1}
ϕ_5	f_{r,ϕ_5}	f_{r,ϕ_7}	f_{r,ϕ_6}	f_{r,ϕ_8}	f_{r,ϕ_1}	f_{r,ϕ_3}	f_{r,ϕ_2}	f_{r,ϕ_4}	f_{ϕ,ϕ_5}	f_{ϕ,ϕ_7}	f_{ϕ,ϕ_6}	f_{ϕ,ϕ_8}	f_ϕ	f_{ϕ,ϕ_2}	f_{ϕ,ϕ_3}	f_{ϕ,ϕ_4}	f_{d_2,ϕ_1}	f_{d,ϕ_1}
ϕ_6	f_{r,ϕ_6}	f_{r,ϕ_8}	f_{r,ϕ_5}	f_{r,ϕ_7}	f_{r,ϕ_2}	f_{r,ϕ_4}	f_{r,ϕ_1}	f_{r,ϕ_3}	f_{ϕ,ϕ_6}	f_{ϕ,ϕ_8}	f_{ϕ,ϕ_5}	f_{ϕ,ϕ_7}	f_{ϕ,ϕ_2}	f_ϕ	f_{ϕ,ϕ_4}	f_{ϕ,ϕ_3}	f_{d_2,ϕ_1}	f_{d,ϕ_1}
ϕ_7	f_{r,ϕ_7}	f_{r,ϕ_5}	f_{r,ϕ_8}	f_{r,ϕ_6}	f_{r,ϕ_3}	f_{r,ϕ_1}	f_{r,ϕ_4}	f_{r,ϕ_2}	f_{ϕ,ϕ_7}	f_{ϕ,ϕ_5}	f_{ϕ,ϕ_8}	f_{ϕ,ϕ_6}	f_{ϕ,ϕ_3}	f_{ϕ,ϕ_4}	f_ϕ	f_{ϕ,ϕ_2}	f_{d_2,ϕ_1}	f_{d,ϕ_1}
ϕ_8	f_{r,ϕ_8}	f_{r,ϕ_6}	f_{r,ϕ_7}	f_{r,ϕ_5}	f_{r,ϕ_4}	f_{r,ϕ_2}	f_{r,ϕ_3}	f_{r,ϕ_1}	f_{ϕ,ϕ_8}	f_{ϕ,ϕ_6}	f_{ϕ,ϕ_7}	f_{ϕ,ϕ_5}	f_{ϕ,ϕ_4}	f_{ϕ,ϕ_3}	f_{ϕ,ϕ_2}	f_ϕ	f_{d_2,ϕ_1}	f_{d,ϕ_1}
d_1	f_{r,d_1}	f_{r,d_1}	f_{r,d_1}	f_{r,d_1}	f_{r,d_2}	f_{r,d_2}	f_{r,d_2}	f_{r,d_2}	f_{d,ϕ_1}	f_{d,ϕ_1}	f_{d,ϕ_1}	f_{d,ϕ_1}	f_{d_2,ϕ_1}	f_{d_2,ϕ_1}	f_{d_2,ϕ_1}	f_{d_2,ϕ_1}	f_d	f_{d,d_2}
d_2	f_{r,d_2}	f_{r,d_2}	f_{r,d_2}	f_{r,d_2}	f_{r,d_1}	f_{r,d_1}	f_{r,d_1}	f_{r,d_1}	f_{d_2,ϕ_1}	f_{d_2,ϕ_1}	f_{d_2,ϕ_1}	f_{d_2,ϕ_1}	f_{d,ϕ_1}	f_{d,ϕ_1}	f_{d,ϕ_1}	f_{d,ϕ_1}	f_{d,d_2}	f_d

Table 5.8. Elements of the Symmetrised F Matrix for the S_4N_4 Molecule Expressed in Terms of Valence Force Constants

Symmetry block	Elements
A_1	$F_{11} = f_r + f_{r,r_2} + f_{r,r_3} + f_{r,r_4} + f_{r,r_5} + 2f_{r,r_6} + f_{r,r_8}$ $\quad F_{12} = f_{r,\phi_1} + f_{r,\phi_2} + f_{r,\phi_3} + f_{r,\phi_4} + f_{r,\phi_5} + f_{r,\phi_6} + f_{r,\phi_7} + f_{r,\phi_8}$ $\quad F_{13} = 2(f_{r,d_1} + f_{r,d_2})$ $F_{21} = f_{r,\phi_1} + f_{r,\phi_2} + f_{r,\phi_3} + f_{r,\phi_4} + f_{r,\phi_5} + f_{r,\phi_6} + f_{r,\phi_7} + f_{r,\phi_8}$ $\quad F_{22} = f_\phi + f_{\phi_1\phi_2} + f_{\phi_1\phi_3} + f_{\phi_1\phi_4} + f_{\phi_1\phi_5} + f_{\phi_1\phi_6} + f_{\phi_1\phi_7} + f_{\phi_1\phi_8}$ $\quad F_{23} = 2(f_{d_1\phi_1} + f_{d_2\phi_1})$ $F_{31} = 2(f_{r,d_1} + f_{r,d_2})$ $\quad F_{32} = 2(f_{d_1\phi_1} + f_{d_2\phi_1})$ $\quad F_{33} = f_d + f_{d_1d_2}$
B_1	$F_{11} = f_r - f_{r,r_2} - f_{r,r_3} + f_{r,r_4} + f_{r,r_5} - 2f_{r,r_6} + f_{r,r_8}$ $\quad F_{12} = f_{r,\phi_1} - f_{r,\phi_2} - f_{r,\phi_3} + f_{r,\phi_4} + f_{r,\phi_5} - f_{r,\phi_6} - f_{r,\phi_7} + f_{r,\phi_8}$ $F_{21} = f_{r,\phi_1} - f_{r,\phi_2} - f_{r,\phi_3} + f_{r,\phi_4} + f_{r,\phi_5} - f_{r,\phi_6} - f_{r,\phi_7} + f_{r,\phi_8}$ $\quad F_{22} = f_\phi - f_{\phi,\phi_2} - f_{\phi,\phi_3} + f_{\phi,\phi_4} + f_{\phi,\phi_5} - f_{\phi,\phi_6} - f_{\phi,\phi_7} + f_{\phi,\phi_8}$
B_2	$F_{11} = f_r + f_{r,r_2} + f_{r,r_3} + f_{r,r_4} - f_{r,r_5} - 2f_{r,r_6} - f_{r,r_8}$ $\quad F_{12} = f_{r,\phi_1} + f_{r,\phi_2} + f_{r,\phi_3} + f_{r,\phi_4} - f_{r,\phi_5} - f_{r,\phi_6} - f_{r,\phi_7} - f_{r,\phi_8}$ $\quad F_{13} = 2(f_{r,d_1} - f_{r,d_2})$ $F_{21} = f_{r,\phi_1} + f_{r,\phi_2} + f_{r,\phi_3} + f_{r,\phi_4} - f_{r,\phi_5} - f_{r,\phi_6} - f_{r,\phi_7} - f_{r,\phi_8}$ $\quad F_{22} = f_\phi + f_{\phi_1\phi_2} + f_{\phi_1\phi_3} + f_{\phi_1\phi_4} - f_{\phi_1\phi_5} - f_{\phi_1\phi_6} - f_{\phi_1\phi_7} - f_{\phi_1\phi_8}$ $\quad F_{23} = 2(f_{d_1\phi_1} - f_{d_2\phi_1})$ $F_{31} = 2(f_{r,d_1} - f_{r,d_2})$ $\quad F_{32} = 2(f_{d_1\phi_1} + f_{d_2\phi_1})$ $\quad F_{33} = f_d - f_{d_1d_2}$
E	$F_{11} = f_r + f_{r,r_2} - f_{r,r_3} - f_{r,r_4}$ $\quad F_{12} = f_{r,r_5} - f_{r,r_8}$ $\quad F_{13} = f_{r,\phi_1} + f_{r,\phi_2} - f_{r,\phi_3} - f_{r,\phi_4}$ $\quad F_{14} = f_{r,\phi_5} - f_{r,\phi_6} + f_{r,\phi_7} - f_{r,\phi_8}$ $F_{21} = f_{r,r_5} - f_{r,r_8}$ $\quad F_{22} = f_r - f_{r,r_2} + f_{r,r_3} - f_{r,r_4}$ $\quad F_{23} = f_{r,\phi_5} + f_{r,\phi_6} - f_{r,\phi_7} - f_{r,\phi_8}$ $\quad F_{24} = f_{r,\phi_1} - f_{r,\phi_2} + f_{r,\phi_3} - f_{r,\phi_4}$ $F_{31} = f_{r,\phi_1} + f_{r,\phi_2} - f_{r,\phi_3} - f_{r,\phi_4}$ $\quad F_{32} = f_{r,\phi_6} + f_{r,\phi_6} - f_{r,\phi_7} - f_{r,\phi_8}$ $\quad F_{33} = f_\phi + f_{\phi,\phi_2} - f_{\phi,\phi_3} - f_{\phi,\phi_4}$ $\quad F_{34} = f_{\phi,\phi_5} - f_{\phi,\phi_6} + f_{\phi,\phi_7} - f_{\phi,\phi_8}$ $F_{41} = f_{r,\phi_5} - f_{r,\phi_6} + f_{r,\phi_7} - f_{r,\phi_8}$ $\quad F_{42} = f_{r,\phi_1} - f_{r,\phi_2} + f_{r,\phi_3} - f_{r,\phi_4}$ $\quad F_{43} = f_{\phi,\phi_5} - f_{\phi,\phi_6} + f_{\phi,\phi_7} - f_{\phi,\phi_8}$ $\quad F_{44} = f_\phi - f_{\phi,\phi_2} + f_{\phi,\phi_3} - f_{\phi,\phi_4}$

in Table 5.9, together with the calculated and observed differences between the frequencies associated with the molecules $S_4{}^{14}N_4$ and $S_4{}^{15}N_4$. Hence it is clear that the observed frequency shifts are closely reproduced by the calculations. Table 5.10 lists the magnitudes of the actual stretching and bending force constants corresponding to the optimum fit of the measured frequencies.

The principal S-N stretching force constant, at 319 N m^{-1}, is of the same order as that calculated for the S_2N_2 molecule (328.5 N m^{-1}) and again much smaller than the empirical relationship between force constant and bond length derived by Glenser et al.[136] might lead one to expect, affording further evidence that this relationship is inapplicable to cyclic sulphur-nitrogen molecules (see also Table 5.11). It is also significantly smaller than the values previously calculated for the S_4N_4 molecule by Bragin and Evans (411 N m^{-1})[122] and by Sawodny et al. (505 N m^{-1}).[160] These discrepancies presumably arise, at least in part, from differences in the assignments, particularly affecting the b_1 fundamentals. The differences might also reflect differences in the off-diagonal elements of the F matrix; the comparatively large values of some of these are indicative of significant mixing of the internal coordinates, which may limit the significance of the force constants.

The differences between cyclic and acyclic sulphur-nitrogen species are also apparent, of course, in the relative magnitudes of the vibrational frequencies, with neither S_4N_4 nor S_2N_2 having a fundamental at a frequency exceeding 950 cm^{-1}. In the case of S_4N_4 in particular, the structure of the molecule dictates that any S-N stretching motion must necessarily involve some deformation of the S_4N_4 ring and vice versa, quite apart from any interaction between the different internal coordinates which may be incurred by the vibrations of a particular symmetry class. This is reflected in the dispersion of the observed frequencies attributable to

Table 5.9. Calculated F Matrix Elements and Isotopic Shifts for the Matrix Isolated S_4N_4 Molecule

Symmetry block	F matrix element	Numerical value[a]	Isotopic shift/cm^{-1} ($S_4{}^{14}N_4$-$S_4{}^{15}N_4$)	
			calc	obs
A_1	F_{11}	434.3	19.2	19.5
	F_{12}	-130.0		
	F_{13}	0.0		
	F_{22}	527.3	0.5	0.0
	F_{23}	120.0		
	F_{33}	225.5	1.8	2.0
B_1	F_{11}	339.0	19.6	-
	F_{12}	115.0		
	F_{22}	93.7	1.5	1.5
B_2	F_{11}	291.2	14.6	14.6
	F_{12}	230.0		
	F_{13}	0.0		
	F_{22}	715.5	13.6	13.7
	F_{23}	170.0		
	F_{33}	106.6	2.3	2.0
E	F_{11}	396.3	25.0	25.9
	F_{12}	72.0		
	F_{13}	20.0		
	F_{14}	-130.0		
	F_{22}	250.9	19.6	-
	F_{23}	-130.0		
	F_{24}	20.0		
	F_{33}	394.1	5.1	-
	F_{34}	0.0		
	F_{44}	722.2	7.1	6.3

Footnote

(a) Units are as follows: $F_{11}, F_{33}(A_1), F_{11}(B_1), F_{11}, F_{33}(B_2), F_{11}, F_{12}, F_{22}(E)$, N m^{-1}; $F_{22}(A_1), F_{22}(B_1), F_{22}(B_2), F_{33}, F_{44}(E)$, N m rad^{-2}; others, N rad^{-1}.

Table 5.10. Calculated Valence Force Constants for the S_4N_4 Molecule

Force constant	Numerical value[a]
f_r	319.4
$f_{r_1r_2}$	54.6
$f_{r_1r_3}$	-16.7
$f_{r_1r_4}$	-4.3
$f_{r_1r_5}$	71.8
$f_{r_1r_6}, f_{r_1r_3}$	0.0
f_d	166.1
$f_{d_1d_2}$	59.5
$f_{r_1d_1}, f_{r_1d_2}$	0.0
f_ϕ	115.2
$f_{\phi_1\phi_2}$	6.3
$f_{\phi_1\phi_3}$	45.6
$f_{\phi_1\phi_4}$	-18.4
$f_{\phi_1\phi_5}$	-22.5
$f_{\phi_1\phi_6}, f_{\phi_1\phi_7}, f_{\phi_1\phi_8}$	0.0
$f_{r_1\phi_1}$	50.9
$f_{r_1\phi_2}$	-32.3
$f_{r_1\phi_3}$	-32.3
$f_{r_1\phi_4}$	40.3
$f_{r_1\phi_5}$	-95.1
$f_{r_1\phi_6}, f_{r_1\phi_7}, f_{r_1\phi_8}$	0.0
$f_{d_1\phi_1}$	32.3
$f_{d_2\phi_1}$	5.7

Footnote

(a) All force constants expressed in N m^{-1}.

Table 5.11. Comparison of S-N Stretching Force Constants in S_4N_4 and S_2N_2 with those of Related Molecules

Molecule	f_{SN}(N m^{-1})	r_{SN}(Å)	Reference
F_3SN	1255	1.42	134
FSN	1071	1.45	161
ClSN	1009	1.45	89
$SO_2(NH_2)_2$	542	1.60	162
NH_2SO_3H	310	1.73	163
$(CF_3S)_3N$	340	1.70	164
SNO	522	~1.62	165
S_2N_2	328	1.65	This work
S_4N_4	319	1.62	This work

fundamentals of the S_4N_4 molecule throughout the range 180-950 cm^{-1} without any obvious gap separating one group from another. The same effect is evident in the magnitudes of the S-S-N bending force constants.

The magnitudes of the interaction force constants of S_4N_4, in common with those of S_2N_2 are consistent with a measure of electron delocalisation (involving for example, π - type interactions). The extent of such delocalisation may be gauged, however, by the fact that appreciable stretch-stretch interaction force constants are found only for pairs of S-N bonds which are adjacent. Comparison of the orbital energy levels of S_4N_4 and S_2N_2 derived from their He(I) and He(II) photoelectron spectra[137] shows certain differences which suggest that the smaller ring size and near-planarity of S_2N_2 are compatible with more extensive electron delocalisation.

The magnitude of the S-S stretching force constant implied by the present calculations (166 N m^{-1}) agrees closely with that deduced by Bragin and Evans[122] and is also comparable with that suggested by Cunningham's calculations.[126] On the other hand, it is five times greater than the value of 31 N m^{-1} proposed by Sawodny *et al.*[160] Although the reason for this discrepancy is not clear, the value obtained in the present study suggests substantial S-S bonding though with a bond order rather less than unity (compare, for example, the S-S stretching force constant of about 250 N m^{-1} estimated for the molecule HSSH[170]). Such a conclusion is consistent with the results of the most recent *ab initio* molecular-orbital calculations,[137] in which positive overlap populations are associated with adjacent pairs of sulphur atoms, albeit at a level significantly inferior to those associated with adjacent sulphur-nitrogen pairs. Similar calculations signify, on the other hand, that cross-ring S-S bonding is absent from the S_2N_2 molecule, interaction between the sulphur atoms being dominated by repulsion between the opposing lone-pair electrons.

Further information about the degree of S-S bonding in the S_4N_4 molecule

may be obtained by consideration of the intensities and depolarisation ratios of the Raman lines, in particular that near 220 cm^{-1} which is associated with the breathing motion of the S_4 tetrahedron. The relatively high intensity and apparent small depolarisation ratio of this line indicate that it is associated with a sizeable mean polarisability derivative suggestive of appreciable S-S bonding, by anology with similar evidence for Hf-B bonding in the molecule $Hf(BH_4)_4$ [166] and for Pb-Pb bonding in the polynuclear hydroxylead complexes $Pb_4(OH)_4^{4+}$ and $Pb_6(OH)_8^{4+}$. [167] On the other hand, the breathing modes of the P_4 units in the molecules P_4 and P_4O_6 occur at much higher frequencies (606 and 562 cm^{-1} respectively), suggesting that S-S bonding in S_4N_4 probably occurs to a somewhat lesser extent than P-P bonding in these two molecules.

5.6 Summary

The main conclusions to be drawn from the vibrational spectra of disulphur dinitride and tetrasulphur tetranitride, as measured and analysed in this project, may therefore be summarised as follows:-

(i) The vibrational frequencies associated with S-N stretching motions of the molecules are substantially lower than those characteristic of acyclic sulphur-nitrogen molecules, and the calculated S-N stretching force constants are conspicuously smaller than the experience of acyclic sulphur-nitrogen molecules would lead one to expect.[136]

(ii) The magnitudes of interaction force constants imply a significant degree of electron delocalisation extending over three or more atomic centres. This delocalisation appears to encompass the whole of the ring in S_2N_2 but to be rather less extensive in relation to the framework of S_4N_4.

(iii) There appears to be substantial cross-ring S-S bonding in S_4N_4, in agreement with the results of molecular-orbital calculations.[137] Some form of S-S interaction appears to be present in S_2N_2 but

molecular-orbital calculations suggest that this takes the form not of a bonding interaction but of a repulsion between the opposing lone-pair electrons.

Chapter 6

MATRIX ISOLATION OF CHROMIUM TRICHLORIDE OXIDE, $CrOCl_3$

6.1 Introduction

The maximum oxidation state exhibited by chromium is the one corresponding to the maximum involvement of its 3d and 4s electrons, namely Cr(VI), but the most stable state in an environment of donor atoms like O, F or Cl is Cr(III) (d^3); octahedral coordination of a Cr(III) centre affords a sort of 'half-filled shell' stability arising from single occupation of each t_{2g} level. The intermediate oxidation states Cr(IV) and Cr(V) do not often give rise to long-lived species in aqueous solution, and until recently were thought to be important under such conditions only as intermediates in redox reactions;[154] however, a stable, water-soluble chromium (V) compound, potassium bis (2-hydroxy-2-methylbutanoato) oxochromate (V) monohydrate, has now been prepared.[171]

In addition, a number of solid chromium (V) compounds have been isolated.[172-175] Thus, the pentafluoride, CrF_5, may be obtained by fluorination of the metal, the trifluoride or the trichloride,[176] whereas treatment of chromium (VI) oxide with a fluorinating agent like ClF_3 or BrF_3 yields the trifluoride oxide $CrOF_3$.[175] There are also known anionic complexes, viz $[CrOX_4]^-$ (X = F or Cl) and $[CrOCl_5]^{2-}$, obtained, for example, by reduction of chromium (VI) oxide with concentrated hydrochloric acid (or glacial acetic acid saturated with hydrogen chloride) in the presence of alkali-metal ions at 0°C.[177]

Chromium trichloride oxide, $CrOCl_3$, was first characterised as a product of the reaction between chromium (VI) oxide and either thionyl chloride or sulphuryl chloride.[178] In a subsequent study, the possibility of preparing chromium trichloride oxide by the following general route has been investigated:[179]

$$CrO_2Cl_2 + 2(X\text{-}Cl) \longrightarrow (X\text{-}O\text{-}X) + CrOCl_3 + \tfrac{1}{2}Cl_2$$

Consideration of the mean bond energies associated with the units X-Cl and X-O-X for a series of chlorides and the corresponding oxides, with due

allowance for the nature of the by-products of the above reaction, leads to the conclusion that boron trichloride is likely to be the most favourable reagent. In fact, the reaction between chromium dichloride dioxide and boron trichloride was the source of the samples of chromium trichloride oxide used in the present study.

Reports suggest that chromium trichloride oxide is photosensitive and thermally unstable, disproportionating at temperatures above $0^{o}C$ to give chromium dichloride dioxide, CrO_2Cl_2, and unidentified chromium (III) species.[178] The measured magnetic moment of 1.80 μ_B corresponds closely to the theoretical 'spin-only' value of 1.73 μ_B for the single unpaired electron associated with a Cr(V) species. An ultraviolet-visible absorption spectrum has also been reported,[180] showing a broad, intense absorption centred at 390 nm (log E ~3.2) with a shoulder at 522 nm (log E ~2.7) (Figure 6.1). The only other physical properties established for chromium trichloride oxide prior to the present study were as follows: (i) the infrared spectrum of a Nujol mull, characterised by very broad and indistinct bands,[181] and (ii) the ultraviolet photoelectron spectrum of the vapour (Fig 6.2);[181] the photoelectron spectrum has been interpreted in terms of a simplified molecular orbital scheme based on SCF-Xα calculations on the manganese trichloride oxide molecule[182] and illustrated in Figure 6.3. This interpretation has been supported by <u>ab initio</u> molecular orbital calculations on the $CrOCl_3$ molecule itself.[183]

The aim of the present study was to attempt the isolation of the molecule $CrOCl_3$ in a solid, inert matrix at low temperatures, and to investigate the effect of varying the nature of the matrix. Once this objective had been achieved, it was hoped to gain some insight into the structure and bonding of $CrOCl_3$ on the basis of the vibrational spectrum of the matrix-isolated molecule. The reasons for carrying out such a study may be summarised as follows:

(i) It afforded the possibility of comparing the main features of the

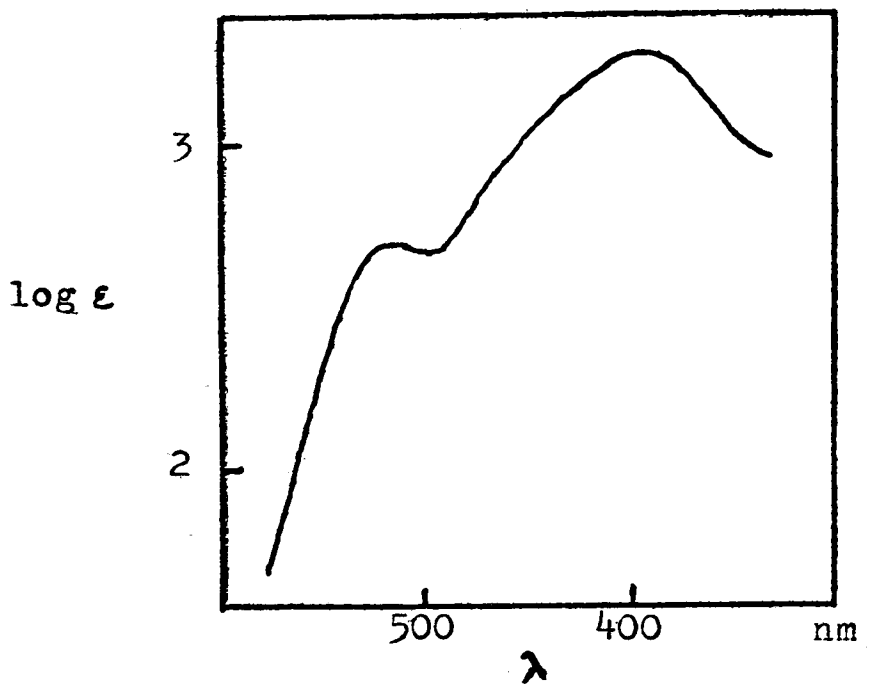

Fig. 6.1. Ultraviolet-visible absorption spectrum of $CrOCl_3$ (ref. 180).

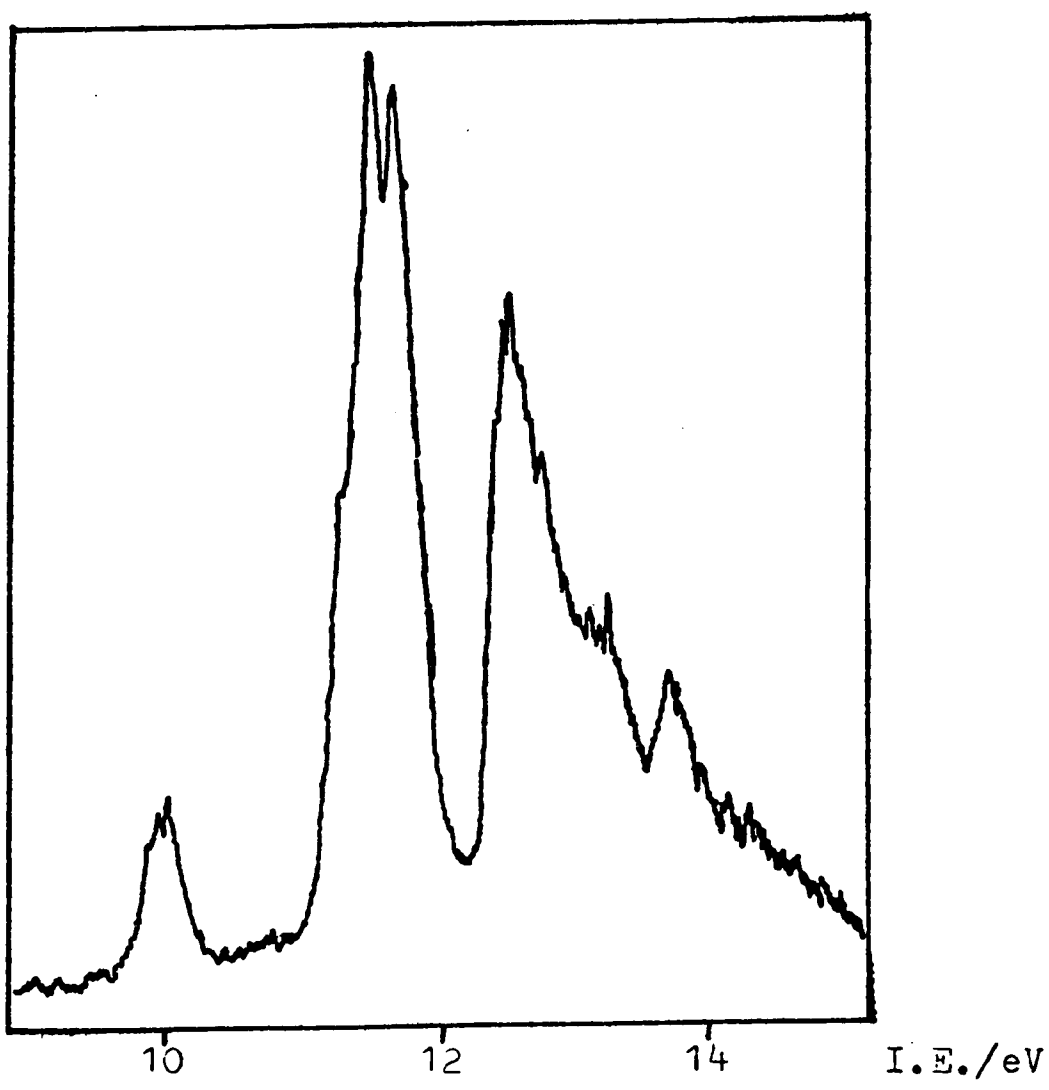

Fig. 6.2. Ultraviolet photoelectron spectrum of $CrOCl_3$ vapour (ref. 181).

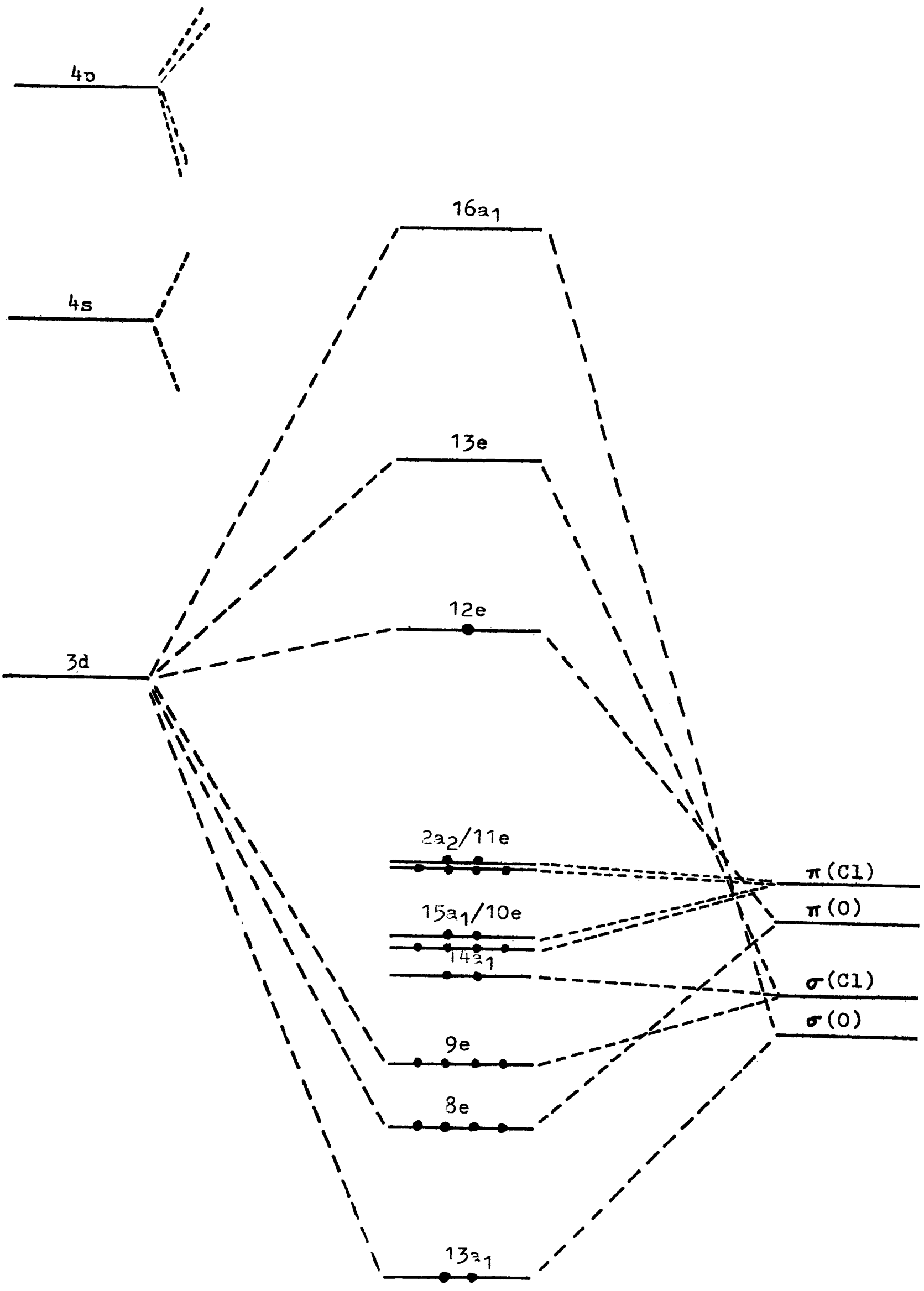

Fig. 6.3. Simplified M.O. scheme for $CrOCl_3$ (refs. 182,183).

vibrational spectrum of the $CrOCl_3$ molecule with those previously established for other molecules of the type MOX_3, such as trifluoramine oxide,[184] the well-defined phosphorous trihalide oxides,[185] and the recently characterised arsenic trihalide oxides.[186, 187]

(ii) The d^1 electronic configuration makes chromium trichloride oxide an ideal model for study by other techniques such as electron paramagnetic resonance[188] and electronic absorption spectroscopy.[189, 190]

(iii) The possible influence of Jahn-Teller distortions on the structure and vibrational properties of a d^1 system like $CrOCl_3$ is a matter of some interest. Consideration of the related VCl_4 molecule reveals that in the u.v.-visible absorption spectrum, the single band expected for a d^1 molecule is split into three components at 6600, 7880 and 9010 cm^{-1}, possibly as a consequence of Jahn-Teller effects.[191] In the vibrational spectrum of this molecule a splitting of up to 40 cm^{-1} on the part of the Raman-active mode $\nu_2(a_1)$ has been predicted.[192] However, no such splitting has been observed in the Raman spectrum measured for vanadium tetrachloride,[193] and it has been suggested that any permanent distortion from tetrahedral geometry is so small as to be undetectable.[194] The Jahn-Teller effect may, of course, not manifest itself in a permanent distortion of the molecule in its ground state; coupling of electronic and vibrational functions may simply lead to more complicated electronic and vibrational states.

(iv) Access to reasonably accurate vibrational frequencies for the ground state of the $CrOCl_3$ molecule is likely to assist the interpretation of fine structure in the u.v.-visible spectrum of the molecule.

(v) Added interest is imparted by the potential importance of chromium (V) species as reaction intermediates in redox reactions of chromium compounds, particularly in the oxidation of organic compounds by chromium (VI) species.[195]

6.2 Experimental

The samples of chromium trichloride oxide used in these experiments were

kindly provided by Mrs V H Thomas, having been prepared by the action of boron trichloride on chromium dichloride dioxide in a sealed vessel at -20°C, followed by sublimation of the product *in vacuo* from a trap held at 0°C to one held at -30°C. The material, consisting of black or very dark red crystals, was stored at liquid nitrogen temperatures in a Pyrex glass U-tube fitted with two Young's greaseless taps (Fig 6.4). Immediately prior to an experiment, the tube, held at 0°C, was opened to the vacuum line and evacuated for a few seconds in an attempt to minimise the amount of the more volatile disproportionation product CrO_2Cl_2 present in the sample.

Initially the U-tube was attached to the vacuum line and deposition attempted using pulses of a pre-mixed sample of the trichloride oxide vapour and matrix gas (matrix gas: $CrOCl_3$ = 500:1). This proved unsuccessful because the trichloride oxide was not sufficiently volatile at the temperatures required to minimise its disproportionation. In the remainder of the experiments, therefore, the U-tube was connected directly *via* a B 24 glass-to-metal tapered joint to the vacuum shroud of the matrix-isolation assembly, and the technique of slow, continuous co-condensation was employed. The sample was first evaporated at -30°C (this temperature being achieved by means of an acetone bath cooled by the addition of solid CO_2) and co-condensed with a stream of argon, deposited at a rate of 3 mmol/hr, over a period of one hour. The infrared spectrum of the resulting yellow deposit is shown in Figure 6.5. The predominance of bands attributable to the molecule CrO_2Cl_2 [196, 197] suggested the possibility of disproportionation and/or hydrolysis of the chromium trichloride oxide at the relatively low pressure used for deposition. In later experiments, therefore, the deposition rate was increased by raising the temperature of the trichloride oxide sample to -20°C and increasing the flow rate of the matrix gas to 4 mmol/hr. Employment of these conditions for a period of 1 - 1.5 hours resulted in an increase in the relative intensities of the bands attributable to the $CrOCl_3$

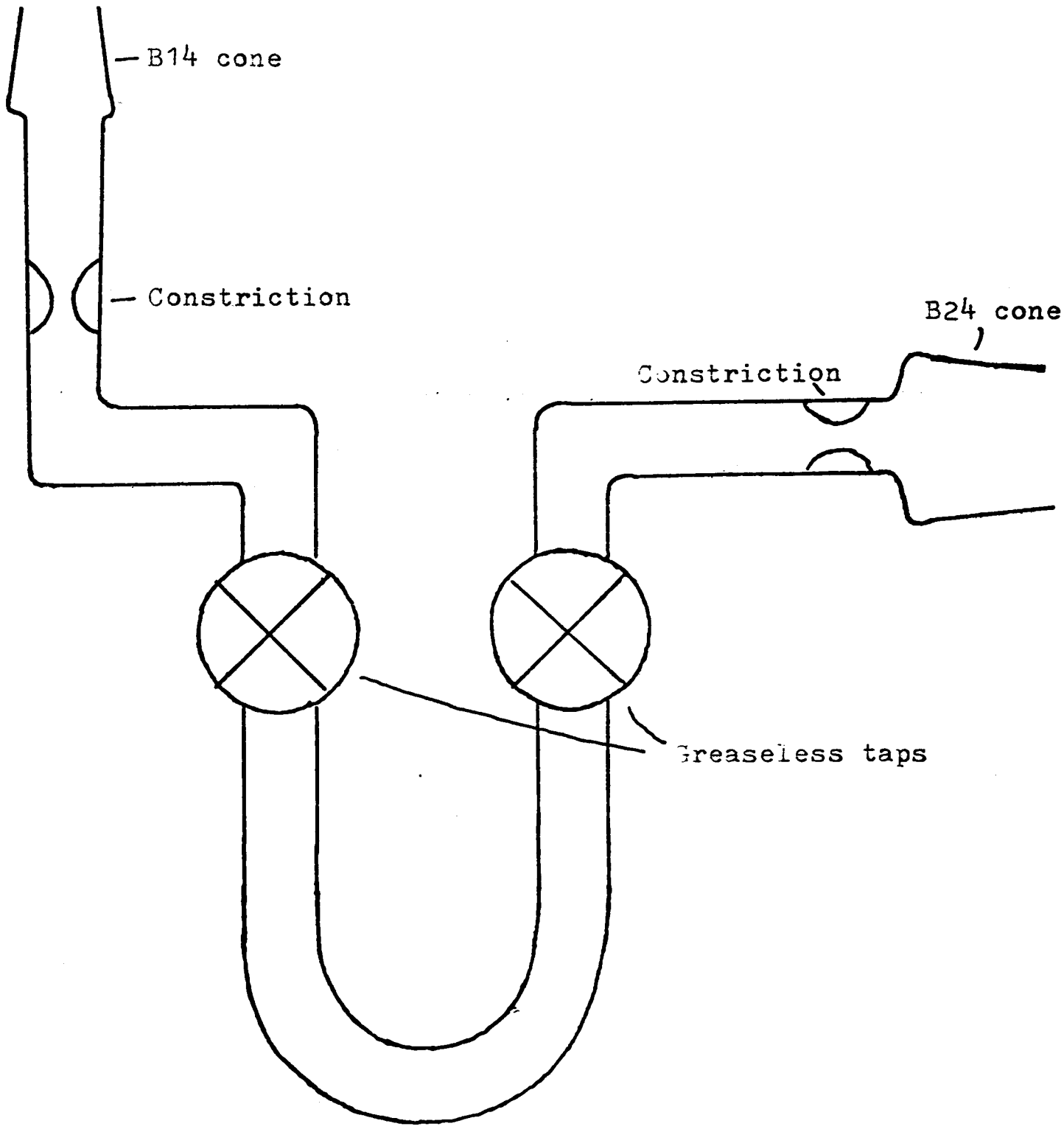

Fig. 5.4. U-tube used in $CrOCl_3$ matrix isolation studies.

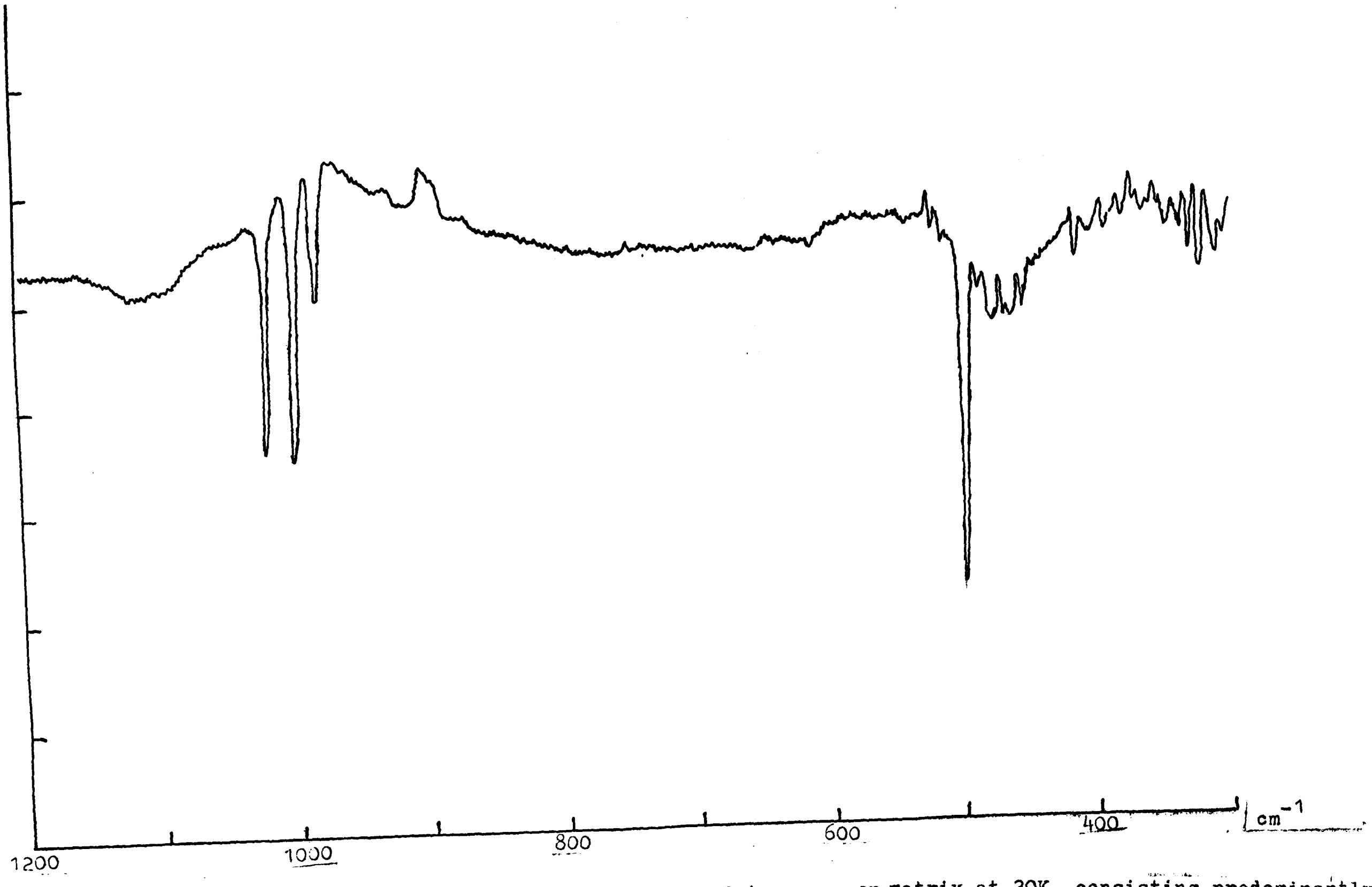

Fig. 6.5. Infrared spectrum of $CrOCl_3/CrO_2Cl_2$ isolated in an argon matrix at 20K, consisting predominantly of bands attributable to the latter.

molecule (Fig 6.6).

For Raman experiments, the temperature at which the sample was evaporated was raised to 0°C while the flow rate of the matrix gas remained at 4 mmol/hr. Total deposition times were in the order of 1.5 hours. Attempts to excite the Raman spectrum of such a deposit using either of the principal lines of the argon ion laser (at 514.5 and 488.0 nm) were unsuccessful even at very low laser powers. It was invariably found that the incident radiation produced a discolouration where it impinged upon the deposit, and in one experiment detached itself from the copper block. Recourse was therefore made to the helium-neon laser despite its deficiencies for matrix-isolation studies, and all the results reported here were obtained using excitation at 632.8 nm with a power level at the sample in the order of 50 mW.

With the production of a deposit relatively free from chromium dichloride dioxide, as judged by its infrared spectrum, the effect of ultraviolet photolysis was investigated. The matrix was irradiated at 20K *via* a water filter with the output from a high-pressure mercury arc and its infrared spectrum re-examined to determine the outcome of this treatment. Photolysis times varied from 10 minutes to about 12 hours, but in no case did irradiation produce any visible effect on the matrix or bring about any change in the infrared spectrum. This is perhaps surprising in view of the broadness of the u.v.-visible absorption band which has been associated with the $CrOCl_3$ molecule,[180] and the extreme sensitivity of matrices containing chromium trichloride oxide to laser irradiation observed in the Raman studies. Future experiments might therefore include investigations of the effect of using the output of the argon-ion laser to irradiate a matrix-isolated sample the behaviour of which is monitored by its infrared spectrum.

6.3 Infrared Spectra

The infrared spectrum initially measured for a mixture of the molecules $CrOCl_3$ and CrO_2Cl_2 in an argon matrix is shown in Figure 6.5. The spectra

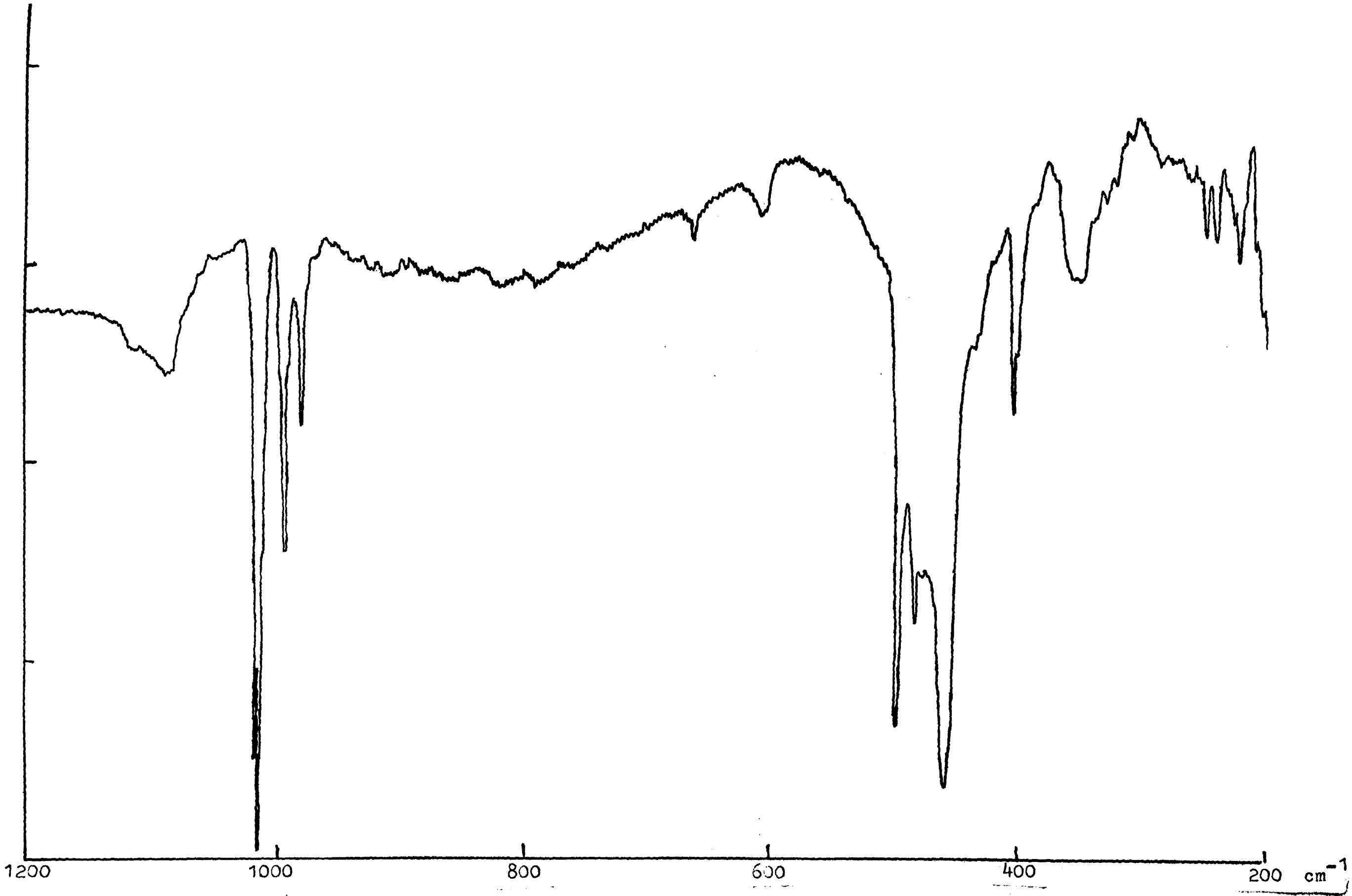

Fig. 6.6. Infrared spectrum of $CrOCl_3/CrO_2Cl_2$ in an argon matrix after alteration of deposition conditions.

subsequently obtained from nitrogen, argon and krypton matrices after alteration of the deposition conditions are shown in Figures 6.7, 6.8 and 6.9, and expanded versions of the relevant portions of these spectra are shown in Figures 6.10 and 6.11. The measured frequencies of the absorptions, with their likely assignments, are listed in Table 6.1.

The identity of the spectral bands thought to arise from the fundamental vibrations of the $CrOCl_3$ molecule has been checked by the invariance of their relative intensities. Assignments have been made on the basis of a simple pyramidal structure of C_{3v} symmetry, for which six fundamental vibrations are expected ($3a_1 + 3e$), all active in both infrared absorption and Raman scattering. Hence the observed frequencies are expected to correspond fairly closely to those of the molecule $VOCl_3$, which are well documented,[185, 198-200] and to those of $AsOCl_3$, recently characterised at low temperatures.[186] In fact, the frequencies, and the assignments of the stretching fundamentals, correspond to those reported as the result of a more recent matrix-isolation study of chromium trichloride oxide carried out independently by Ogden and co-workers.[201] The following assignments have been made.

(a) Chromium-oxygen stretching mode, $\nu_1(a_1)$. Three bands were generally observed in the region of the infrared spectrum associated with Cr = O stretching motions, the measured frequencies being typically 1018.6, 1000.2 and 988.4 cm^{-1} (for an argon matrix). The first of these is assigned to $\nu_1(a_1)$, the Cr = O stretching fundamental of $CrOCl_3$; the corresponding fundamental of the gaseous $VOCl_3$ molecule occurs at 1042.5 cm^{-1} [185] and that of the matrix-isolated $AsOCl_3$ molecule at *ca* 995 cm^{-1}.[186] The two bands at lower frequency are assigned to the Cr = O stretching fundamentals of CrO_2Cl_2 (recently reported to occur at 995 and 981 cm^{-1} in an argon matrix[202]). The band at 1018.6 cm^{-1} exhibited splitting with components separated by intervals in the order of 1 cm^{-1}. This was reproduced in several experiments and with all

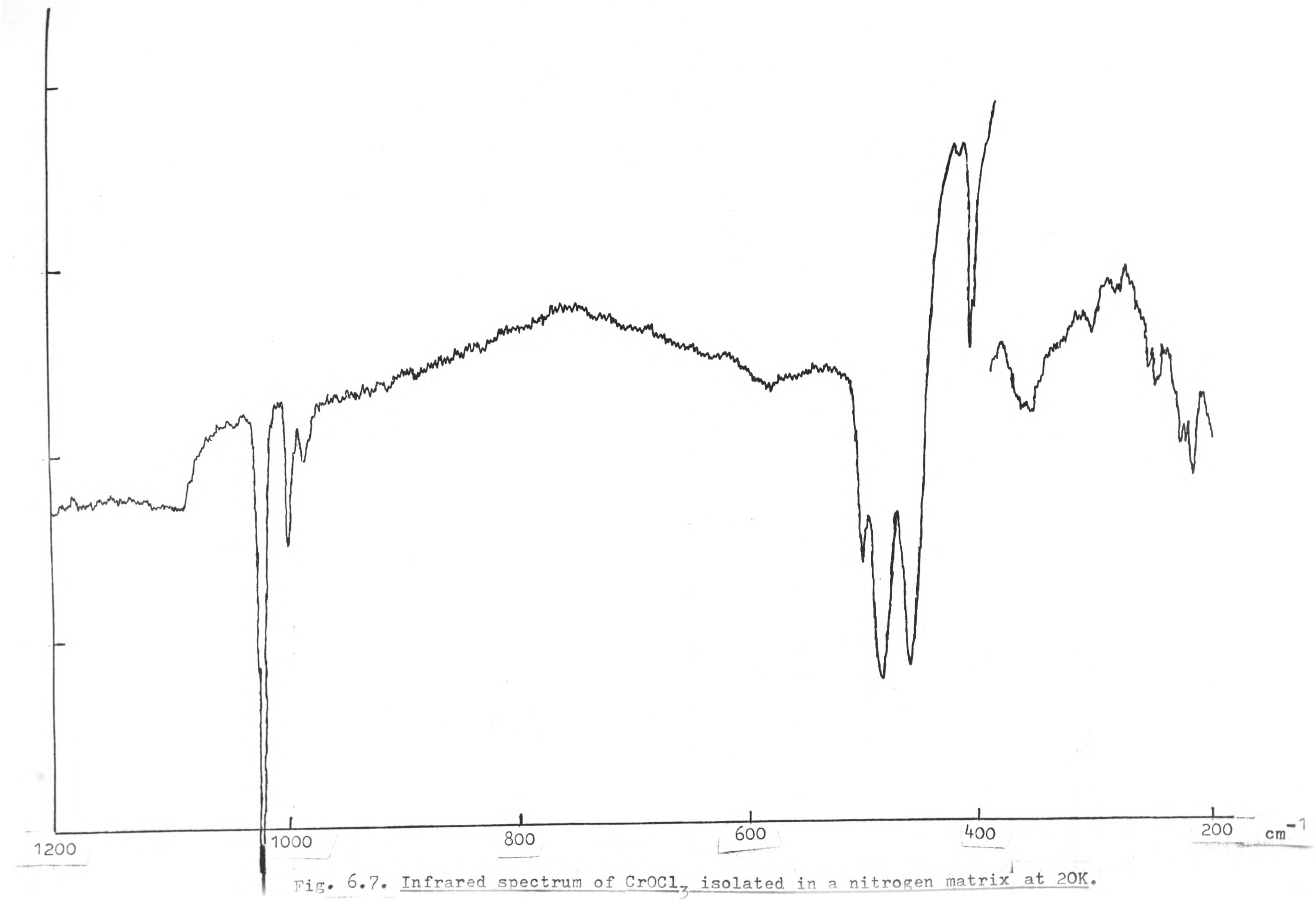

Fig. 6.7. Infrared spectrum of $CrOCl_3$ isolated in a nitrogen matrix at 20K.

Fig. 6.8. Infrared spectrum of $CrOCl_3$ isolated in an argon matrix at 20K.

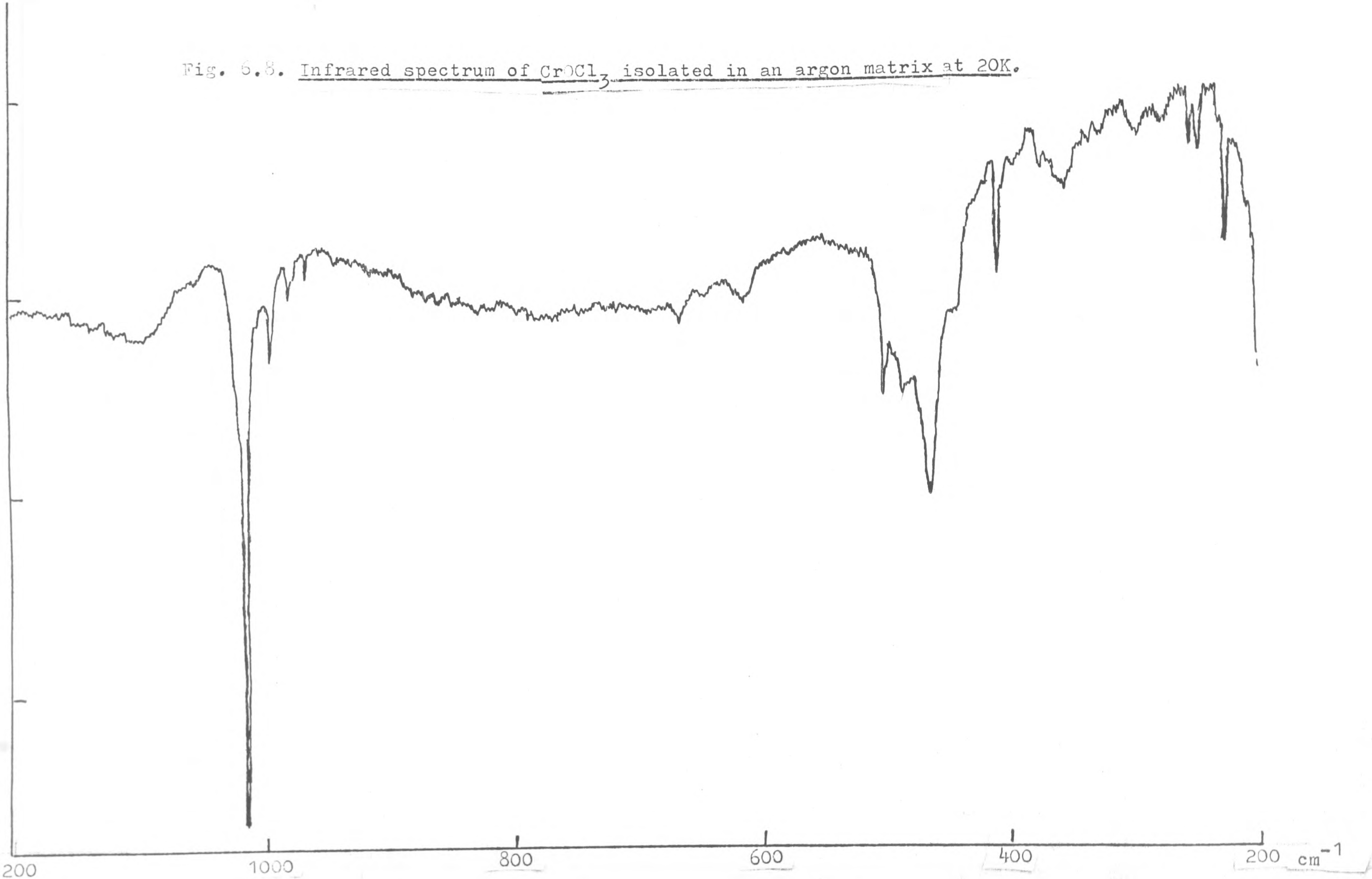

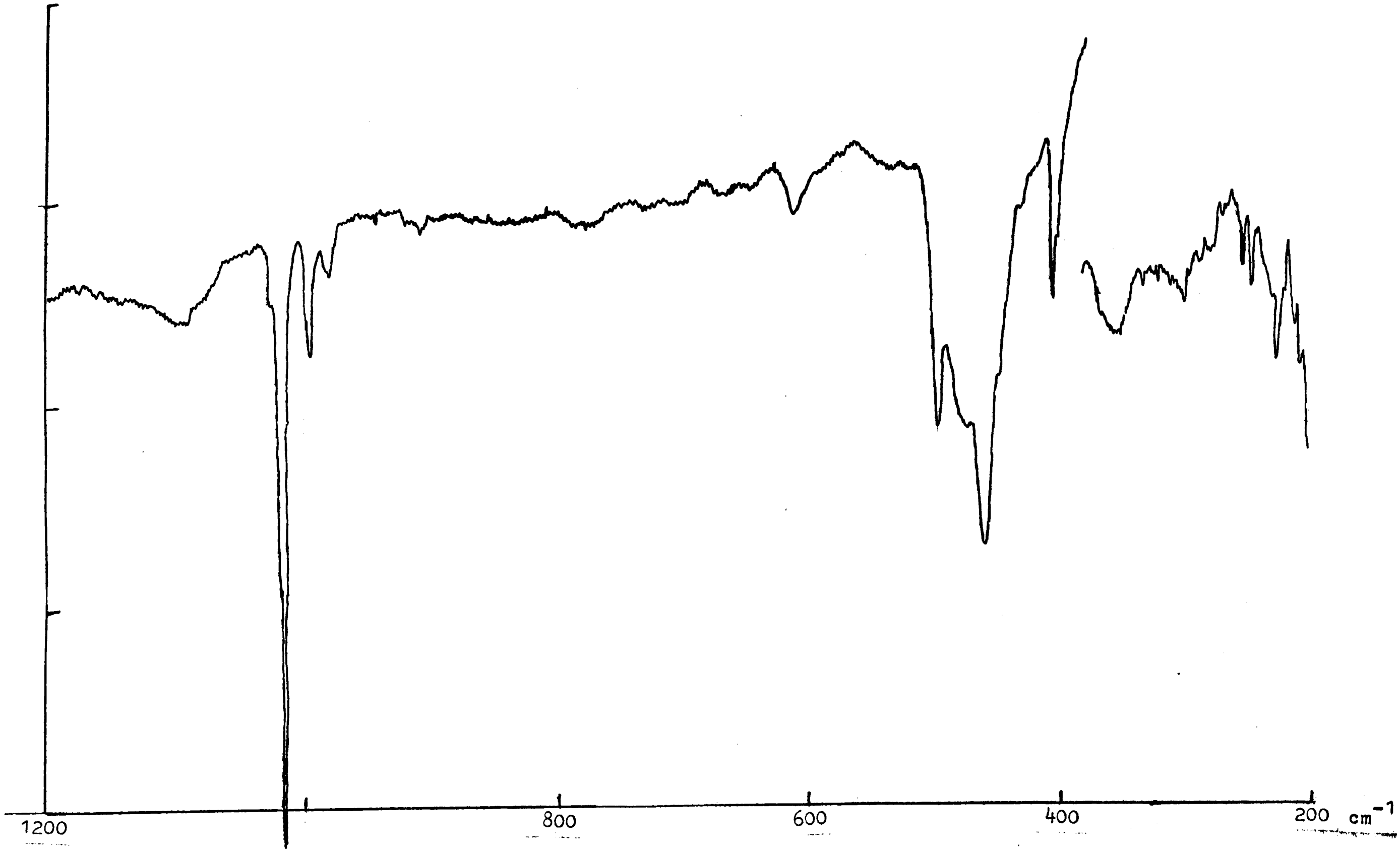

Fig. 6.9. Infrared spectrum of $CrOCl_3$ isolated in a krypton matrix at 20K.

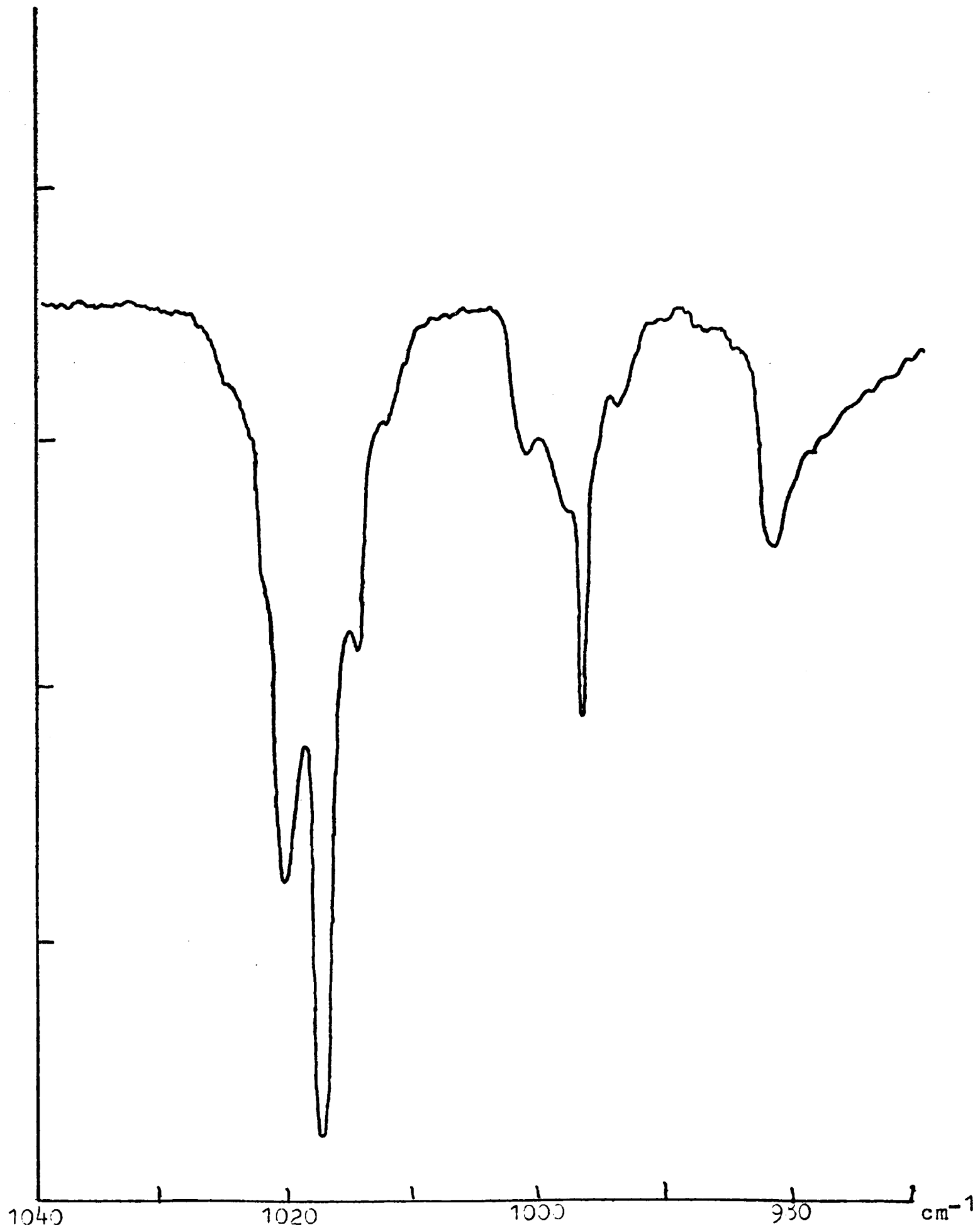

Fig. 6.10. Bands in the infrared spectrum of $CrOCl_3/CrO_2Cl_2$ isolated in an argon matrix.

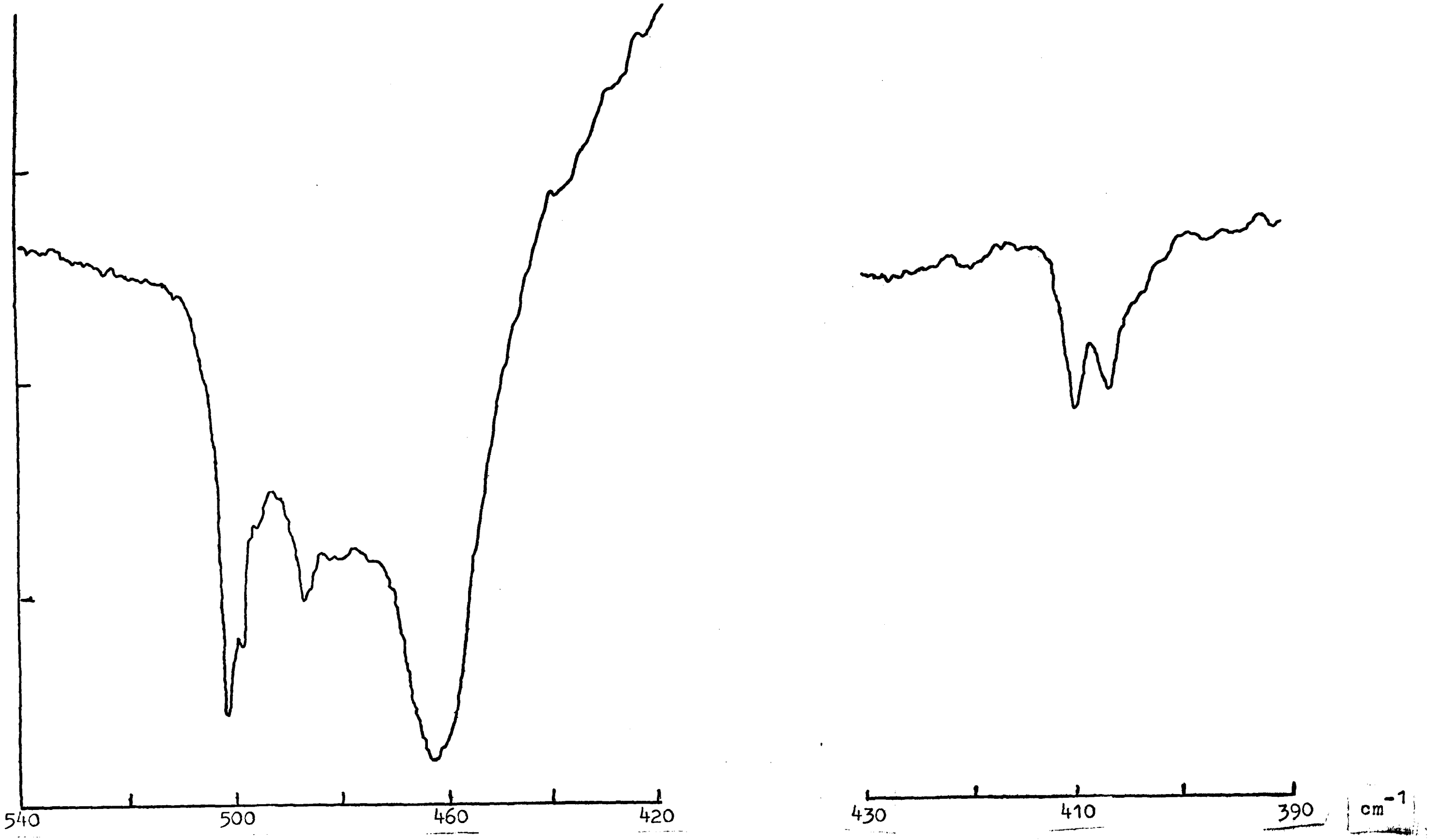

Fig. 6.11. Bands in the infrared spectrum of $CrOCl_3$ isolated in an argon matrix.

Table 6.1. Frequencies and Assignments of Infrared Bands Observed in $CrOCl_3$ Matrix Isolation Studies

Frequency/cm^{-1}				Assignment
Solid, 30K	N_2 matrix, 20K	Ar matrix, 20K	Kr matrix, 20K	
1020	1024.3 1022.0 1019.8 1017.4	1021.4 1013.6 1016.0	1018.5 1016.2 1013.7	$\nu_1(a_1)CrOCl_3$
989	999.6	1000.2	995.0	$\nu_6(b_1)CrO_2Cl_2$
975	985.0	988.4	983.1	$\nu_1(a_1)CrO_2Cl_2$
490	499.2	501.2	498.5	$\nu_8(b_2)CrO_2Cl_2$
480	483	486	483	?
463	458.0	462.0	459.3	$\nu_4(e)\ CrOCl_3$
408	408.2 405.0	406.7 403.4	407.0 403.9	$\nu_2(a_1)CrOCl_3$
368	360	361	355	$\nu_3(a_1)CrO_2Cl_2$
300	303	308	302	?
264	254.0	253.6	253.9	$\nu_9(b_2)CrO_2Cl_2$
251	247.8	248.0	248.2	?
225	225.9	226.5	226.6	$\nu_5(e)\ CrOCl_3$?

three of the matrix gases used. The possibility that the splitting arises from isotopic variations at the chromium atom was considered, but initially discounted on the grounds that the intensity pattern of the multiplet did not correspond to the natural abundances of the different isotopes (^{50}Cr, ca 4%; ^{52}Cr, 84%; ^{53}Cr, 10% and ^{54}Cr, 2%[203]). Another possibility is that the splitting arises from chlorine isotopic effects, which should result in four bands with intensities in order of decreasing frequency in the ratio 27:27:9:1; if this interpretation were correct, it would indicate significant coupling between the a_1 modes ν_1 and ν_2 which involve mainly stretching of the Cr = O and Cr-Cl bonds respectively. Again, however, the observed intensity pattern did not fit in with this interpretation. It has been suggested by Ogden[201] that the observed multiplet may arise from a superposition of chromium isotope patterns resulting from the occurrence of different trapping sites in the matrix.

(b) Chromium-chlorine stretching modes, $\nu_2(a_1)$ and $\nu_4(e)$. Several bands were observed between 400 and 500 cm^{-1}, within the range of frequencies associated with Cr-Cl stretching vibrations.[197] Two of these, with measured frequencies in an argon matrix of 462.0 and 406.7 cm^{-1}, appeared to vary in intensity in the same manner as the band at 1018.6 cm^{-1}, and have therefore been assigned to the Cr-Cl stretching fundamentals of $CrOCl_3$ (the corresponding frequencies of the gaseous $VOCl_3$ molecule are 503 and 409.5 cm^{-1};[185] those of matrix-isolated $AsOCl_3$ are ca 434 and 375 cm^{-1}.[186]). The absorption lower in frequency is assigned to ν_2 (a_1) and that higher in frequency to ν_4 (e) by analogy with other species of the type O = MX_3 (M = metal atom; X = halogen) wherein the symmetric M-X stretching fundamental tends to be lowered in energy by mixing with the M = O stretching vibration belonging to the same symmetry class.[204] The band at 406.7 cm^{-1} exhibited splitting with components separated by intervals in the order of 2-3 cm^{-1}; in this case the splitting probably does arise from chlorine isotopic effects, as proposed by Ogden.[201] A

band observed at 501.2 cm^{-1} was often the strongest in the spectrum, particularly in the earlier experiments; its frequency is consistent with its assignment to ν_8 (b_2) of the matrix-isolated CrO_2Cl_2 molecule.[202] The origin of the band at 486 cm^{-1} is uncertain but may be found in other disproportionation products of chromium trichloride oxide.

(c) Deformation modes. The deformation modes of the gaseous molecule $VOCl_3$, ν_3 (a_1), ν_5 (e) and ν_6 (e) occur at 163.0, 246.0 and 124.5 cm^{-1} respectively.[185] Hence, in the case of $CrOCl_3$, the first and third of these are likely to occur at frequencies too low to allow observation in the present study, which was confined to the region 200–4000 cm^{-1}. However, if the frequencies are similar to those attributed to $VOCl_3$, the mode ν_5 (e), corresponding to the $CrCl_3$ rocking motion, should be observable. In fact, several bands were located at the low-frequency end of the spectrum, but these were often indistinct and barely identifiable above the 'noise' level (made worse in this region by the absorptions due to the rotational spectrum of atmospheric water vapour). A band at 226.5 cm^{-1} exhibited by an argon matrix may be assignable to ν_5 (e) of $CrOCl_3$ (cf ν_5 (e) = ca 249 cm^{-1} for matrix-isolated $AsOCl_3$[186]), although this frequency does not correspond very closely to that of the Raman scattering thought to arise from the same mode (see next section). Some of the bands observed at low frequencies presumably originate in deformation modes of the molecule CrO_2Cl_2; for example, the broad absorption at 360 cm^{-1} corresponds closely in frequency to that (356 cm^{-1}) reported for ν_3 (a_1) of the CrO_2Cl_2 molecule in an argon matrix.[202]

6.4 Raman Spectra

The light scattering excited at 632.8 nm from samples formed by co-deposition of chromium trichloride oxide with one of various matrix gases is illustrated in Figures 6.12 to 6.14. The measured frequencies of the Raman lines, together with their likely assignments, are listed in Table 6.2. Attempts to measure

Fig. 6.12. Raman spectrum of $CrOCl_3$ isolated in a nitrogen matrix.

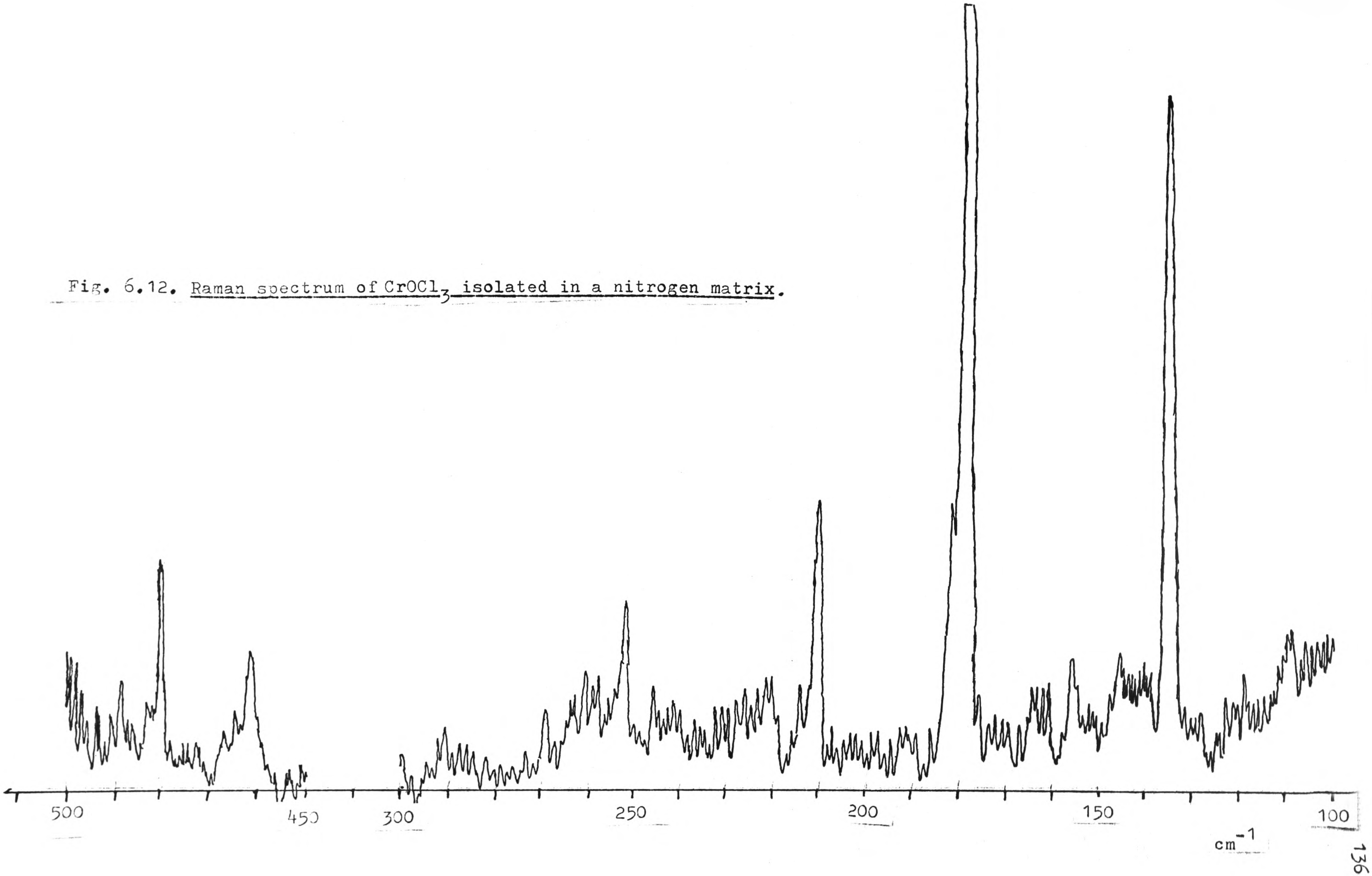

Fig. 6.13. Raman spectrum of $CrOCl_3$ isolated in an argon matrix.

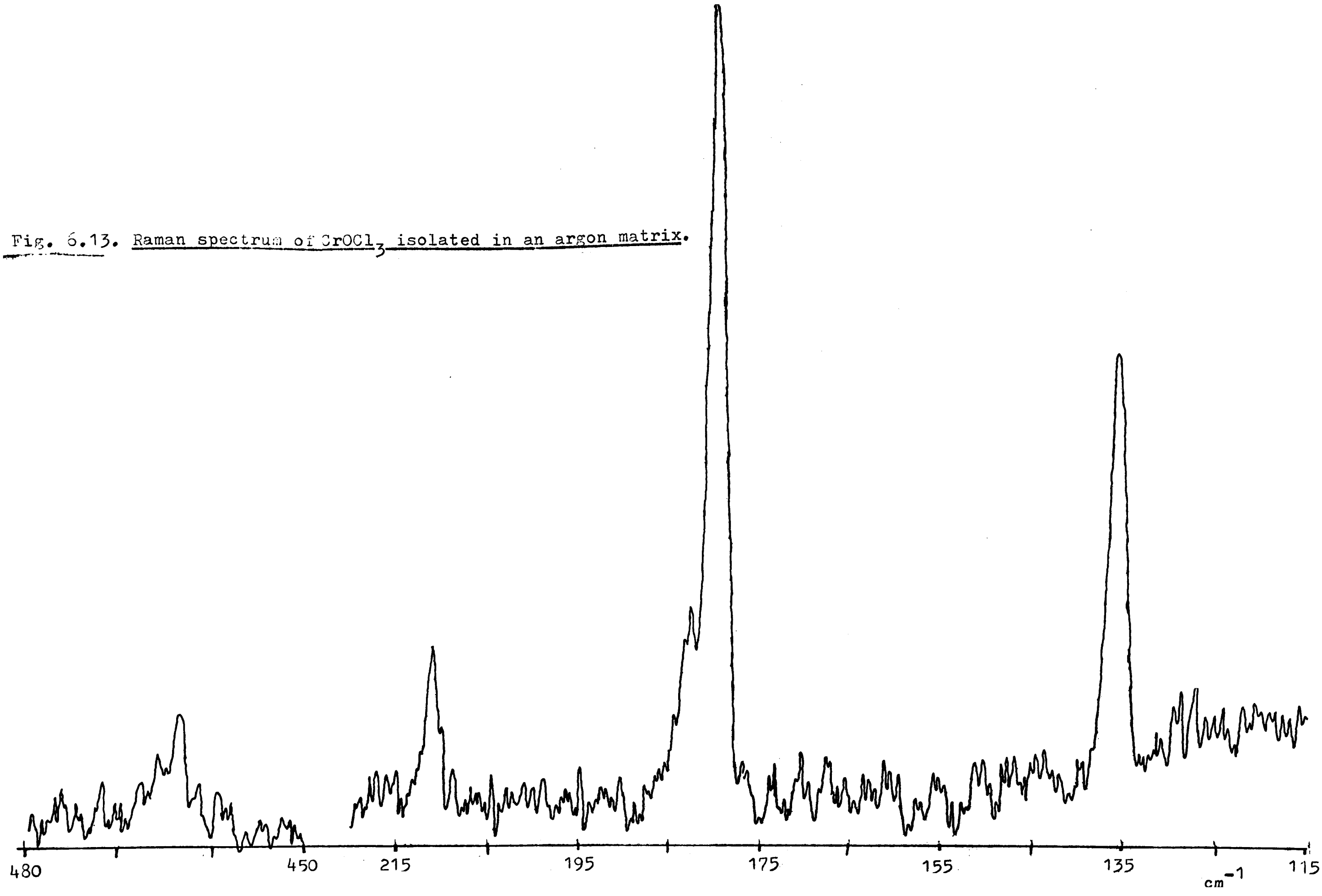

Fig. 6.14. Raman spectrum of $CrOCl_3$ isolated in a krypton matrix.

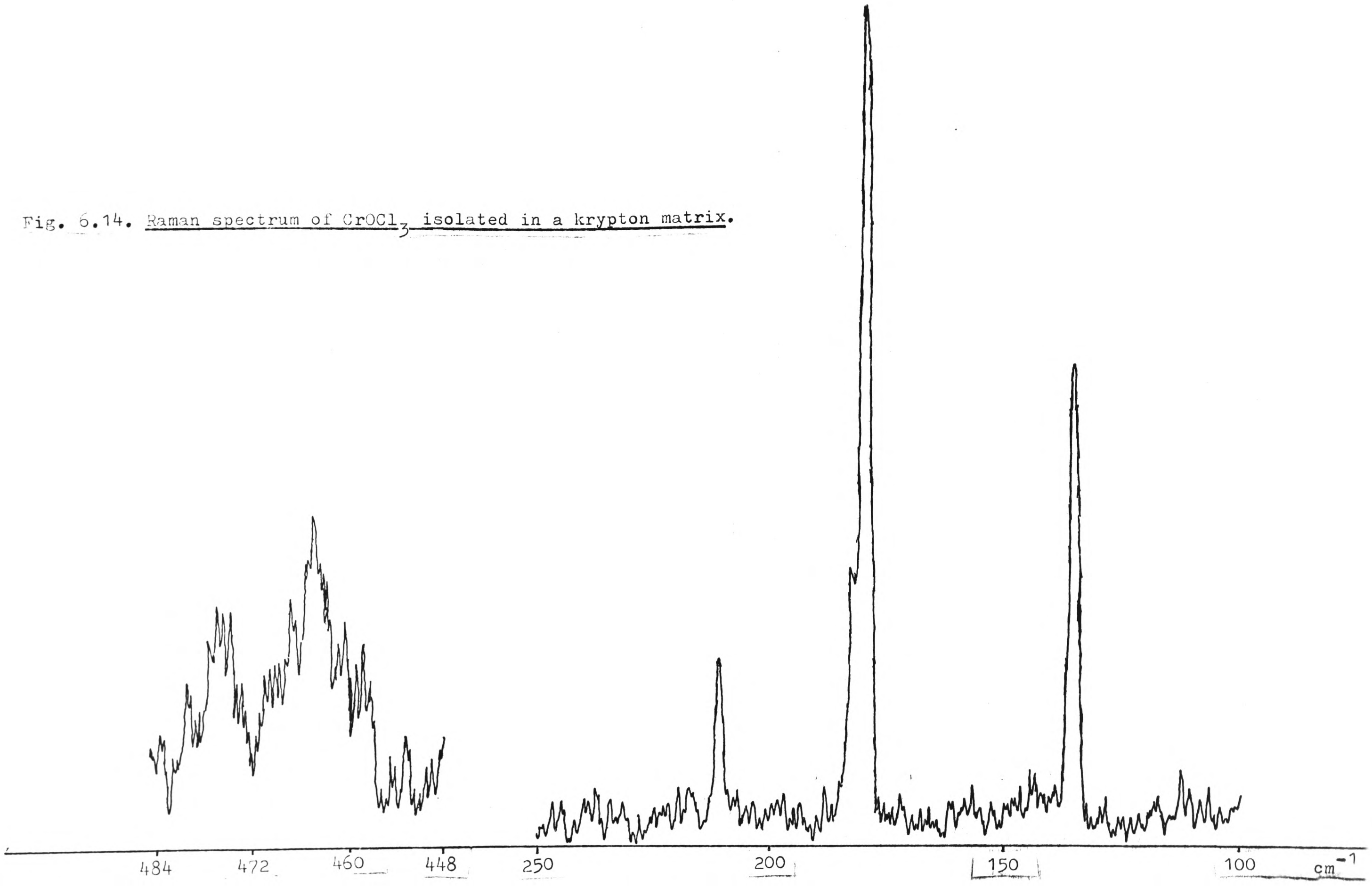

Table 6.2. Frequencies and Assignments of Raman Bands Observed in $CrOCl_3$ Matrix Isolation Studies

Frequency/cm^{-1}			Assignment
N_2 matrix,20K	Ar matrix,20K	Kr matrix,20K	
464	463	465	$\nu_4(e)CrO_2Cl_2$
210.4	211.4	211.1	$\nu_5(e)$ $CrOCl_3$
178.6	178.9	179.3	$\nu_3(a_1)CrOCl_3$
135.0	134.7	134.8	$\nu_6(e)$ $CrOCl_3$

the depolarisation ratios of the observed features were unsuccessful, probably because the matrices were too frosty. The difficulty experienced in measuring the Raman spectrum of matrix-isolated chromium trichloride oxide, particularly using the argon-ion laser, is scarcely surprising in view of the intensity of the visible absorption which the molecule exhibits.[180]

The observed Raman spectra show just three strong bands of constant relative intensity; the measured frequencies for an argon matrix are 211.4, 178.9 and 134.7 cm^{-1}. Consideration of both the Raman spectrum of the $VOCl_3$ molecule[109] and the infrared spectrum of the matrix-isolated $CrOCl_3$ molecule described in the preceding section suggests that these frequencies can be reasonably assigned to the three deformation modes of $CrOCl_3$, namely $\nu_5(e)$, $\nu_3(a_1)$ and $\nu_6(e)$ respectively. For species of the type $O = MX_3$ it is generally observed that the frequency of the a_1 deformation mode lies between those of the other two modes both belonging to the e symmetry class.[205]

However, if the strong lines observed in the present study are genuinely attributable to the matrix-isolated $CrOCl_3$ molecule, a surprising feature of the Raman spectrum is that little or no scattering could be observed in the frequency ranges associated with Cr = O or Cr-Cl stretching fundamentals. In fact no scattering could be discerned in the region near 1000 cm^{-1}, in stark contrast to the infrared spectrum of the matrix-isolated $CrOCl_3$ molecule, and the only feature reproducibly observed in the region 400-500 cm^{-1} characteristic of Cr-Cl stretching modes was a broad, comparatively weak band near 460 cm^{-1}, corresponding quite closely to the infrared band previously assigned to $\nu_4(e)$, the antisymmetric Cr-Cl stretching mode of $CrOCl_3$. The absence of features attributable to the CrO_2Cl_2 molecule is also surprising, but reference to the visible absorption spectrum of this molecule (Fig 6.15)[197] indicates quite strong absorption even at 632.8 nm; in fact the

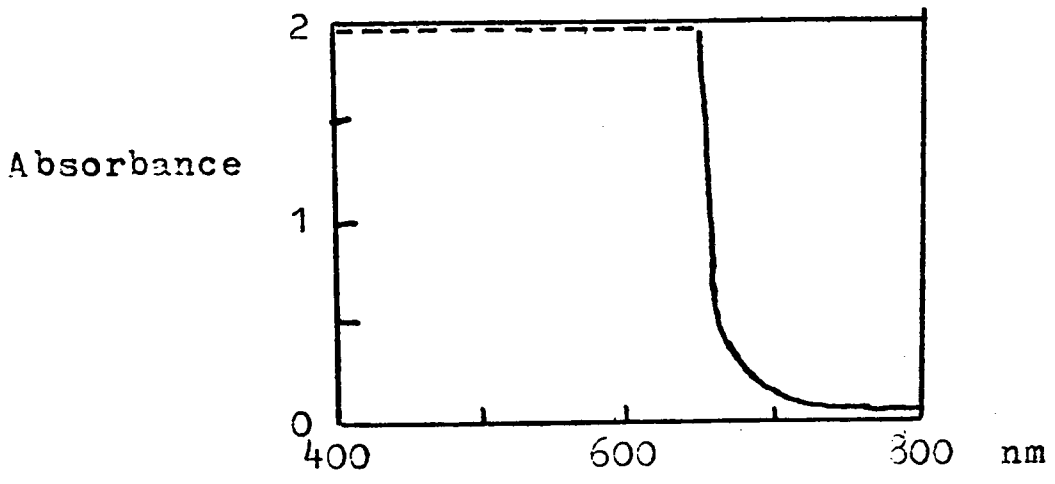

Fig. 6.15. Visible absorption spectrum of CrO_2Cl_2 (ref. 197).

Raman spectrum of chromium dichloride dioxide previously reported[197] was excited by the so-called D-lines in the emission spectrum of a potassium arc, which occur at 766.5 and 769.9 nm.

One explanation for the apparent enhancement in intensity of certain Raman bands relative to others is the occurrence of a resonance Raman effect.[42-44] The usual requirement for such an effect is that the excitation frequency is close to the frequency of an allowed electronic transition; this requirement could well be fulfilled in the present case by excitation at 632.8 nm, in view of the broad and intense nature of the visible absorption bands exhibited by chromium trichloride oxide.[180] It is normally observed that the bands which exhibit a pronounced enhancement of intensity are those corresponding to modes which are vibronically active in an allowed electronic transition.[42-44]

If the exciting frequency ν_o is well removed from that of any electronic transition and the initial and final vibrational states both involve the electronic ground state, the scattered intensity I is given by

$$I = \frac{2^7\pi^5}{3^2c^4} I_0 (\nu_0 \pm \nu_i)^4 \sum_{ij} |(\alpha_{ij})|^2 \qquad (6.1)$$

where I_o is the incident intensity, $\nu_o \pm \nu_i$ represents the scattered frequency and the α_{ij}'s are the components of the polarisability tensor. The breakdown of this expression under resonance conditions has been rationalised by Albrecht[43, 206, 207] using the so-called adiabatic approximation, in which the electronic and vibrational wavefunctions are assumed to be completely separable allowing the former to be expressed as a Taylor series in terms of the nuclear displacements. The scattering tensor is then expressed as the sum of an A term and a B term, which respectively lead to the following expressions for the frequency dependence of the scattered intensity (e and f referring to the appropriate electronic states):

$$\text{A Term:} \qquad I \propto (\nu_0 - \nu_i)^4 \left[\frac{\nu_e^2 + \nu_0^2}{(\nu_e^2 - \nu_0^2)^2} \right]^2 \qquad (6.2)$$

$$\text{B Term:} \qquad I \propto (\nu_0 - \nu_i)^4 \left[\frac{\nu_e \nu_f + \nu_0^2}{(\nu_e^2 - \nu_0^2)(\nu_f^2 - \nu_0^2)} \right]^2 \qquad (6.3)$$

The A term corresponds to vibrational interaction with a single excited electronic state by means of a Franck-Condon overlap integral and is non-zero only in the case of totally symmetric modes, which are always active in resonance Raman scattering. The B term, on the other hand, corresponds to vibronic mixing of two states, and is found to be non-zero for any vibration belonging to a symmetry species which is contained in the direct product of the representations of these two states.

In the case of the chromium trichloride oxide molecule, the a_1 modes will be subject to enhancement <u>via</u> the A term; in addition, the e modes may also be enhanced, in this case <u>via</u> the B term. Moreover, with certain exceptions (eg NO_2 [51]), it is normally found that resonance enhancement is more marked for stretching than for deformation modes; comparison of the results obtained in the present study with the published Raman spectra of the molecules $VOCl_3$ [185] and $AsOCl_3$ [186] (Fig 6.16) indicates just the opposite for the Raman scattering attributed to the matrix-isolated $CrOCl_3$ molecule. It is difficult therefore to explain the present observations in terms of a resonance Raman effect. In fact, studies of the u.v.-visible absorption spectrum of the matrix-isolated $CrOCl_3$ molecule carried out by Ogden and co-workers, [201] and shown in Figure 6.17, indicate that the exciting frequency actually coincides with a dip in the absorption and that there is slightly increased absorption at longer wavelengths, which might account for the virtual extinction of Raman lines displaced by more than about 400 cm^{-1} on the low-frequency side of the Rayleigh line. Alternatively,

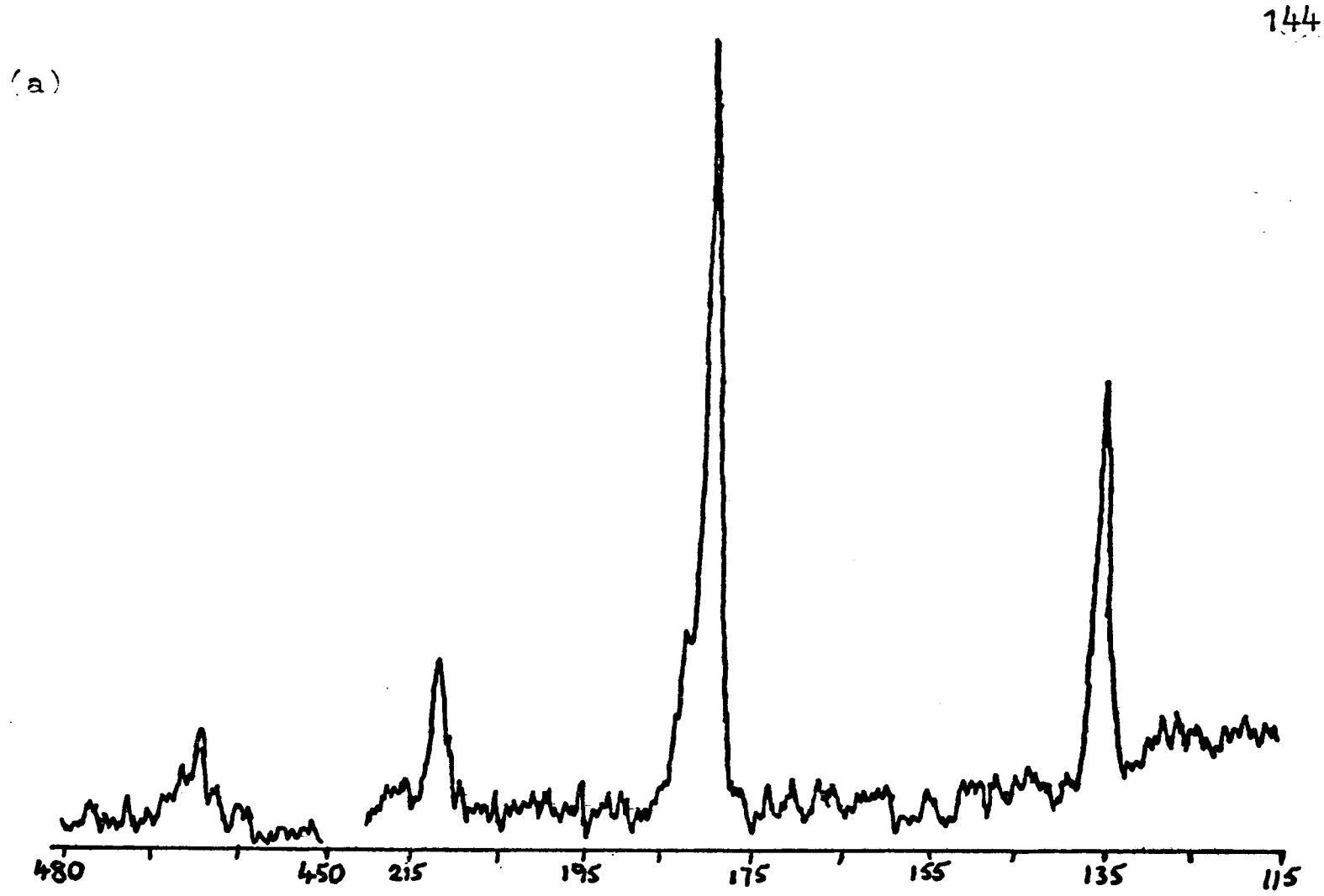

Fig. 6.16. Raman spectra of (a) $CrOCl_3$, Ar matrix (this work); (b) $VOCl_3$, vapour phase (ref. 199); (c) $AsOCl_3$, Ar matrix (ref. 137).

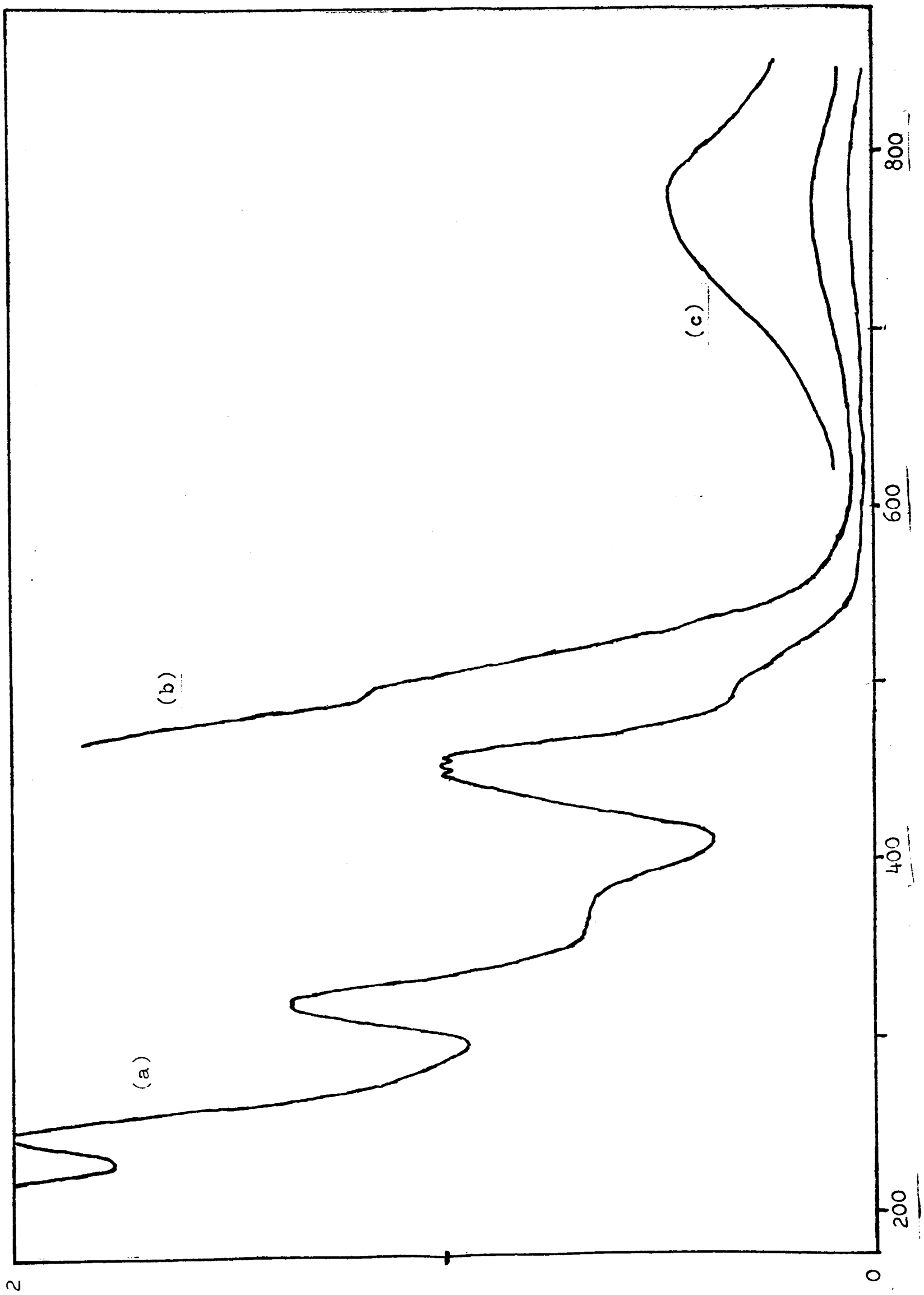

Fig. 5.17. U.v.-visible absorption spectrum of the matrix-isolated $CrOCl_3$ molecule (ref.201).

the observed bands may be due either to fluorescence or to electronic Raman transitions; low frequency features in the Raman spectrum of chromocene, $Cr(C_5H_5)_2$, have recently been attributed to the electronic Raman effect, [208, 209] and in the case of chromium trichloride oxide, spin-orbit and/or Jahn-Teller effects could easily give rise to low-lying excited electronic states. Clearly there is a need for further studies of the Raman scattering excited at different frequencies.

In spite of the doubts thus raised concerning the exact significance of the observed Raman spectra, it is difficult to see how the scattering could have arisen, if not from the matrix-isolated $CrOCl_3$ molecule. There is, for example, no correspondence between the observed features and those of the Raman spectrum previously reported for the molecule CrO_2Cl_2. [197] However, it is impossible to judge how well isolated the chromium trichloride oxide is in the Raman experiments; it is possible that the deposit is really a rather concentrated matrix and that the Raman lines are really due to $CrOCl_3$ aggregates, in which case the comparison between the infrared and Raman spectra may well not be a comparison of like with like. Nevertheless, in the absence of any clearcut alternative, the three strong bands consistently observed in the present Raman experiments have been assigned to the deformation modes of the $CrOCl_3$ molecule, and the discussion which follows is based on this interpretation.

6.5 Calculations

With the attribution of a complete set of vibrational frequencies to the normal modes of the $CrOCl_3$ molecule, it is a natural aim to attempt the calculation of at least an approximate set of molecular force constants. In order to do this, however, it is necessary first to construct the appropriate G matrix, which in turn requires some knowledge of the molecular dimensions. In the absence of any definitive structural details, it has been necessary to make certain assumptions, based partly on the dimensions established for

related molecular species. Thus, electron diffraction studies of the molecules CrO_2Cl_2 [210] and $VOCl_3$ [211] have yielded the molecular parameters listed in Table 6.3, on the basis of which bond lengths of 2.12Å and 1.56Å have been assigned to the Cr-Cl and Cr = O bonds respectively in the molecule $CrOCl_3$. In addition, there is the possibility, for a molecule of the type $O = MX_3$ having C_{3v} symmetry, of estimating the bond angles from the relative intensities in infrared absorption of the a_1 and e M-X stretching fundamentals, assuming that the ratio of the intensities of the matrix-isolated molecule is comparable with that of the gaseous molecule.[212] Provided that there is no interaction between the M-X stretching and other internal coordinates, and with certain other simplifying assumptions, it can be shown[213] that the intensities of the two infrared absorptions are related by the expression

$$\frac{I_e}{I_{a_1}} = \tan^2 \theta \qquad (6.4)$$

Here θ is the angle subtended by the M-X oscillators with respect to the C_3 axis; hence θ is related to α, the X-M-X bond angle, by the equation

$$\sin \theta = \sqrt{\frac{2}{3}} \sin \frac{\alpha}{2} \qquad (6.5)$$

From the relative intensities, as judged by peak areas, of the two infrared absorptions assigned to these fundamentals of the $CrOCl_3$ molecule isolated in various matrices, values for the Cl-Cr-Cl bond angle have been estimated, and these are listed in Table 6.4; the mean value is about 111°.

Although the estimates of the Cl-Cr-Cl bond angle thus obtained appear quite reasonable for a molecule of this type, several assumptions are implicit in the derivation of the expression for the intensity ratio. The most important of these are as follows:-

(i) The individual bond dipole moment vectors coincide with the axes of the bonds being considered.

Table 6.3. Molecular Parameters of CrO_2Cl_2 and $VOCl_3$

Parameter	CrO_2Cl_2	$VOCl_3$
r(M-Cl) (Å)	2.12	2.14
r(M-O) (Å)	1.57	1.56
∠(Cl-M-Cl)	113.0°	111.3°
∠(O-M-Cl)	109.5°	107.6°

Table 6.4. Values of Cl-Cr-Cl Bond Angle in $CrOCl_3$ Calculated from Infrared Band Intensities

Matrix	I_e (arbitrary units)	I_{a_1} (arbitrary units)	θ (see text)	α (see text)
N_2	637	51	74.2°	112.8°
Ar	708	73	71.6°	110.5°
Kr	407	42	72.2°	111.0°

(ii) The individual bond dipole moment vectors are additive, their sum corresponding to the total molecular dipole moment.

(iii) The molecule does not possess a permanent dipole moment; for molecules having such a dipole moment, a rotational correction term arises for vibrations having the same symmetry as a molecular rotation, because the central atom is then constrained to move so as to conserve angular momentum.

Although the rotational correction term may be estimated if the molecular geometry and permanent dipole moment are known, [214, 215] serious doubts have been expressed[213] regarding the feasibility of calculating bond angles on the basis of the intensities in infrared absorption of the stretching fundamentals of adjacent bonds having a common central atom. Hence the fact that reasonable results have been obtained for the $CrOCl_3$ molecule may be rather fortuitous; in any case, valence-shell electron pair repulsion arguments[216] might suggest a Cl-Cr-Cl bond angle somewhat less than the tetrahedral angle (109.5°), although the presence of the unpaired electron is undoubtedly a complicating factor.

The internal coordinates chosen for the construction of the $\underset{\sim}{G}$ matrix are illustrated in Figure 6.18 and the internal symmetry coordinates derived from these are listed in Table 6.5; the numerical values of the elements of the symmetrised $\underset{\sim}{G}$ matrix, based on the molecular dimensions given above, are presented in Table 6.6. A set of approximate force constants has been derived for the $CrOCl_3$ molecule using the limited information available by setting all the off-diagonal elements in the symmetrised $\underset{\sim}{F}$ matrix equal to zero. The diagonal elements of the $\underset{\sim}{F}$ matrix are related to the actual force constants of a valence force field by the expressions given in Table 6.7. The observed frequencies are then accommodated satisfactorily by the force constants listed in Table 6.8, and are listed, together with the frequencies calculated from these force constants for comparison, in Table 6.9.

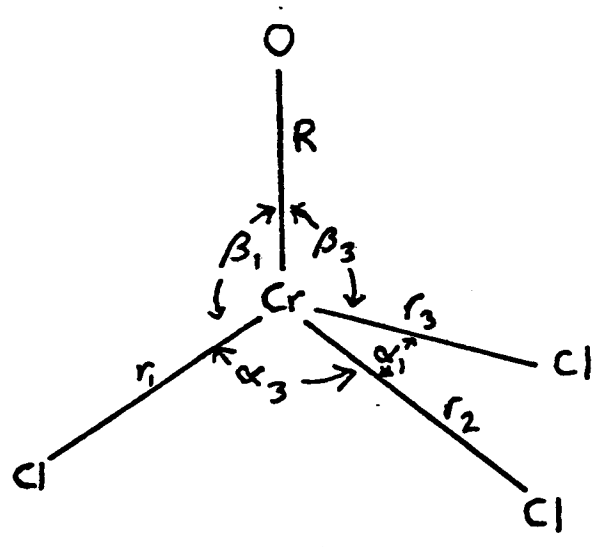

Fig. 6.18. Internal coordinates of the $CrOCl_3$ molecule.

Table 6.5. Internal Symmetry Coordinates Used in the Normal Coordinate Analysis of the $CrOCl_3$ Molecule

(See Figure 6.19 for an explanation of the symbols)

Symmetry block	Coordinate
A_1	$S_1 = R$ $S_2 = \frac{1}{\sqrt{3}}(r_1 + r_2 + r_3)$ $S_{3a} = \frac{1}{\sqrt{6}}(\alpha_1 + \alpha_2 + \alpha_3 - \beta_1 - \beta_2 - \beta_3)$ $S_{3b} = \frac{1}{\sqrt{6}}(\alpha_1 + \alpha_2 + \alpha_3 + \beta_1 + \beta_2 + \beta_3)$
E	$S_{4a} = \frac{1}{\sqrt{6}}(2r_1 - r_2 - r_3)$ $S_{5a} = \frac{1}{\sqrt{6}}(2\alpha_1 - \alpha_2 - \alpha_3)$ $S_{6a} = \frac{1}{\sqrt{6}}(2\beta_1 - \beta_2 - \beta_3)$ $S_{4b} = \frac{1}{\sqrt{2}}(r_2 - r_3)$ $S_{5b} = \frac{1}{\sqrt{2}}(\alpha_2 - \alpha_3)$ $S_{6b} = \frac{1}{\sqrt{2}}(\beta_2 - \beta_3)$

Footnote

The redundancy affecting the a_1 coordinates has been retained in the first instance and eliminated at a later stage as a zero root in the solution of the secular equation.

Table 6.6. Numerical Values of the Symmetrised G Matrix Elements for the $CrOCl_3$ Molecule[a]

Symmetry block	Element	Value[a]
A_1	G_{11}	0.81732
	G_{12}	-0.11120
	G_{13}	0.20958
	G_{22}	0.34636
	G_{23}	-0.12119
	G_{33}	0.35405
E	G_{44}	0.53838
	G_{45}	0.17089
	G_{46}	-0.21713
	G_{55}	0.27075
	G_{56}	-0.11334
	G_{66}	0.63191

Footnote

(a) Actual values multiplied by 10, as calculated using the computer program GMAT.

Table 6.7. Diagonal Elements of the Symmetrised F Matrix for the $CrOCl_3$ Molecule Expressed in Terms of Valence Force Constants

A_1 block

Coordinate			
(Cr=O)	(Cr-Cl)	(Cl-Cr-Cl) redundant	(Cl-Cr-Cl)
f_R			
	$f_r + 2f_{rr}$		
		$\frac{r^2}{2}(f_\alpha + 2f_{\alpha\alpha}) + r\sqrt{rR}(f'_{\alpha\beta} + 2f_{\alpha\beta}) + \frac{rR}{2}(f_\beta + 2f_{\beta\beta})$	
			$\frac{r^2}{2}(f_\alpha + 2f_{\alpha\alpha}) - r\sqrt{rR}(f'_{\alpha\beta} + 2f_{\alpha\beta}) + \frac{rR}{2}(f_\beta + 2f_{\beta\beta})$

E block

Coordinate		
(Cr-Cl)	(Cl-Cr-Cl)	(O-Cr-Cl)
$f_r - f_{rr}$		
	$r^2(f_\alpha - f_{\alpha\alpha})$	
		$rR(f_\beta - f_{\beta\beta})$

Table 6.3. Calculated Force Constants for the $CrOCl_3$ Molecule

$\underset{\sim}{F}$ matrix element or valence force constant	Numerical value[a]
F_{11}	736.5
F_{22}	290.7
F_{33}	70.7
F_{44}	217.1
F_{55}	51.2
F_{66}	50.5
f_R	736.5
f_r	241.6
f_{rr}	24.5
$f_\alpha - f_{\alpha\alpha}$	11.4
$f_\beta - f_{\beta\beta}$	15.3

Footnote

(a) Units are as follows: F_{11}, F_{22} and F_{44}, N m^{-1}; F_{33}, F_{55} and F_{66}, N m rad^{-2}; f_R, f_r, f_{rr}, f_α, $f_{\alpha\alpha}$, f_β and $f_{\beta\beta}$, N m^{-1}.

Table 6.9. Comparison of Observed and Calculated Frequencies for $CrOCl_3$

Mode	Observed frequency	Calculated frequency
$\nu_1(a_1)$	1018.6	1018.6
$\nu_2(a_1)$	406.7	406.7
$\nu_3(a_1)$	178.9	179.0
$\nu_4(e)$	462.0	462.0
$\nu_5(e)$	211.4	211.6
$\nu_6(e)$	134.7	134.0

The force constants deduced for the $CrOCl_3$ molecule may be compared with those previously reported for the related molecules $POCl_3$,[187] and $AsOCl_3$ [187] and $VOCl_3$ [217, 218] (Table 6.10). The principal Cr-Cl and Cr = O stretching force constants, with values of 242 and 737 N m^{-1} respectively, correspond quite closely to their counterparts in $VOCl_3$ and CrO_2Cl_2;[202, 219] the bending force constants in the three molecules $CrOCl_3$, $VOCl_3$ and CrO_2Cl_2 are also comparable in magnitude. It appears therefore that the $CrOCl_3$ molecule complies with a force field very similar to those operative in $VOCl_3$ and CrO_2Cl_2. Any comparison must clearly be treated with caution in view of the comparatively limited amount of information available in the case of $CrOCl_3$, although the ultraviolet photoelectron spectra [183, 220] would seem to suggest a close structural relationship between the molecules $CrOCl_3$, $VOCl_3$ and VCl_4. There is no indication here that the unpaired electron affects significantly either the structure or the bonding of the $CrOCl_3$ molecule; thus, the relative magnitudes of the force constants for $CrOCl_3$ and $VOCl_3$ imply that it is practically non-bonding in character. For a better insight into the structure of the $CrOCl_3$ molecule and the nature of its force field, however, more information is clearly needed.

6.6. Conclusions

During the course of the present study, a set of vibrational frequencies has been assigned to the chromium trichloride oxide molecule as trapped in solid, inert matrices at low temperatures and characterised by its infrared and Raman spectra. Hence an approximate force field has been derived, and the results of the vibrational analysis indicate that, in terms of both structure and bonding, the $CrOCl_3$ molecule is closely akin to $VOCl_3$ and CrO_2Cl_2. There must be some doubt, however, about the significance of some of the results obtained, particularly in the case of the Raman experiments. In order to draw more definite conclusions about the structure and bonding of the $CrOCl_3$ molecule, it would be desirable to carry out further investigations of its vibrational properties. Such

Table 6.10. Comparison of Force Constants Calculated for $CrOCl_3$ with those of Related Molecules[a]

Force constant	Molecule			
	$CrOCl_3$	$VOCl_3$	$POCl_3$	$AsOCl_3$
f_R	736.5	741.7	1039.4	758.7
f_r	241.6	251.5	236.1	233.4
f_{rr}	24.5	25.9	39.7	0.0
$f_{\alpha} - f_{\alpha\alpha}$	11.4	9.3	34.4	12.5
$f_{\beta} - f_{\beta\beta}$	15.3	21.5	47.5	23.1

Footnote

(a) All force constants expressed in N m^{-1}.

investigations might profitably include the following:

(a) The preparation and spectroscopic characterisation of ^{18}O-enriched chromium trichloride oxide. An economical means of producing a different isotopic version of the molecule is an essential prerequisite to further progress. In fact, a set of frequencies for the molecule $^{18}OCrCl_3$ has actually been predicted on the basis of the simplified force field defined by the potential constants given in Table 6.8, and these are listed in Table 6.11.

(b) Further studies of the Raman scattering of chromium trichloride oxide using a range of different frequencies for excitation (made possible, for example, with access to a krypton-ion or dye laser) and preferably higher power levels at the sample.

(c) Further studies of the photolysis of chromium trichloride oxide, with particular reference to the effect on the infrared spectrum of irradiating the trapped molecule with visible light, eg the blue or green lines of the argon-ion laser.

(d) Investigations of the effect of controlled warming on a deposit of chromium trichloride oxide with the aim of identifying its disproportionation products; these, along with its photolysis products, may have an important bearing on its chemistry.[181]

Table 5.11. Vibrational Frequencies Predicted for the Molecule $^{18}OCrCl_3$

Mode	Observed for $^{16}OCrCl_3$	Calculated for $^{18}OCrCl_3$
$\nu_1(a_1)$	1018.6	975.9
$\nu_2(a_1)$	406.7	405.1
$\nu_3(a_1)$	178.9	177.8
$\nu_4(e)$	462.0	461.9
$\nu_5(e)$	211.4	211.4
$\nu_6(e)$	134.0	128.5

Chapter 7

STUDIES OF PHOSPHORUS AZIDES

7.1 Introduction

The azide group, consisting of a linear chain of three nitrogen atoms, occurs in a large number of compounds, the first of which was prepared as long ago as 1864.[221] Azides may be divided into two major categories. First, there are the compounds which contain more-or-less discrete N_3^- ions and have the properties of ionic salts, eg NaN_3. Second, there are the molecular azides, which include the majority of organic and inorganic azides, containing the N_3 group covalently bonded to another atom.[222-224] Azides are generally prepared *via* exchange reactions involving hydrogen azide or the sodium salt,[225] and a number of organometallic azides have been synthesised in this manner.[226] The following are representative examples:-

$$Et_2AlCl + NaN_3 \longrightarrow Et_2AlN_3 + NaCl$$

$$(NPCl_2)_3 + 6NaN_3 \longrightarrow [NP(N_3)_2]_3 + 6NaCl$$

$$(CF_3)_2 PCl + LiN_3 \longrightarrow (CF_3)_2 PN_3 + LiCl$$

The structure of the simplest molecular azide, hydrogen azide, as determined by electron diffraction,[227] shows that the three nitrogen atoms are collinear and the HNN bond angle is 112°, while the two N-N distances differ considerably, $HN-N_2$ being 1.24Å and HN_2-N 1.13Å. These values are comparable to those reported for other molecular azides.[224] On the other hand, investigation of the structures of ionic azides by X-ray diffraction[223-225] show that the azide ion is also linear, but with two equal N-N distances of about 1.16Å. These structures have been discussed at various levels of sophistication in terms of molecular orbitals;[228-230] thus, the sixteen valence electrons of hydrogen azide can be regarded as being distributed between two lone pairs, three σ-bonds and two π-bonds, with the remaining two electrons occupying a π-orbital which is more-or-less non-bonding in

character (Fig 7.1).[231] The bond angles are accounted for by approximate sp^2 hybridisation of the nitrogen atom through which coordination occurs and sp hybridisation of the other two nitrogen atoms.

Azides tend to be unstable with respect to loss of molecular dinitrogen. Such decomposition may be explosive but in many cases a slower, more controlled reaction may be induced by photolysis.[225, 226] Consideration of the absorption spectra of molecular azides indicates that this requires ultraviolet irradiation; for example, appreciable absorption by hydrogen azide sets in near 220 nm and increases towards shorter wavelengths,[232] while the spectrum of methyl azide consists of a weak, broad band centred at 285 nm and a considerably stronger band with a long wavelength limit near 240 nm.[233] In fact, thermochemical studies[234] indicate that in covalent azides of the type RN_3 the weakest bond is the $RN-N_2$ linkage, and that the primary step of photolytic decomposition is generally the breaking of this bond.

The primary products of the photolysis of a molecular azide RN_3 are generally dinitrogen and an electron-deficient species of the type RN: which tends to undergo further reactions such as dimerisation,[235] rearrangement[236] and insertion.[237] If the azide is trapped in a low-temperature matrix, the primary products of photolysis may be retained and identified spectroscopically, and the course of subsequent reactions followed by investigating the effects of warming on the matrix. The advantages afforded by azides as a source of new nitrogen-containing molecules, particularly in matrix-isolation experiments, may be summarised as follows:

(i) The other product is usually N_2, which is not only inert (and therefore counteracts any 'cage' effects) but also free from complicating infrared absorptions.

(ii) On the evidence of other studies, they seem to be highly photosensitive with respect to ultraviolet radiation (in other words

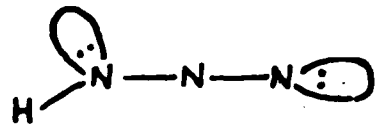

(a) Lone pairs and σ-bonds.

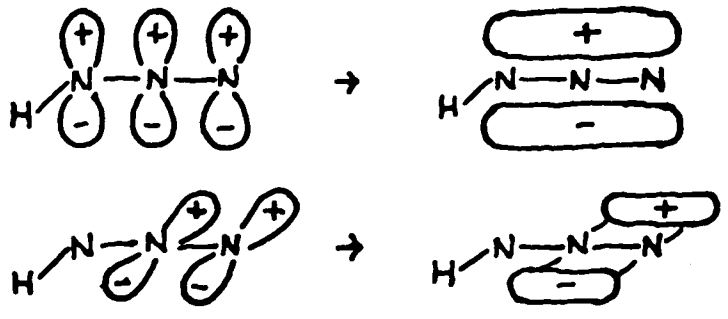

(b) Bonding π-molecular orbitals.

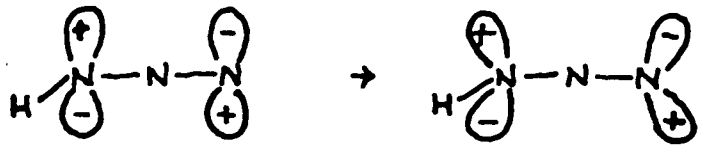

(c) Non-bonding π-molecular orbital.

Fig. 7.1. Molecular orbital description of the bonding in HN_3.

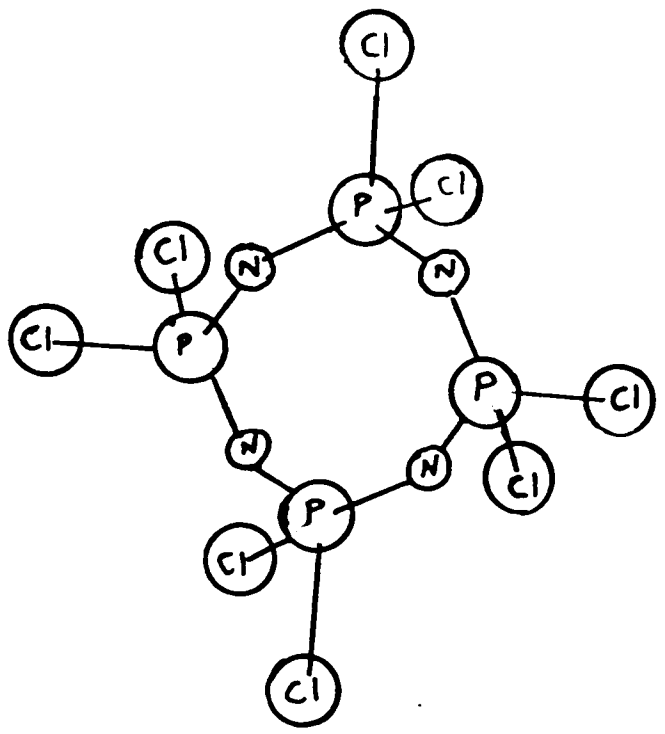

Fig. 7.2. The $(NPCl_2)_4$ molecule.

the quantum yields of the photochemical changes are high).

(iii) The infrared absorptions due to the coordinated azide group are fairly well defined, and so the fate of the azide is easily monitored.

(iv) They provide one of the simplest and best-controlled means of producing molecules containing nitrogen multiply bonded to a heavy atom.

Thus the molecules NH and N_2H_2 have been detected as products of the photolysis of the matrix-isolated HN_3 molecule,[238] while similar treatment of the halogen azides has been shown to give rise to the molecules FN, ClN and BrN.[239] Photolysis of matrix-isolated azidomethane affords the molecule CH_2NH followed by HNC as a secondary product;[233, 240] on the other hand, HNSi is the only product which has been detected on photolysis of matrix-isolated azidosilane, SiH_3N_3.[241] Yet again, a recent investigation of the photolysis of matrix-isolated trimethylazidosilane, $(CH_3)_3 SiN_3$, discloses an unusual rearrangement reaction with resultant Si-H bond formation.[242]

The present study was particularly concerned with the generation of species in which the azide group is bonded to a phosphorus atom, with a view to bringing about the removal of dinitrogen from such molecules by photolysis. Azide groups can generally be introduced into phosphorus compounds by treating the appropriate halide with an alkali-metal azide, and in fact claims have recently been laid to the synthesis by this method of phosphorus triazide, $P(N_3)_3$, pentazide, $P(N_3)_5$, and triazide oxide, $OP(N_3)_3$.[243] However, all three compounds are unstable at normal temperatures and tend to explode on removal of the acetonitrile in which the reactions are carried out. In contrast, several organophosphorus azides appear to exhibit fair thermal stability; this is true, for example, of diphenylazidophosphine, $(C_6H_5)_2PN_3$,[244] and bis(trifluromethyl) azidophosphine, $(CF_3)_2PN_3$,[245] formed by treatment of the appropriate chloro-derivatives with lithium azide. Phosphorus (V) azides of the type $R_2P(X)N_3$, with R = CH_3 or C_2H_5 and X = O or S, have been obtained by similar methods.[246] There are no reports,

however, that any matrix-isolation studies have been carried out on molecules of this type.

The first part of the present study was concerned with the reaction between phosphorus trichloride and sodium azide. The formation of the triazide $P(N_3)_3$ by this route has already been referred to; by using the correct proportions of the reagents, it was hoped to prepare the monosubstituted derivative Cl_2PN_3, thereby allowing the possibility of carrying out at low temperatures the photolytic transformation

$$Cl_2PN_3 \xrightarrow{h\nu} Cl_2P \equiv N + N_2$$

Dichlorophosphazene, Cl_2PN, has not been isolated in the monomeric form, and although adducts such as $POCl_3.NPCl_2$ [247] and $NPCl_2.2PCl_5$ [248] have been reported, these almost certainly have the structures $Cl_2\overset{O}{\underset{\|}{P}}-N = PCl_3$ and $[Cl_3P = N-PCl_3]^+ [PCl_6]^-$ respectively. The only known species having the empirical formula $NPCl_2$ are the cyclic oligomers $(NPCl_2)_n$ (the best known being those with n = 3 and n = 4) consisting of rings of alternating phosphorus and nitrogen atoms with two chlorine atoms bonded to each phosphorus (Fig 7.2).[249, 250] Attempts to isolate the Cl_2PN monomer by trapping the products of pyrolysis of the trimer and tetramer in low temperature matrices led to inconclusive results.[125] It would be interesting to be able to compare the properties of the $Cl_2P \equiv N$ molecule with those of its sulphur counterpart $ClS\equiv N$, particularly with respect to its behaviour on controlled warming.

The second part of the present study was concerned with the attempted matrix isolation of the hitherto unknown dimethylazidophosphine $(CH_3)_2 PN_3$, again prepared <u>via</u> the reaction between the appropriate chloro-derivative and sodium azide. The lack of any previous references to the existence of this compound is a matter of some surprise in view of the comparative stability, already referred to, of the related molecules $(C_6H_5)_2PN_3$ [244] and $(CF_3)_2PN_3$; [245] the arsenic and bismuth analogues, $(CH_3)_2AsN_3$ and $(CH_3)_2BiN_3$, have been prepared, moreover, and characterised by their vibrational spectra.[251]

Once again, it was hoped that the successful matrix isolation of the $(CH_3)_2PN_3$ molecule would allow an investigation of the effects of ultra-violet irradiation, with the possibility of generating the species $(CH_3)_2PN$ and of comparing the behaviour of the matrix-isolated $(CH_3)_2PN_3$ molecule with that of $(CH_3)_3SiN_3$ under similar conditions.[242]

7.2 Experimental

The materials used in these experiments, together with their sources and the methods of purification employed, are listed in Table 7.1. Previous studies of reactions of this nature[243-246] have employed reaction media such as acetone and acetonitrile; in the present study diglyme (bis[2-methoxyethyl] ether) was chosen because of its relatively low volatility (vapour pressure at room temperature ~1.5 mm Hg [252]) which was expected to facilitate its separation from the molecular azides formed as reaction products. All manipulations were carried out on the vacuum line, incorporating a train of traps, shown in outline in Figure 7.3; the reactions actually took place in ampoules of the type illustrated in Figure 7.4, which could be sealed and removed from the vacuum line if required.

In a typical study of the reaction between phosphorus trichloride and sodium azide, about 50 mg (0.77 mmol) of sodium azide was introduced into the reaction ampoule, which was then attached to the vacuum line *via* a B10 ground-glass cone. An approximately equimolar quantity of phosphorus trichloride, measured by volume (about 0.07 ml), was then transferred into the ampoule together with about 1 ml of diglyme, and the mixture allowed to stand for about 12 hours at room temperature. At the end of this period, the volatile materials present were transferred to the train of traps, where fractionation was attempted by allowing the vapour of the reaction products to pass through traps held at -23°C (carbon tetrachloride slush), -95°C (toluene slush) into one held at -196°C (liquid nitrogen). Diglyme, with a vapour pressure in the order of 10^{-2} mm Hg at -23°C, was expected to condense mainly in the first trap, while the reaction products should

Table 7.1 Materials Used in Studies of Phosphorus Azides

Material	Source and purity claimed	Method of purification
PCl_3	BDH (98.5%)	Distillation in air followed by fractionation through traps held at -23°, -126° and -196°C and collection of the middle fraction
$(CH_3)_2PCl$	Strem Chemicals Inc (99%)	Distillation *in vacuo*
NaN_3	BDH (99%)	Dried by heating to 80°C in vacuo for several hours
Diglyme	BDH (99%)	Refluxing over calcium hydride for one day, followed by distillation on to molecular sieve

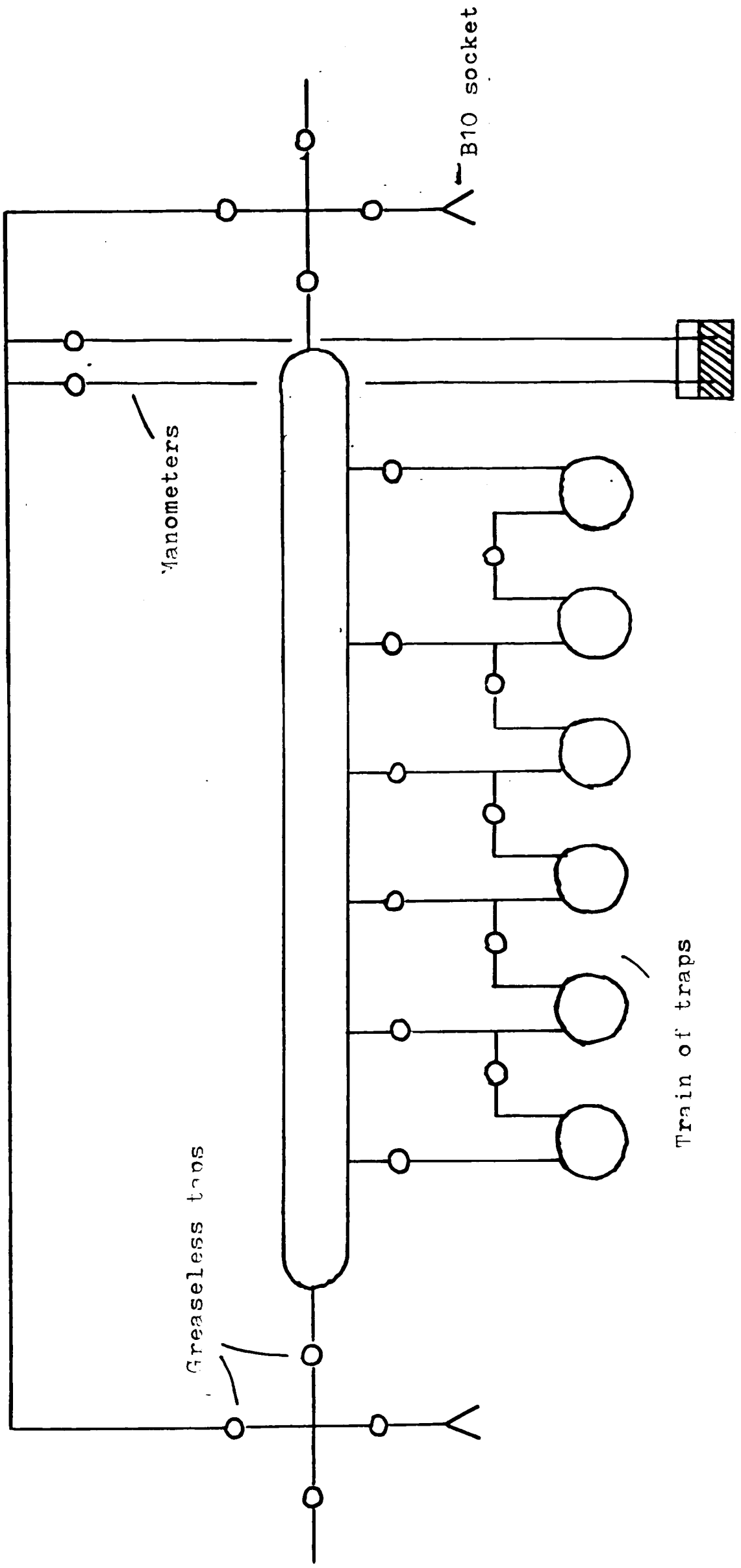

Fig. 7.3. Schematic diagram of the vacuum line used in studies of phosphorus azides.

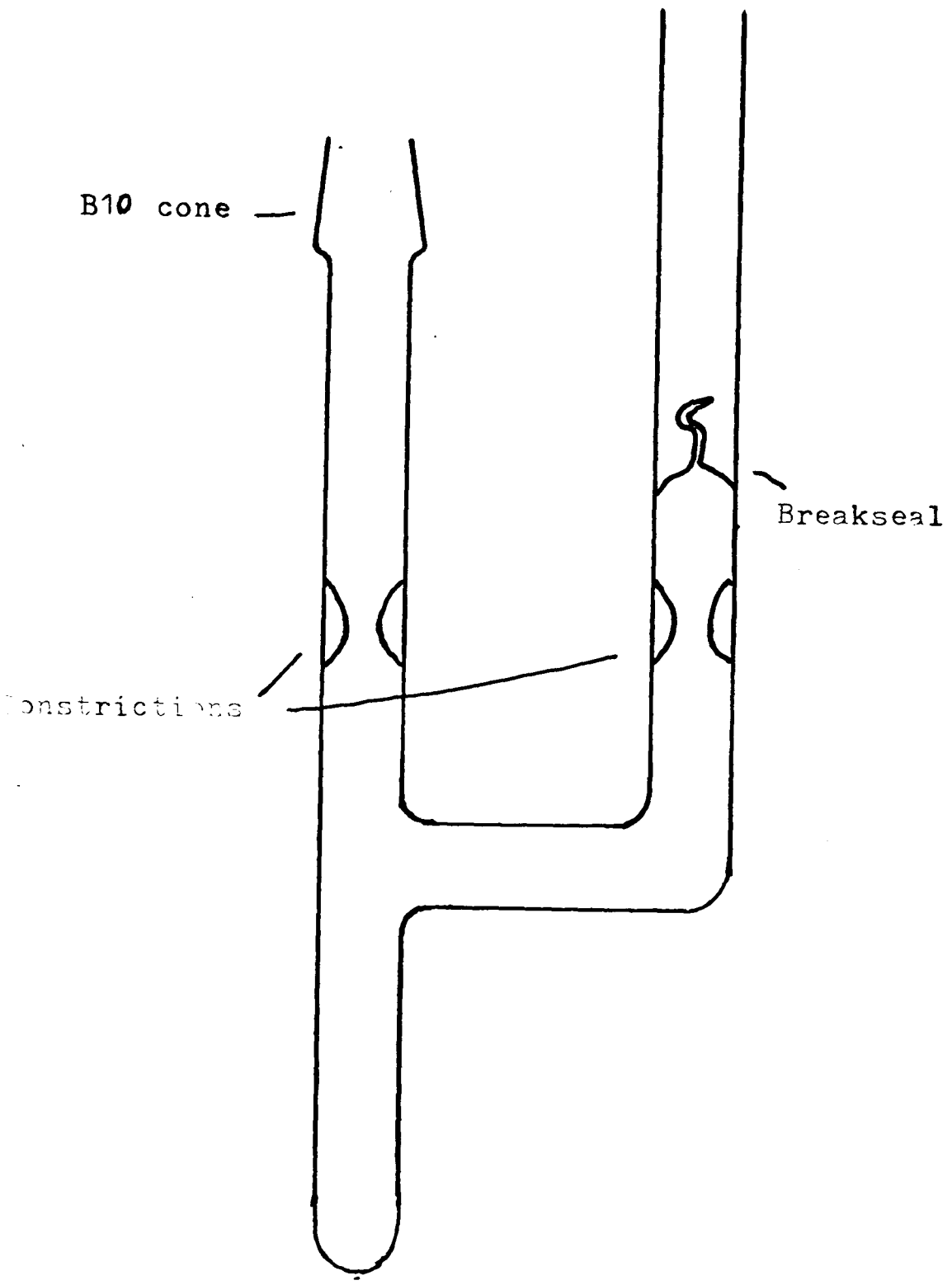

Fig. 7.4. Ampoule used in studies of phosphorus azides.

condense mainly in the second. Infrared studies of the products were carried out by evaporation from the trap, normally held at -63°C (chloroform slush), on to the cold window of the cell described in Section 3.6(g).

The reaction between dimethylchlorophosphine and sodium azide was carried out under similar conditions and for a similar duration except that the sodium azide was now present in excess, typical quantities being 100 mg (1.55 mmol) of sodium azide and 0.05 ml (0.64 mmol) of dimethylchlorophosphine (the scales of the preparations were kept small in both studies in order to minimise the risk of explosion). The products of the reaction were again found to condense in a trap held at -95°C, and an initial infrared study of these products condensed on a caesium iodide window held at 77K was again carried out using a procedure similar to that outlined in the preceding paragraph. Attempts were made in subsequent experiments to isolate the products in low-temperature matrices. Since the products were found to have a vapour pressure of about 2 cm Hg at room temperature, it was possible to achieve matrix isolation by pulsed deposition of a pre-mixed sample of products and matrix gas (products: matrix gas = 1:500).

7.3 The Reaction Between Phosphorus Trichloride and Sodium Azide

Infrared spectra typical of those obtained in the study of the reaction between phosphorus trichloride and sodium azide are illustrated in Figures 7.5 to 7.7, and the measured frequencies listed in Table 7.2; all these spectra refer to solid products held on a caesium iodide window at 77K. Figures 7.5 and 7.6 show the spectra of the fractions collected at -95°C in each of two separate experiments. The spectrum of a sample collected under similar conditions in a third experiment is shown in Figure 7.7(a), and that of the same sample after ultraviolet irradiation (*via* a water filter) at 77K for a period of one hour appears in Figure 7.7(b). Annealing the deposits formed at 77K did not appear to produce any significant change in the infrared spectra beyond causing a sharpening of the bands and giving better-resolved spectra.

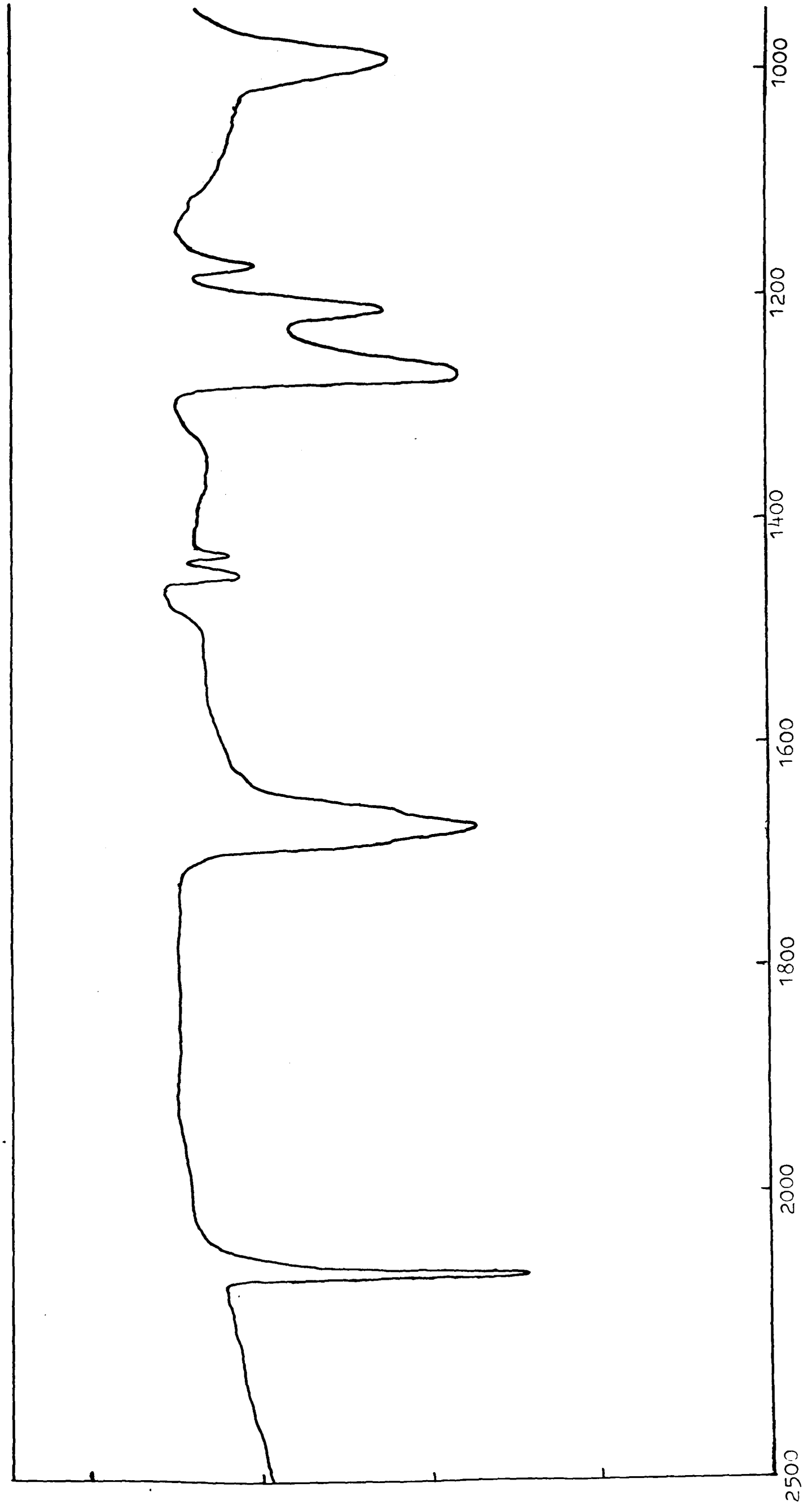

Fig. 7.5. Infrared spectrum of the volatile products of the reaction between PCl_3 and NaN_3 (1).

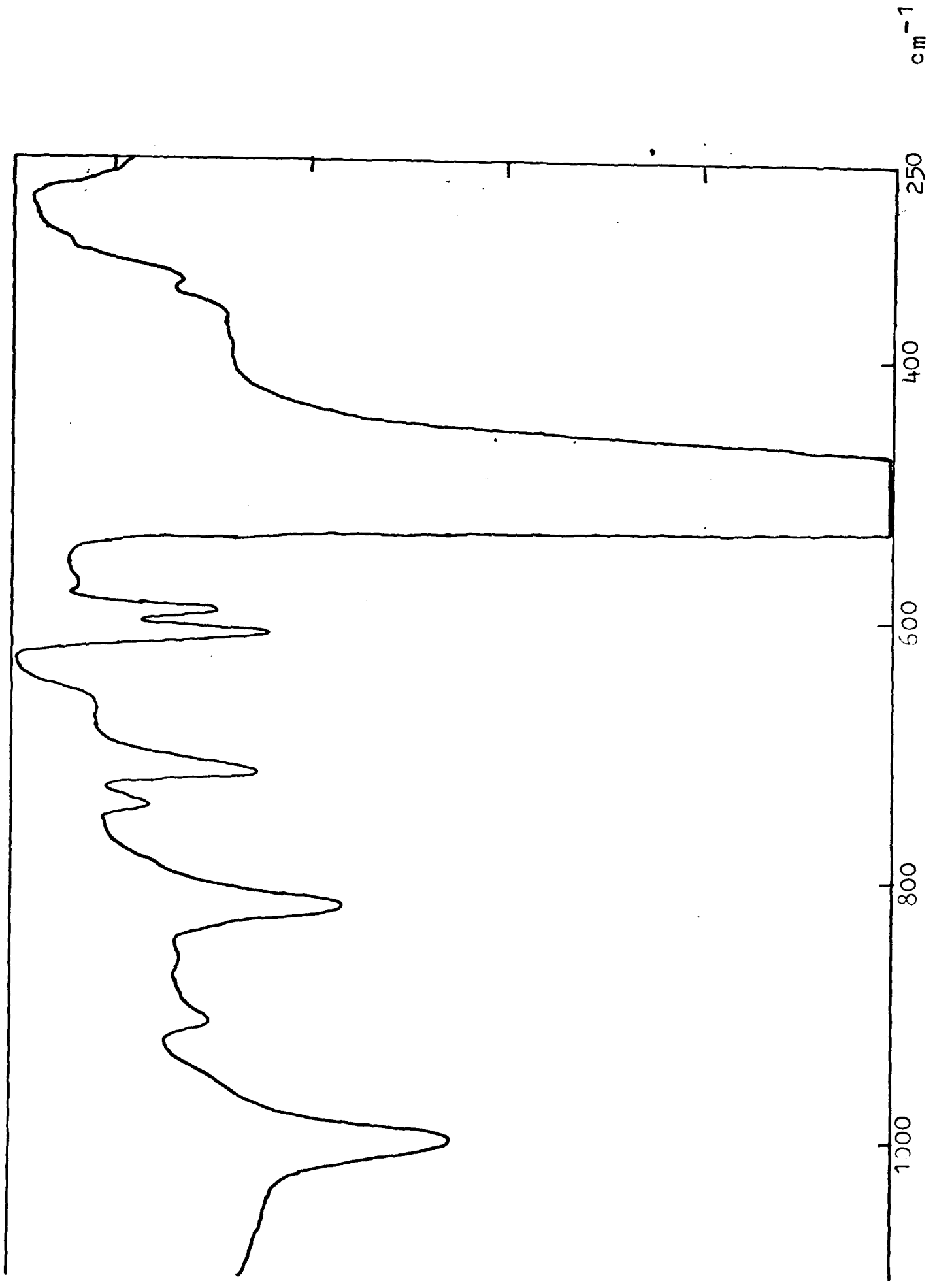
cm⁻¹
250
400
600
800
1000

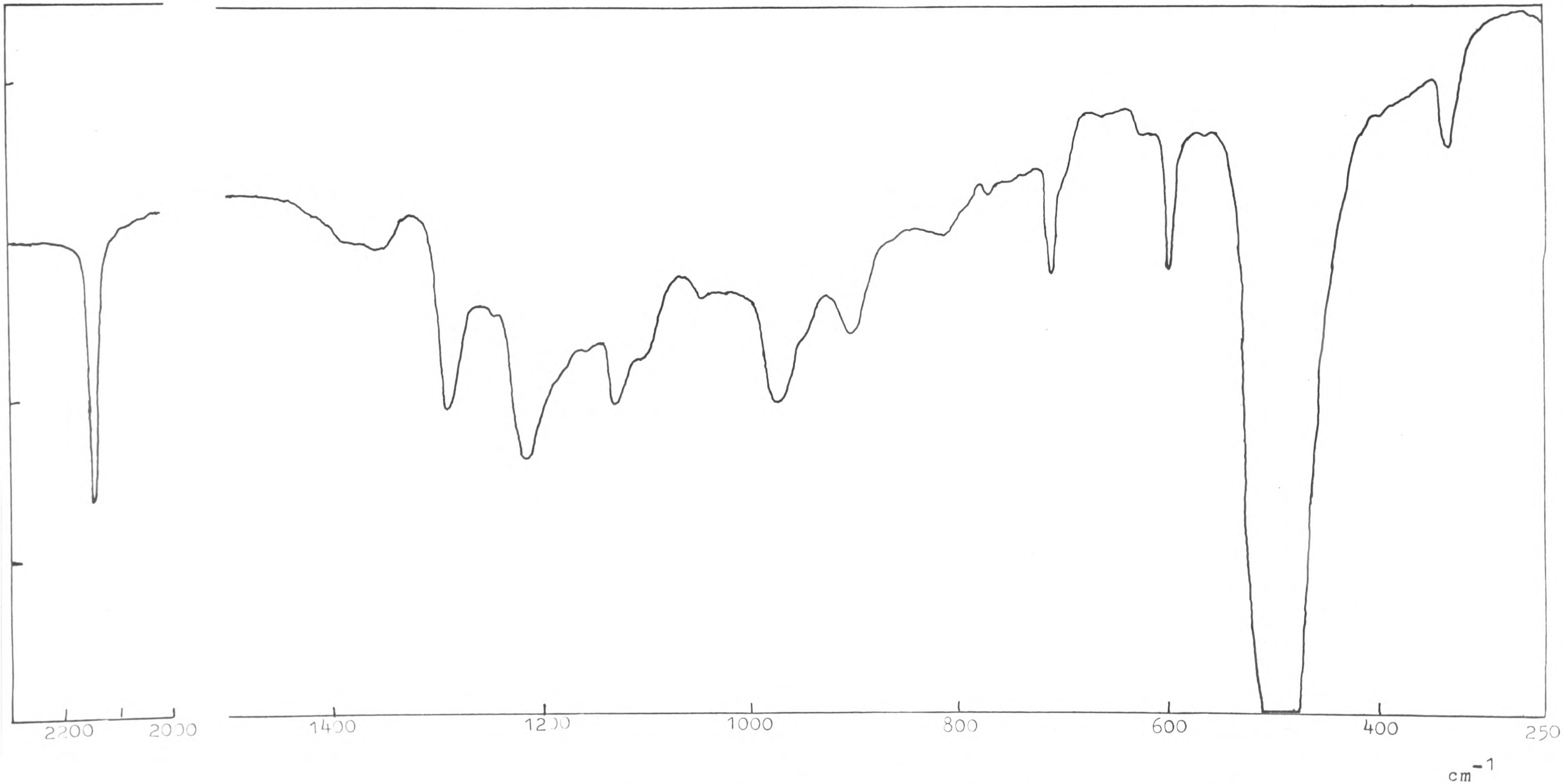

Fig. 7.6. Infrared spectrum of the volatile products of the reaction between PCl_3 and NaN_3 (2).

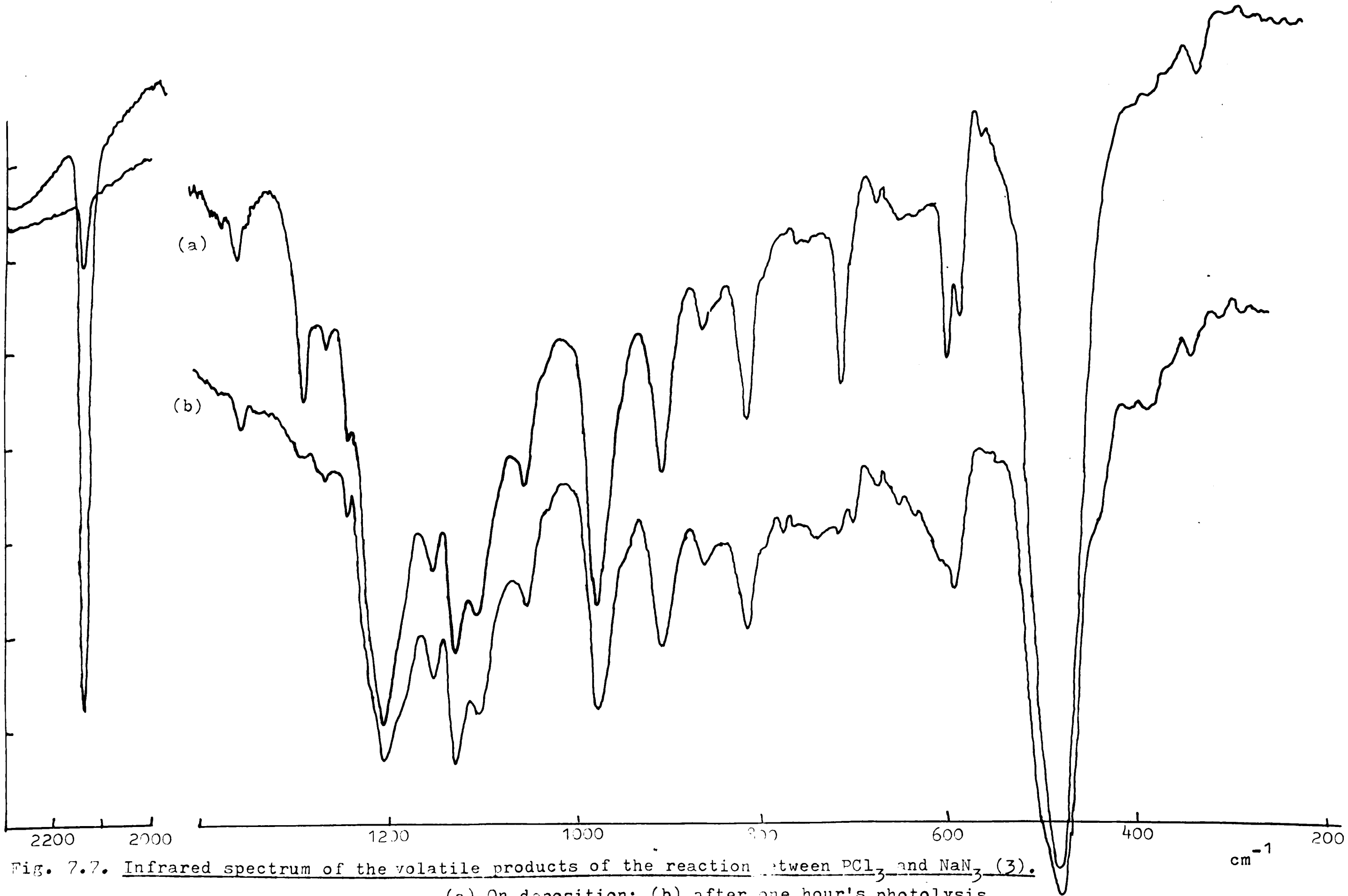

Fig. 7.7. Infrared spectrum of the volatile products of the reaction between PCl_3 and NaN_3 (3). (a) On deposition; (b) after one hour's photolysis.

Table 7.2. Observed Infrared Frequencies in Studies of the Reaction Between Phosphorus Trichloride and Sodium Azide

Expt. 1 (Fig. 7.5)	Expt. 2 (Fig. 7.6)	Expt. 3 (Fig. 7.7)
2147s	2144s	2140s
1676s		
1458w		
1440w		
		1352w
1235s	1290m	1285m
		1263w
		1240vw
1217m	1216m	
		1204s
1181w		
		1150w
	1131w	1128m
		1103w
	1050vw	1050w
996m		
	975m	974m
905w	907w	906m
		361w
818m	820vw	813m
739w		
717m	714m	712m
608m	603m	600m
590m		538m
~490vs	~490vs	430vs
340w	342w	338w

Consideration of the relative intensities of the infrared bands of the solid deposits formed at 77K indicates the presence of several distinct molecules in the volatile reaction products, although attempts to separate these products, whatever they might be, by further fractionation proved unsuccessful. One possibility is that some of the observed infrared bands arise from the presence of solvent in the samples, although this should have been removed by fractionation and there appears to be little, if any, correlation between the spectra observed in the present study and the infrared spectrum of diglyme previously reported.[253] On the other hand, the presence of hydrolysis products, resulting, for example, from the action of the vacuum grease, cannot be completely ruled out. It is also possible that at least some of the bands originate in oligomers of the $Cl_2P \equiv N$ molecule; in particular, those at 1204, 1128, 861 and 588 cm^{-1} could arise from the presence of the well-characterised cyclic trimer $(NPCl_2)_3$.[126, 254]

Despite the complexity of the observed spectra, it is possible to make certain observations about the results obtained. In particular, the band near 2140 cm^{-1}, which showed up quite strongly in some of the spectra obtained but was found to be absent from others, is probably associated with the antisymmetric stretching fundamental of a coordinated azide group. Consideration of the infrared spectra reported[243-246] for molecular azides related to species like Cl_2PN_3 indicates that this is invariably the strongest of the three infrared absorptions associated with the fundamentals of the azide group itself, and that the symmetric stretching and deformation modes generally give rise to absorptions near 1250 and 650 cm^{-1} respectively. The band s observed at 1285 and 600 cm^{-1} in the present study might therefore arise from such fundamentals of an azidophosphine such as Cl_2PN_3. The assignment of the band at 2140 cm^{-1} to an azide linkage is supported by its considerable decrease in intensity on ultraviolet photolysis of the solid deposit at 77K (see Figure 7.7).

Comparison of the spectra exhibited by different samples apparently of the same origin (Figs 7.5, 7.6), and consideration of the effects of ultraviolet irradiation of the solid deposit on the intensities of the bands, suggest that the features observed at 712 and 336 cm^{-1}, and possibly one at 813 cm^{-1}, are associated with the same molecule as are the features already attributed to the presence of an azide linkage. If this species is the dichloroazidophosphine molecule, Cl_2PN_3, the band at 712 cm^{-1} may be assigned to the P-N stretching fundamental, again by analogy with the vibrational spectra of related molecules;[243, 246] its virtual disappearance on photolysis is consistent with such an assignment. The interpretation of the band at 813 cm^{-1}, if it does arise from the same species as the others, is less certain but that at 338 cm^{-1} presumably represents a deformation mode of the molecule concerned. In addition, of course, the presence of strong bands attributable to P-Cl stretching fundamentals is also expected. The broad, intense absorption near 480 cm^{-1} might include these, but, in view of the complex nature of the spectra, this is probably associated with the presence of several molecules, possibly including unchanged phosphorus trichloride.[255]

There are grounds therefore for believing that the Cl_2PN_3 molecule is one of the products of the reaction between sodium azide and phosphorus trichloride, although the presence of other molecular species containing the azide linkage cannot be ruled out. The behaviour observed on ultraviolet photolysis is interesting in view of the virtual disappearance of certain bands, but inconclusive in that no new bands were seen to develop and no pre-existing bands to increase significantly in intensity, with the exception of the weak feature at 1240 cm^{-1}. This frequency is of the same order of magnitude as that quoted for the gaseous PN molecule (1337 cm^{-1});[256] otherwise there is no clear evidence for the formation of a molecule containing a P≡N bond.

The complexity of the observed spectra prevents any definite conclusions

from being drawn about the course of the reaction between phosphorus trichloride and sodium azide or about the effects of photolysing the reaction products at 77K. Further investigations are clearly needed in order to arrive at a more definite interpretation but for the purposes of the present research it was decided that the products did not lend themselves to matrix-isolation experiments.

7.4 The Reaction Between Dimethylchlorophosphine and Sodium Azide

The infrared spectrum, again recorded at 77K, of the products volatile at -23°C of the reaction between dimethylchlorophosphine and sodium azide is shown in Figure 7.8, together with that of the same material after ultraviolet irradiation of the deposit held at 77K for a period of one hour. For comparison, Figure 7.9 shows the infrared spectrum of gaseous dimethylchorophosphine, which is in agreement with the spectrum previously reported.[257, 258] The simplicity and reproducibility of the spectra as compared with those described in the previous section encouraged the performance of a matrix-isolation study of the products, the results of which, for argon and krypton matrices respectively, are shown in Figures 7.10 to 7.13. Finally, the effect of twelve hours' ultraviolet irradiation of the product isolated in an argon matrix at 20K is illustrated in Figure 7.14. The measured frequencies are listed in Table 7.3.

The spectra obtained from the volatile products of the reaction between sodium azide and dimethylchlorophosphine are more readily interpreted than those for the corresponding reaction between sodium azide and phosphorus trichloride. If dimethylazidophosphine $(CH_3)_2PN_3$, is formed, then there should be some correspondence with the infrared spectra previously reported for the compounds $(CH_3)_2AsN_3$ and $(CH_3)_2BiN_3$.[251] Again the strong band at 2136 cm^{-1} is almost certainly associated with the antisymmetric stretching fundamental of a coordinated azide group. Comparison with the spectrum of dimethylazidoarsine[251] suggests, on the basis of relative intensities, that the band at 1199 cm^{-1} is associated with the corresponding symmetric

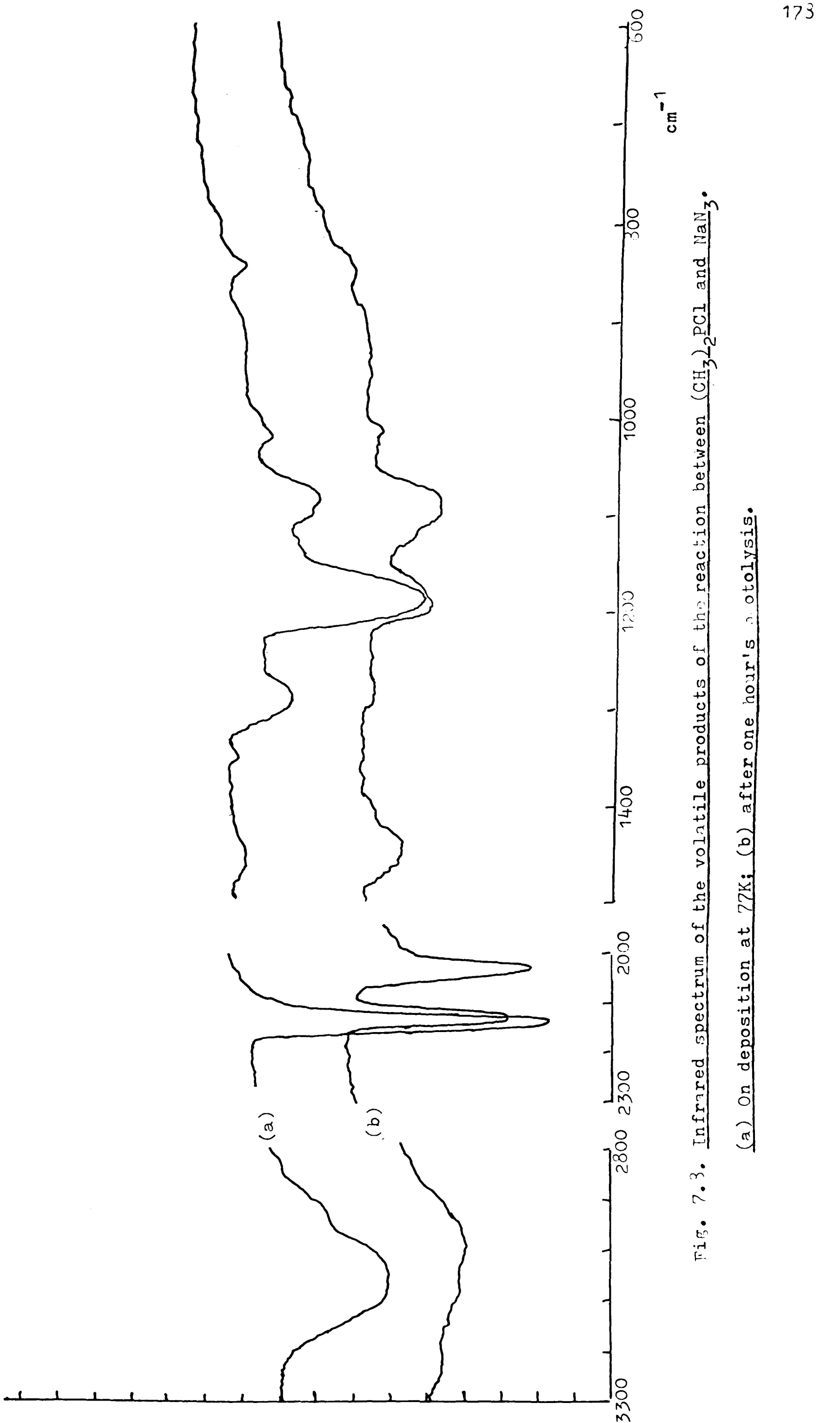

Fig. 7.3. Infrared spectrum of the volatile products of the reaction between $(CH_3)_2PCl$ and NaN_3.

(a) On deposition at 77K; (b) after one hour's photolysis.

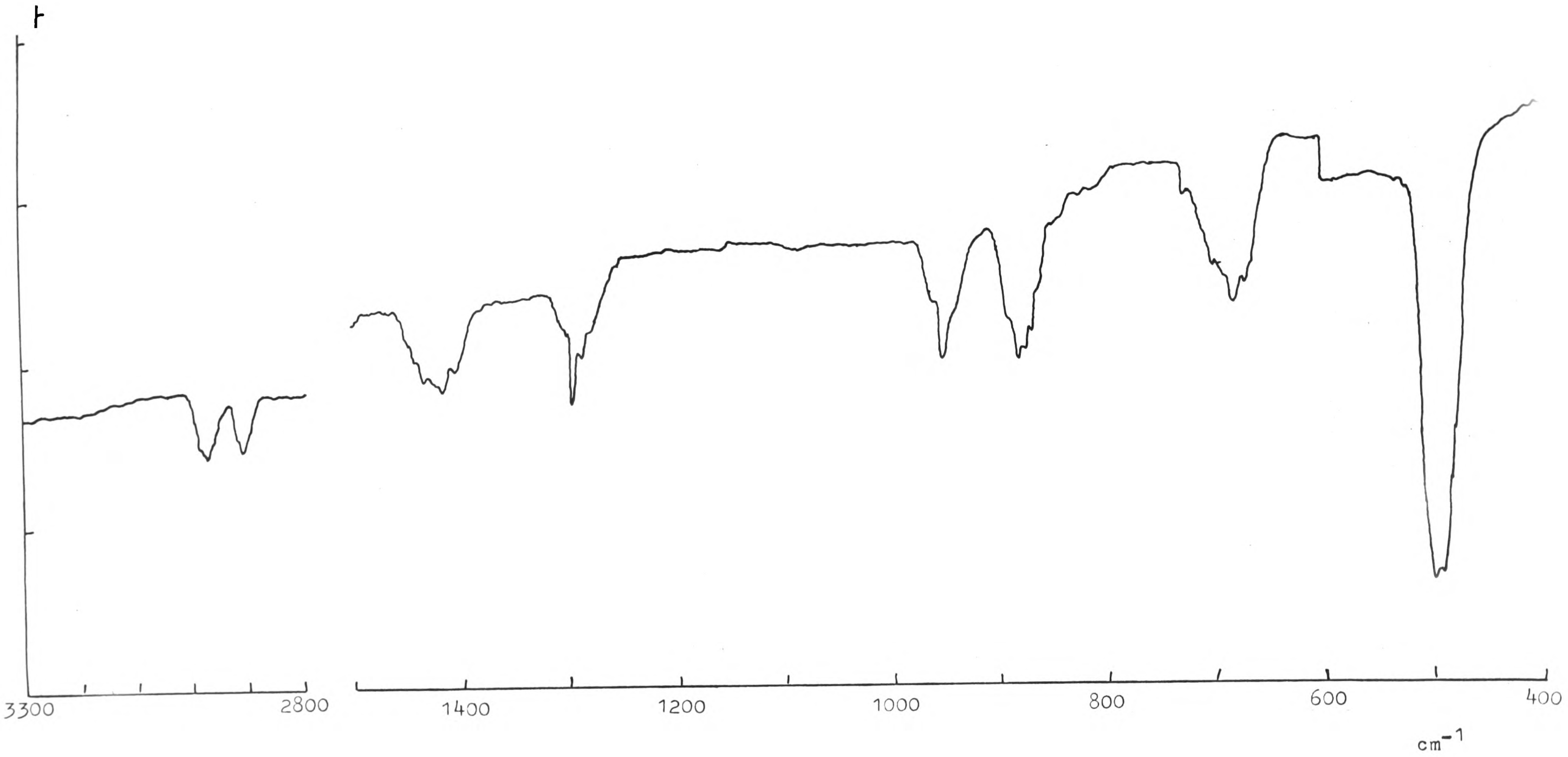

Fig. 7.9. Infrared spectrum of gaseous $(CH_3)_2PCl$.

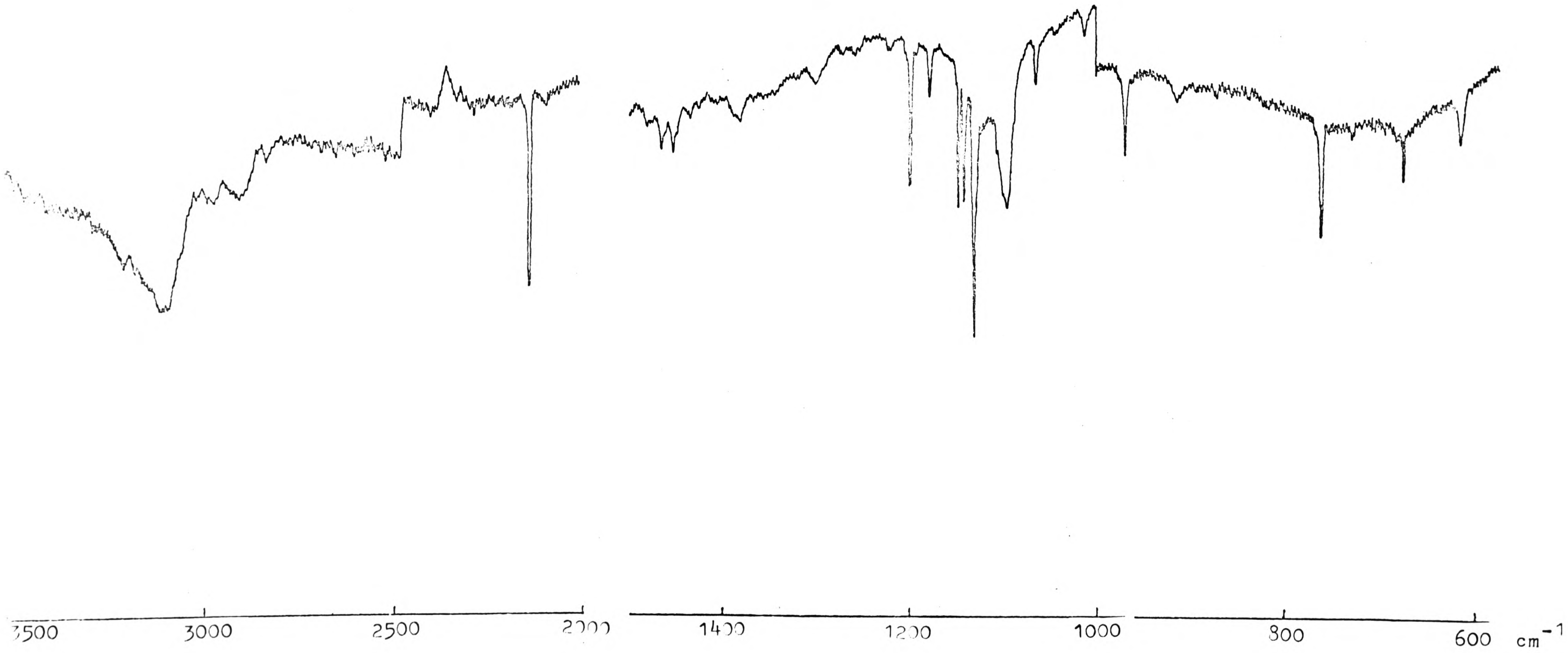

Fig. 7.10. Infrared spectrum of the products of the reaction between $(CH_3)_2PCl$ and NaN_3 isolated in an argon matrix.

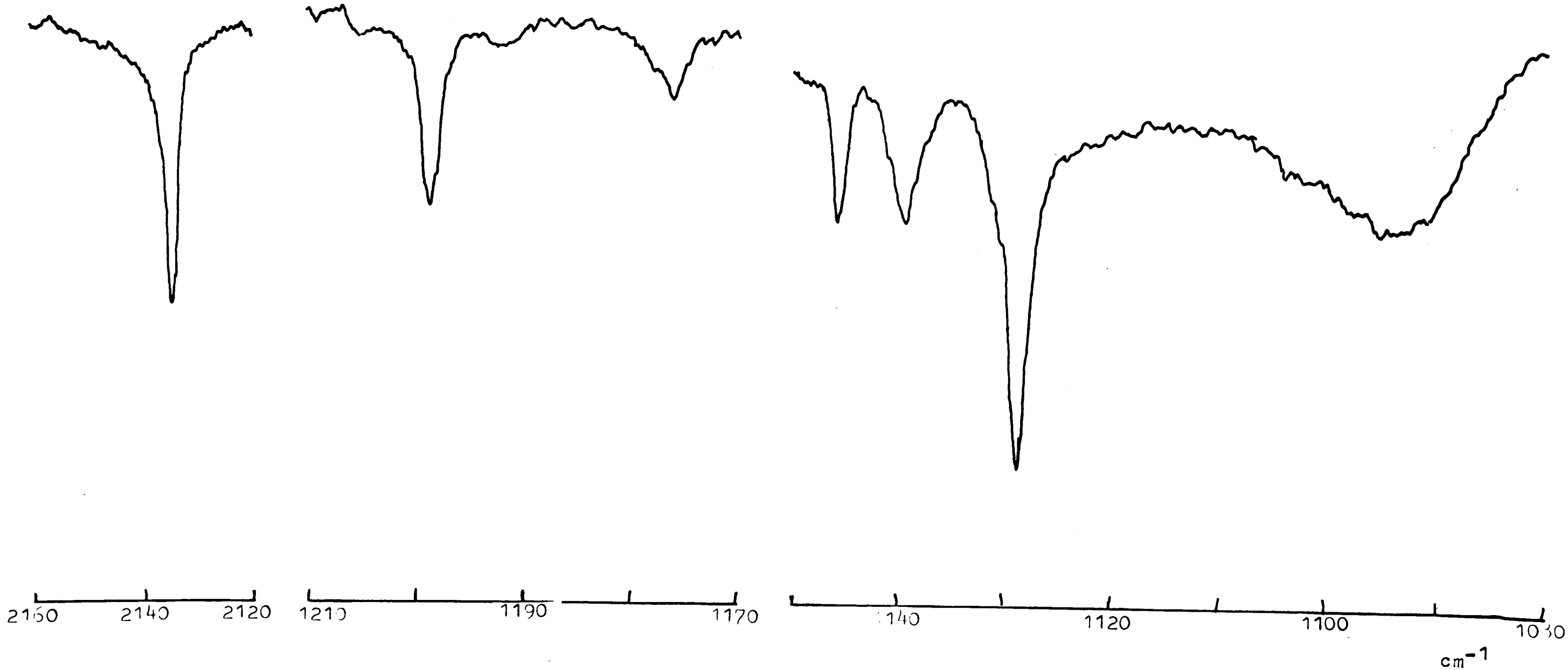

Fig. 7.11. Bands in the infrared spectrum of the products of the reaction between $(CH_3)_2PCl$ and NaN_3 isolated in an argon matrix.

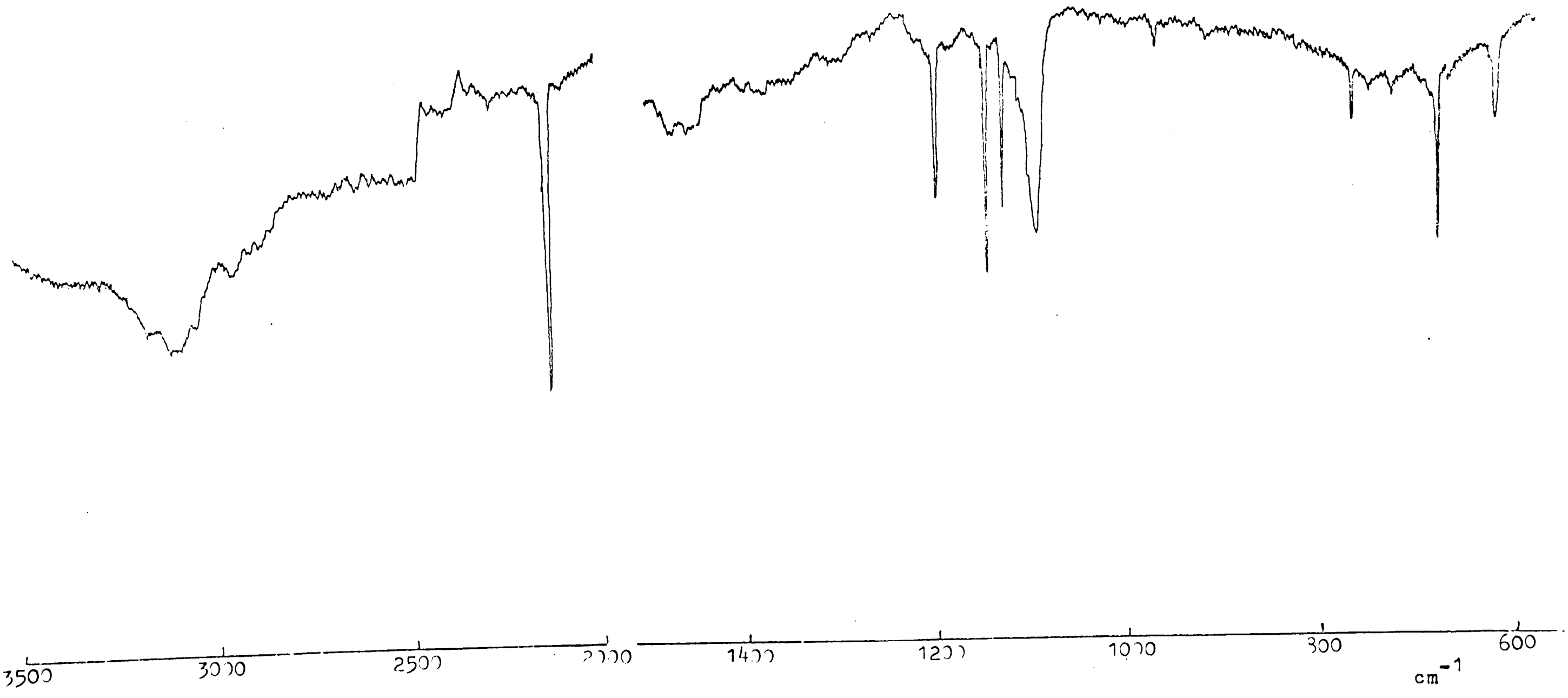

Fig. 7.12. Infrared spectrum of the products of the reaction between $(CH_3)_2PCl$ and NaN_3 isolated in a kryoton matrix.

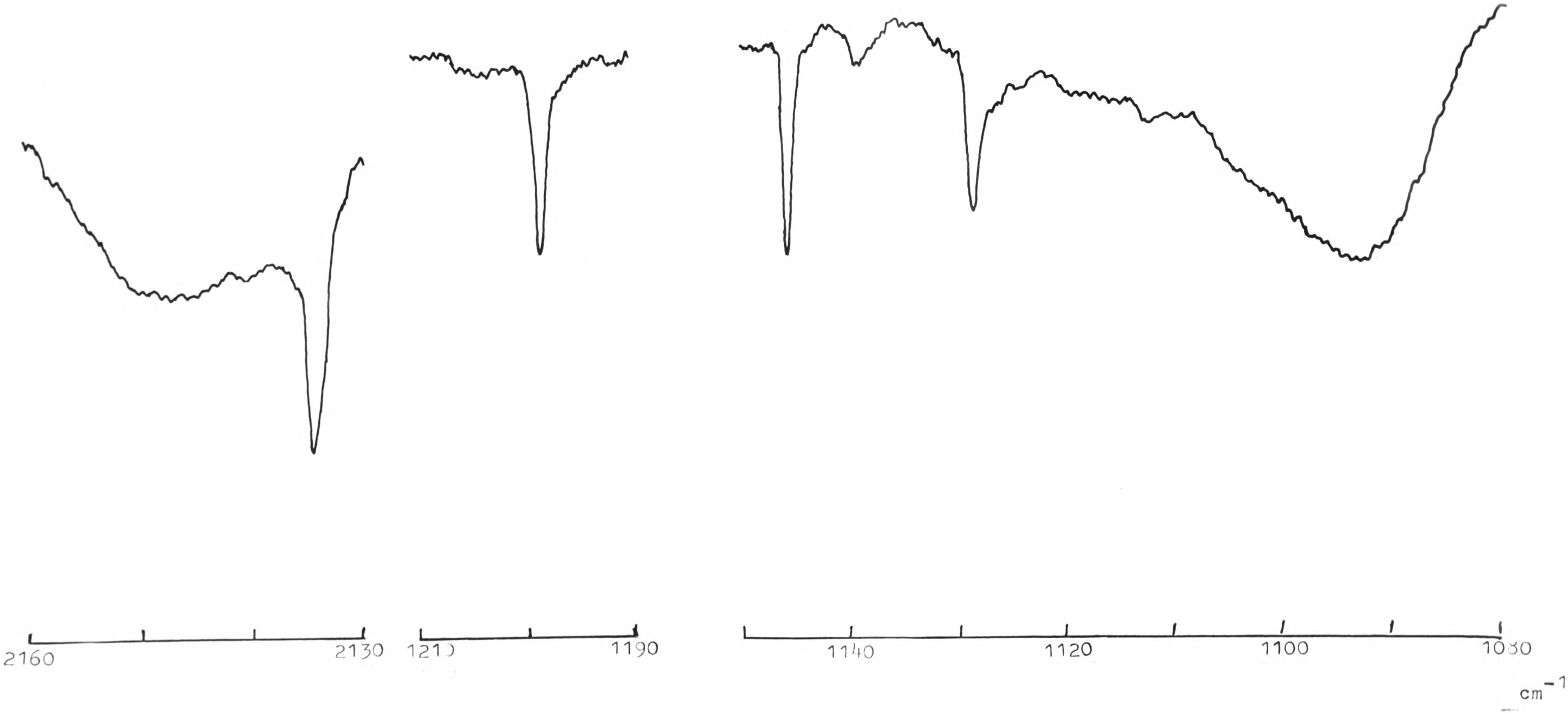

Fig. 7.13. Bands in the infrared spectrum of the products of the reaction between $(CH_3)_2PCl$ and NaN_3 isolated in a krypton matrix.

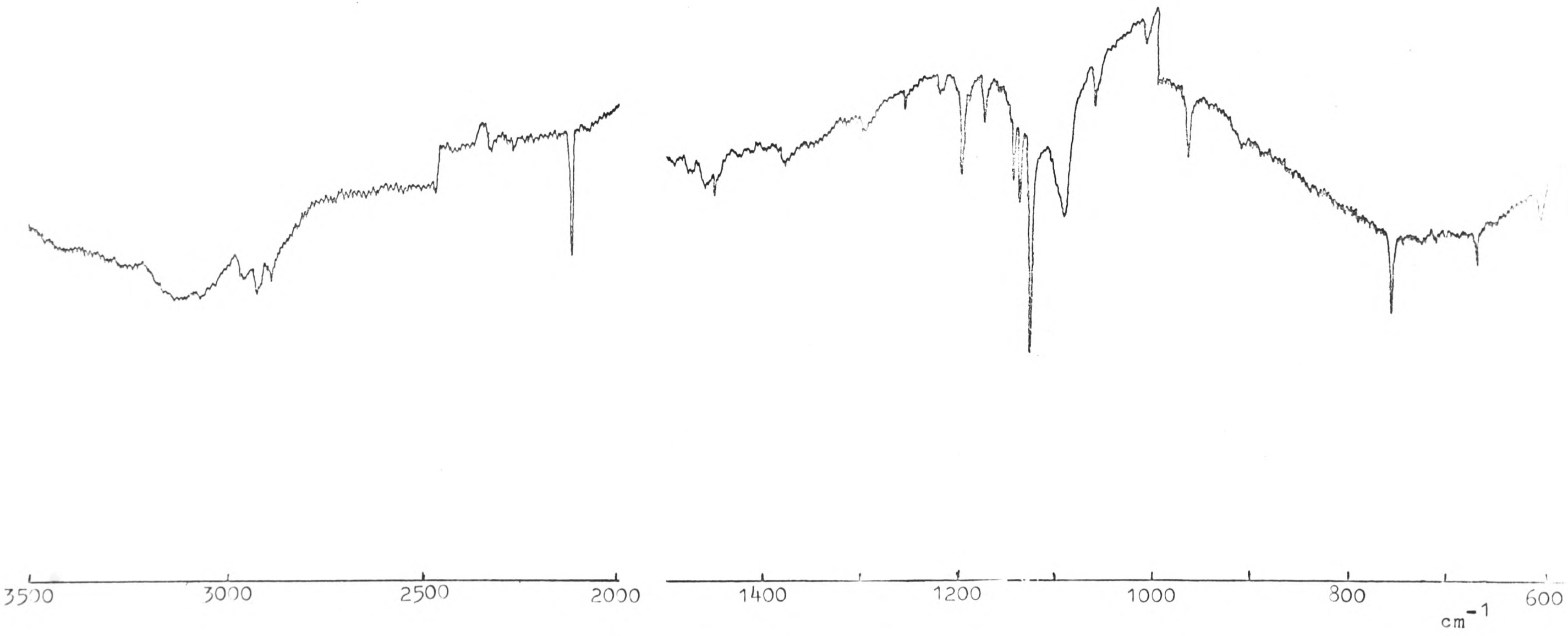

Fig. 7.14. Infrared spectrum of an argon matrix containing the products of the reaction between $(CH_3)_2PCl$ and NaN_3 after overnight photolysis.

Table 7.3. Observed Infrared Frequencies in Studies of the Reaction Between Dimethylchlorophosphine and Sodium Azide

(1) Solid, 77K	(2) Ar matrix, 20K	(3) Kr matrix, 20K
~3050	~3100	~3100
2135	2136	2134
	1466	1474
1450	1453	1456
1353		
1290	1300	
1185	1199	1198
	1176	
	1146	1146
	1139	1139
	1129	1128
1084	1094	1093
1022		
	968	965
838	838	
	762	760
	674	671
	612	610

stretching vibration, although it is slightly lower in frequency than would normally be expected (~ 1250 cm^{-1}). The bending mode of the N_3 group can then be ascribed to the band at 674 cm^{-1}.

Of the other absorptions in the spectrum of the solid at 77K, the broad feature near 3000 cm^{-1} presumably arises from C-H stretching vibrations; the presence of methyl groups in the product could also explain the weak features at 1454 and 838 cm^{-1}, which have counterparts in the spectra described for the molecules $(CH_3)_2AsN_3$ and $(CH_3)_2BiN_3$.[251] In addition, if the reaction products do contain dimethylazidophosphine, then there should be a band in the spectrum which is attributable to the P-N stretching fundamental; the band of medium intensity at 762 cm^{-1} is a plausible candidate (cf the assignment of the band at 712 cm^{-1} to such a vibration in Cl_2PN_3 or some related molecule in the previous section). There should also be several bands at lower frequencies (< 500 cm^{-1}) associated with skeletal deformation modes of the $(CH_3)_2PN_3$ molecule, but no such bands were observed in the present study. Nevertheless, the bands displayed by the solid deposit may be tentatively assigned to the $(CH_3)_2PN_3$ molecule in accordance with the proposals listed in Table 7.4, where the corresponding frequencies of the $(CH_3)_2AsN_3$ and $(CH_3)_2BiN_3$ molecules are also included for comparison.

Although clear evidence supporting the formation of the molecule $(CH_3)_2PN_3$ has thus been obtained, there are still several features of the observed spectra which remain unexplained, and, as in the case of the reaction between sodium azide and phosphorus trichloride, the products probably include two or more distinct molecular species which could not be separated by the methods of trap-to-trap distillation. In particular, the spectrum of the matrix-isolated products contains several strong bands near 1100 cm^{-1} which it is difficult to associate with any fundamental vibrations of the $(CH_3)_2PN_3$ molecule; there also appears to be no correlation between the

Table 7.4. Proposed Infrared Frequency Assignments for the $(CH_3)_2PN_3$ Molecule and Comparison with the Spectra of $(CH_3)_2AsN_3$ and $(CH_3)_2BiN_3$

Molecule			
$(CH_3)_2PN_3$	$(CH_3)_2AsN_3$	$(CH_3)_2BiN_3$	Assignment
3100	2990 2910	3000 2915	$\nu(CH_3)$
2136	2077	2043	$\nu_{as}(N_3)$
1454	1412	1383	$\delta_{as}(CH_3)$
1199	1255	1268	$\nu_s(N_3)$
838	395 332	307 748	$\rho(CH_3)$
674	656	673	$\delta(N_3)$
762	440	352	ν (M-N)

additional bands observed in the present study and the infrared spectra previously reported for dimethylchlorophosphine[258] and diglyme.[253] One possible explanation is analogous to that suggested in the previous section, namely, that the reaction products include one or more oligomers of the $(CH_3)_2P \equiv N$ molecule. No such oligomers are known, although a polymeric substance formulated as $[(CH_3)_2PN]_n$ has been reported as a product of the reaction between dimethylchlorophosphine and chloramine.[259] Again it is difficult to reach any definite conclusions on the basis of the evidence available from the present study.

The other puzzling feature of the spectra obtained from the products of the reaction between sodium azide and dimethylchlorophosphine is the effect of ultraviolet irradiation on the infrared spectrum of the matrix-isolated sample. Apart from a slight decrease in the intensity of the bands assigned to the fundamental vibrations of the azide group, very little change in the spectrum was observed even after prolonged irradiation of the sample. By contrast, the spectra of the solid products held at 77K indicate quite a marked effect following ultraviolet irradiation; bands associated with the vibrations of the azide group undergo a considerable decrease in intensity, and the simultaneous appearance of a broad band at 1400 cm^{-1} is possibly a sign of the formation of a molecule containing a $P \equiv N$ bond. More difficult to explain, however, is the appearance of a strong band at 2020 cm^{-1}. One possibility is that photolysis induces a rearrangement reaction similar to that observed in the case of matrix-isolated trimethylazidosilane[242] and resulting in the formation of a product containing a P-H bond, but the frequency of 2020 cm^{-1} is slightly too low to be easily attributable to a P-H stretching vibration.[35] A more likely explanation for the appearance of this band is the formation of some other azide-containing species.

Despite the uncertainties which have been raised by the results obtained in the present study, it is probable that dimethylazidophosphine is a major

product of the reaction between sodium azide and dimethylchlorophosphine. In order to confirm this, to produce more definite vibrational assignments for this product and to establish the nature of the other products of the reaction, further studies are plainly needed. The obvious methods of characterising the products, in addition to infrared spectroscopy, are gas chromatography (particularly to determine the complexity of the mixture) and mass spectroscopy. When dimethylazidophosphine has been properly characterised and isolated free from other compounds, a fuller spectroscopic investigation might be carried out, including the following:

(i) A more extensive investigation of the effects of ultraviolet irradiation, particularly on matrix-isolated samples, including a greater degree of selectivity in the choice of wavelengths.

(ii) Measurements of the Raman spectra of dimethylazidophosphine and the products of any photochemical changes which it may undergo.

(iii) The preparation and spectroscopic characterisation of different isotopic versions of both the $(CH_3)_2PN_3$ molecule itself and the products of any photochemical changes which it may undergo, using either deuteriated dimethylchlorophosphine or ^{15}N-labelled sodium azide.

REFERENCES

1 G N Lewis and D Lipkin, J Amer Chem Soc, 1942, 64, 2801.

2 J Dewar, Proc Roy Soc, 1901, 68, 360.

3 L Vegard, Nature, 1924, 113, 716.

4 E Whittle, D A Dows and G C Pimentel, J Chem Phys, 1954, 22, 1943.

5 G Porter, Science, 1968, 160, 1299.

6 M S Matheson and L F Dorfman, 'Pulse Radiolysis', M I T Research Monographs in Radiation Chemistry, M I T Press, 1969.

7 A J Barnes and H E Hallam, Quart Rev, 1969, 23, 392.

8 H E Hallam, Ann Reports (A), 1970, 67, 117.

9 T S Hermann and S R Harvey, Appl Spectroscopy, 1969, 23, 435.

10 G A Ozin, The Spex Speaker, 1971, XVI, no 4.

11 B Meyer, Science, 1970, 168, 783.

12 P H Kasai, Accounts Chem Res, 1971, 4, 329.

13 T K McNab, H Micklitz and P H Barrett, Phys Rev (B), 1971, 4, 3787.

14 A Kaldor and R F Porter, Inorg Chem, 1971, 10, 775.

15 A J Barnes and H E Hallam, Trans Faraday Soc, 1970, 66, 1920.

16 R A Frey, R L Redington and A L K Aljibury, J Chem Phys, 1971, 54, 344.

17 H H Claassen, G L Goodman and H Kim, J Chem Phys, 1972, 56, 5042.

18 A J Rest and J J Turner, J C S Chem Comm, 1969, 1026.

19 J K Burdett, A J Downs, G P Gaskill, M A Graham, J J Turner and R F Turner, Inorg Chem, 1978, 17, 523.

20 L Andrews and G C Pimentel, J Chem Phys, 1967, 47, 3637.

21 D E Milligan and M E Jacox, J Chem Phys, 1967, 47, 703.

22 J S Anderson and J S Ogden, J Chem Phys, 1969, 51, 4189.

23 J S Ogden and M J Ricks, J Chem Phys, 1970, 52, 352.

24 J S Ogden and M J Ricks, J Chem Phys, 1970, 53, 896.

25 J S Ogden and M J Ricks, J Chem Phys, 1972, 56, 1658.

26 L A Woodward, Introduction to the Theory of Molecular Vibrations and Vibrational Spectroscopy, Oxford University Press, 1972.

27 E B Wilson, J C Decius and P C Cross, Molecular Vibrations, McGraw-Hill, New York, 1955.

28 F A Cotton, Chemical Applications of Group Theory, 2nd ed, Wiley-Interscience, New York, 1971.

29 S D Ross, Inorganic Infrared and Raman Spectra, McGraw-Hill, London, 1972.

30 K Nakamoto, Infrared and Raman Spectra of Inorganic and Coordination Compounds, 3rd ed, Wiley-Interscience, New York, 1978.

31 J C D Brand, J C Speakman and J K Tyler, Molecular Structure, 2nd ed, Edward Arnold, 1975.

32 T Shimanouchi, Pure Appl Chem, 1963, 7, 131.

33 G Herzberg, Infrared and Raman Spectra of Polyatomic Molecules, Van Nostrand, New York, 1945.

34 L W Fung and E F Barker, Phys Rev (2nd Series), 1934, 45, 238.

35 E K Lee and C K Wu, Trans Faraday Soc, 1939, 25, 1366.

36 J S Ogden, in Cryochemistry (ed M Moskovits and G A Ozin), Wiley, New York, 1976.

37 G Placzek, Handbuch der Radiologie, Band VI Teil II, Leipzig, 1934.

38 M Wolkenstein, Compt Rend Acad Sci USSR, 1941, 30, 791.

39 D A Long, Proc Roy Soc, 1953, 217A, 203.

40 R E Hester, in Raman Spectroscopy (ed H A Syzmanski), Plenum Press, New York, 1967, p101.

41 J Behringer, ibid, p168.

42 J Behringer, in 'Molecular Spectroscopy', Chem Soc Specialist Periodical Reports, Vol 2 (1974) p100, and Vol 3 (1975) p163.

43 J Tang and A C Albrecht, in Raman Spectroscopy (ed H A Szymanski), Volume 2, Plenum Press, New York, 1970.

44 R J H Clark, in Advances in Infrared and Raman Spectroscopy, Volume 1, Heyden, London, 1975.

45 P P Shorygin, Izv Akad Nauk SSSR, 1953, 17, 581.

46 A H Kalantar, E S Franosa and K K Innes, Chem Phys Lett, 1972, 17, 335.

47 W Kiefer, Appl Spectroscopy, 1974, 28, 576.

48 J A Koningstein and B F Gachter, J Opt Soc Am, 1973, 63, 892.

49 W F Howard and L Andrews, J Amer Chem Soc, 1973, 95, 2056.

50 L Andrews and R C Spiker, J Chem Phys, 1973, 59, 1863.

51 D E Tevault and L Andrews, Spectrochim Acta, 1974, 30A, 969.

52 J S Ogden and J J Turner, Chem Brit, 1971, 7, 186.

53 A J Downs and S C Peake, in 'Molecular Spectroscopy', Chem Soc Specialist Periodical Reports, Volume 1 (1973), p 523.

54 B M Chadwick in 'Molecular Spectroscopy', Chem Soc Specialist Periodical Reports, Vol 3 (1975), p281 and Vol 6, (1979), p72.

55 H E Hallam, ed Vibrational Spectroscopy of Trapped Species, Wiley, London, 1973.

56 S Cradock and A J Hinchcliffe, Matrix Isolation, Cambridge University Press, 1975.

57 G A Ozin and A Vander Voet, Prog Inorg Chem, 1975, 19, 105.

58 I R Beattie, G A Ozin and R O Perry, J Chem Soc A, 1970, 2071.

59 R E Barletta, H H Claassen and R L McBeth, J Chem Phys, 1971, 55, 2049.

60 A Snelson, J Phys Chem, 1970, 74, 2574.

61 L Y Nelson and G C Pimentel, Inorg Chem, 1967, 6, 1758.

62 L Y Nelson and G C Pimentel, J Chem Phys, 1967, 47, 3671.

63 L Andrews, B S Ault, J M Grzybowski and R O Allen, J Chem Phys, 1975, 62, 2461.

64 W L S Andrews and G C Pimentel, J Chem Phys, 1966, 44, 2361.

65 W L S Andrews and G C Pimentel, J Chem Phys, 1966, 44, 2527.

66 L Andrews, J Phys Chem, 1967, 71, 2761.

67 E D Becker and G C Pimentel, J Chem Phys, 1956, 25, 224.

68 A J Barnes and H E Hallam, Quart Rev, 1969, 23, 392.

69 M M Rochkind, Science, 1968, 160, 196.

70 M M Rochkind, Spectrochim Acta, 1971, 27A, 547.

71 R N Perutz and J J Turner, J Chem Soc Faraday Trans II, 1973, 69, 452.

72 R Stevenson, J Chem Phys, 1957, 27, 656.

73 J W Hastie, R H Hauge and J L Margrave, in Spectroscopy in Inorganic Chemistry (ed C N R Rao and J R Ferraro), Academic Press, 1970, Vol 1, p57.

74 A D Buckingham, Trans Faraday Soc, 1960, 56, 753.

75 M Allavena, R Rysink, D White, V Calder and D E Mann, J Chem Phys, 1969, 50, 3399.

76 G C Pimentel and S W Charles, Pure Appl Chem, 1963, 7, 111.

77 P H Kasai and E B Whipple, Mol Phys, 1965, 9, 497.

78 G A Ozin, The Spex Speaker, 1971, XVI, no 4.

79 J S Shirk and H H Claassen, J Chem Phys, 1971, 54, 3237.

80 D Boal, G Briggs, H Huber, G A Ozin, E A Robinson and A Vander Voet, Nature Phys Sci, 1971, 231, 174.

81 J W L Kohler, Scientific American, 1965, 212, 119.

82 Technical Manual for 'Displex' Closed Cycle Refrigerators, Air Products and Chemicals (1973).

83 IUPAC Commission on Molecular Structure and Spectroscopy. 'Tables of Wavenumbers for the Calibration of Infrared Spectrometers.' Butterworths, 1961.

84 A R Downie, M C Magoon, T Purcell and B Crawford, J Opt Soc Am, 1953, 43, 941.

85 Operation and Maintenance Manual for Ramalog 5 Spectrometer, Spex Industries Inc, 1974.

86 A R Striganov and N S Sventitskii, Table of Spectral Lines of Neutral and Ionised Atoms, Plenum Data Corporation, New York, 1968.

87 M A Graham, Ph D Thesis, University of Cambridge, 1972.

88 M Moskovits and G A Ozin, Appl Spectroscopy, 1972, 26, 481.

89 S C Peake and A J Downs, J Chem Soc Dalton Trans, 1974, 859.

90 Gmelin, Handbuch der Anorganichen Chemie, Schwefel, B3, Verlag Chemie, Weinheim, 1963, p1536.

91 J M Dyke, A Morris and I R Trickle, J Chem Soc Faraday Trans II, 1977, 73, 147.

92 W L Jolly, Advances in Chemistry Series, 1972, 110, 92.

93 A W Cordes, R F Kruh and E K Gordon, Inorg Chem, 1965, 4, 681.

94 P Friedman, Inorg Chem, 1969, 8, 692.

95 M Becke - Goehring and M Fluck, in Developments in Inorganic Nitrogen Chemistry (ed C B Colburn), Elsevier, Amsterdam, 1966.

96 O Glemser, Angew Chem Int Ed Engl, 1963, 2, 530.

97 H G Heal, in Inorganic Sulphur Chemistry (ed G Nickless), Elsevier, Amsterdam, 1968.

98 H G Heal, Adv Inorg Chem Radiochem, 1972, 15, 375.

99 A J Banister, in MTP International Review of Science, Inorganic Chemistry, Series Two, Volume 3, Butterworth, London, 1975.

100 M Becke - Goehring, Inorg Syn, 1960, 6, 123.

101 F Feher, in Handbook of Preparative Inorganic Chemistry (ed G Brauer), Volume 1, Academic Press, New York, 1963, p409.

102 R L Patton and W L Jolly, Inorg Cher, 1969, 8, 1389.

103 A Douillard, J-F May and G Vallet, Compt Rend, 1969, 269C, 212.

104 A Douillard, J-F May and G Vallet, Ann Chim, 1971, 6, 257.

105 M J Cohen, A F Garito, A J Heeger, A G MacDiarmid, C M Mikulski, M S Saran and J Kleppinger, J Amer Chem Soc, 1976, 98, 3844.

106 R L Patton and K N Raymond, Inorg Chem, 1969, 8, 2426.

107 S C Abrahams, Acta Crystallogr, 1965, 8, 661.

108 A J Banister, Nature Phys Sci, 1972, 237, 92.

109 R Adkins, D Dell and A G Turner, J Mol Structure, 1976, 31, 403.

110 D R Salahub and R P Messmer, J Chem Phys, 1976, 64, 2039.

111 M P S Collins and B J Duke, J C S Chem Comm, 1976, 701.

112 V V Walatka, M M Labes and J H Perlstein, Phys Rev Lett, 1973, 31, 1139.

113 C Hsu and M M Labes, J Chem Phys, 1974, 61, 4640.

114 R L Greene, P M Grant and G B Street, Phys Rev Lett, 1975, 34, 89.

115 A A Bright, M J Cohen, A F Garito, A J Heeger, C M Mikulski, P J Russo and A G MacDiarmid, Phys Rev Lett, 1975, 34, 206.

116 R L Greene, G B Street and L J Suter, Phys Rev Lett, 1975, 34, 577.

117 P Love, H I Kao, G H Myer and M M Labes, J C S Chem Comm, 1978, 301

118 R H Baughman, R R Chance and M J Cohen, J Chem Phys, 1976, 64, 1869.

119 J Berkowitz, J Chem Phys, 1958, 29, 1386.

120 D White, K S Seshadri, D F Dever, D E Mann and M J Linevsky, J Chem Phys, 1963, 39, 2463.

121 J R W Warn and D Chapman, Spectrochim Acta, 1966, 22, 1371.

122 J Bragin and M V Evans, J Chem Phys, 1969, 51, 268.

123 A J Downs and S C Peake, unplublished observations.

124 W L Jolly, K D Maguire and D Rabinowitch, Inorg Chem, 1963, 2, 1304.

125 M Becke-Goehring and H P Latscha, Z Anorg Allgem Chem, 1964, 333, 181.

126 R D Cunningham, Part II Thesis, Oxford, 1972.

127 C M Mikulski, P J Russo, M S Saran, A G MacDiarmid, A F Garito and A J Heeger, J Amer Chem Soc, 1975, 97, 6358.

128 S Bhagavantam and T Venkatarayudu, Proc Indian Acad Sci, 1939, 9A, 224.

129 S Bhagavantam, Proc Indian Acad Sci, 1941, 13A, 543.

130 G Turnell, Infrared and Raman Spectra of Crystals, Academic Press, London, 1972.

131 H Temkin and D B Fitchen, Solid State Comm, 1976, 19, 1181.

132 A Muller, N Mohan, S J Cyvin, N Weinstock and O Glemser, J Mol Spectr, 1976, 59, 161.

133 H Richert and O Glemser, Z Anorg Allgem Chem, 1961, 307, 328.

134 W Sawodny, K Ballein and A Fadini, Spectrochim Acta, 1965, 21, 995.

135 H J Becher and R Mattes, Spectrochim Acta, 1967, 23, 2449.

136 O Glemser, A Muller, D Bohler and B Krebs, Z Anorg Allgem Chem, 1968, 357, 184.

137 R H Findlay, M H Palmer, A J Downs, R G Egdell and R Evans, Inorg Chem, in press.

138 W Gregory, J Pharm, 1835, 21, 315.

139 M Villena-Blanco and W L Jolly, Inorg Syn, 1967, 9, 98.

140 H J Emeleus, Endeavour, 1973, 32, 76.

141 C S Lu and J Donohue, J Amer Chem Soc, 1944, 66, 818.

142 B D Sharma and J Donohue, Acta Crystallogr, 1963, 16, 891.

143 D Chapman and T C Waddington, Trans Faraday Soc, 1962, 58, 1679.

144 A Caron and J Donohue, Acta Crystallogr, 1965, 18, 562.

145 I Lindqvist, J Inorg Nucl Chem, 1958, 6, 158.

146 A Bondi, J Phys Chem, 1964, 68, 441.

147 A G Turner and F S Mortimer, Inorg Chem, 1966, 5, 906.

148 J Mason, J Chem Soc A, 1969, 1567.

149 R Gleiter, J Chem Soc A, 1970, 3174,

150 P Cassoux, J F Labarre, O Glemser and W Koch, J Mol Structure, 1972, 13, 405.

151 M J S Dewar, E A C Lucken and M A Whitehead, J Chem Soc, 1960, 2423.

152 A J Banister, Nature Phys Sci, 1972, 239, 69.

153 K I Tobelko, Z V Zvonkova and G S Zhdanov, Dokl Akad Nauk SSSR, 1954, 96, 749.

154 F A Cotton and G Wilkinson, Advanced Inorganic Chemistry, 3rd ed, Wiley-Interscience, New York, 1972.

155 M S Gopinathan and M A Whitehead, Canad J Chem, 1975, 53, 1343.

156 C A Coulson, Valence, 2nd ed, Oxford University Press, 1961.

157 E R Lippincott and M C Tobin, J Chem Phys, 1953, 21, 1559.

158 W P Griffith and K J Rutt, J Chem Soc A, 1968, 2331.

159 D W Scott, J P McCullough and F H Kruse, J Mol Spectr, 1964, 13, 313.

160 A Turowski, R Appel, W Sawodny and K Molt, J Mol Structure, 1978, 48, 313.

161 A Muller, G Nagarajan, O Glemser and S J Cyvin, Spectrochim Acta, 1967, 23A, 2683.

162 I W Herrick and E L Wagner, Spectrochim Acta, 1965, 21, 1569.

163 J Goubeau, Angew Chem, 1966, 78, 565.

164 H Burger, G Pawelke, A Haas, H Willner and A J Downs, Spectrachim Acta, 1978 34A, 287.

165 A J Downs and M Hawkins, unpublished observations.

166 T T A Keiderling, W T Wozniak, R S Gray, D Jurkowitz, E R Bernstein and S J Lippard, Inorg Chem, 1975, 14, 576.

167 V A Maroni and T G Spiro, Inorg Chem, 1968, 7, 188.

168 Y M Bosworth, R J H Clark and D M Rippon, J Mol Spectr, 1973, 46, 240.

169 I R Beattie, K M S Livingston, G A Ozin and P J Reynolds, J Chem Soc A, 1970, 449.

170 D W Scott and J P McCullough, J Amer Chem Soc, 1958, 80, 3544.

171 M Krumpolc, B G DeBoer and J Rocek, J Amer Chem Soc, 1978, 100, 145.

172 R D Peacock, Prog Inorg Chem, 1960, 2, 193.

173 G W A Fowles, Preparative Inorganic Reactions, 1964, 1, 126.

174 A D Beveridge and H C Clark, in Halogen Chemistry (ed V Gutmann), Academic Press, New York, 1967, Vol 3, p179.

175 J E Ferguson, ibid, p227.

176 H von Wartenburg, Z Anorg Chem, 1941, 247, 135 and 1942, 249, 100.

177 R F Weinland and M Fiederer, Ber, 1906, 39, 4042 and 1907, 40, 2090.

178 H L Krauss and G Munster, Z Naturforsch, 1962, 17B, 344.

179 R B Johannesen and H L Krauss, Chem Ber, 1964, 97, 2094.

180 H L Krauss, M Leder and G Munster, Chem Ber, 1963, 96, 3008.

181 E A Seddon, K R Seddon and V H Thomas, Transition Metal Chem, 1978, 3, 318.

182 J P Jasinski and S L Holt, Inorg Chem, 1975, 14, 1267.

183 M Doran, I H Hillier, E A Seddon, K R Seddon, V H Thomas and M F Guest, Chem Phys Lett, 1979, 63, 612.

184 W B Fox, J S Mackenzie, N Vanderkooi, B Sukornuk, C A Wamser, J R Holmes, R E Eibeck and B B Stewart, J Amer Chem Soc, 1966, 88, 2604.

185 R J H Clark and D M Rippon, Mol Phys, 1974, 28, 305.

186 F W S Benfield, A J Downs, G P Gaskill and S E Staniforth, J C S Chem Comm, 1976, 856.

187 G P Gaskill, D Phil, Thesis, Oxford, 1978.

188 C D Garner, I H Hillier, F E Mabbs, C Taylor and M F Guest, J Chem Soc Dalton Trans, 1976, 2258.

189 C D Garner, J Kendrick, P Lambert, F E Mabbs and I H Hillier, Nature, 1975, 258, 138.

190 C D Garner, J Kendrick, P Lambert, F E Mabbs and I H Hillier, Inorg Chem, 1976, 15, 1287.

191 C J Ballhausen and J de Heer, J Chem Phys, 1965, 43, 4304.

192 L L Lohr and W N Lipscomb, Inorg Chem, 1963, 2, 911.

193 R J H Clark, B K Hunter and P D Mitchell, J Chem Soc Faraday Trans II, 1972, 68, 476.

194 C A Coulson and B M Deb, Mol Phys, 1969, 16, 545.

195 F Hasan and J Rocek, J Amer Chem Soc, 1976, 98, 6574, and preceding papers.

196 W E Hobbs, J Chem Phys, 1958, 28, 1220.

197 F A Miller, G L Carlson and W B White, Spectrochim Acta, 1959, 15, 709.

198 F A Miller and L R Cousins, J Chem Phys, 1957, 26, 329.

199 R J H Clark and P D Mitchell, J Chem Soc Dalton Trans, 1972, 2429.

200 I R Beattie, K M S Livingston, D J Reynolds and G A Ozin, J Chem Soc A, 1970, 1210.

201 W Levason, J S Ogden and A J Rest, J Chem Soc Dalton Trans, 1980, 419.

202 E L Varetti and A Muller, Spectrochim Acta, 1978, 34A, 895.

203 C M Lederer, J M Hollender and I Perlman, Table of Isotopes, 6th ed, Wiley, New York, 1967.

204 A Muller, B Krebs, A Fadini, O Glemser, S J Cyvin, J Brunvoll, B N Cyvin, I Elvebredd, G Hagen and B Vizi, Z Naturforsch, 1968, 23A, 1656.

205 W A Seth-Paul, J Mol Structure, 1969, 3, 403.

206 A C Albrecht, J Chem Phys, 1961, 34, 1476.

207 J Tang and A C Albrecht, J Chem Phys, 1968, 49, 1144.

208 L V Haley, T Paraneswaran, J A Koningstein and V T Aleksanyan, Chem Phys Lett, 1976, 42, 13.

209 T Paraneswaran, J A Koningstein, L V Haley and V T Aleksanyan, J Chem Phys, 1978, 68, 1285.

210 J K Palmer, J Amer Chem Soc, 1938, 60, 2360.

211 K I Karakida and K Kuchitsu, Inorg Chim Acta, 1975, 13, 113.

212 H Selig and H H Claassen, J Chem Phys, 1966, 44, 1404.

213 W M A Smit, J Mol Structure, 1973, 19, 789.

214 D C McKean and P N Schatz, J Chem Phys, 1956, 24, 316.

215 A D Dickson, I M Mills and B Crawford, J Chem Phys, 1957, 27, 445.

216 R J Gillespie and R S Nyholm, Quart Rev, 1957, 11, 339.

217 P B Rao and K S Murtz, Current Sci (India), 1960, 29, 14.

218 S P So, Z Phys Chem Neue Folge, 1975, 97, 47.

219 H Stammreich, K Kawai and Y Tavares, Spectrochim Acta, 1959, 15, 438.

220 P A Cox, S Evans, A Hamnett and A F Orchard, Chem Phys Lett, 1970, 7, 414.

221 P Griess, Phil Trans Roy Soc, 1864, 13, 377.

222 B L Evans, A D Yoffe and P Gray, Chem Rev, 1959, 59, 515.

223 P Gray, Quart Rev, 1963, 17, 441.

224 A D Yoffe, in Developments in Inorganic Nitrogen Chemistry, Vol 1 (ed C B Colburn), Elsevier, Amsterdam, 1966, p72.

225 K G Mason, in Mellor's Comprehensive Treatise on Inorganic and Theoretical Chemistry, Vol 8, Suppl II, Nitrogen, Part II, Longmans, London, 1967, p16.

226 J S Thayer, Organometal Chem Rev, 1966, 1, 157.

227 V Schomaker and R Spurr, J Amer Chem Soc, 1942, 64, 1884.

228 K Singh, Proc Roy Soc, 1954, 225A, 519.

229 A Bonnemay and R Daudel, Compt Rend, 1950, 230, 2300.

230 T W Archibald and J R Sabin, J Chem Phys, 1971, 55, 1821.

231 W J Orville Thomas, Trans Faraday Soc, 1953, 49, 855.

232 A O Beckman and R G Dickinson, J Amer Chem Soc, 1928, 50, 1870.

233 D E Milligan, J Chem Phys, 1961, 35, 1491.

234 P Gray and T C Waddington, Proc Roy Soc, 1956, 235A, 481.

235 A Bertho, Ber, 1924, 57B, 1138.

236 S K Deb and A D Yoffe, Proc Roy Soc, 1960, 256A, 528.

237 D H R Barton and L R Morgan, J Chem Soc, 1962, 622.

238 K Rosengren and G C Pimentel, J Chem Phys, 1965, 43, 507.

239 D E Milligan and M E Jacox, J Chem Phys, 1964, 40, 2461.

240 D E Milligan and M E Jacox, J Chem Phys, 1963, 39, 712.

241 S Cradock and J F Ogilvie, J C S Chem Comm, 1966, 364.

242 R N Perutz, J C S Chem Comm, 1978, 762.

243 W Buder and A Schmidt, Z Anorg Allgem Chem, 1975, 415, 263.

244 K L Paciorek and R Kratzer, Inorg Chem, 1964, 3, 594.

245 G Tesi, C P Haber and C M Douglas, Proc Chem Soc, 1960, 219.

246 H F Schoder and J Muller, Z Anorg Allgem Chem, 1975, 418, 247.

247 M Becke-Goehring and E Fluck, Inorg Syn, 1966, 8, 92.

248 M Becke-Goehring and E Fluck, Inorg Syn, 1966, 8, 94.

249 A Wilson and D F Carroll, J Chem Soc, 1960, 2548.

250 J A A Ketelaar and T A de Vries, Rec Trav Chim, 1939, 58, 1081.

251 J Muller, Z Anorg Allgem Chem, 1971, 381, 103.

252 D R Stull, Ind Eng Chem, 1947, 39, 517.

253 K Machida and T Miyazawa, Spectrochim Acta, 1964, 20, 1865.

254 I C Hisatsune, Spectrochim Acta, 1965, 21, 1899.

255 R J H Clark and D M Rippon, J Mol Spectr, 1974, 52, 58.

256 G Herzberg, Molecular Spectra and Molecular Structure - 1. Spectra of Diatomic Molecules, Van Nostrand, Princeton, 1950.

257 J Goubeau, R Baumgartner, W Koch and U Muller, Z Anorg Allgem Chem, 1965, 337, 174.

258 J R Durig and J E Saunders, J Mol Structure, 1975, 27, 403.

259 H H Sisler, Fr Patent 1,497,470 (1967).

SUMMARY

This thesis is concerned with the study of a variety of molecules trapped in low temperature matrices using the tools of vibrational spectroscopy. The concept of matrix isolation is introduced in Chapter 1, where the applicability of the technique to both normally unstable and relatively stable species is indicated. The usefulness of vibrational spectroscopic methods in particular is noted, and effects of the matrix environment such as simplification and sharpening of spectral features are outlined briefly.

Chapter 2 is concerned with the background to the methods of vibrational spectroscopy. The relationship between observed frequencies and molecular force constants is demonstrated on an essentially classical mechanical basis, while the selection rules for infrared absorption and Raman scattering are explained in quantum mechanical terms. Also described in the case of Raman scattering are the phenomena observed when the frequency of the exciting radiation approaches or coincides with that of an electronic transition of the molecule under investigation.

The principles of matrix isolation are discussed in more detail in Chapter 3. The various methods of production of matrix isolated molecules are outlined and the effects of the matrix environment on their vibrational spectra, such as frequency shifts and splitting of bands, are discussed at greater length. A section is then devoted to the particular advantages of Raman spectroscopy as applied to matrix isolated molecules, as well as the difficulties arising from its relative insensitivity. Finally, the experimental techniques, both cryogenic and spectroscopic, employed in the present study are described.

Observation of the vibrational spectra of cyclic sulphur-nitrogen compounds under the conditions of matrix isolation is the subject of Chapters 4 and 5. The former is concerned with the simplest such molecule, namely disulphur dinitride, S_2N_2. The infrared spectrum of polycrystalline disulphur dinitride contains five bands, three of which have previously been assigned to the infrared

active fundamentals of the molecule; as a result of the present investigation the other two are attributed to two distinct intermediates in the polymerisation of S_2N_2. The Raman spectrum of matrix isolated S_2N_2 contains just three bands. The assignment of these to the Raman active fundamentals of S_2N_2 is supported both by their polarisation properties and by the normal coordinate analysis of the molecule, and the possibility of Fermi resonance, suggested by the close proximity of two of them, is discounted. The vibrational spectra of the precursor of S_2N_2, namely tetrasulphur tetranitride, S_4N_4 observed under conditions of matrix isolation, are consistent with previous observations made in the solid state and in solution, and with the well-established cage structure of the molecule.

Measurement of the vibrational spectra of different isotopic versions of the molecules, namely $S_2{}^{15}N_2$ and $S_4{}^{15}N_4$, has enabled a complete normal coordinate analysis of both disulphur dinitride and tetrasulphur tetranitride to be carried out. The principal S-N stretching force constants are found to be much lower than those predicted on the basis of observations made for related acyclic molecules, possibly reflecting the strain imposed by the cyclic structures. The magnitudes of the interaction force constants are consistent with the existence of delocalised π -bonding, which appears to extend throughout the ring in the case of S_2N_2 but to be slightly more restricted in the larger S_4N_4 cage. Further evidence is afforded for substantial cross-ring S–S bonding in S_4N_4, while on the other hand the results obtained for S_2N_2 may be explained in terms of repulsive non-bonded S–S interactions, in accordance with the results of *ab initio* molecular orbital calculations.

Chapter 6 describes a matrix isolation study of a chromium (V) compound, namely chromium trichloride oxide, $CrOCl_3$, which as might be expected is rather unstable at normal temperatures, tending to decompose by disproportionation and/or hydrolysis. The infrared spectrum of matrix-isolated $CrOCl_3$ contains bands attributable to the vibrational fundamentals of a pyramidal molecule of C_{3v}

symmetry, by analogy with other similar molecules, particularly $VOCl_3$. In addition, several other bands, indicating the presence of CrO_2Cl_2 and possibly other decomposition products, are observed. The Raman spectrum is rather more puzzling in that just three strong bands are observed, all below 250 cm^{-1}. The possibility of a resonance Raman effect is considered but it is thought more likely that the exciting line coincides with a dip in the absorption spectrum leading to increased absorption at longer wavelengths; fluorescence and the occurrence of an electronic Raman effect are possible alternative explanations. Normal coordinate analysis of $CrOCl_3$, based on the assumption that the observed Raman lines arise from its deformation fundamentals, indicates a force field very similar to those in the related molecules $VOCl_3$ and CrO_2Cl_2.

The seventh and final chapter is concerned with the attempts to generate molecules containing an azide group bonded to a phosphorus atom, in the hope of carrying out the photolytic transformation $>P\text{-}N_3 \longrightarrow >P \equiv N + N_2$. The infrared spectrum (measured at 77K) of the volatile products of the reaction between phosphorus trichloride and sodium azide indicates the presence of several molecules. Although these probably include Cl_2PN_3, it was decided that this apparently complex mixture did not lend itself to a matrix isolation study. Such a study was carried out on the products of the reaction between dimethylchlorophosphine and sodium azide, which almost certainly include $(CH_3)_2PN_3$ as a major component. However, the reaction again appears to be rather complex and several observations, particularly the effects of ultraviolet photolysis, remain unexplained.

In conclusion, although the present investigation has yielded some interesting results relating to a variety of molecular species, further studies are clearly desirable in several areas; for example, those described in Chapters 4 and 5 might be extended to other cyclic sulphur-nitrogen systems, thus enabling more general comparisons to be made. Secondly, the origin of the Raman scattering of chromium trichloride oxide might be made clearer by further studies using a range of excitation frequencies, while investigation of the effects of controlled

warming and photolysis might lead to identification of its disproportionation products. In the case of the studies described in Chapter 7, application of other techniques such as mass spectrometry might lead to more definite characterisation of the reaction products, while if, for example, dimethylazidophosphine can be isolated free from other compounds, a fuller spectroscopic investigation, including measurement of its Raman spectrum, might be carried out.